Epigenetics in Health and Disease: Focus on epigenetic mechanisms as systems of change and adaptability

Dissertation

zur Erlangung des Grades

Doktor der Naturwissenschaften

Am Fachbereich Biologie

der Johannes Gutenberg-Universität Mainz

Tamer Butto

geb. am 12.12.1992 in Petah Tikva, Israel

Mainz, den

Supervisor: Prof. Dr. Susanne Gerber

Date of oral examination: 15.10.2021

Table of Contents

Chapter 2 – Case studies

Chapter 3 – Overall discussion and outlook

Abstract

Epigenetics can be described as the field that studies the distinct molecular mechanisms that modulate gene expression without entailing actual changes in the genetic sequence. The regulation of gene expression is a fundamental process in cellular and molecular biology, which ultimately promotes cellular adaptation in response to internal and external environmental stimuli. Epigenetic mechanisms such as DNA methylation, histone post-translational modification (PTM), and non-coding RNA are the most broadly studied epigenetic mechanisms shown to play a vital role in the regular maintenance of distinct cellular populations as well as in the pathology of a variety of health-associated maladies.

The current thesis presents a collection of studies addressing the distinctive roles of epigenetic mechanisms as systems of change and adaptability and their association with different healthy/diseased phenotypes. Such studies will focus on research topics involved in 1) Epigenetic treatment of genomic imprinting disorder, 2) transcriptional and epigenetic alterations associated with resilient behavior to chronic stress, 3) host-gut microbiota communication network associated with the stress-response system, and 4) transcriptional alterations associated with mTOR inhibition in adult neurons. In addition, several studies will highlight the progression of various methodologies used to monitor the diverse epigenetic alterations and their influence on gene expression changes. Each study provides a unique prospect emphasizing the role of the epigenetic mechanism in the referred health-associated condition as well as its broad function as an evolutionary tool of change and adaptability.

Lastly, this thesis will present a novel outlook and concepts aiming to properly define and sub-classify the distinct epigenetic mechanisms based on their capacity of alteration and their necessity in various cellular populations. Such novel views could provide a stimulating re-evaluation of the distinct epigenetic mechanisms, which will encourage further examination of the basic models of epigenetics and will herewith contribute to the field's further progression.

Zusammenfassung

Das Forschungsfeld der Epigenetik interessiert sich für verschiedene molekulare Mechanismen, welche die Genexpression modulieren, ohne zu tatsächlichen Veränderungen in der genetischen Sequenz zu führen. Die Regulation der Genexpression ist ein fundamentaler Prozess im zentralen Dogma der Molekularbiologie, der letztlich die zelluläre Anpassung als Reaktion auf interne und externe (Umwelt)reize fördert. DNA-Methylierung, posttranslationale Histon-Modifikation (PTM) und die Aktivität nicht-kodierender RNAs sind die am besten untersuchten epigenetischen Mechanismen. Diese spielen eine wichtige Rolle, insbesondere bei der zellulären Homöostase, der Adaptation an externe Faktoren, sowie, bei Fehlfunktion, für die Pathologie einer Vielzahl von Krankheiten.

Die vorliegende Arbeit stellt eine Sammlung von aufeinander aufbauenden Studien vor, die sich jeweils mit der Rolle epigenetischer Mechanismen als Werkzeug der Anpassungsfähigkeit befassen und den Zusammenhang zwischen gesunden/krankhaften Phänotypen analysieren. Diese Studien konzentrieren sich auf Forschungsthemen in Bezug auf: 1) Epigenetische Behandlung von genomischen Imprinting-Störungen, 2) transkriptionelle und epigenetische Veränderungen, die mit resilientem Verhalten gegenüber chronischem Stress assoziiert sind, 3) Kommunikationsnetzwerk zwischen Wirt und Darm-Mikrobiota, das mit dem Stress-Reaktionssystem assoziiert ist, und 4) transkriptionelle Veränderungen, die mit mTOR-Inhibierung in reifen Neuronen assoziiert sind. Darüber hinaus wird mehrfach vergleichend auf die aktuellen methodologischen Fortschritt eingegangen, welche eine immer genauere Untersuchung und Analyse der verschiedenen epigenetischen Veränderungen und ihres Einflusses auf Veränderungen der Genexpression erlauben. Jede Studie beschäftigt sich jeweils auch perspektivisch mit der Rolle der jeweiligen epigenetischen Mechanismen, sowie deren Funktion als evolutionäres Werkzeug der Anpassung.

Abschließend werden in dieser Arbeit neue Perspektiven und Konzepte vorgestellt, die darauf abzielen, die verschiedenen epigenetischen Mechanismen auf Grundlage ihrer Veränderungsfähigkeit und ihrer Notwendigkeit in einer Vielzahl von Zellpopulationen richtig zu definieren und zu klassifizieren. Solche neuartigen Ansichten könnten eine anregende Neubewertung der verschiedenen epigenetischen Mechanismen liefern, welche wiederum zu einer weiteren Untersuchung der grundlegenden Modelle der Epigenetik anregen und hierdurch zur weiteren Entwicklung des Feldes beitragen können.

List of abbreviations

PTM – Post-translational modification

5mC – (5' cytosine-phosphate-gunosie3')

DNMTs – DNA methyltransferase

TET – ten-eleven translocation proteins

HATs – Histone acetyltransferase

HDAC – Histone deacetylase

HMT – Histone methyltransferase

KDM/LSD – Lysine-specific demethylase

XCI - X chromosome inactivation

H3K4me – methylation of histone 3 lysine 4 residue

H3K27ac – Acetylation of histone 3 lysine 27 residue

ORF – Open reading frame

miRNA – microRNA

RISC – RNA induced silencing complex

ICR – *imprinted control regions*

HPA – Hypothalamic-pituitary-adrenal axis

IEG – immediate early gene

CSD – Chronic social defeat

PFC – prefrontal cortex

vHIP – ventral hippocampus

CSS – Chronic social stress

BBIDS – Birk-Barel intellectual disability syndrome

mTOR – mechanistic target of rapamycin

FANS – Fluorescence-assisted nuclei sorting

INTACT – "Isolation of Nuclei Tagged in Specific Cell Types"

nucRNA-seq – nuclear RNA sequencing

DEGs – Differentially expressed genes

DEMs – Differentially expressed miRNAs

DAR – Differentially accessible regions

GO analysis – Gene ontology analysis

sRNA- small RNA

scRNA-seq – Single cell RNA-sequencing

Chapter 1 – General Introduction

1.1 The basics of epigenetics: concepts and importance

The term "epigenetics" consists of the Greek word *epi-* meaning "above" or "over", and *genetics,* which is the field in biology that studies gene heritability and its variations (Nightingale 2016). Thereby, epigenetics describes a form of regulation that is above the expression of genes (i.e. genetics). Conrad Hal Waddington introduced the term epigenetics in the 1940s, while describing a mechanism by which environmental signals (both internal and external) interact with genes, giving rise to novel phenotypes (Waddington 1942, Tronick and Hunter 2016). Since then, a modern definition of epigenetics describes it as the heritable and reversible changes that occur in gene expression without altering the genetic sequence i.e. DNA (Watson 2014).

The completion of the human genome project in 2005 (Belmont et al. 2005) and analysis of additional mammalian genomes (Carninci et al. 2005) marked a milestone in the field of genomics, highlighting the importance of the field of epigenetics by revealing a few unexpected outcomes regarding the complexity of the mammalian genome. For instance, the number of genes identified in mammalian genomes (~20-25,000 genes) was not proportional to the genome size of approximately 3 billion nucleotides. This puzzling observation hinted that the complexity of higher eukaryotic organisms was not attributed to the number of genes, but rather to the structural organization of the chromatin, its dynamic expression and varied functional outcomes. Secondly, sequencing analyses of such mammals revealed that 98% of what was considered "junk DNA" could also be transcribed. However, these transcripts did not appear to encode functional proteins (Statello et al. 2020). Therefore, it has been postulated that these non-coding RNA (ncRNA) populations could comprise an additional role in regulating gene expression (Lee, Zhang and Krause 2019). These observations led to the recognition of multiple layers of epigenetic regulation that govern and affect the complexity of higher eukaryotic cells and triggered scientists to continue and explore the multi-faceted field of epigenetics.

1.2 The role of epigenetics in the central dogma of molecular biology

The central dogma of molecular biology relates to the conversion of biological information, from the genetic material (DNA), to its transcription (RNA) and ultimately, the formation of a functional translated outcome (protein) (Morange 2009). Each step is tightly regulated allowing functional activity of the cellular system. Through its distinct branches, epigenetic regulation provides a "gate" between the existing environmental stimuli and the internal regulation of gene expression thereby allowing the cells to respond and adapt to their environment (Figure 1).

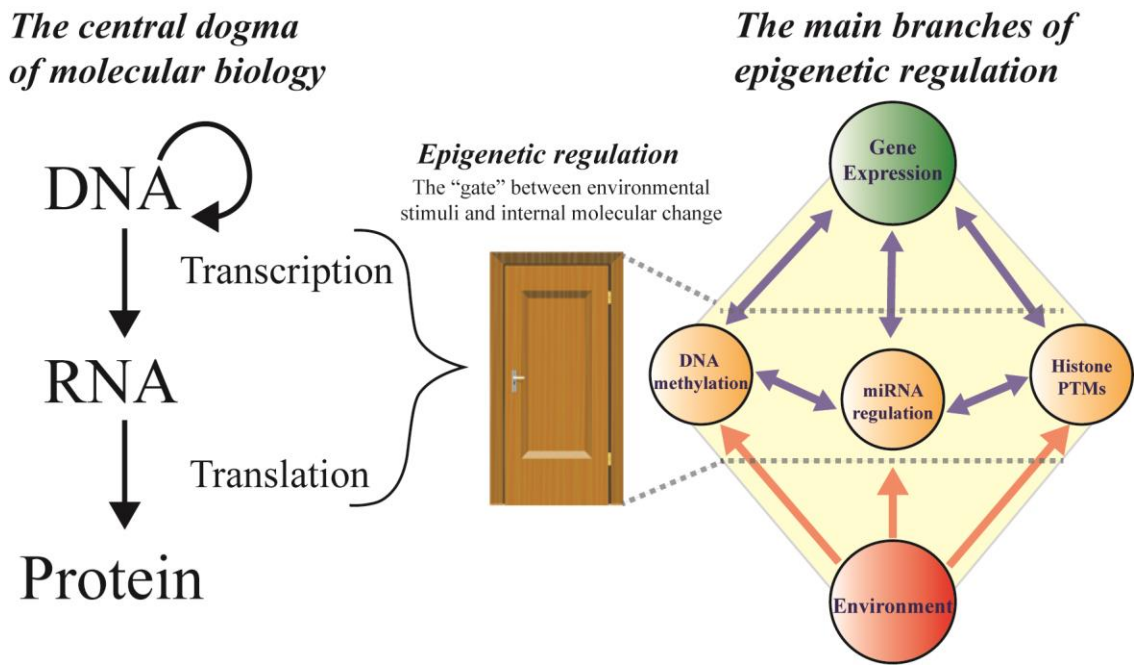

Figure 1: The relationship between the central dogma of biology and epigenetic regulation. (The right part of the illustration is slightly modified version of Figure 4 from Villota-Salazar et al. 2016)

While all cells in a single organism contain relatively similar genetic content, the gene expression and activity vary from cell to cell. The interest in such phenomena led scientists to explore the different attributes of specific cell populations in order to identify their characteristics, roles, and purpose within an organism. More specifically, it was recognized that epigenetic regulation provides a unique blueprint that controls and expresses a specific set of genes required for cell-type-specific populations. Therefore, epigenetic regulation offers how the cells differentiate and adapt in response to external and internal stimuli.

There are three main epigenetic branches including DNA methylation, histone post-translational modification (PTM) and non-coding RNA, which include miRNA regulation which will be addressed in this thesis (Villota-Salazar et al. 2016). Each epigenetic branch comprises various protein components and specific mechanisms that ultimately ensure a purposeful regulation of gene expression. The following sections will summarize the main epigenetic branches, their respective mechanisms of actions and key constituents involved in regulating gene expression.

1.3 The main branches of epigenetics

1.3.1 DNA methylation

The conventional branch of DNA methylation relates to the chemical modification of the genomic DNA by deposition of a methyl group on cytosine ring of a CpG site (5' cytosine-phosphate-gunosie3' or 5mC) (Prachayasittikul et al. 2017; Skvortsova, Iovino and Bogdanović, 2018). In 1975, it was proposed that DNA methylation was responsible for controlling gene expression during differentiation and development (Holliday and Pugh 1975; Riggs 1975). Such deposition has been associated initially with transcriptional repression (Ben-Hattar et al. 1988, Watt et al. 1988, Iguchi –Ariga et al. 1989). However, depending on the genomic region and associated chromatin binding proteins, it was demonstrated that 5mC could be associated with actively transcribed genes (Greenberg and Bourc'his 2019). Further studies have identified CpG-rich regions (CpG islands) in the mammalian genome of which two-thirds are located at promoter regions (Gardiner-Garden and Frommer 1987, Larsen et al. 1992). These regions alongside with neighboring genomic regions such as CpG shores (located up to 2 kb from CpG islands) play a crucial role in gene regulation and transcriptional activation.

DNA methyltransferases (DNMTs) mediate the deposition of the methyl groups on the DNA. In contrast, ten-eleven translocation (TETs) are the main enzymes which mediate DNA demethylation through active or passive mechanisms (Kohli and Zhang 2013). Since the discovery of such regulatory role, DNA methylation has been associated with a variety of biological processes such as repression of transposons elements (Walsh, Chaillet & Bestor 1998), germ-line specific gene silencing (Borgel et al. 2010) and most predominantly genomic imprinting (Li, Beard & Jaenisch 1993) and X chromosome inactivation (XCI) (Mohandas, Sparkes & Shapiro 1981, Greenberg & Bourc'his 2019) (Figure 2A).

1.3.2 Histone post-translational modification

Histone modification relates mainly to the post-translational modification of the arginine (R) or lysine (K) residues located on the histone tails (Li, Carey and Workman 2007). Despite the identifying various histone modifications (Kouzarides 2007), histone methylation and acetylation are the most predominantly studied, identifying their diverse deposition pattern on histone tails and their varied regulative roles in chromatin structure remodeling and gene expression.

Acetylation of Histone 3 and 4 (H3 and H4) or distinct methylation configurations of H3K4 are associated with active transcription located on genomic regions termed euchromatin (Yan and Boyd 2006). Such modifications are mediated by distinct enzymes which deposit or remove the modification from the histone

tails. For instance, histone acetyltransferases (HATs) and histone deacetylases (HDACs) mediate the acetyl deposition or removal on the histone tails, respectively (Yang and Seto 2007). Similarly, histone methyltransferases (HMTs) and histone demethylases (KDM/LSD) mediate the deposition or removal of methyl modifications from the histone tails, respectively (Teperino, Schoonjans and Auwerx 2010, Dimitrova, Turberfield and Klose 2015).

The diverse modification array revealed a complex and dynamic regulatory network that provides a relatively flexible form of transcriptional regulation on the entire genome. An example of such variation is observed in the distinct methylation forms of H3K4 that were shown to be enriched in specific genomic regions associated with active transcriptional. For instance, H3K4 monomethylation (H3K4me1) has been shown to enriched in active enhancer and poised promoters (Bae and Lesch 2020), whereas H3K4 trimethylation (H3K4me3) is enriched around active promoter regions, transcription start sites (TSS), and 5'end of the open reading frame (ORF) (Pokholok et al. 2005). Another example of a transcriptionally active mark is the acetylation of H3K27 residue (H3K27ac), which was discovered to be deposited by the histone acetyltransferase CBP/p300 and enriched in active enhancer and promoter region thereby associating the mark with active transcription (Tie et al. 2009, Creyghton et al. 2010, Rada-Iglesias et al. 2011).

On the contrary, inactive genomic regions known as heterochromatin, were shown to be enriched with methylation marks at H3K9 and H3K27 residues (Hyun et al. 2017). For instance, methylation of H3K9 (particularly mono- and di-methylation) has been shown to be associated with inactivate chromatin region and overall silenced transcription (Tachibana et al. 2002). Similarly, H3K9 tri-methylation (H3K9me3) is a widely studied mark associated with transcriptional inhibition. H3K9me3 promotes gene regulation by forming large repressive domains, which provide constraint during embryo development and promote stability in differentiated cell types (Becker, Nicetto and Zaret 2016).

In the case of the methylated H3K27 residue, various studies have shown the divergent role of this residue in transcriptional activity. For instance, H3K27me1 was shown to be enriched at the active promoter, whereas H3K27me3 is associated with inactive yet poised gene promoters (Barski et al. 2007, King et al. 2016). These few examples display the dynamic roles of histone modifications and their vast regulative potential varying depending on the genomic region, modified histone residue, and type of modification (Figure 2B).

1.3.3 miRNA regulation

microRNAs (miRNAs) are classified as small, single stranded non-coding RNA molecules of approximately 20-23 nt which inhibit translation by binding to the 3'-end of mRNA promoting mRNA decay or translational inhibition (Vishnoi and Rani 2017, Dexheimer and Cochella 2020). miRNAs were initially discovered in *C.elegans,* identifying a mechanism by which a small RNA can bind to complementary mRNA, thereby regulating its translation (Lee, Feinbaum and Ambros 1993). miRNA regulation provides a substantial genome-wide transcriptional regulation where multiple miRNAs can target and regulate one mRNA, and similarly, a single miRNA can regulate multiple mRNAs targets (Saetrom et al. 2007). For instance, it is estimated that mammalian miRNAs regulate approximately 30% of all protein-coding genes (Filipowicz, Bhattacharyya and Sonenberg 2008). Since then, miRNAs have been detected and annotated in most eukaryotic systems, with currently 48,860 annotated miRNA in 271 organisms, according to miRBase (Kozomara, Birgaoanu and Griffiths-Jones 2019).

In mammals, the miRNA biogenesis can be divided into a two-step cleavage process occurring in the nucleus and in the cytoplasm. The process of miRNA biogenesis involves transcription of pri-miRNA, which is cleaved by RNase III endonuclease Drosha (in association with DGCR8/Pasha), creating the precursor pre-miRNA (Lee et al. 2002, Lee et al. 2003). The pre-miRNA is transported to the cytoplasm (through exportin 5) amd further cleaved by the RNAse III endonuclease Dicer creating the mature miRNA containing the "seed" sequence complementary to a specific 3'UTR motif of the mRNA it regulates (Lai 2002). The mature miRNA is next loaded into RNA induced silencing complex (RISC) containing that catalytic subunit Argonaute (AGO) protein which ultimately down-regulates the target gene by mRNA cleavage (Hutvágner and Zamore 2002) or by repression of translation (Lai 2002) (Figure 2C).

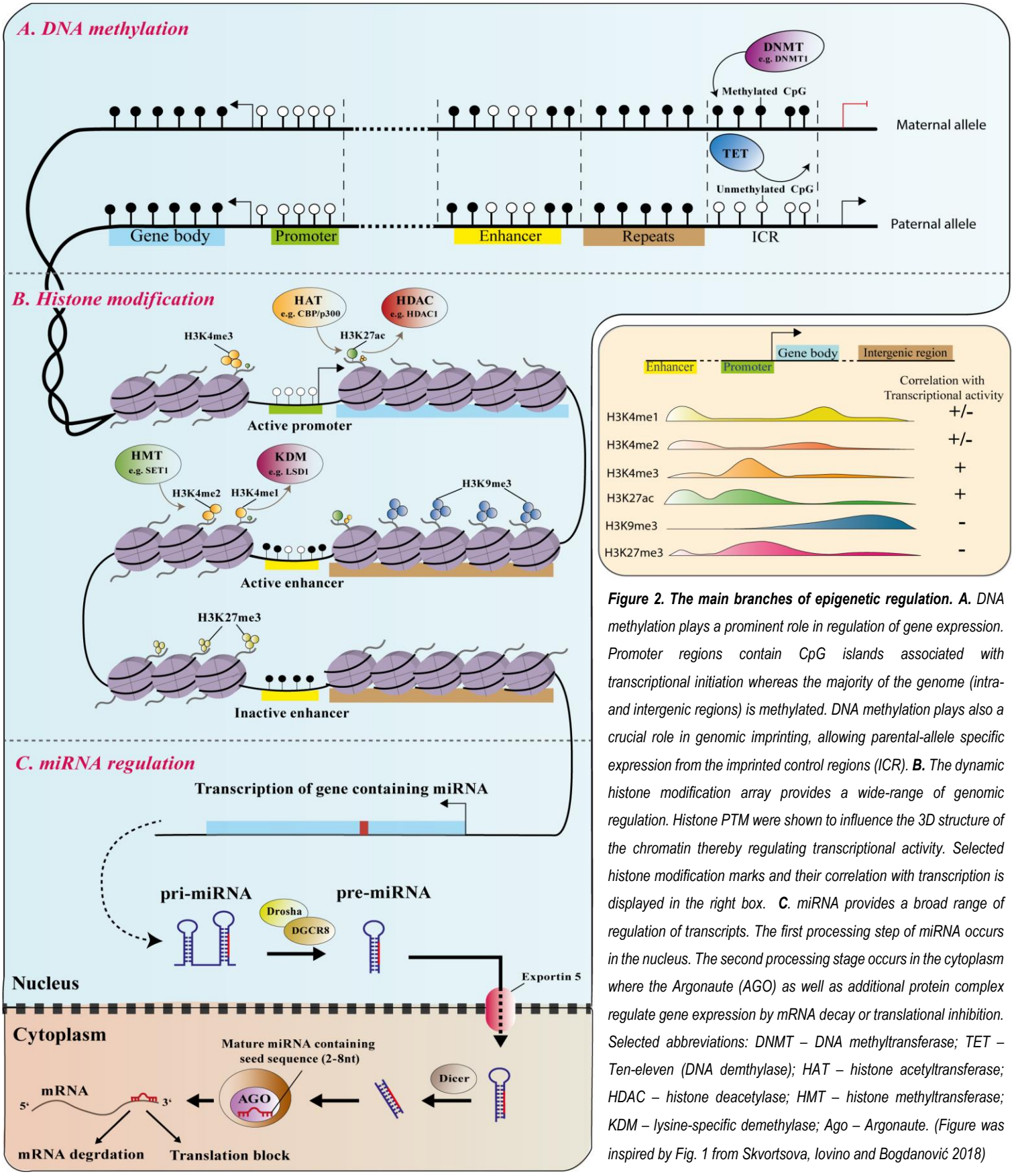

Figure 2. The main branches of epigenetic regulation. A. *DNA methylation plays a prominent role in regulation of gene expression. Promoter regions contain CpG islands associated with transcriptional initiation whereas the majority of the genome (intra- and intergenic regions) is methylated. DNA methylation plays also a crucial role in genomic imprinting, allowing parental-allele specific expression from the imprinted control regions (ICR).* ***B.*** *The dynamic histone modification array provides a wide-range of genomic regulation. Histone PTM were shown to influence the 3D structure of the chromatin thereby regulating transcriptional activity. Selected histone modification marks and their correlation with transcription is displayed in the right box.* ***C.*** *miRNA provides a broad range of regulation of transcripts. The first processing step of miRNA occurs in the nucleus. The second processing stage occurs in the cytoplasm where the Argonaute (AGO) as well as additional protein complex regulate gene expression by mRNA decay or translational inhibition. Selected abbreviations: DNMT – DNA methyltransferase; TET – Ten-eleven (DNA demthylase); HAT – histone acetyltransferase; HDAC – histone deacetylase; HMT – histone methyltransferase; KDM – lysine-specific demethylase; Ago – Argonaute. (Figure was inspired by Fig. 1 from Skvortsova, Iovino and Bogdanović 2018)*

1.4 Epigenetics in health and disease

The continuous study of the distinct epigenetic mechanisms has revealed their importance not only in the regulation and regular maintenance of active cellular systems but also in their involvement in disease pathology. Early work has associated distinctive epigenetic mechanisms mainly with cancer and presently, it is associated with various other diseases including autoimmune diseases, congenital disorders, neuropsychiatric disorders and many others (Zhang, Lu and Chang 2020, Portela and Esteller 2010, Fraga et al. 2015).

The association between disease and its manifestation can be linked to the concept of Genes x Environment (G x E) or "Nature versus Nurture" (Crews et al. 2014). Such a relationship describes the link between an individual's genetic composition and acquired behavioral traits (environmental), which lead to the expression of the overall individual's phenotype (Figure 3). Such a concept can be applied to the notion of health preservation or disease manifestation as a sum of the genetic constitution ("Nature") and individual differences in various traits, including physiology, cognition, and behavior ("Nurture") (Powledge 2011). Unlike genetic alterations, which are more challenging to reverse, epigenetic alterations are reversible. They, therefore, provide a promising avenue for pharmaceutical intervention, which can be potentially targeted and reversed back to healthy states (Figure 3).

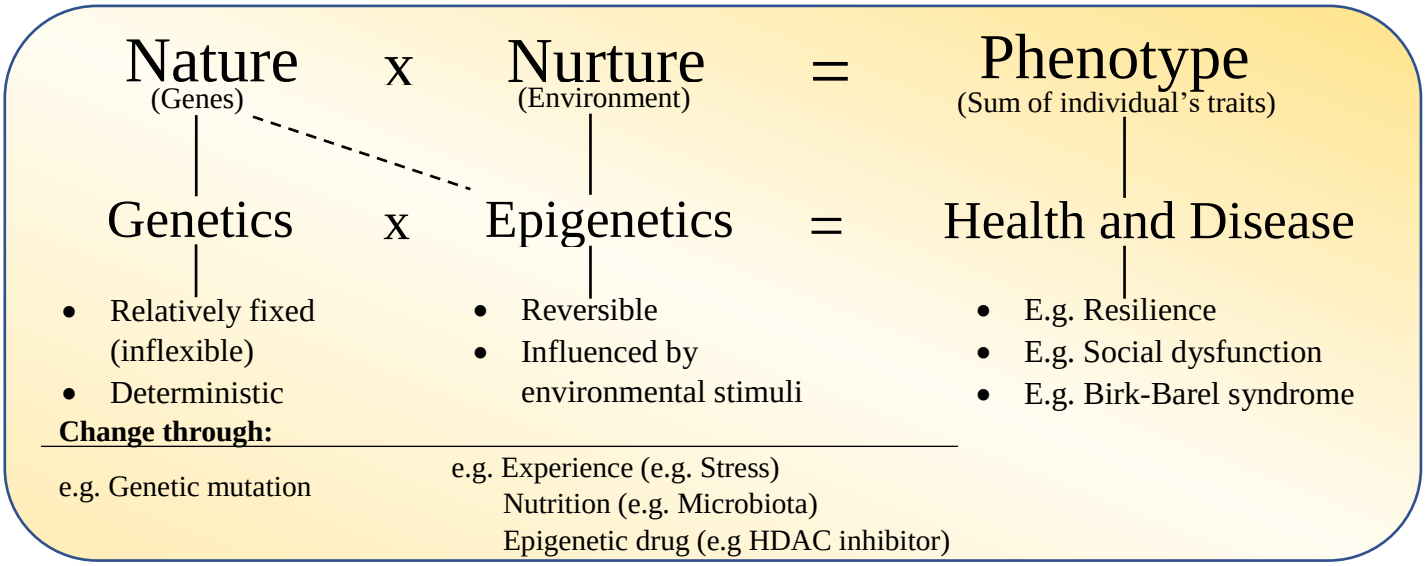

Figure 3. The relationship between "Nature versus Nurture" in association with health and disease. *The overall phenotypic expression is influenced by the genetic constitution (genetics) and its given gene expression (epigenetics) in response to environmental stimuli. Changes in the genetic constitution (through mutations) or in individual traits (experience, nutrition etc.) can shift the phenotypic expression towards health preservation or disease manifestation.*

The following sections will introduce subjects linked to the case studies addressed in this thesis and present their relationship with distinct epigenetic mechanisms and their involvement in health and disease.

1.4.1 Stress-resilience

1.4.1.1 Basic concepts of stress

Stress can be defined as a physiological response to a stimulation followed by an effort of the body to overcome the stimuli and adapt to the new state (Anisman and Merali 1999). Hans Selye, also known as "the father of stress", further attempted to deepen the understanding of stress by describing two situations of how stress can be experienced. The first scenario describes stress as a positive and a healthy response, allowing the body to overcome a challenge, adapt to a new state and eventually become stronger. This type of stress was termed eustress. In contrast, when the body cannot handle the stimulation, it fatigues and risks developing a physiological disorder. This harmful stress was termed distress (Salleh 2008).

These basic concepts led to developing further conceptual ideas of stress adaptation such as allostasis, which refers to "maintenance of stability through change" (Sterling and Eyer 1988, Karatsoreos and McEwen 2011, McEwen and Karatsoreos 2015). Unlike homeostasis, which concerns the physiological and chemical stability of internal states such as body temperature, oxygen levels, and pH regulation, allostasis requires an external stimulus to promote change. This process involves multiple systems including the hypothalamic-pituitary-adrenal axis (HPA), metabolic systems, autonomic nervous system, and immune system (Kinlein and Karatsoreos 2020). All these systems work in cooperation, influencing one another and ultimately creating a network that allows the organism to change, adapt and ultimately achieve stability (i.e. allostasis) (Sterling and Eyer, 1988, McEwan 2000). If such equilibrium is not reached, the risk of developing a physiological disorder increases.

1.4.1.2 Impact of chronic stress on health – the concept of resilience

Nowadays, stress exposure, and more specifically chronic stress, can significantly impact mood-related phenotypes and behavior. Chronic stress exposure has been linked with a wide variety of illnesses, including cardiovascular disease, asthma, and diabetes, as well as a variety of mood-related disorders such as anxiety, social dysfunction, and depression (McEwen and McEwen 2017). Interestingly, while some appear to be more susceptible, resulting in the development of the associated disorders, most individuals seem to overcome the stress thus remaining resilient. This remark has gained attention in recent years, shifting the focus of research from disease-oriented to a health-driven investigation. More specifically, the subject of stress-resilience has gained interest in recent years, aiming to understand the phenomenon by which an

individual or group of people maintain their mental health despite exposure to psychological or physical adversity (Kalisch et al. 2017).

1.4.1.3 Relationship between stress-resilience and epigenetics

Several studies have documented the relationship between epigenetic alterations and resilient behavior, uncovering the changes occurring in gene expression of the selected cellular population in distinct brain regions, which ultimately influence behavior (Cadet 2016, Zannas and west 2013). Moreover, the link between resilience and epigenetic mechanisms provides an attractive avenue to investigate the influence of external stimulation (e.g. stress) on internal molecular changes (e.g. gene expression), which contribute to the maintenance of health (e.g. resilience) or development of disease (e.g. susceptibility). Recent data support the idea that resilient phenotype is an active process by which different epigenetic programs act at specific brain regions, leading to alteration in gene expression and ultimately altering of the synaptic and neuronal circuit (Faye et al. 2018).

An example of such an active process is the induction of immediate early genes (IEGs) following stress stimulation. Early studies in the field used IEGs such as *Arc*, *c-Fos* or *Egr1* to monitor the active neuronal populations (Schreiber et al. 1991, Senba and Ueyama 1997). Upon stimulation, IEGs are the first set of genes to be active in the neurons inducing specific transcriptional and translational programs that ultimately promote neuronal plasticity (Gallo et al. 2018). Chronic stress has been associated with decreased activity of IEGs such Arc in the hippocampus and prefrontal cortex both in humans and animal models (Lee et al. 2012, Gallo et al. 2018). The activity of IEGs is associated with short and long-lasting chromatin accessibility changes, which influence further gene expression, therefore having a broader extent of regulation on the short and long time periods (Su et al. 2017).

1.4.1.4 Animal models and behavioral paradigms

Distinct animal models and behavioral paradigms have been developed to uncover both behavioral and molecular alterations occurring in an organism following stress exposure (Krishnan and Nestler 2008). Additionally, distinct behavioral paradigms have been established to test the stress effect separately in male and female animals mainly due to dissimilar induction and influence of the HPA system in both sexes, which leads to different behavioral outputs (Franklinm, Saab and Mansuy 2012). For instance, chronic social defeat (CSD) is a behavioral test where typically C57bl/6 male mice are defeated by a more aggressive strain (CD1) for an extensive period of at least seven days (Krishnan et al. 2007). The stressed mice are subjected to behavioral evaluation using social interaction (SI) test to measure the stress effect and behavioral phenotype. Such paradigm has been widely used to test the effect of long-lasting stress exposure and evaluate the

behavioral patterns, which can include depression-like behavior (susceptibility) or apparent regular behavior (resilience) (Krishnan et al. 2007). An example of the female behavioral paradigm used in this thesis includes chronic social stress (CSS), which was recently adapted to uncover the behavioral phenotypic changes following stress exposure in female mice. CSS consists of group housing of 4 female mice where the stressed group undergoes a seven week cage interchange (twice per week) while the control mice are kept in the initial composition of grouped mice. The lack of hierarchical establishment within the female groups was shown to inflict substantial stress-effect which can be measured using modified SI test as well as additional parameters (Enderes lab).

The topic of stress-resilience is addressed in case studies 2.2 and 2.3

1.4.2 Gut microbiota

1.4.2.1 Introduction to gut microbiota

The gut microbiota comprises all microbial communities inhabiting the gut, living in a dynamic symbiotic relationship within the host (Chang and Kao 2019). Such microbial communities produce and secrete a wide variety of metabolites, including small molecules and endogenous compounds that modulate gene expression and ultimately influence the host's cellular activity to adapt to external environmental changes (i.e. bacterial modulators) (Rooks and Garret 2016, Kim et al. 2017).

1.4.2.2 Relationship between gut microbiota and stress

Several studies have shown a strong connection between the composition of the gut microbiota and the appearance of various disorders such as neurological and mood-related disorders (Jiang et al. 2015, Dinan and Cryan 2017, Rogers et al. 2016, Misiak et al. 2020). The gut microbiome influences the regulation of key neurotransmitters such as serotonin (Yano et al. 2015, Kelly et al. 2015, Mittal et al. 2017), the inflammatory response system (Wong et al. 2016, Belkaid and Hand 2014, Lazar et al. 2018), and various behavioral changes in response to stress (De Palma et al. 2015, Zheng et al. 2016, Bridgewater et al. 2017). For instance, studies showed that the presence of specific probiotic strains of bacterial species such as *Bifidobacterium* or *Lactobacillus* is sufficient to confer resilience to chronic stress defeat (Yang et al. 2017; Bravo et al. 2011). This connection links the gut-brain axis to a much broader extent of neurological and behavioral regulation through the enteric nervous system and the neuroendocrine systems.

1.4.2.3 Epigenetics and gut microbiota

The gut microbial communities have a direct link with host gene regulation since many of the epigenetic marks such as acetylation and methylation rely on the processing of substrate metabolic compounds produced by both the host and the microbial cells (Miro-Blanch and Yanes 2019). The available "resources"

supplied by the host (e.g. nutrition) constantly influence such communities, allowing the survival of the microbial populations within the host. This connection is also known as the "microbiota- nutrient metabolism-epigenetic axis" (Miro-Blanch and Yanes 2019).

In recent years, the focus of study has shifted towards the interaction between these microbial communities, the host, and the various forms of communication between these two biological systems. Arguably, the external changes produced by the bacterial communities are in a continuous dynamic cross-talk with host cells and have an enormous potential for reciprocal regulation of cellular and gene expression activities (Rooks and Garrett 2016). An interesting rising hypothesis suggests that small RNAs (sRNAs), including micro RNAs (miRNAs) and other small non-coding RNAs (ncRNAs), could mediate the connection between the bacteria and host transcriptional regulation thereby, providing a potential communication network between the two systems (Liu et al. 2016, Zhou, Li and Wu 2018, Hewel et al. 2019). This observation of trans-kingdom miRNA exchange was reported between bacteria and plants (Weiberg et al. 2014, Hudzik et al. 2020) and recently in animals such as *C. elegans* (Kaletsky et al. 2020), suggesting a potential evolutionary conserved mechanism. An additional indication of such trans-kindom miRNA regulation is observed in mitochondrial (Purohit and Saini 2020, Fan et al. 2019, Jeong et al. 2017, Indrieri et al. 2019) chloroplast (Ruwe and Schmitz-Linnweber 2012, Fang et al. 2019) transcript regulation. Such observations suggest an evolutionary conserved role of miRNA regulation between the host and the ancestral bacterial species. *The topic miRNA-gut microbiota association is addressed in case study 2.2*

1.4.3 Genomic imprinting and neurodevelopmental disorders

1.4.3.1 The basics of genomic imprinting

The mechanisms of DNA methylation are involved in a wide variety of molecular and biological functions, from cellular differentiation and proliferation to development and disease (Li and Zhang 2014). One of the most prominent roles includes the process of genomic imprinting. This important mechanism, relates to the parental-specific monoallelic expression required during early development and normal functional cellular activity. (Fergurson–Smith et al. 1993, Stöger et al. 1993, Li, Beard and Jaenisch 1993, Monk et al. 2019). Genomic imprinting is a form of intergenerational epigenetic inheritance where the parent-of-origin-dependent methylation influences the expression of the imprinted gene (Monk et al. 2019). Aberrant alterations in the methylation or subsequent expression and function of these imprinted genes can lead to imprinting disorders (Eggermann et al. 2015).

An example of an imprinting disorder addressed in this thesis is the Birk-Barel intellectual disability (ID) syndrome (BBIDS or *KCNK9* imprinting syndrome; Case study 2.1). BBIDS is an autosomal dominant maternally-inherited disease that occurs as a result of a missense mutation in the maternal allele of the *KCNK9* gene (Barel et al. 2008). BBIDS is typically associated with congenital central hypotonia, developmental delay, intellectual disability, severe feeding problems, and hyperactivity (Barel et al. 2008). *KCNK9* encodes a potassium channel subunit TASK3, where the paternal copy of *KCNK9* is embryonically paternally silenced as part of an imprinted cluster, allowing brain-specific gene expression in both mice and humans (Ruf et al. 2007, Court et al. 2014).

1.4.3.2 Use of epigenetic drugs for treatment of neurological disorders

Epigenetic drugs (or modulators), are often synthetic or natural chemical compounds that alter the activity of specific epigenetic mechanism (Duncan and Campbell 2018). Such modulators include a repertoire of inhibitors of DNA and histone demethylases/methyltransferases as well as histone deacetylases/acetyltransferases (Heerboth et al. 2014, Toth 2020). The discovery and application of epigenetic drugs were first directed towards cancer treatment (Ganesan et al. 2019, Morel et al. 2020). However, nowadays, there is an increased interest in applying such drugs for the potential treatment of distinct cardiovascular, metabolic and neurological disorders (Heerboth et al. 2014, Toth 2020). In the latter case, epigenetic modulation is an attractive avenue for therapy neurological disorders since the cellular populations in the brain are known to respond to external stimuli, creating rapid effects in brain circuits and plasticity (Toth 2020).

1.4.3.3 mTOR signaling pathway

The mTOR signaling pathway plays significant role in cellular stability and homeostasis (Liu and Sabatini 2020). At its core stands the mechanistic target of rapamycin (mTOR), a serine/threonine protein kinase that orchestrates a wide array of cellular functions such as nutrient homeostasis, regulation of cell growth, metabolic regulation, and protein synthesis (Liu and Sabatini 2020). mTOR activity is regulated intracellularly by nutrients, energy level, and stress factors (e.g., hypoxia) and extracellularly by growth factors, hormones (e.g., insulin), neurotransmitters, and cytokines (Liu and Sabatini 2020). The regulation of mTOR activity and subsequent signaling pathways has been shown to adjust the cellular stress-response system, promoting cellular adaptability by regulating of distinct translational and transcriptional machinery (Arambru et al. 2014). In eukaryotes, mTOR constitutes the catalytic subunit of two distinct protein complexes known as mTORC1 and mTORC2. mTORC1 was shown to transcriptionally regulate genes involved in glycolysis, lipid and lysosome biogenesis, and mitochondrial metabolism (Düvel et al. 2010, Chapman et al. 2018). In the brain, the mTOR signaling pathway controls various cellular processes such as neuronal differentiation, neuronal

cell size determination, axon guidance, dendritogenesis, and synaptic plasticity (Garza-Lombó and Gonsebatt 2016). Dysregulation of the mTOR pathway has been associated with a variety of neurodevelopmental and neuropsychiatric disorders such as autism spectrum disorders (ASD), intellectual disability (ID), schizophrenia, and depression (Costa-Mattioli and Monteggia 2013).

As the term mTOR suggests, rapamycin was the first compound discovered to target the mTOR signalling pathway, mainly by inhibiting the kinase activity of mTORC1 (Heitman, Movva and Hall 1991, Kunz et al. 1993). Since the discovery of rapamycin, an increasing amount of studies are aspiring to identify and characterize additional mTOR inhibitors due to their potential therapeutic properties in a variety of diseases (Benjamin et al. 2011,Xu et al. 2020, Schreiber et al. 2019).

The topic genomic imprinting and epigenetic modulation is addressed in case study 2.1, and the mTOR signaling pathway is addressed in case study 2.4.

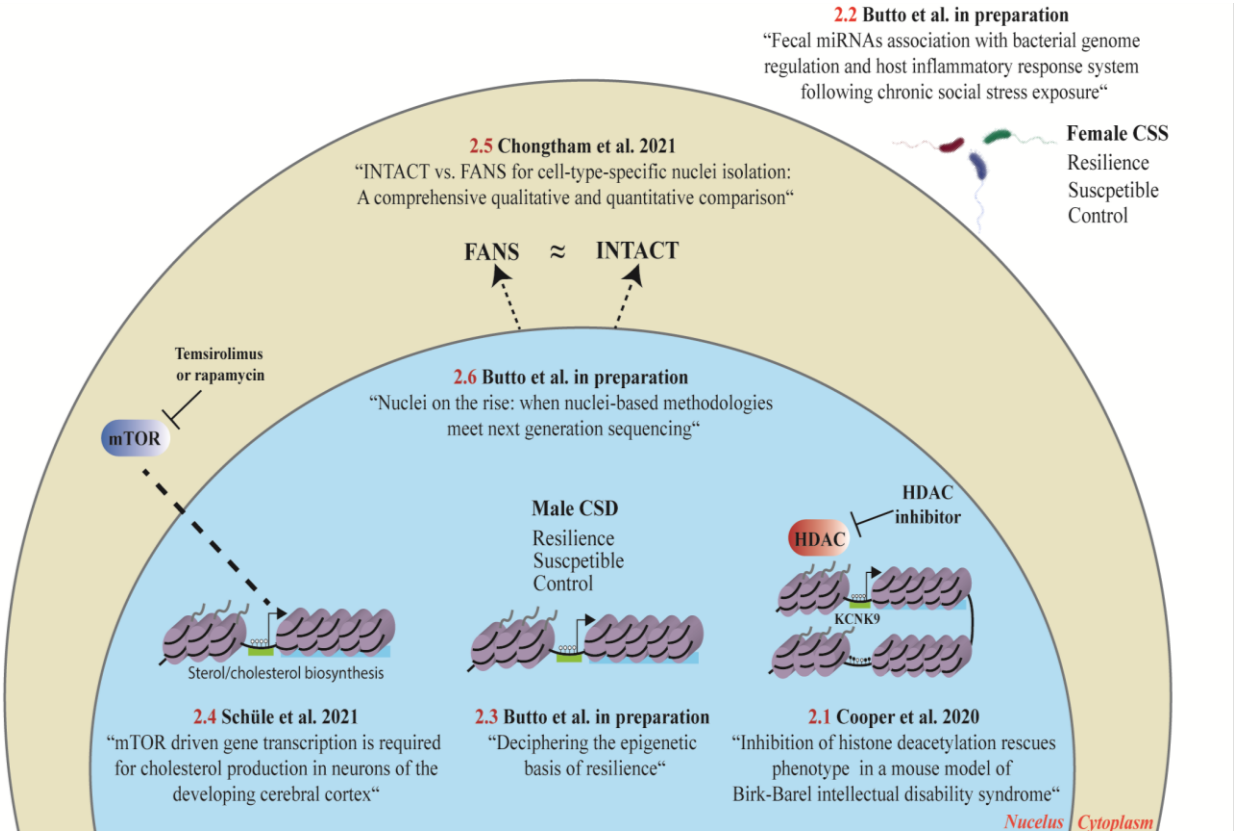

Figure 4: Overview of all the studies described in the thesis and the role of epigenetic mechanisms as systems of change and adaptability. *The numbers represent the order of the presented studies. (See section "1.6 Scope and outline of the thesis" for further information)*

1.5 Assays and methodologies for epigenetic studies

Since the discovery and establishment of the different branches of epigenetics, the research field has significantly increased, grasping the importance of its extensive forms of regulation on the cellular systems, from early stages of fertilization and development to later stages of unique-differentiated cell populations. Additionally, the aspiration to understand the distinctive cellular blueprints of unique populations has led scientists to develop innovative assays to measure and analyze the varied epigenetic mechanisms existing in eukaryotic cells. The following sections will describe the main methodologies applied throughout this thesis.

1.5.1 The use of nuclei for epigenetic research

In the last decade, there has been an upsurge in the application of nuclei-based studies, particularly in association with genome-wide (e.g. transcriptomic and epigenomic) next-generation sequencing approaches. Such studies use nuclei to identify novel nuclear properties or cell-type-specific traits in combination with supplementary molecular biology techniques. The eukaryotic nucleus contains the chromatin-histone protein complex, and therefore the mechanisms of DNA methylation and histone post-translational modifications are also present and regulated in the nucleus (Wang, Peterson and Loring 2014). With the increased interest in epigenetic regulation mechanisms, particularly combined with high-throughput sequencing, nuclei were found to be sufficient for such studies (Figure 5A). Nonetheless, transcriptomic analyses require a vigorous examination to prevent technical biases based on the RNA content, RNA quality, and library preparations strategies (Figure 5B).

Case study 2.6 provides a perspective of the possible reasons for the increased use of nuclei for scientific research and the advantages and disadvantages of such use. Finally, future considerations to use nuclear material are discussed. Additionally, nuclei isolation was used in studies 2.3 and 2.5 to identify the molecular differences between neuronal activated nuclei following chronic social defeat (CSD) stress exposure as well as to uncover the molecular differences between two rising techniques, “Fluorescence-assisted nuclei sorting” (FANS) and “Isolation of Nuclei Tagged in Specific Cell Types” (INTACT), respectively.

1.5.2 Nuclear RNA-seq

Nuclear RNA-seq (nucRNA-seq) comprises of high-throughput sequencing of RNA isolated solely from nuclei. With the increased use of nuclei as part of multi-omic studies, nucRNA-seq has been more frequently used in the last decade. Similar to regular RNA-seq, RNA is isolated from nuclei and converted to cDNA libraries. The library is often processed using a Poly(A) or ribo-depletion approaches, in order to enrich desired RNA population for sequencing (Stark, Grzelak and Hadfield 2019) (Figure 6A). However, since

nuclear RNA consists of a portion of the entire cellular RNA population, the study of nucRNA-seq data requires critical analyses, as pointed out in case study 2.2. Using nucRNA-seq, it is possible to compare the transcriptional states and thus to identify the differentially expressed genes (DEGs) between different experimental conditions. Further downstream analyses aim to identify shared mechanisms using for instance, gene ontology enrichment analysis (GO terms) and ultimately reveal significant changes that are altered between the different conditions (Figure 6A).

Nuclear RNA-seq is used in case studies 2.2 and 2.4 to identify the transcriptional alterations between two rising techniques (FANS and INTACT) and identify transcriptional differences between neuronal activated nuclei following chronic social defeat stress, respectively.

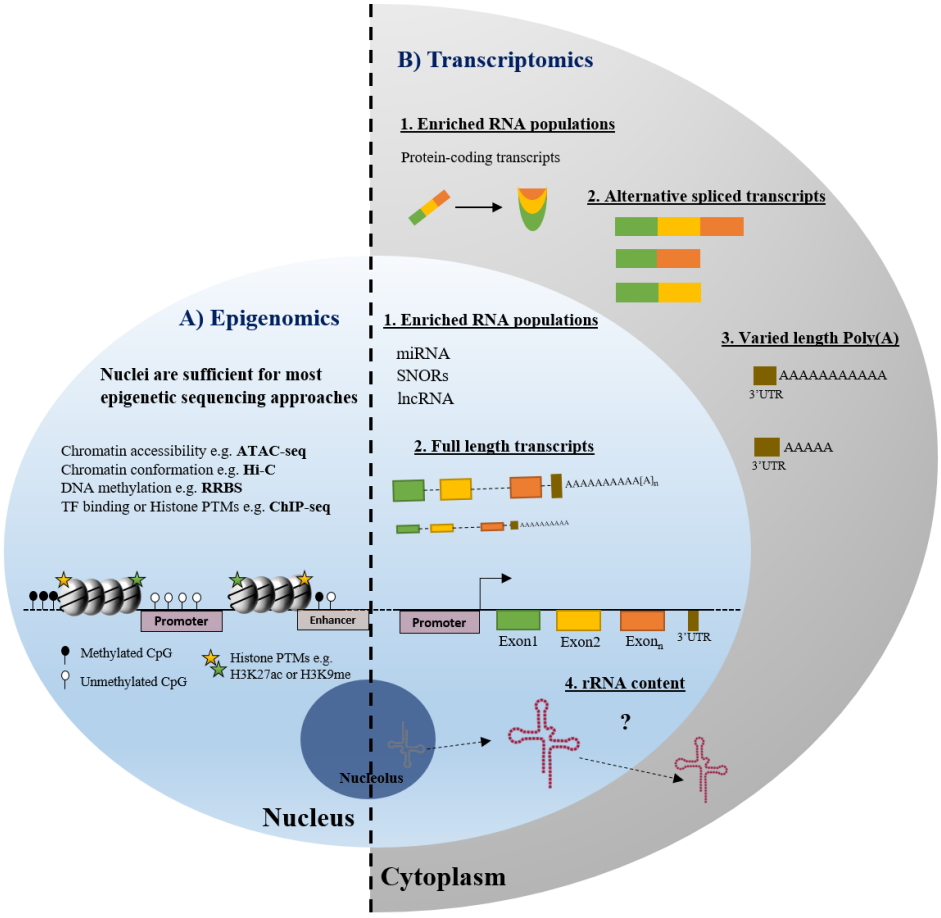

Figure 5. Overview of the application of nuclei-based studies with next-generation sequencing approaches. *A. Epigenomic - The use of nuclei is sufficient for most epigenetic sequencing approaches as the content of interest (e.g. Histones and chromatin-associated modifications) is located within the nucleus. B. Transcriptomics- Differences between nuclear and cytoplasmic transcripts in terms of 1. Distinct enriched RNA populations, 2. Distinct intronic and exonic transcript ratio, 3. Distinct length of poly-adenylated transcripts, 4. Distinct rRNA content. Figure taken from case study 2.6*

1.5.3 Small RNA-seq

Small RNA-seq involves sequencing of small RNA populations, including microRNAs (depending on the application). The selection of the RNA fragment size can be determined by the library predation strategy. Similar to common RNA-seq library, small RNA populations are converted into cDNA and barcodes are attached to 5'and 3' of amplified fragments (Figure 6B). Following amplification of selected barcoded fragments, the desired small RNA population is selected based on their size using a gel-excision size selection step. Finally, the selected library is sequenced, and data is analyzed using the same principles as in regular RNA sequencing. However, in the case of miRNA enrichment, differentially expressed miRNAs (DEMs) are identified, and their relevant shared mechanism between different experimental conditions are uncovered (Figure 6B).

Small RNA-seq was used in case study 2.1 to identify differentially expressed fecal miRNA following exposure to chronic social stress, the association of such miRNA with bacterial gene regulation.

1.5.4 Assay for transposase-accessible chromatin (ATAC-seq)

The technique assay for transposase-accessible chromatin, also known as ATAC-seq, is an assay to monitor chromatin accessibility states within a given cellular population. The method relies on a hypersensitive Tn5 transposase activity that incorporates selected barcodes at chromatin accessible regions thereby, allowing the detection of genome-wide chromatin accessibility states (Buenrostro 2013, Buerostro et al. 2015). Its relatively short and straightforward protocol made ATAC-seq a rapidly growing technique for identifying chromatin accessibility states, which often indicate active transcriptional loci (Li et al. 2019) (Figure 6C). Using ATAC-seq, the differentially accessible regions (DARs) are identified between different experimental conditions. Analyses of DARs at promoter and enhancer regions could indicate transcriptional active states in a genome-wide context, providing a broader view of the genomic activity (Figure 6C).

ATAC-seq was used in case studies 2.3, 2.4, and 2.5 for identification of chromatin accessibility states in active neuronal population of chronically defeated mice (Study 2.3), Temsirolimus (mTOR inhibitor) treated neurons (Study 2.4) and comparison between two rising techniques (INTACT and FANS) (Study 2.5).

1.5.5 Chromatin immunoprecipitation (ChIP)

Chromatin Immunoprecipitation is a method used to identify histone modification or chromatin-bound proteins that can be combined with high throughput sequencing (ChIP-seq) or quantitative PCR (ChIP-qPCR) (Barski et al. 2007, Mikkelsen et al. 2007, Johnson et al. 2007). Initially, samples containing the cell-type of interest are cross-linked to capture the DNA-bound proteins/histone modifications. Next, the chromatin is fragmented following antibody immunoprecipitation step to enrich for specific histone/protein bound to the chromatin. Finally, samples are purified, obtaining the DNA fragments which were previously bound to the protein of interest and quantified to detect changes in different experimental conditions (Figure 6D).

ChIP-qPCR was used in Case study 2.1 and 2.4 for identification the effects of HDAC inhibition on selected histone marks in BBIDS mouse model (Study 2.1) and NFY-A binding occupancy at selected promoter region following temsirolimus treatment (Study 2.4).

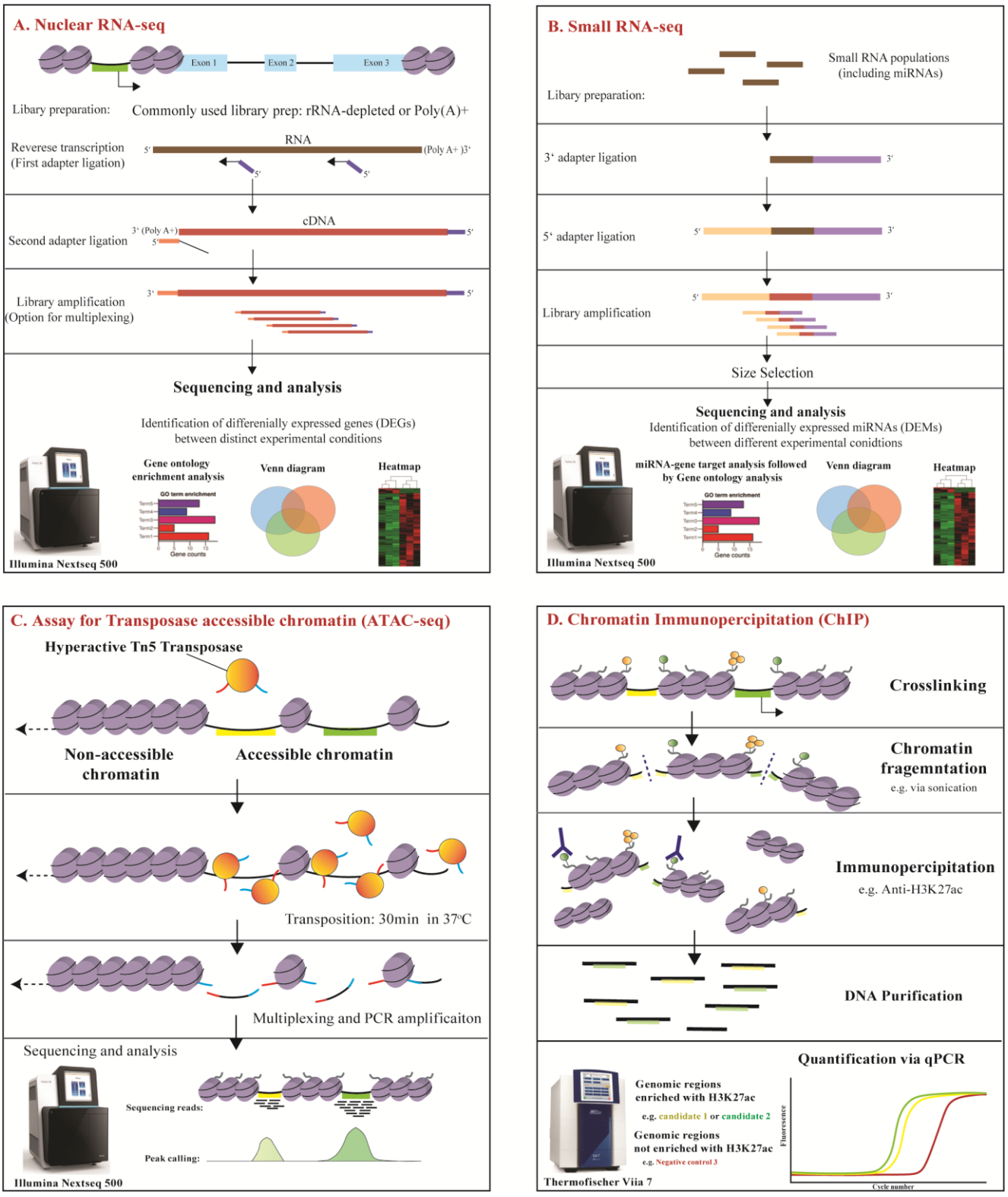

Figure 6. Main transcriptomic and epigenetic assays used in the thesis. *A. Outline of nuclear RNA-seq library preparation and analyses. B. Outline of small RNA-seq library preparation and analyses. C. Outline of ATAC-seq processing steps and analyses D. Outline of ChIP-qPCR processing and target sequences quantification using qPCR.*

1.6 Scope and outline of the thesis

The following thesis describes a multi-disciplinary compilation of studies aimed to address the distinct roles of epigenetic mechanisms as a system of change and adaptability in health and disease. For structural purposes, the studies under consideration will be divided into two sections:

Section 1: Case studies reviewing the relationship between external stimuli and distinct epigenetic alterations.

- **Case study 1- Epigenetic drug treatment of BBIDS in a mouse model.** This study focuses on the maternally inherited disorder Birk-Barel intellectual disability syndrome studies on the mouse model *Kcnk9*KO^{mat} and the potential therapeutic applications using an HDAC inhibitor (CI-994) to partially rescue a genomic imprinting disease.
- **Case study 2 – Fecal miRNA-gut microbiota communication following stress exposure.** This study explores the relationship between specific miRNAs and gut-microbial population using a novel alignment strategy (Hewel et al. 2019). Chronic social stress (CSS) was used to inflict behavioral stress and, using small RNA-seq, differentially expressed miRNA (DEMs) between the classified resilient, susceptible and control mice. The study provides evidence of how stress exposure influences the presence of fecal miRNA and how these could associate with microbial populations.
- **Case study 3 – Transcriptional and epigenetic alterations in active neuronal population following the chronic social defeat.** This study investigates the transcriptional and chromatin accessibility changes occurring in active neuronal populations isolated from chronic social defeated mice. The focus of this study was to identify molecular properties associated with resilience behavior, focusing on the neuronal population that was active during the social defeat.
- **Case study 4 – mTOR driven transcription of cholesterol genes in developing cerebral cortex neurons.** This study examines the transcriptional alterations occurring in developing and adult neurons following treatment with mTOR inhibitor compounds. Such study aims to identify gene targets located downstream of the mTOR signaling pathway, influenced by mTOR inhibition, and characterize their role in differentially developed neurons.

This section aims to present the general concept of stimuli-change-adaptation, which will be discussed in *Chapter 3 – Overall discussion and outlook* and the role epigenetic mechanisms as the core system to inflict cellular change.

Section 2 – Literature and methodological overview of frequently used techniques for epigenetic studies.

- **Case study 5 – Qualitative and quantitative comparison of the nuclei isolation techniques: INTACT and FANS.** This study compares two frequently used techniques INTACT and FANS, both their influence in the nuclear membrane as well as the transcriptional (nucRNA-seq) and chromatin accessibility (ATAC-seq) following nuclei sorting.
- **Case Study 6 – Overview of nuclei-based studies with next-generation sequencing methodologies.** The presented study examines the reasons for the increase of nuclei-based studies, providing a broad and trending overview of selected next-generation sequencing coupled with nuclei isolation techniques. The study highlights the benefits and challenges of nuclei-based studies, emphasizing their coupling with selected transcriptomic and epigenetic sequencing approaches.

This section aims to provide a literature overview of the biological tools and distinct assays frequently applied for transcriptional and epigenetic analyses and used in this thesis.

Table 1 - Overview of case studies presented in this thesis

Section 1 - Case-studies reviewing the relationship between the role of distinct epigenetic mechanisms and their influence in health/diseased phenotypes		
Case studies in consideration	**Molecular mechanism and assay used in the investigation**	**Health/diseased phenotype investigated**
Case study 1	➢ Histone marks quantification (ChIP-qPCR -H3K27ac and H3K4me1)	➢ Birk-Barel intellectual disability syndrome (BBIDS) Mouse model - *Kcnk9*KO^{mat}
Case study 2	➢ Fecal miRNA (small RNA-seq and miRNA-qPCR)	➢ Chronic social stress (CSS) ➢ Mouse model – Arc-sun1GFP
Case study 3	➢ Transcriptional analysis (nucRNA-seq) and chromatin accessibility (ATAC-seq)	➢ Chronic social defeat (CSD) Mouse model – Arc-sun1GFP
Case study 4	➢ Chromatin accessibility (ATAC-seq) and Chromatin-transcription factor binding (ChIP-qPCR - NFYA)	➢ Pre- and postnatal effect of mTOR inhibition in neurons (association with neurodevelopmental disorders)
Section 2 - Literature overview and methodological comparison of frequently used techniques for epigenetic studies		
Case studies in consideration	**Molecular mechanisms and assay used in the investigation**	**Comparative literature overview**
Case study 5	• Transcriptional analysis (nucRNA-seq) and chromatin accessibility (ATAC-seq)	• FANS and INTACT
Case study 6	-	• General literature overview of frequently used transcriptional and epigenetic analyses

Chapter 2 – Case studies

2.1 Inhibition of histone deacetylation rescues phenotype in a mouse model of Birk-Barel intellectual disability syndrome

Authors: Alexis Cooper, **Tamer Butto**, Niklas Hammer, Somanath Jagannath, Desiree Lucia Fend-Guella, Junaid Akhtar, Konstantin Radyushkin, Florian Lesage, Jennifer Winter, Susanne Strand, Jochen Roeper, Ulrich Zechner & Susann Schweiger

This article is published in *Nature communication*, **11,** 480 (2020). https://doi.org/10.1038/s41467-019-13918-4

My contributions to this article are listed in section 4.2 Contributions to individual publications.

nature COMMUNICATIONS

ARTICLE

https://doi.org/10.1038/s41467-019-13918-4 OPEN

Inhibition of histone deacetylation rescues phenotype in a mouse model of Birk-Barel intellectual disability syndrome

Alexis Cooper[1], Tamer Butto[2,10], Niklas Hammer[3,10], Somanath Jagannath[3], Desiree Lucia Fend-Guella[1], Junaid Akhtar[2], Konstantin Radyushkin[4], Florian Lesage[5], Jennifer Winter[1,4], Susanne Strand[6], Jochen Roeper[3,11], Ulrich Zechner[1,7,11]* & Susann Schweiger[1,4,8,9,11]*

Mutations in the actively expressed, maternal allele of the imprinted *KCNK9* gene cause Birk-Barel intellectual disability syndrome (BBIDS). Using a BBIDS mouse model, we identify here a partial rescue of the BBIDS-like behavioral and neuronal phenotypes mediated via residual expression from the paternal *Kcnk9* (*Kcnk9*^{pat}) allele. We further demonstrate that the second-generation HDAC inhibitor CI-994 induces enhanced expression from the paternally silenced *Kcnk9* allele and leads to a full rescue of the behavioral phenotype suggesting CI-994 as a promising molecule for BBIDS therapy. Thus, these findings suggest a potential approach to improve cognitive dysfunction in a mouse model of an imprinting disorder.

[1] Institute of Human Genetics, University Medical Center of the Johannes Gutenberg University Mainz, Langenbeckstr. 1, 55131 Mainz, Germany. [2] Institute for Developmental Biology and Neurobiology, Johannes Gutenberg University Mainz, Staudingerweg 9, 55128 Mainz, Germany. [3] Institute of Neurophysiology, Goethe University Frankfurt, Theodor-Stern-Kai 7, 60590 Frankfurt, Germany. [4] Focus Program Translational Neuroscience, Center for Rare Diseases, University Medical Center of the Johannes Gutenberg University Mainz, Langenbeckstr. 1, 55131 Mainz, Germany. [5] Université Côte d'Azur, INSERM, Centre National de la Recherche Scientifique, Institut de Pharmacologie Moléculaire et Cellulaire, Labex ICST, 660, route des Lucioles Sophia Antipolis, 06560 Valbonne, France. [6] Department of Internal Medicine I, University Medical Center of the Johannes Gutenberg University Mainz, Obere Zahlbacher Straße 63, 55131 Mainz, Germany. [7] Senckenberg Center of Human Genetics, Weismüllerstraße 50, 60314 Frankfurt, Germany. [8] Center for Orphan Diseases of the Central Nervous System, University Medical Center of the Johannes Gutenberg University Mainz, Langenbeckstr. 1, 55131 Mainz, Germany. [9] German Resilience Centre, University Medical Center of the Johannes Gutenberg University Mainz, Langenbeckstr. 1, 55131 Mainz, Germany. [10] These authors contributed equally: Tamer Butto, Niklas Hammer [11] These authors jointly supervised this work: Jochen Roeper, Ulrich Zechner, Susann Schweiger *email: u.zechner@senckenberg-humangenetik.de; susann.schweiger@unimedizin-mainz.de

Birk-Barel intellectual disability (ID) dysmorphism syndrome (BBIDS or *KCNK9* imprinting syndrome, OMIM 612292) is typically associated with congenital central hypotonia, developmental delay, intellectual disability, severe feeding problems, and hyperactivity[1,2]. The disease is inherited autosomal dominantly with maternal-only transmission[1], as the *KCNK9* gene is embryonically paternally silenced (imprinted) in man and mouse. It encodes the potassium channel subunit TASK3, which dimerizes to form two-pore domain potassium (K2P) leak channels[3]. The mouse *Kcnk9* gene maps to an imprinted cluster on mouse chromosome 15 together with further imprinted genes, i.e., the brain-specific maternally expressed genes *Ago2*, *Chrac1*, and *Trappc9* and the paternally expressed *Peg13* gene[4].

Kcnk9 mRNA expression is widespread in the central nervous system[5,6]; in rodents with notably high levels in cerebellar granule neurons, the locus coeruleus (LC), the dorsal raphe nuclei, hippocampal CA1 and CA3 pyramidal neurons, and several hypothalamic nuclei[7,8]. Homozygous deletion of *Kcnk9* in the mouse (*Kcnk9*KO^{hom}) reduces the resting potassium conductance and enhances spike firing accommodation in adult cerebellar granule neurons[9]. *Kcnk9*KO^{hom} mice further display increased nocturnal motor activity, cognitive deficits, as well as a reduced sensitivity to inhalation anesthetics and the cannabinoid receptor agonist WIN55212-2 mesylate [10-12]. More recently, RNAi-based knockdown of *Kcnk9* and expression of a dominant-negative mutant KCNK9, which had been associated with the human disease phenotype were shown to impair neuronal migration during mouse cortical development[13]. However, the phenotype of mice with heterozygous deletion of the active maternal *Kcnk9* allele (*Kcnk9*KO^{mat}) thus mimicking BBIDS has not yet been characterized.

DNA methylation is well established as a key player in imprinting regulation by multiple studies, which characterized the kinetics and mechanisms of methylation reprogramming at imprinting control regions (ICRs). The critical involvement of post-translational histone modifications in transcriptional regulation, in general, is also well accepted, but much less explored for ICRs[14]. It is assumed that an interplay between DNA methylation and histone acetylation is essential for proper erasure and resetting of imprints in the germline as well as selective imprint maintenance during postzygotic reprogramming[15]. A differentially methylated region (DMR) which is methylated on the maternal allele and assumed to be involved in *Kcnk9* gene regulation has been only identified in the promoter region of *Peg13*[16,17]. Promoter CpG islands of *Kcnk9* are unmethylated, but display high levels of active histone H3 lysine 4 monomethylation (H3K4me1) and histone H3 lysine 27 acetylation (H3K27ac) chromatin marks in brain tissues[4].

Here, we characterize the behavioral and neuronal phenotype of mice with heterozygous deletion of the active maternal *Kcnk9* allele (*Kcnk9*KO^{mat}). We demonstrate partial behavioral rescue in these animals compared with full knockout animals and show that epigenetic manipulation stimulates *Kcnk9*^{pat} expression sufficiently, to rescue the behavioral phenotypes, thereby opening new avenues for treatment of cognitive dysfunctions in BBIDS.

Results

Deletion of Kcnk9 leads to impaired behavior. To assess behavioral deficits along the BBIDS phenotype in *Kcnk9*KO mice, we performed in vivo experiments in adult wild type (WT) as well as *Kcnk9*KO^{mat} and *Kcnk9*KO^{hom} mice with a deletion of *Kcnk9* exon 2 as previously described[18] (Fig. 1a). Following the strictly monoallelic expression pattern of *Kcnk9* in mouse brain (<1% paternal expression)[3], we expected largely concordant phenotypes in mice carrying a deletion of both *Kcnk9* alleles (*Kcnk9*KO^{hom}) or only the maternal *Kcnk9* allele (*Kcnk9*KO^{mat}), respectively. No differences in behavior between *Kcnk9*KO^{hom}, *Kcnk9*KO^{mat}, and WT littermates were seen in elevated plus maze and open field testing for anxiety (Supplementary Fig. 1a, b) and in the rotarod-test for motor coordination (Supplementary Fig. 1c). Given the described intellectual disability in BBIDS patients, we then examined whether working memory was affected in *Kcnk9*KO mice. Spontaneous alternation relies on the natural tendency of rodents to explore a novel environment and can be quantified using a Y-maze task. The ability to remember the immediately preceding choice is considered an indicator for active working memory. In the Y-maze, spontaneous alternation was defined as consecutive entries into all three arms without revisiting an arm. The average percentage of spontaneous alternation made by *Kcnk9*KO^{hom}, *Kcnk9*KO^{mat}, and WT mice across a 10-min trial was analyzed and revealed a significant reduction of spontaneous alternation by about 10% in both *Kcnk9*KO^{hom} and *Kcnk9*KO^{mat} mice compared with WT littermates (Fig. 1b). There was no significant difference in the extent of the working memory impairment between *Kcnk9*KO^{hom} and *Kcnk9*KO^{mat} mice (Fig. 1b). Our findings indicate an impaired working memory in *Kcnk9*KO^{hom} and *Kcnk9*KO^{mat} mice, which is consistent with previously reported observations in *Kcnk9*KO^{hom} mice[10].

Circadian rhythms in mammals are endogenously coordinated oscillations of biological parameters such as the sleep/wake cycles with an overall period length of about 24 h[19]. KCNK9 channels are expected to contribute to the in vivo electrical activity of neurons in those brain regions associated with the regulation of circadian rhythms and arousal[10-12,20]. Spontaneous motor activity analysis during light (resting) and dark (active) phase was performed, resembling day and night in diurnal humans, respectively. A significantly increased overall locomotor activity during the dark phase was found in *Kcnk9*KO^{hom} and *Kcnk9*KO^{mat} mice compared with WT controls, describing an exaggerated nocturnal activity in *Kcnk9*KO animals (Fig. 1c), which is in consensus with previous observations[10]. Surprisingly, an intermediate phenotype for dark phase activity was observed in the *Kcnk9*KO^{mat} animals with statistically significant differences to both WT and *Kcnk9*KO^{hom} animals. No significant differences between genotypes were observed in the overall locomotor activity during the light phase (Fig. 1c, Supplementary Table 1).

Together, these data demonstrate that the loss of *Kcnk9* in mice results in the impairment of behavioral parameters resembling components of the BBIDS phenotype. Interestingly, we found an intermediate phenotype for nocturnal locomotor activity in animals with a loss of only the actively expressed maternal allele (*Kcnk9*KO^{mat}) suggesting the involvement of the silenced paternal allele.

Non-canonical imprinting of Kcnk9 in the mouse brain. In human and mouse brain *KCNK9* was reported to be mono- allelically expressed from the maternal allele[3,4] while the paternal allele is silenced. To elucidate if the intermediate phenotype of *Kcnk9*KO^{mat} animals was due to residual expression from the paternal allele, we analyzed the parent-of-origin allele-specific expression pattern of *Kcnk9* in different brain regions of F1 hybrid animals from crosses between C57BL/6 (B6) and Mus musculus castaneus (Cast/Ei) mouse strains [(C57BL/6xCast/Ei) F1][3]. As expected, we observed a predominant expression of the maternal *Kcnk9* allele in all analyzed brain regions (Fig. 1d). However, we also detected significant expression from the repressed paternal allele, which represented 1-14% of all

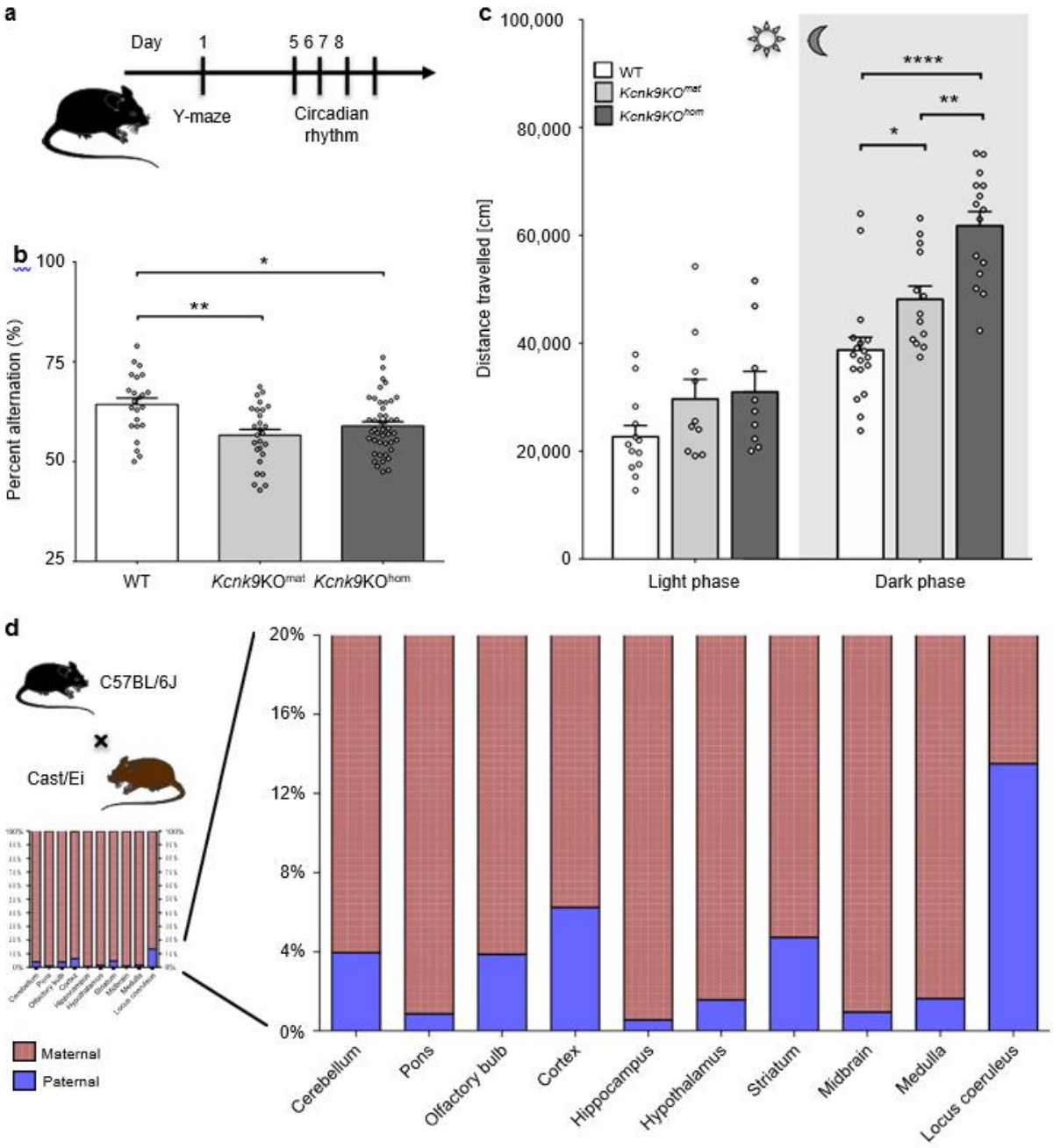

Fig. 1 Deletion of non-canonical imprinted *Kcnk9* gene leads to impaired behavior of *Kcnk9*KO mice. a Schematic representation of the sequence of mouse behavioral experiments. b Y-maze percentage alternation analysis of WT ($n = 23$), *Kcnk9*KO^{mat} ($n = 27$), and *Kcnk9*KO^{hom} ($n = 44$) mice. A spontaneous alternation was defined as consecutive entries into all three arms without revisiting an arm. *Kcnk9*KO mice display a significant decrease in percentage alteration compared with WT mice. One-way ANOVA: $F(2, 91) = 7.261$, $P = 0.0012$; followed by Bonferroni's multiple comparison post hoc test, $^*P < 0.05$, $^{**}P < 0.01$. c Total locomotor activity (distance traveled in the home cage) in light (12 h, sun symbol)/dark (12 h, moon symbol) phase. The left section shows no difference in distance traveled in the light phase of WT ($n = 13$), *Kcnk9*KO^{mat} ($n = 10$) and *Kcnk9*KO^{hom} ($n = 9$) mice. One-way ANOVA: $F(2, 29) = 2.281$, $P = 0.1203$. The right section depicts the nocturnal activity of WT ($n = 18$), *Kcnk9*KO^{mat} ($n = 13$) and *Kcnk9*KO^{hom} ($n = 15$) mice. *Kcnk9*KO^{mat} and *Kcnk9*KO^{hom} mice display significantly increased nocturnal hyperactivity compared with WT littermates with activity scores of *Kcnk9*KO^{mat} mice intermediate between *Kcnk9*KO^{hom} and WT mice. One-way ANOVA: $F(2, 43) = 22.70$, $P < 0.0001$; followed by Bonferroni's multiple comparison post hoc test, $^*P < 0.05$, $^{**}P < 0.01$, $^{****}P < 0.0001$. b, c Behavioral experiments were performed in seven independent sessions. d Non-canonical *Kcnk9* imprinting in (C57BL/6xCast/Ei)F1 hybrid mice. Quantification of Allele-Specific Expression by Pyrosequencing (QUASEP) of several brain regions from (C57BL/6xCast/Ei)F1 hybrid mice; maternal allele (red) and paternal allele (blue). Cerebellum $n = 14$, pons $n = 10$, olfactory bulb $n = 12$, cortex $n = 14$, hippocampus $n = 14$, hypothalamus $n = 9$, striatum $n = 5$, midbrain $n = 5$, medulla $n = 5$, and locus coeruleus $n = 4$; n = biologically independent samples. a–d Data are means ± 1 SEM (standard error of the mean). Statistical analyses and approaches are provided in Supplementary Table 1. Source data are provided as a Source Data file. The mouse images in this figure were created using Servier Medical Art templates, which are licensed under a Creative Commons Attribution 3.0 Unported License; https://smart.servier.com.

transcripts depending on the brain region analyzed (Fig. 1d, suppl. Fig. 2c). Highest paternal expression was observed in the LC (Fig. 1d). Accuracy of the LC tissue-punches was demon- strated through elevated gene expression levels of tyrosine hydrolase (TH) in LC samples (Supplementary Fig. 2a, b).

These data demonstrate a brain region-specific leakiness of the imprint on the *Kcnk9*^{pat} allele with a peak in the LC. This leakiness might be responsible for the observed intermediate phenotype in *Kcnk9*KO^{mat} animals and suggested a particular importance of LC *Kcnk9* expression for locomotor activity during the active (dark) phase.

Kcnk9 knockdown in the LC induces elevated nocturnal activity. To test the role of functional *Kcnk9* expression in LC neurons for the control of nocturnal activity, we bilaterally infused AAV vectors for expression of eGFP and shRNAmir sequences, either scrambled (pAAV-Syn-shRNAmir-scrambled- EF1a-eGFP) or specifically targeting *Kcnk9* mRNA (pAAV-Syn- shRNAmir-*Kcnk9*-EF1a-eGFP), into the LC of WT mice under stereotactic control (Fig. 2a). Efficiency of the used shRNA sequence was pre-tested in vitro (Fig. 2b) and validated by RT- qPCR from mouse brain tissue (Fig. 2c). Targeting efficiency and selectivity of stereotactically guided infusion was demonstrated by eGFP immunohistochemistry (Fig. 2a). Twenty-one days after injection, animals were tested for circadian activity and working memory. A significant and selective increase of nocturnal activity was detected in the shRNAmir-*Kcnk9* injected animals compared with age-matched control animals injected with the scrambled shRNAmir virus (Fig. 2d). These results demonstrated that altering local expression of *Kcnk9* in the LC was sufficient to selectively affect dark-phase activity in mice. Furthermore, it identified LC as an important neural hub for mediating the behavioral effects of altered *Kcnk9* expression, which warranted further mechanistic analysis of these neurons. Interestingly, a clear trend toward impaired working memory was also observed in shRNAmir-*Kcnk9* injected animals (Fig. 2e), suggesting that *Kcnk9* expression also controls working memory-related activity of LC neurons.

Increased dark-phase LC pacemaking activity in Kcnk9KO^{hom} but not Kcnk9KO^{mat} mice. Electrical activity of LC neurons drives periods of wakefulness and arousal[21-23]. Indeed, selective optogenetic activation of LC neurons revealed their causal role in sleep-to-wake transitions and locomotor arousal by demonstrat- ing that sustained 3-Hz LC neuronal stimulation enhanced spontaneous locomotion (total track length) by about 50%[24]. As we detected a similar increase of spontaneous locomotion during the active (dark) phase of *Kcnk9*KO^{hom} mice compared with WT controls, we reasoned that KCNK9-dependent differences in LC pacemaking activity might contribute to this phenotype.

By recording from synaptically isolated (including inhibition of somatodendritic alpha2-autoreceptors), spontaneously active LC neurons in brainstem slices from adult mice, we observed a dark phase-selective, about 70% increase of pacemaker frequency in LC neurons from *Kcnk9*KO^{hom} mice (Fig. 3a-d). In contrast, no significant dark-phase increase of LC pacemaker frequency was observed in WT animals (Fig. 3c, d). These results demonstrate that some degree of KCNK9 channel expression is necessary to selectively dampen enhanced pacemaker activity during the dark phase, which is present in *Kcnk9*KO^{hom} mice. Interestingly, LC neurons from *Kcnk9*KO^{mat} animals displayed no significant increase in pacemaker activity in the dark phase (Fig. 3c, d), but a significant difference in pacemaker activity in the dark was observed between *Kcnk9*KO^{hom} and *Kcnk9*KO^{mat} animals. This indicated that a certain level of functional expression of KCNK9 channels from the *Kcnk9*^{pat} allele in LC is present in *Kcnk9*KO^{mat} animals to prevent the full nocturnal in vitro pacemaker frequency increase. This level of *Kcnk9* expression might at the same time not be sufficient to dampen in vivo LC activity, which is also driven by synaptic inputs from neuronal networks, in line with the observed intermediate behavioral phenotype regarding dark-phase locomotion in *Kcnk9*KO^{mat} mice. In line with this argument, we show below that boosting further expression of KCNK9 channel subunits from paternal alleles indeed also restores the WT motor activity phenotype.

CI-994 activates the paternally repressed Kcnk9 allele. The paternally inherited *Kcnk9/KCNK9* gene is epigenetically silenced yet structurally unimpaired. Our behavioral and gene expression experiments suggest a contribution of paternally expressed *Kcnk9* to the intermediate phenotype of the *Kcnk9*KO^{mat} mice and the possibility of upregulation of the paternal allele in the case of loss of the maternal allele. We, therefore, speculated that exogenous application of epigenetic modulators might alter the structure at the *Kcnk9* promoter region and result in further derepression of the *Kcnk9*^{pat} allele. We hypothesized that this could fully com- pensate for the loss of the maternal allele and rescue the BBIDS- like phenotype of *Kcnk9*KO^{mat} mice.

To investigate the paternally derived *Kcnk9* transcript levels after epigenetic drug treatment, we isolated E14 mouse primary cortical neurons (mPCNs) from WT and *Kcnk9*KO^{mat} animals from crosses between WT males and *Kcnk9*KO^{hom} females (Fig. 4a). We then chose six different compounds representing different classes of epigenetic modulators for treatment (Fig. 4b). Murine PCNs were treated for 3 days with the epigenetic modulators and *Kcnk9* expression was analyzed by RT-qPCR. mPCNs treated with DZNep (20 µM), SAHA (30 µM), VPA (5 mM), and CI-994 (40 µM) exhibited a significantly increased *Kcnk9*^{pat} expression (RT-qPCR) compared with *Kcnk9*KO^{mat} mPCNs treated with dimethyl sulfoxide (DMSO) (control vehicle) (Fig. 4c). By contrast, treatment with the compounds Zebularine and C646 did not show any differential *Kcnk9* expression in *Kcnk9*KO^{mat} mPCNs compared with control conditions (Supplementary Fig. 3a).

For further investigations, we focused on the benzamide-based second-generation histone deacetylase inhibitor (HDACi) CI-994, a selective inhibitor of class I HDACs, which is a potent inhibitor of HDAC1 and 3 isoenzymes relative to HDAC6 and HDAC8[25]. CI-994 showed the most efficient upregulation of *Kcnk9*^{pat} expression in *Kcnk9*KO^{mat} mPCNs (Fig. 4c). Furthermore, a previous study reported that intraperitoneal administration of CI- 994 in WT mice resulted in long-lasting CI-994 levels in the brain without affecting the overall behavioral phenotype of mice[26].

The effect of CI-994 in *Kcnk9*KO^{mat} mPCNs was further tested in a dose-response experiment. *Kcnk9*KO^{mat} mPCNs were treated with increasing concentrations of CI-994 for 24 h, and *Kcnk9* expression was analyzed using RT-qPCR in comparison to DMSO-treated *Kcnk9*KO^{mat} and WT control cells (Fig. 4d). As expected, the *Kcnk9*^{pat} expression in DMSO-treated *Kcnk9*KO^{mat} mPCNs was significantly reduced compared with that of WT mPCNs. After CI-994 treatment of *Kcnk9*KO^{mat} mPCNs, we observed a strong linear correlation between the increase of *Kcnk9*^{pat} expression and CI-994 dosage suggesting a specific, dose-dependent effect of CI-994. Notably, *Kcnk9* expression in 80 µM CI-994-treated *Kcnk9*KO^{mat} mPCNs exceeded that of DMSO-treated WT mPCNs in vitro (Fig. 4d). Treatment of *Kcnk9*KO^{mat} mPCNs with 20 µM CI-994 showed a consistent increase of *Kcnk9*^{pat} expression even after 10 days suggesting a prolonged and stable in vivo effectiveness (Fig. 4e). Cell viability analysis after treatment of *Kcnk9*KO^{mat} mPCNs with

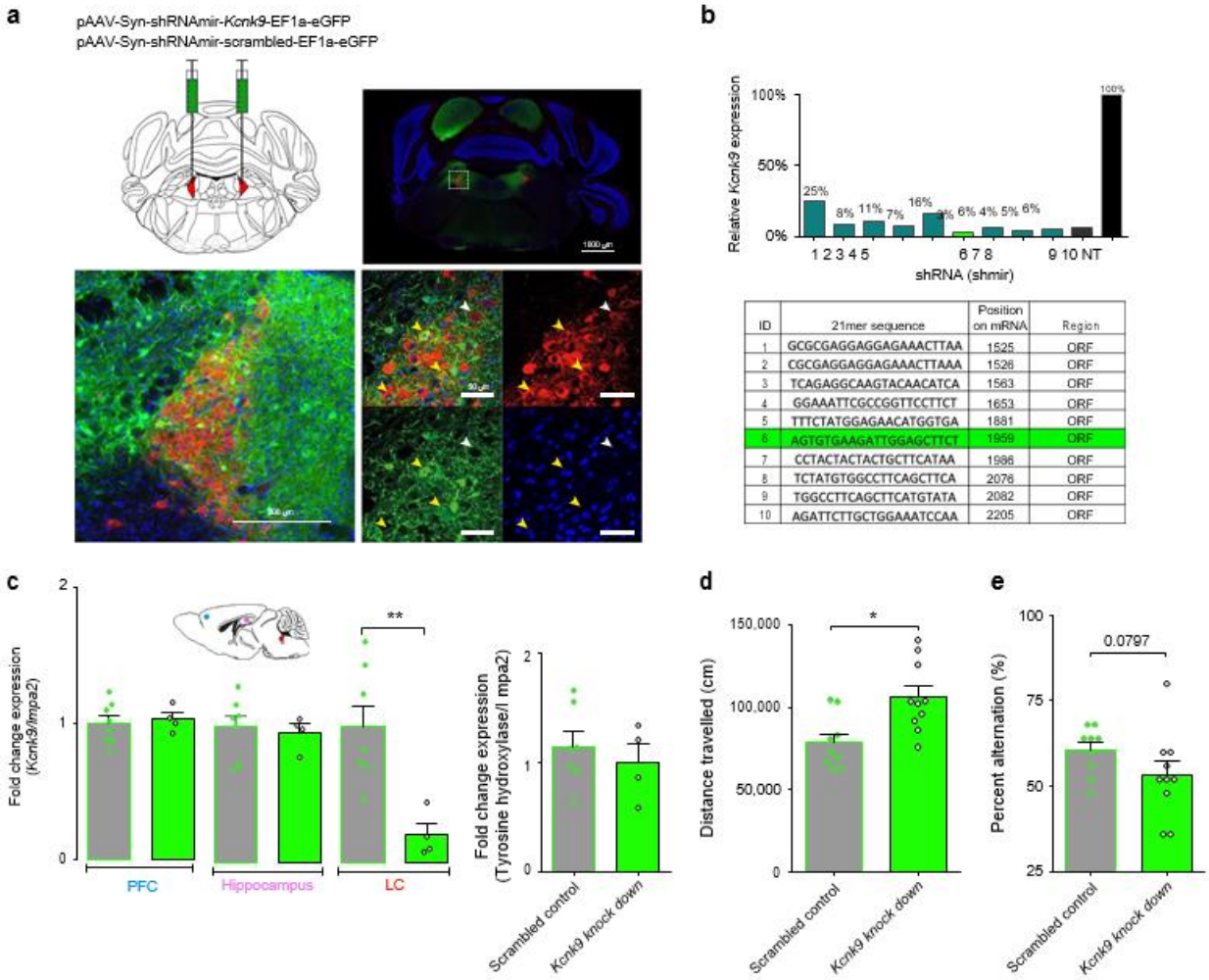

Fig. 2 *Kcnk9* knockdown in the locus coeruleus induces elevated nocturnal activity. a Bilateral virus injection with pAAV-Syn-shRNAmir-Kcnk9-EF1a-eGFP (KD) or Syn-shRNAmir-scrambled-EF1a-eGFP (SC) in the locus coeruleus (LC): Top left: schematic coronal section of the mouse brain at the position −5.4 relative to bregma[43]; red triangles represent the LC; top right: Immunofluorescence staining of a coronal section. Scale represents 1000 μm (4×). Bottom left: Images of the LC. Scale represents 200 μm (20×); bottom right: Magnification of LC cells. Scale represents 50 μm (60×), majority of tyrosine hydroxylase (TH; red) expressing cells co express GFP (green) (yellow arrows), while also GFP negative TH expressing cells could be observed (white arrow). Blue, DAPI; green, GFP; red, TH (TH serves as a norepinephrine marker). b Cell-based quantification of *Kcnk9* gene knockdown (*Kcnk9* KD) using *Kcnk9*-specific shRNAs by RT-qPCR compared with negative control (NT). Validated shRNAs with KD > 80%: 2, 3, 4, 5, 6, 7, 8, 9, and 10. ShRNA 6 was utilized for AAV generation in 293T cells. Arithmetic means of *Kcnk9* expression of presented IDs were provided by Sirion Biotech. c Left: *Kcnk9* knockdown efficiency validation in vivo. *Kcnk9* expression analysis in the prefrontal cortex (PFC, blue circle, SC $n = 8$, KD $n = 4$), hippocampus (pink circle, SC $n = 7$, KD $n = 4$) and LC (red circle, SC $n = 7$, KD $n = 4$) by RT-qPCR revealed a significant down-regulation of *Kcnk9* gene expression in the LC of *Kcnk9* KD mice compared with mice injected with scrambled controls. Mann–Whitney U: $P = 0.004$. Right: Tyrosine hydroxylase (TH) RT-qPCR expression analysis in the LC to validate accuracy of tissue collection. LC samples of *Kcnk9* KD ($n = 4$) and scrambled controls ($n = 7$) exhibit similar TH levels demonstrating sample collection accuracy. n = biologically independent mice. d Total locomotor activity in dark (12 h) phase, 21 days after AAV-injections. Mice injected with pAAV-Syn-shRNAmir-*Kcnk9*-EF1a-eGFP ($n = 10$) display increased nocturnal activity compared with pAAV-Syn-shRNAmir-scambled-EF1a-eGFP ($n = 9$) injected controls. Mann–Whitney U: $P = 0.0101$. e Y-maze percentage alternation analysis reveals tendency toward impaired working memory in *Kcnk9* KD mice ($n = 10$) compared with age-matched controls ($n = 10$); n = biologically independent mice. Mann–Whitney U: $P = 0.0797$. Values are means ± SEM. Statistical analyses and approaches are provided in Supplementary Table 1. Source data are provided as a Source Data file.

10 or 20 μM CI-994 did not reveal any toxic effect (Supplementary Fig. 4c). Intriguingly, CI-994 treatment did not affect the expression of other nearby imprinted genes within the imprinted cluster on mouse chromosome 15 in vitro (Supplementary Fig. 3b).

CI-994 rescues the behavioral phenotype of Kcnk9KO^{mat} animals. The detection of *Kcnk9*^{pat} allele expression in several brain regions, prominently among them the LC, as well as the observation of intermediate phenotypes in *Kcnk9*KO^{mat} animals led us to hypothesize that epigenetic manipulation could further stimulate paternal gene expression and thereby boost the phenotypical rescue.

For testing, either DMSO (100%) or CI-994 (30 mg/kg of body weight in 100% DMSO) were injected daily over 14 days in the peritoneum (Fig. 5a). After injections, *Kcnk9*^{pat} expression was induced up to ~3-fold compared with DMSO-treated controls in several brain regions including the cerebellum, hippocampus,

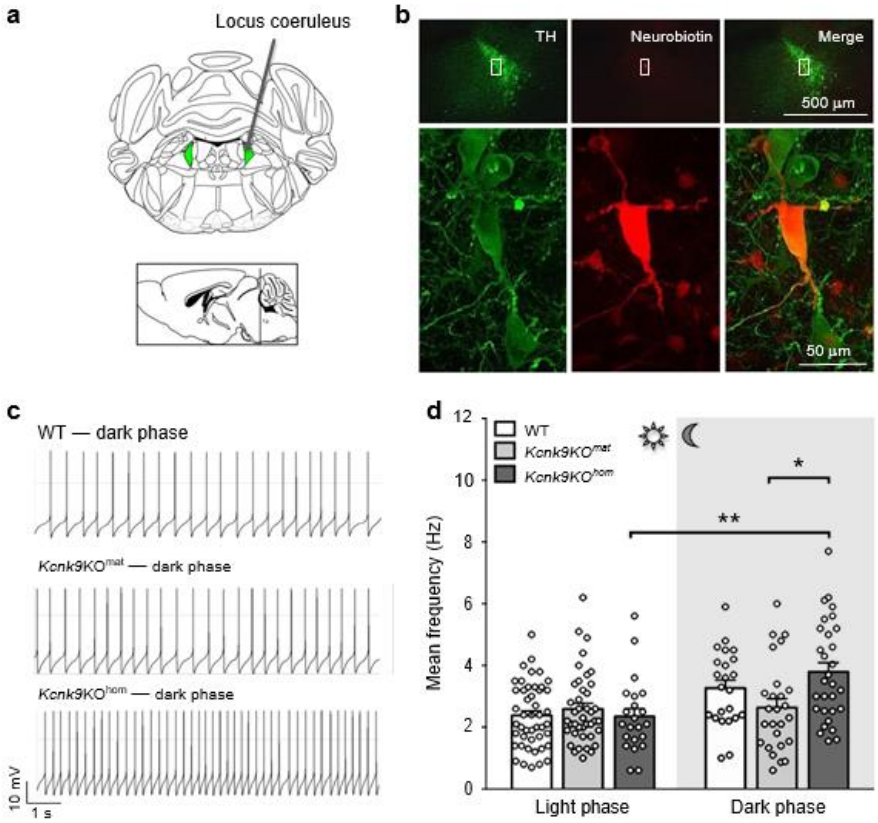

Fig. 3 Electrophysiological analysis of LC neurons. a Schematic overview of the locus coeruleus (LC) and its position in the adult mouse brain, bregma−5.40 and −5.52 (the coordinates were according to the mouse brain atlas[43]). Green triangles represent the LC. b Confocal images showing TH-positive signal (green), neurobiotin-positive signal (red) and a merge of both signals (yellow). Upper images show an overview of the LC at a low-magnification (×4) and lower images display signals of analyzed single-cell at high-magnification (×60 oil). c Electrophysiological traces of single cells in the night phase of WT, *Kcnk9*KO^{mat} and *Kcnk9*KO^{hom} animals. Recordings from synaptically isolated spontaneously active LC neurons reveal increased pacemaker frequency in LC neurons from *Kcnk9*KO^{hom} mice during dark phase. d Scatter dot-plot of mean frequencies including all analyzed cells in the day and night phase of WT (light $n = 46$, $N = 5$, dark $n = 23$, $N = 3$), *Kcnk9*KO^{mat} (light $n = 41$, $N = 5$, dark $n = 26$, $N = 4$) and *Kcnk9*KO^{hom} (light $n = 22$, $N = 3$, dark $n = 30$, $N = 5$) animals. Ordinary one-way ANOVA with Bonferroni's multiple comparison post hoc test, $^{*}P < 0.05$, $^{**}P < 0.01$. Values are means ± SEM. N = number of mice, n = total number of cells. Statistical analyses and approaches are provided in Supplementary Table 1. Source data are provided as a Source Data file.

pons, hypothalamus, olfactory bulb, and the LC (Fig. 5b). Importantly, this drug-induced rescue also included brain regions like the hippocampus, where only a small degree (<1%) of spontaneous expression from paternal alleles was observed in the *Kcnk9*KO^{mat} mice. In an allele-specific assay using WT (C57BL/ 6xCast/Ei)F1 hybrids, we found that CI-994 affects specifically expression of the *Kcnk9*^{pat} allele (Supplementary Fig. 4b). Only a very weak upregulation of global (maternal plus paternal) *Kcnk9* expression was seen in WT animals after CI-994 treatment (Fig. 5c, Supplementary Fig. 4c). Importantly, and in line with the in vitro observations, expression of only *Kcnk9* but no other of the genes located within the imprinting cluster on mouse chromosome 15 was found to be increased after CI-994 injection in vivo (Fig. 5d).

To assess whether CI-994-mediated enhancement of *Kcnk9* expression also promotes behavioral recovery, WT, *Kcnk9*KO^{mat}, and *Kcnk9*KO^{hom} mice were subjected to behavioral testing after treatment with either DMSO (100%) or CI-994 (30 mg/kg of body weight). In the Y-maze task, CI-994 treatment led to a significant increase of spontaneous alternation in the *Kcnk9*KO^{mat} mice compared with DMSO-treated *Kcnk9*KO^{mat} control mice (Fig. 5e). Post hoc testing for multiple comparisons showed no difference between CI-994-treated *Kcnk9*KO^{mat} animals and either DMSO- or CI-994-treated WT animals (Fig. 5e). WT mice treated with either DMSO or CI-994 did not exhibit deficits in working memory and significant differences in the Y-maze. By contrast, no increase of spontaneous alternation was seen in the CI-994 treated *Kcnk9*KO^{hom} animals suggesting that the paternal allele silenced in the *Kcnk9*KO^{mat} animals carries the effect of the treatment (Supplementary Fig. 5a).

We then asked whether CI-994 treatment also alters nocturnal activity in *Kcnk9*KO^{mat} or in *Kcnk9*KO^{hom} mice. Indeed, *Kcnk9*KO^{mat} mice showed a significant decrease in horizontal nocturnal activity during the 12-h dark phase after CI-994 treatment (Fig. 5f). Again, post hoc analysis of multiple comparisons showed no significant difference between CI-994 -treated *Kcnk9*KO^{mat} and DMSO- or CI-994-treated WT animals suggesting full rescue of the nocturnal hyperactivity phenotype in the *Kcnk9*KO^{mat} animals. No drug effect was observed in *Kcnk9*KO^{hom} animals and total locomotor activity in the light phase was not altered by CI-994 treatment irrespective of the genotype of the animals (Fig. 5f, Supplementary Fig. 5b).

CI-994 interferes with H3K27 acetylation at the Kcnk9 locus. Imprinting of the *Kcnk9/KCNK9* gene is thought to be regulated by a maternally methylated germline differentially methylated region (DMR) in the promoter of the *Peg13/PEG13* gene[3].

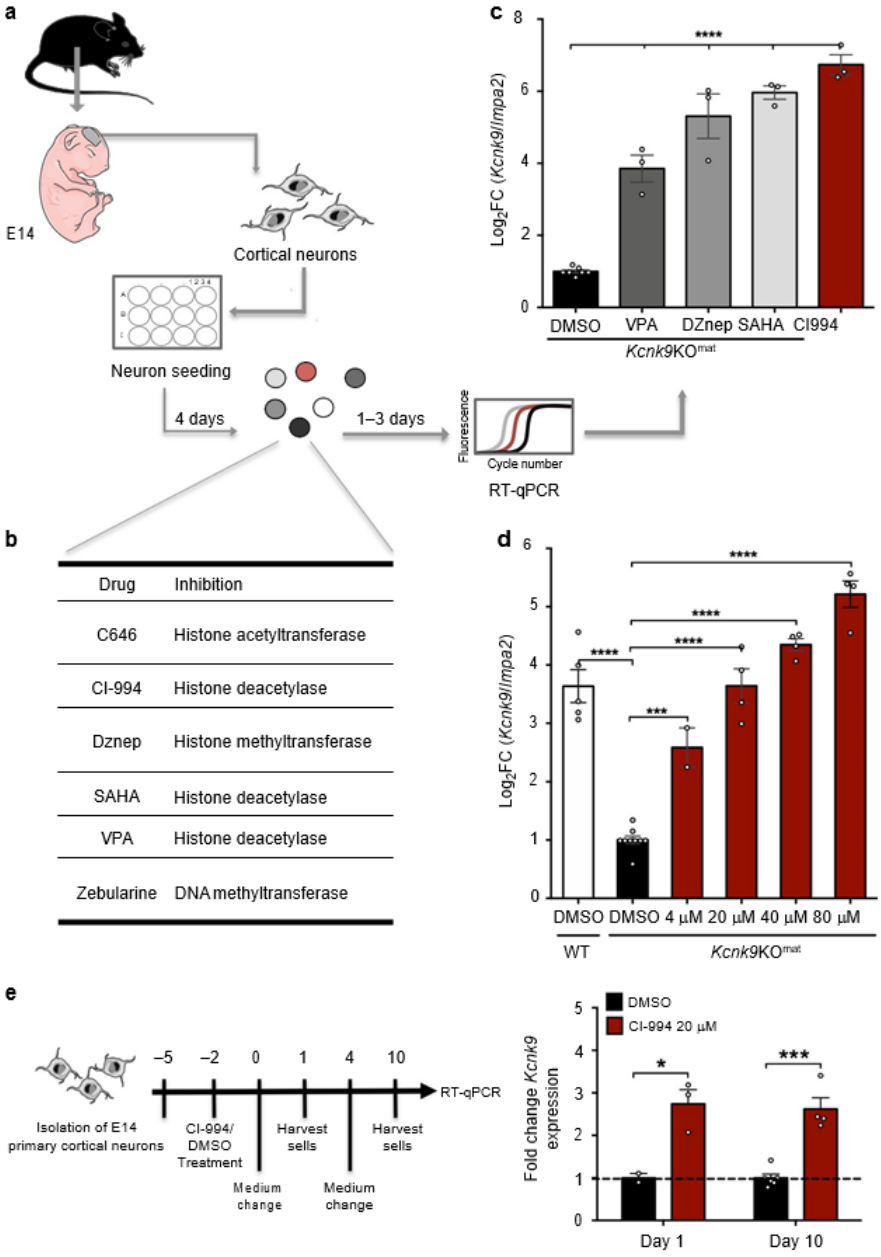

Acetylation of histone 3 lysine 27 (H3K27ac), monomethylation of histone 3 lysine 4 (H3K4me1) as well as DNA methylation at the maternally methylated DMR in the human *PEG13* promoter region have been suggested to control human *KCNK9* expression[4] (Fig. 6a, Supplementary Fig. 6a-d). CI-994 is a second-generation class I histone deacetylase inhibitor inhibiting HDACs1 and 3 with high specificity[25]. To clarify the epigenetic mechanism underlying the induction of the *Kcnk9*^{pat} allele through CI-994 we investigated the methylation status of two subregions of the *Peg13*-DMR (*Peg13* DMR1 and *Peg13* DMR2) in adult hippo- campus and LC of DMSO- and CI-994-treated *Kcnk9*KO^{mat} mice using bisulfite pyrosequencing. Methylation levels of about 40-50% typical for imprinted gene DMRs in somatic cells were determined for both DMRs in the two brain regions of *Kcnk9*KO^{mat} mice. These methylation levels were not significantly altered by CI-994 treatment of *Kcnk9*KO^{mat} mice (Supplementary Fig. 6c, d). Our results indicate that the upre- gulation of *Kcnk9* mRNA in various brain regions of *Kcnk9*KO^{mat} mice after CI-994 treatment was independent of the DNA methylation status at the *Peg13*-DMR.

The human *PEG13*-DMR has been further demonstrated to bind CTCF-cohesin which conveys chromatin looping between a brain-specific enhancer region, marked by H3K27ac and H3K4me1, and the *PEG13* and *KCNK9* promoters to supposedly control brain-specific *KCNK9* expression[4]. To determine the effect of CI-994 on the *Kcnk9* locus in the hippocampus and LC of *Kcnk9*KO^{mat} mice, we performed Chromatin immunoprecipi- tation (ChIP)-qPCR for H3K27ac and H3K4me1 marks following CI-994 or vehicle treatment. Using several public mouse brain ChIP-seq datasets, we did not find an orthologous region in the

Fig. 4 Identification of epigenetic modulators upregulating *Kcnk9*^{pat} expression in mPCNs. a Workflow of murine primary cortical neurons (mPCN) isolation, drug treatment, and RT-qPCR analysis. b Epigenetic modulators used for treatment of mPCNs (left column) with enzymatic activities inhibited by them (right column). c Significant upregulation of paternal allele-derived *Kcnk9* mRNA in DZnep-, SAHA-, VPA- and CI-994-treated E14 *Kcnk9*KO^{mat} mPCNs compared with DMSO-treated *Kcnk9*KO^{mat} mPCNs detected by RT-qPCR (3-day treatment, normalization to *Impa2*, DMSO $n = 7$ cultures/group, DZnep (20 μM) SAHA (30 μM), VPA (5 mM) and CI-994 (40 μM) $n = 3$ cultures/group). One-way ANOVA: $F(5, 22) = 75.51$, $P < 0.0001$; followed by Bonferroni's multiple comparison post hoc test to *Kcnk9*KO^{mat} DMSO control, ****$P < 0.0001$. d Upregulation of paternal allele-derived *Kcnk9* mRNA after treatment of *Kcnk9*KO^{mat} mPCNs with different CI-994 concentrations compared with paternal allele-derived *Kcnk9* mRNA of DMSO-treated *Kcnk9*KO^{mat} mPCNs and *Kcnk9* mRNA of DMSO-treated WT mPCNs detected by RT-qPCR (1 day treatment, normalization to *Impa2*, *Kcnk9*KO^{mat} DMSO $n = 9$; 4 μM $n = 2$; 20–80 μM $n = 4$ and WT DMSO $n = 5$ cultures/group). One-way ANOVA: $F(5, 22) = 75.51$, $P < 0.0001$; corrected with Bonferroni's multiple comparison post hoc test to *Kcnk9*KO^{mat} DMSO mPCNs, ***$P < 0.001$****, $P < 0.0001$, c, d performed in 2–4 independent experiments. e Duration of *Kcnk9* derepression in vitro. Workflow is illustrated in schematical representation (left). After 1 and 10 days, *Kcnk9* is significantly upregulated after CI-994 treatment in mPCN compared with DMSO controls. One day DMSO $n = 2$, 1 day CI-994 $n = 3$, day 10 DMSO $n = 6$, day 10 CI-994; $n = 4$; n = samples (3–5 wells/sample; 6 embryos pooled). Day 1: $P = 0.0297$, day 10: $P = 0.0001$, Mann–Whitney U. c–e Values are means ± SEM. Statistical analyses and approaches are provided in Supplementary Table 1. Source data are provided as a Source Data file. Images displaying the mouse, the embryo and the neurons in this figure were created using Servier Medical Art templates, which are licensed under a Creative Commons Attribution 3.0 Unported License; https://smart.servier.com.

mouse displaying a brain-specific enhancer chromatin signature similar to that identified at the human imprinted domain on chromosome 8q24. Thus, we focused our analysis on the promoter and intronic region of the *Kcnk9* locus, which are enriched for both marks in the mouse brain ChIP-seq datasets (Fig. 6a). Due to the small size of the LC, we opted to use a novel low-input ChIP-method[27] for both regions (LC and hippocam- pus) and validated this by conventional ChIP-qPCR in the hippocampus (Supplementary Fig. 7b). Upon CI-994 treatment, we observed a significant more than two-fold increase in H3K27ac depositions at the two *Kcnk9* regions both in the hippocampus and LC of *Kcnk9*KO^{mat} mice (Fig. 6b). The levels of H3K27ac were also increased in the hippocampus of WT littermates however the increase was not as prominent as in the *Kcnk9*KO^{mat} animals (Supplementary Fig. 7i, j). An intergenic region, lacking H3K27ac or H3K4me1 modifications, was used as negative control (Supplementary Fig. 8c-j). Looking at allele- specific H3K27ac deposition in the hippocampus of (C57BL/ 6xCast/Ei)F1 hybrid animals using two different SNPs in intron 1 of *Kcnk9*, we found that, as expected, the maternal allele had a higher degree of H3K27ac association than the paternal allele. CI- 994 treatment of *Kcnk9*KO^{mat} mice, however, led to a higher degree of H3K27ac deposition at the paternal than at the maternal *Kcnk9* allele (Fig. 6c).

In addition, we tested the deposition of H3K4me1 both in the LC and hippocampus to assess if histone acetylation inhibition leads to additional changes in other histone marks. Treatment with CI-994 led to only a slight, but not significant increase of H3K4me1 deposition at the *Kcnk9* promoter region (Supplemen- tary Fig. 7f-h). Our findings indicate that CI-994 treatment affects histone acetylation consistently at the promoter and intronic regions of *Kcnk9* of the investigated brain tissues and has diverging effects on H3K4me1 deposition at the investigated *Kcnk9* locus.

Taken together, our findings demonstrate that the paternal allele of *Kcnk9* is not fully silenced in the brain, further derepressed in the case of loss of the maternal allele and substantially activated upon exogenous epigenetic modulation. Our data provide evidence for a promising therapeutic effect of the class I HDAC inhibitor CI-994, in a mouse model for BBIDS with maternal loss of *Kcnk9*.

Discussion

Kcnk9/*KCNK9* is an imprinted gene in mouse and man that is expressed from the maternal allele. Pathogenic variants present on only the maternal allele, therefore, cause disease in patients[1,2]. In a study comparing full *Kcnk9* knockout animals (*Kcnk9*KO^{hom}) with maternal *Kcnk9* knockout animals (*Kcnk9*KO^{mat}) and WT littermates in a behavioral battery, we surprisingly found an intermediate phenotype in nocturnal locomotor activity in *Kcnk9*KO^{mat} animals. Furthermore, elec- trophysiological analysis of tyrosine hydroxylase (TH)-positive neurons in the LC, a region involved in regulation of arousal and locomotor activity in mice, displayed significantly increased spontaneous firing frequencies only during the active dark phase in full knock-outs in contrast to WT, while it was fully rescued in the *Kcnk9*KO^{mat} animals. Allele-specific expression analysis of *Kcnk9* mRNA in (C57BL/6JxCast/Ei)F1 hybrid animals revealed significant residual paternal expression of up to 14% of total *Kcnk9* expression in the LC in the *Kcnk9*KO^{mat} animals. Daily i.p. injection of the second-generation HDAC inhibitor CI-994 could increase this expression up to three-fold and resulted in a full rescue of the behavioral phenotypes of *Kcnk9*KO^{mat} animals.

We show here that an increase in dark-phase locomotion in the *Kcnk9*KO^{hom} animals is associated with an increase of in vitro pacemaker frequency in the LC. Deletion of the active maternal *Kcnk9* allele in the mouse is supposed to lead to a phenotype comparable to the full knockout. Surprisingly, however, our study identified an intermediate behavioral phenotype in nocturnal (hyper)activity in the *Kcnk9*KO^{mat} animals, as well as a fully rescued cellular phenotype (LC firing frequency) (Figs. 1c, 3). Extended allele-specific expression analysis using (C57BL/ 6JxCast/Ei)F1 mouse hybrids demonstrated residual *Kcnk9* expression from the paternal allele in several brain regions with a significant peak in the LC of 14% of total *Kcnk9* expression coming from the paternal allele.

The LC plays an essential role in arousal and sleep-wake transitions[28] and, as the origin of noradrenergic neurons pro- jecting into the hippocampus and the prefrontal cortex, is also involved in the regulation of long-term and working memory, two essential building blocks of higher cognition/brain func- tions[29]. In a knockdown experiment using shRNAmir containing AAVs targeting the *Kcnk9* mRNA specifically injected into the LC we found a similar behavior phenotype in circadian activity as seen in the full and maternal *Kcnk9* knockout animals demon- strating an essential and causal contribution of *Kcnk9* expression within the LC in the control of nocturnal locomotor activity. Interestingly, our electrophysiological data show full rescue of in vitro pacemaker firing frequency through *Kcnk9*^{pat} expression in the LC in *Kcnk9*KO^{mat} animals on the one hand and only a partial rescue of dark-phase activity on the other. This might indicate different levels of *Kcnk9* expression isolated pacemaker function, which typically oper- ates with very small ionic currents of a few picoamps, compared

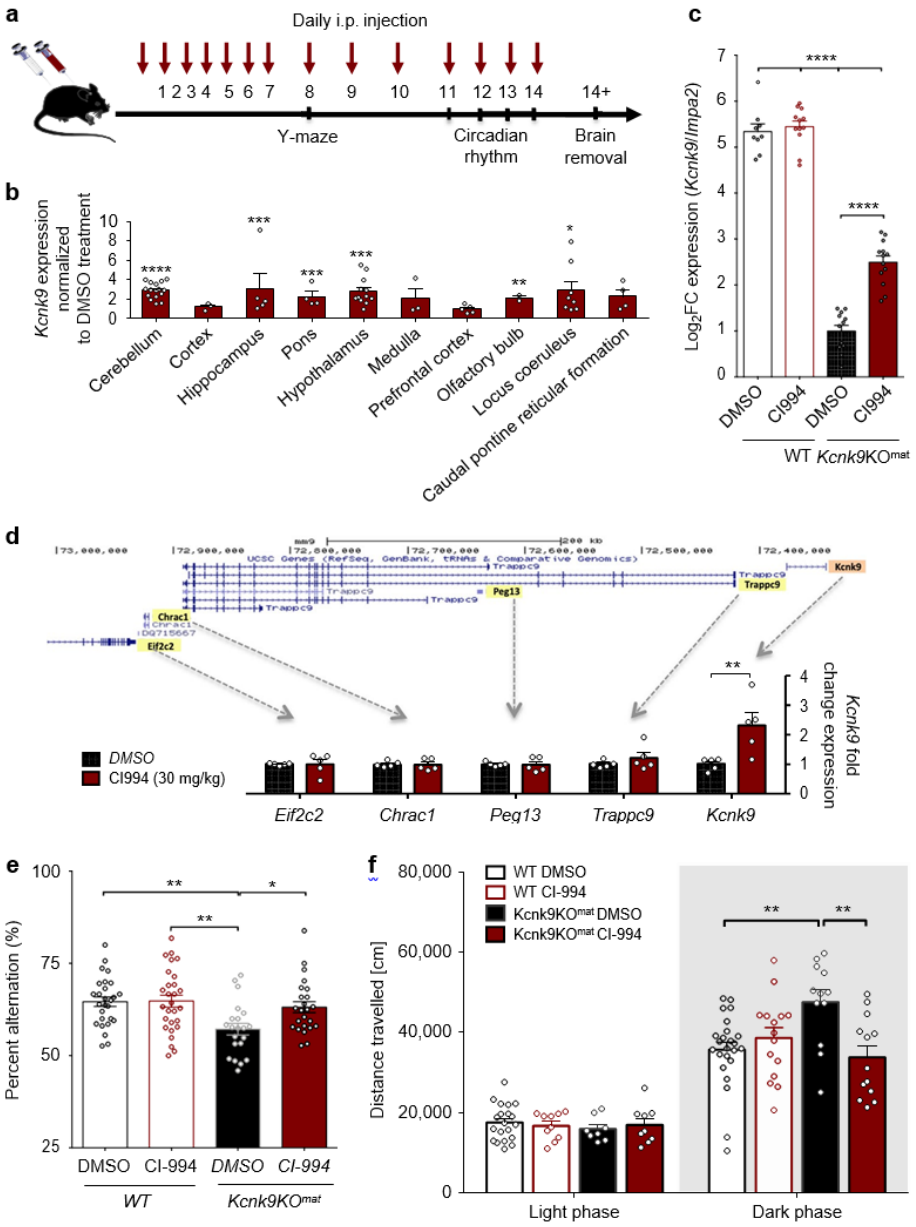

Fig. 5 Effects of CI-994 histone deacetylase inhibitor treatment in vivo. a Experimental design of the mouse study. CI-994 or DMSO was intraperitoneally injected. b Significant upregulation of *Kcnk9* after CI-994 treatment in several brain regions normalized to DMSO treatment, Mann–Whitney U test. Regions from left to right, DMSO/CI-994, n = 12/13; 6/9; 12/14; 7/8; 9/12; 6/6; 9/9; 6/6; 7/8 and 7/4. c Upregulation of *Kcnk9* in the cerebellum of CI-994-treated *Kcnk9*KO^{mat} mice ($n = 13$), but not of CI-994-treated WT mice ($n = 12$), each compared with DMSO-treated *Kcnk9*KO^{mat} ($n = 12$) and WT mice ($n = 9$). Two- way ANOVA and subsequent Bonferroni's multiple comparisons test, $^{****}P < 0.0001$ (all comparisons except DMSO:WT vs. CI-994:WT). d RT-qPCR expression analysis of known genes in the imprinting cluster on mouse chromosome 15. CI-994 treatment (30 mg CI-994/kg body weight) did not affect expression of *Trappc9, Peg13, Chrac1*, and *Eif2c2* in the hippocampus of *Kcnk9*KO^{mat} mice. Significant increase of *Kcnk9* expression after CI-994 treatment, $n = 5$, $P = 0.0079$, Mann–Whitney U test. e Y-maze percentage alteration was examined for DMSO-treated WT mice ($n = 20$), CI-994-treated WT mice ($n = 18$), DMSO-treated *Kcnk9*KO^{mat} mice ($n = 21$) and CI-994 treated *Kcnk9*KO^{mat} ($n = 24$) mice. CI-994 or DMSO-treated WT mice and CI-994-treated *Kcnk9*KO^{mat} mice did not exhibit deficits in working memory. CI-994-treated *Kcnk9*KO^{mat} mice showed a significant increase in percent spontaneous alteration compared with DMSO- treated *Kcnk9*KO^{mat} mice. Two-way ANOVA, Tukey post hoc test, $^{*}P < 0.05$, $^{**}P < 0.01$. f Distance traveled in the home cage in light (12 h) phase (left section) and the dark (12 h) phase (right section). No differences between DMSO-treated WT ($n = 20$), CI-994-treated WT ($n = 10$), DMSO-treated *Kcnk9*KO^{mat} ($n = 8$) and CI-994-treated *Kcnk9*KO^{mat} ($n = 9$) mice in the distance traveled in the light phase were detected. DMSO-treated *Kcnk9*KO^{mat} ($n = 12$) mice displayed a significant increase of nocturnal activity compared with DMSO-treated WT mice ($n = 24$) and CI-994-treated *Kcnk9*KO^{mat} ($n = 13$) mice as well as a visible, but not significant increase of nocturnal activity compared with CI-994-treated WT mice ($n = 15$). Two-way ANOVA, Bonferroni's post hoc test, $^{**}P < 0.01$. b–f n = sample or data arising from biologically independent animals. e, f Behavioral experiments were performed in nine independent sessions. b–e Values are means ± SEM (±indicates the standard error). Statistical analyses and approaches are provided in Supplementary Table 1. Source data are provided as a Source Data file. The mouse image in this figure was created using Servier Medical Art templates, which are licensed under a Creative Commons Attribution 3.0 Unported License; https://smart.servier.com.

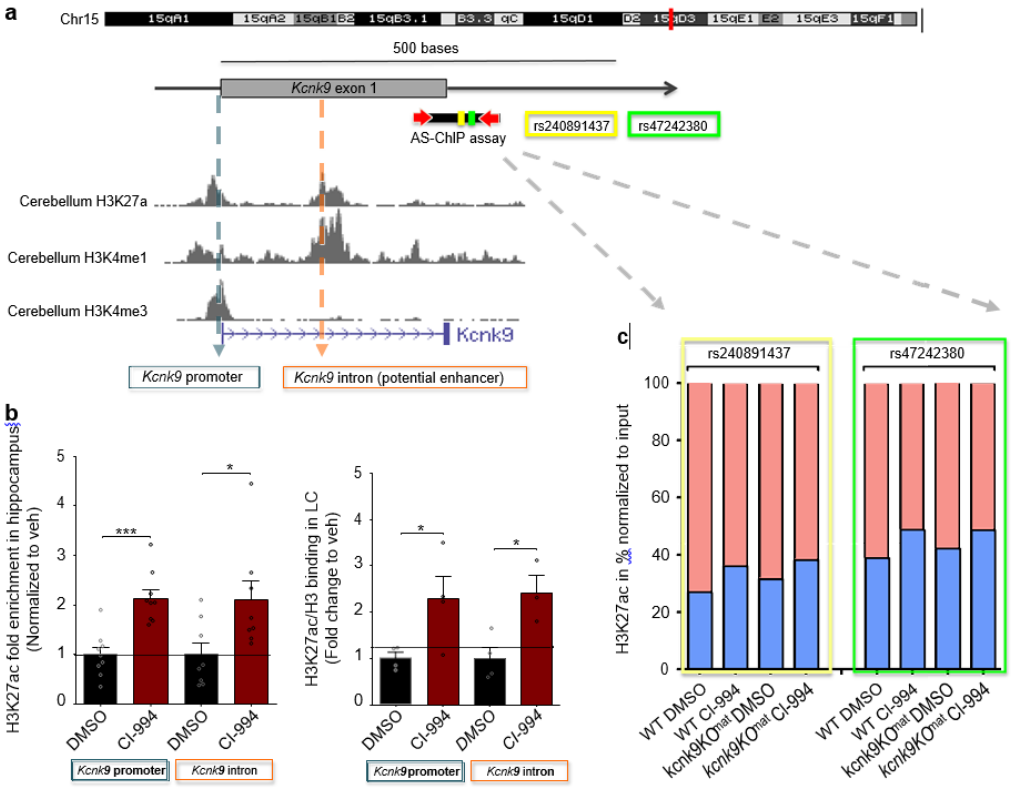

Fig. 6 Treatment with CI-994 affects H3K27 acetylation at the *Kcnk9* locus. a Schematic presentation of the *Kcnk9* locus on distal mouse chromosome 15. The murine *Kcnk9* gene is shown with the corresponding H3K27ac, H3K4me1 and H3K4me3 peaks in mouse cerebellum (UCSC Genome Browser on Mouse July 2007 (NCBI37/mm9) Assembly). b Increased deposition of H3K27ac marks at the promoter and intronic region of *Kcnk9* in hippocampus and locus coeruleus (LC) in *Kcnk9*KO^{mat} mice following treatment with CI-994 (normalized to veh). Hippocampus (left): in *Kcnk9* promoter, DMSO ($n = 9$) vs. CI-994 ($n = 9$), $P = 0.0001$; in *Kcnk9* intron, DMSO ($n = 8$) vs. CI-994 ($n = 8$), $P = 0.0270$. LC (right) in *Kcnk9* promoter, DMSO ($n = 4$) vs. CI-994 ($n = 4$), $P = 0.0450$; in *Kcnk9* intron, DMSO ($n = 4$) vs. CI-994 ($n = 3$), $P = 0.0202$. Values are means ± SEM, $*P \le 0.05$, $***P < 0.001$, by Student's *t* test. c Chromatin Immunoprecipitation followed by pyrosequencing reveals allele-specific chromatin deposition of H3K27ac. Two SNPs (rs240891437 and rs47242380) in the intronic region of the *Kcnk9* in the hippocampus of (C57BL/6xCast/Ei)F1 hybrid mice were analyzed; maternal allele (red) and paternal allele (blue). Untreated state (DMSO) reveals higher acetylation levels in maternal allele compared with the paternal allele. The paternal allele exhibits higher H3K27 acetylation enrichment after CI-994 treatment compared with the maternal allele. WT:DMSO $n = 3$, WT:CI-994 $n = 4$, *Kcnk9*KO^{mat}:DMSO $n = 6$, and *Kcnk9*KO^{mat}:CI-994 $n = 4$. b, c n = biologically independent animals. Data generated in two independent experiments. Statistical analyses and approaches are provided in Supplementary Table 1. Source data are provided as a Source Data file.

with in vivo function for behavioral control, where neurons are embedded in active networks and larger currents are necessary to alter their firing patterns. Our data suggest that the influence of KCNK9 on pacemaker frequency and potentially in vivo activity could be feasible as a therapeutical strategy for attention deficit and hyperactivity disorder (ADHD). However, future studies should directly record from LC neurons in vivo in awake behaving mice as well as from *Kcnk9*KO^{mat} and *Kcnk9*KO^{hom} animals to better define the functional role of KCNK9/TASK3 channels.

Nocturnal activity values (measured as distance traveled, in cm) of WT mice showed considerable variability between experiments. This variability may be attributed to various factors such as different treatments (naïve vs. injected) of the analyzed mice as well as different timepoints and environmental conditions at which the experiments were performed. It is well-known, that animal behavior heavily relies on environmental conditions within animal facilities and that these conditions can slightly change with time[30]. For example, in our animal facility, maintenance work was carried out in the time between the circadian locomotor activity experiments for the first manuscript version and those including treatment of *Kcnk9*KO^{hom} mice with CI-994 for the revised manuscript version. In light of these limitations, we strongly argue that a comparison of nocturnal activity values makes only sense within the same experiment but not across the different experi- ments performed. A recent study has suggested histone methylation as a potential therapeutic target for another imprinting disorder, the Prader- Willi syndrome (PWS)[31]. The authors showed that UNC0642, a selective inhibitor of euchromatic histone-lysine N-methyl-transferase-2, derepressed the maternal copies of paternally expressed PWS candidate genes and promoted the growth and survival of mouse pups with a paternal deletion of the PWS region without altering DNA methylation at the PWS-ICR. We show here that derepression of the paternal allele in *Kcnk9*KO^{mat} animals leads to a significant increase in *Kcnk9* expression in selected brain regions and that this is enough to substantially influence the behavioral phenotype in domains likely to be regulated by LC activity. Furthermore, we found that the second- generation HDAC inhibitor CI-994 is another attractive option for treatment of imprinting disorders such as BBIDS. CI-994 treatment of *Kcnk9*KO^{mat} mice as a mouse model of BBIDS substantially activated the repressed paternal allele of *Kcnk9* in several brain areas resulting in a

significant increase in *Kcnk9* expression. This led to the full rescue of specific domains of brain function impaired in BBIDS. Our data for the first time shows successful phenotypic rescue of impaired brain function in a mouse model for an imprinting disorder using an epigenetic modulator.

Similar to the findings in the UNC6042-treated mouse model of PWS[31], activation of the *Kcnk9*^{pat} allele was not accompanied by changes of DNA methylation at the *Peg13* DMR, which is assumed to play a key role in regulation of *Kcnk9* imprinting also in the mouse[3]. Notably, the bisulfite technique did not allow us to dis- criminate between 5-methylcytosine and 5-hydroxymethylcytosine levels possibly affected by CI-994. Though, our data strongly argue that CI-994-mediated derepression of the *Kcnk9*^{pat} allele is pri- marily caused by an increase of H3K27ac at regulatory elements in the promotor and intronic region of the *Kcnk9* gene. However, the treatment did not display significant differences in H3K27ac deposition between the LC and hippocampus tissues suggesting a region-independent effect of the HDAC inhibitor. Such effects have commonly been reported in multiple genome-wide studies investigating the effect of HDAC inhibitors[32]. Interestingly, CI-994 as a histone deacetylase inhibitor did not only selectively increase H3K27ac but also slightly increased H3K4me1 at the *Kcnk9* pro- moter region. This is not unexpected since crosstalk mechanisms between histone-modifying enzymes often affect the binding and activity of further histone-modifying enzymes. For instance, treatments with HDAC inhibitors were reported to affect globally the histone methylation marks specifically of H3K4me1[32]. These observations are repeatedly described in the literature suggesting a broad effect of HDAC inhibitors on chromatin structure and transcription[33,34].

In general, epigenetic modulation is supposed to rather unspecifically target numerous genes and their expression in the genome. Side effects of all sorts including tumor development and metabolic dysregulation are believed to be likely with such substances. Also, interference with brain function leading to cognitive impairment and mental dysfunction cannot be excluded. However, valproic acid, a first generation HDAC inhibitor has been used in anti-epileptic therapy for decades without severe tumorigenic or metabolic long-term effects. CI- 994 is a second-generation, specific class I HDAC inhibitor. Although a relatively broad effect of CI-994 on gene expression has been demonstrated in vivo, it is being used in several clinical trials for anti-cancer therapy having proven inhibitory potency of epithelial-mesenchymal transition processes[35]. Accumulating evidence also suggests that CI-994 provides neuroprotective effects in the central nervous system and cell survival in vitro[36]. Regarding brain function in WT mice no effect of CI-994 treatment has been seen in the open field[26]. In our experiments, no significant influence of two weeks CI-994 injection was seen on working memory or circadian locomotor activity in WT animals. Furthermore, an increase of *Kcnk9*^{pat} expression after CI-994 injections was only seen in selected brain regions, but not in, e.g., cortex or prefrontal cortex, and mainly in the maternal knockout animals (only very weakly in WT animals). Allele-specific ChIP-qPCR of (C57BL/6JxCast/Ei)F1 hybrids showed that the CI-994 effect is more pronounced on the paternal allele (Fig. 6c). This leads to a visible increase in expression of the paternal but not the maternal allele (Supplementary Fig. 4a) and might be due to the high acetylation status of the active maternal allele. Furthermore, CI-994 treatment did not affect the expression of other nearby imprinted genes within the imprinted cluster on mouse chromosome 15 in vitro and in vivo. Taken together these data suggest a rather specific epigenetic action of CI-994 in *Kcnk9*KO^{mat} animals, which might make CI-994 safe for usage in BBIDS patients.

However, so far all CI-994 related studies have been carried out in vitro or in adult animals. If used in patients, early treatment during development might be more efficient. In order to make this possible, further studies on CI-994 specificity and possible adverse and teratogenic effects in young mice have to be conducted.

In summary, we show here that brain region-specific upregu- lation of the paternally silenced *Kcnk9* allele particularly in the LC of *Kcnk9*KO^{mat} animals modulates nocturnal hyperactivity, a central phenotype of *Kcnk9* knockout animals. We further show that the class I HDAC inhibitor CI-994 leads to a significant additional increase of *Kcnk9*^{pat} expression in several brain regions and fully rescues behavioral alterations in *Kcnk9*KO^{mat} animals. This rescue is associated with an increase of H3K27 histone acetylation at the promotor and intronic region of the *Kcnk9* gene but not with changes in DNA methylation at the differentially methylated region in the *Peg13/Kcnk9* locus. Our data suggest epigenetic modulation by CI-994 as a promising therapeutic strategy in patients with BBIDS and, more generally, derepression of imprinted gene alleles as a sustainable approach for the treatment of imprinting disorders.

Methods

Mice. All experimental procedures were performed in accordance with institu- tional animal welfare guidelines and were approved by the ethical committee of the state government of Rhineland-Palatinate, Germany (ID: 23 177-07/G 17-1-022). *Kcnk9*KO^{hom} mice were provided by Florian Lesage, Institut de Pharmacologie Moléculaire et Cellulaire, Valbonne, France. The gene targeting strategy of *Kcnk9*KO^{hom} mice was based on a cre-mediated deletion of exon 2 encoding pore domains P1 and P2, transmembrane domains M2–M4 as well as the cytoplasmic C-terminus[18]. Breeding of two heterozygous animals revealed homozygous, het- erozygous and WT animals at a proportion of 1:2:1. WT littermates were used as controls. WT and heterozygous *Kcnk9*KO mice with inactivation of the maternal *Kcnk9* allele (*Kcnk9*KO^{mat}) were obtained by crossing male WT mice with female *Kcnk9*KO^{mat} mice. Finally, breeding of homozygous female and heterozygous male mice resulted in *Kcnk9*KO^{mat} and *Kcnk9*KO^{hom} mice. The mice were kept under specific-pathogen-free (SPF) conditions on a 12 h light/12 h darkness cycle in standard polystyrene cages with free access to water and food. Using tail tip DNA, mice were genotyped by assessing exon 2 excision using the primers flanking this region (F, 5′TGCGAGCTTCAGAGAGAGGATG-3′ and R, 5′-ATGCTC-TAATCTCCAGTCTG-3′) producing fragments for WT and mutant alleles.Additional primers within exon 2 were applied to generate a control product for the WT allele (F, 5′-CACCACGCCATGTACTTCCT-3′ and R, 5′-GGACCG-GAAGTAGGTGTTCC-3′). Male mice at 8–10 weeks of age were used for expression analysis and to investigate the behavioral phenotype with and without drug treatment. Allele-specific expression analyses were carried out with total RNA from F1 offspring derived from crosses between female WT C57BL/6J or *Kcnk9*KO^{hom} mice and male WT Mus musculus castaneus (Cast/Ei) mice.

Behavioral testing. Littermate WT and *Kcnk9*KO mice were tested in 4–8 cohorts of mice, with testing beginning at 8–10 weeks of age. All experimenters were blinded to the genotype of the mice throughout the studies and behavioral analyses. Immediately after the behavioral tests, animals were sacrificed and whole brains were rapidly removed and incubated in RNAlater® (Sigma) for subsequent expression analysis.

Drug administration in vivo. Nine weeks old male *Kcnk9*KO^{mat} and WT mice were injected intraperitoneally once daily with CI-994 (ApexBio) or dimethyl sulfoxide (DMSO) (control vehicle) for 7 consecutive days before behavior experiments were initiated (Fig. 5a). On days of testing, mice were injected 2 h before behavior experiments. A single injection contained either 20 µl DMSO or 20 µl CI-994 (35 mg/kg) dissolved in 100 % DMSO.

Toxicity/viability test in CI-994 treated mPCNs. mPCNs were washed with PBS and fixed with 4% paraformaldehyde for 2 h. Subsequently, cells were incubated for 20 min in 0.4% Triton X-100 in PBS at 37 °C and further rinsed three times with PBS. After blocking with 10% sheep serum at 37 °C for 1 h, cells were washed for a further three times with PBS. Next, neurons were incubated overnight at 4 °C with anti-neuron-specific nuclear protein NeuN monoclonal antibody (cat. # ab104225; dilution 1:200 in PBS), followed by five washes with PBS for 5 min each.

The neurons were subsequently incubated with an Alexa Fluor 488-conjugated goat anti-mouse secondary antibody (cat # ab150077; dilution 1:200 in PBS) for 1 h at 37 °C and washed for a further five times in PBS. After staining, cells on coverslips were mounted onto microscope slides and counterstained with mounting medium containing 2 µg/mL Hoechst 33258 (Cat # H3569).

Tissue collection. Whole mouse brains were removed and incubated in RNAlater® (Sigma) and stored for 2 days at 4 °C. After the dehydration process, several brain regions were dissected and further processed or stored at −80 °C. For LC samples, coronal brain sections (80 µm) between bregma −5.40 and −5.52[37] were generated, and 0.51 µm punches bilaterally of each brain region were collected with the Brain Punch Tissue Set (Leica). The accuracy of the LC tissue collection was validated by performing tyrosine hydroxylase (TH) expression analyses and comparing the expression levels to those of WT cerebellum and hippocampus samples. Samples with non-adequate TH levels were excluded from analysis. Tyrosine hydroxylase, which serves as a norepinephrine marker, was expressed ~400-fold higher compared with hippocampus samples, indicating a precise tissue dissection (Supplementary Fig. 2).

Cell culture. *Kcnk9*KO^{mat} primary cortical neurons (mPCNs) were isolated from E14 embryos derived from matings between female *Kcnk9*KO^{hom} mice and WT males. After collection of brains, cortices were dissected out and mechanically separated into single cortical cells through resuspension. The mPCNs were plated on Poly-L-Ornithine (Sigma)- and Laminin (Sigma)-coated plates and maintained in culture medium containing Neurobasal medium (Gibco), supplemented with 2%B27 plus vitamin A (Gibco) and 1% Glutamax (Gibco), in a humidified incubator at 37 °C and 5% CO_2.

In vitro drug treatment. We cultured murine primary cortical neurons (mPCNs) for 4 days in 6- or 12 well-plates and treated them with epigenetic compounds diluted in culture medium for 24 or 72 h. To investigate the duration of *Kcnk9* unsilencing, mPCNs were cultured for 3 days and treated with 20 µM CI-994. After 2 days of treatment, cells were washed with 37 °C culture medium. After 1 day, some cells were harvested. Medium change was conducted after additional three days. Six days later, on 10 days, remaining cells were harvested and analyzed via RT-qPCR.

AAV generation and *Kcnk9* knockdown in WT mice. Viral constructs were purchased from Sirion Biotech (Martinsried, Germany). Generation and evaluation of shRNAmir sequence targeting the gene *Kcnk9* were performed using SIRION's RNAiONE platform as previously described[38]. Ten different 21mer shRNAmir sequences against *Kcnk9* were selected using algorithms listed in Fig. 2a. Corresponding shRNA template oligonucleotide cassettes were cloned into a shuttle plasmid under the control of the human U6 promoter. The coding region of the cDNA was PCR-amplified and cloned into the validation vector pVal downstream of the EGFP coding region resulting in pVal-target. The promoter-shRNA regions of the shRNA shuttle plasmids along with a shuttle plasmid encoding for a NT-shRNA as control were then transferred into pVal-target by recombinational cloning. Cells were then transfected with the validation plasmids and were incubated for 48 h. Total RNA was subsequently isolated and 1 µg was reverse transcribed using a mixture of random hexamer and oligo-dT primer. The silencing efficiency of each shRNA was determined by quantification of the EGFP-target cDNA expression levels relative to NT-shRNA control vector. The expression cassette was then cloned into an AAV transfer vector (pAAV-Syn-shRNAmir-*Kcnk9*-EF1a-eGFP and pAAV-Syn-shRNAmir-scrambled-EF1a-eGFP) and ITRs integrity was then validated by restriction analysis. 293T cells were utilized for AAV production, which were generated via co-transfection and transferred to 1E13 VG in vivo buffer. We infused 8-week-old C57BL/6J mice (CLR) with either AAV1-hSyn-shRNAmir-*Kcnk9*-EF1a-eGFP (Sirion, Germany) to knockdown the *Kcnk9* expression or AAV1-hSyn-shRNAmir-scrambled-*Kcnk9*-EF1a-eGFP (Sir- ion, Germany) as a control bilaterally in the LC. Animals where anesthetized with isoflurane (1–2%) and received a subcutaneous injection of carprofen (4 mg/kg). Three hundred nanoliters of virus was infused with a rate of 100 nl/min in the LC (AP: −5.4, ML: ±1.0, DV: 3.0, in mm, relative to bregma) under stereotaxic control (Kopf Instruments, USA) using a 1 µl Hamilton syringe with a glass capillary.Twenty-one days after surgery spontaneous alteration and circadian rhythm were tested.

RNA Isolation, cDNA synthesis, and RT-qPCR. The total RNA extraction with TRIzol reagent from brain tissue was prepared as suggested by Invitrogen Life Technologies. High Pure RNA Tissue Kit (Roche) and High Pure RNA Isolation Kit (Roche) were applied to extract total RNA from small tissue and cell samples using spin columns. The purity, quantity, and integrity of the RNA were measured with a NanoDrop 1000 spectrophotometer and an Agilent 2100 Bioanalyzer. The cDNA samples were synthesized from 200 to 1000 ng total RNA using the Pri- meScript™ RT Master Mix cDNA (Takara) as recommended by the manufacturer. Quantitative real-time PCR (qRT-PCR) was carried out using SYBR® Premix Ex Taq™ II (Tli RNaseH Plus) and 10 µM primers (final concentration), according to the manufacturer's instructions. Allele-specific RT-qPCR reactions were performed on an ABI StepOnePlus™ Real-Time PCR System using exon–exon junction primers with the following conditions: 95 °C/30 s, 40 cycles of 95 °C/5 s, 68.5 °C/30 s, 72 °C/30 s. All additional RT-qPCR reactions were performed with the following conditions: 95 °C/30 s, 40 cycles of 95 °C/5 s, 60 °C/30 s, 72 °C/30 s. All reactions were measured in triplicates, and median cycles to threshold (Ct) values were used for analysis. The housekeeping gene *Impa2* was used to normalize against experimental genes, and relative gene expression was determined using the 2−ΔΔCT methods[39]. *Impa2* forward primer 5′-CGTGCGGGACAAATCATCA G-3′ and reverse primer 5′-CGTGCGGGACAAATCATCAG-3′.

Allele-specific expression analysis by QUASEP. For allele-specific expression analysis, the synthesized cDNA of (C57BL/6JxCast/Ei)F1 hybrid mice was amplified in a PCR applying one non-biotinylated forward primer: 5′-GCCTGTACCT TCACCTAC-3′ and one biotinylated reverse primer: 5′-CACAACTATCGGATATGGACATGC-3′. To distinguish the origin of the alleles we subsequently analyzed the RT-PCR products in allele-specific expression analysis, using the C/T-SNP rs225149059 (Ensembl; GRCm38.p5) and QUASEP method as previously descri- bed[3]. A *Kcnk9*-specific pyrosequencing primer: 5′-TGCCGCGGTGTTC-3′, was designed flanking the allele-specific SNP and pyrosequencing was carried out on a PyroMark Q96 instrument (Qiagen).

DNA methylation analysis. Approximately 500 ng DNA was subjected to sodium bisulfite treatment and purified using the EZ DNA Methylation Direct™ kit (Zymo Research). Bisulphite PCR primers for the *Peg13*-DMR1 and *Peg13*-DMR2 (located from +195 to +833 bp relative to the 5′end of the *Peg13* transcript) were designed using the Pyrosequencing Assay Design Software (Qiagen). PCR amplification was performed with 1 µg bisulfite converted DNA and specific primers at 42 cycles in a bisulfite PCR analysis. We amplified two CpG-rich regions, *Peg13*-DMR1 and *Peg13*-DMR2, associated with the mouse *Kcnk9* gene regulation with the following primers: *Peg13*-DMR1, forward 5′-TTGGATGAGTTATTATATAAGGTTTAAAA-3′ and reverse 5′-ACAACTACCTACATTCCAAATCT-3′-biotinylated (product size: 175 bp), sequencing 5′-AAATTTTAATAAGATGGGTTAAT-3′. *Peg13*-DMR2, forward 5′-AGATTTGGAATGTAGGTAGTTGTGA-3′and reverse 5′-CC TCAATAAAACCATTCTAATCAACTAT-3′-biotinylated (product size: 198 bp), sequencing 5′-GGTAATTTGTTAGGTGGAGATATA-3′. The pyrosequencing was carried out on the PyroMark Q96 instrument (Qiagen).

Chromatin Immunoprecipitation (ChIP)-qPCR. ChIP experiments were performed as described in Akhtar et al. with minor modifications for brain tissue processing[27]. Briefly, brain tissues were dissected in cold PBS and homogenized with a pestle. Following dissection, tissues were fixed with 1% formaldehyde in PBS for 10 min at room temperature, followed by quenching of the fix with 125 mM glycine for 5 min. Fixed cells were resuspended in 140 mM RIPA (10 mM Tris-Cl pH 8.0, 140 mM NaCl, 0.1 mM EDTA pH 8.0, 1% Triton X-100, and 0.1% SDS) and subjected to 18 cycles of sonication on Bioruptor Pico (Diagenode), with 30 secs "ON"/ "OFF" at high settings. After sonication, samples were centrifuged at 14,000 × *g* for 10 min at 4 °C and supernatant was transferred to a fresh tube. The extracts were incubated overnight with 1 µg (1:500 dilution) of H3K27ac (Abcam, Cat # ab4729), H3K4me1 (Active motif, Cat # 39297), H3 (Abcam, Cat # ab1791) or IgG control (Diagenode, Cat # C15410206) antibody at 4 °C with head-over tail rotations. After overnight incubations, 20 µl of blocked Protein A and G Dyna- beads (Diagenode) were added to the tubes and further incubated for 3 h to capture the antibodies. Bead separation was carried out using a magnetic rack and washed as following; once with 140 mM RIPA (10 mM Tris-Cl pH 8.0, 140 mM NaCl, 0.1 mM EDTA pH 8.0, 1% Triton X-100, and 0.1% SDS), four times with 250 mM RIPA (10 mM Tris-Cl pH 8.0, 250 mM NaCl, 0.1 mM EDTA pH 8.0, 1% Triton X- 100, and 0.1% SDS) and twice with TE buffer pH 8.0 (10 mM Tris-Cl pH 8.0 and 0.1 mM EDTA pH 8.0). For reversal of cross-linking, samples were RNase-treated (NEB) and subjected to Proteinase K treatment for 12 h at 37 °C and at least 6 h at 65 °C after the immunoprecipitation. After proteinase K treatment, the DNA was extracted using the phenol-chloroform method. After precipitating and pelleting, DNA was dissolved in 30 µl of TE buffer pH 8. The real-time PCR was performed using SYBR Green chemistry (ABI) on the ABI StepOnePlusTM Real-Time PCR System. The input and chromatin immunoprecipitated material were processed identically across the samples. The fluorescent signal of the amplified DNA was normalized to H3 binding or input with the following primers: *Kcnk9* promoter F5′-CGTGTGCGCTACATCTCCTA-3′and R 5′-ATTCGCCGGTTCCTTCTACT-3′; *Kcnk9* intron F 5′-AGGGCAGATGCTTAAGAGGA-3 and R 5′-CATCTGTTCTGTACCCCATCC-3′; *Intergenic region 3 (Ig3)* F 5′-ATGCCCCTCAGCTATC ACAC-3′ and R 5′-GGACAGACATCTGCCAAGGT-3′. The low amount chro- matin immunoprecipitation (TAF-ChIP) was performed according to Akhtar et al.[27].

Allele-specific ChIP followed by pyrosequencing. For allele-specific ChIP analysis, DNA of WT and *Kcnk9*KO^{mat} (C57BL/6JxCast/Ei)F1 hybrid mice, treated either with DMSO or CI-994, was amplified in a PCR applying one non-biotinylated forward primer: 5′-AAATTCGCCGGTTCCTTCTAC-3′ and one biotinylated reverse primer: 5′-GAGATGTAGCGCACACGAAGC-3′. To distinguish the origin of the alleles we subsequently analyzed the PCR products in an allele-specific

manner, using two neighboring SNPs, rs240891437 and rs47242380 (Ensembl; GRCm38.p5). The quantification of enrichment was performed using the pyrosequencing technique. A *Kcnk9*-specific pyrosequencing primer: 5′-AAGGAATG GGTGTGC-3′ was designed and pyrosequencing was carried out on a PyroMark Q96 instrument (Qiagen).

Behavioral analyses. Brief descriptions of the behavioral tests are provided below. Male mice between 8 and 10 weeks of age were used for behavioral tests, as described below.

Circadian locomotor activity. Mice were individually placed in transparent polypropylene cages (38 × 22 × 15 cm) with standard beddings. Food and water were available and accessible at all times. The cages were placed in a sound-prove room under dimed light during the light phase and under infrared LED lights during the dark cycle. The horizontal locomotor activity of the mice was recorded in the light and in the dark phase using a video tracking software (EthovisionXT, Noldus software). The circadian rhythm activity was measured after 48 h accli- matization for 24 h and analyzed with EthovisionXT, Noldus software. The results show the distance traveled (in cm) in the light and in the dark phase.

Spontaneous alternation. Spatial working memory was assessed in a Y-maze test as described previously[40]. During a 10-min session in a Y-maze the spon- taneous alternation behavior was recorded. The spontaneous alternation test is based on the willingness of rodents to explore new environments, therefore to enter the arm of a Y-maze that had not been recently explored, i.e., the arm that was not entered in the previous choice. Mice were placed in a gray plexiglass Y maze in a sound proof room. Each maze consisted of three arms. Each arm was 40-cm long, 20-cm high, and 10-cm wide, and the arms converged to an equi- lateral triangular central area. Each mouse was placed at the end of the start arm, in which the mouse starts to explore and move freely through the maze during the 10-min session. The series and order of arm entries was observed manually and considered to be completed when the hind paws of the mouse had com- pletely entered the arm. Transitions between arms were scored as either correct or incorrect alternations by the observer. Healthy animals (controls) show a high change rate. This shows that the animal can remember which arm was last entered. The percentage of alternation was calculated as the ratio of actual to possible alternations multiplied by 100%, either for a 10 min session or 25 initial decisions. Each of the arms of the Y maze was cleaned with 70% ethanol solution between trials.

In vitro brain slice patch-clamp recordings of LC neurons. Adult mice were anesthetized and perfused with ice-cold ACSF as previously described[41]. The brainstem slices containing the LC were sectioned after intracardial perfusion using ice-cold ACSF (50 mM sucrose, 125 mM NaCl, 2.5 mM KCl, 25 mM $NaHCO_3$, 1.25 mM NaH_2PO_4, 2.5 mM glucose, 6.2 mM $MgCl_2$, 0.1 mM $CaCl_2$, and 2.96 mM kynurenic acid; Sigma-Aldrich GmbH), oxygenated with 95% O_2/5% CO_2). Slices were continuously perfused with oxygenated ACSF (2–4 ml min^{-1}, 36 °C; 22.5 mM sucrose, 125 mM NaCl, 3.5 mM KCl, 25 mM $NaHCO_3$, 1.25 mM NaH_2PO_4, 2.5 mM glucose, 2 mM $MgCl_2$, and 2 mM $CaCl_2$; 95% O_2/5% CO_2) for ≥45 min and then transferred to a recording chamber. CNQX (12.5 µM; Biotrend), AP-5 (10 µM; Biotrend), gabazine (SR95531, 4 µM; Biotrend), and yohimbine (1 µM; Biotrend) were added to inhibit fast excitatory and inhibitory synaptic transmission as well as activity of somatodendritic alpha2 adrenoreceptors, respectively. The electrophysiological recordings (whole-cell patch-clamp recordings) and data acquisition were performed as previously described[42].

Histology. Animals were injected with phenobarbital and perfused with fixation solution containing 4% paraformaldehyde, 15% picric acid in phosphate buffer solution (PBS). The removed brains were post-fixed overnight, 60 µm brain sections were sliced using a microtome (VT1000S, Leica). Free-floating sections were washed in PBS and incubated with blocking solution (10% horse serum, 0.5% Triton X-100% and 0.2% BSA in PBS) for 1 h at room temperature. Then, sections were incubated with primary antibodies in carrier solution (1% horse serum, 0.5% Triton X-100% and 0.2% BSA in PBS) at room temperature over- night. After washing the sections with PBS, they were incubated with secondary antibodies in carrier solution overnight. The following primary antibodies were used: monoclonal mouse anti-tyrosine hydroxylase (TH, catalog #MAB318, 1:1000, Millipore), polyclonal rabbit anti-GFP (catalog #A11122, 1:1000, Life Technology). The following secondary antibodies were used: Alexa Fluor 488 goat anti-rabbit (catalog #A11008, 1:1000, Thermo Fisher Scientific, Invitrogen) and Alexa Fluor 568 goat anti-mouse (catalog #A11004, Thermo Fisher Scien- tific, Invitrogen). On the third day, sections were washed with PBS, incubated inPBS containing 0.02% 4′,6′-diamidin-2-phenylindol (DAPI, catalog #D1306, Molecular Probes, Invitrogen) for 5 min and washed in PBS for 10 min. Afteward, sections where mounted on slides, coverslipped and stored at 4 °C until confocal images were taken.

Statistical analyses and graphical illustrations. All analyses and graphical illustrations were performed using Prism 7 (Graphpad Software, San Diego, CA) Assumptions concerning normal distribution were applied (Kolmogorov–Smirnov test) before statistical analyses were implemented. Statistical analyses and approaches are provided in Supplementary Table 1. Concerning annotation, the sample/cell number is expressed with n and number of mice is noted with N.

For animal studies and RT-qPCR expression analysis, data were compared using a one-way ANOVA and two-way ANOVA with and without repeated measures by multiple comparisons followed by Tukey's or Bonferroni's multiple comparison post hoc test. The numbers of biologically independent experiments, sample size, statistical results and ages of the animals are all indicated in the main text or figure legends and Supplementary Table 1. Values were only excluded if they were identified as outliers based on a Grubbs' test. Unless stated otherwise, the data given in figures and text are expressed as mean ± SEM. $P < 0.05$ was considered to be statistically significant.

Reporting summary. Further information on research design is available in the Nature Research Reporting Summary linked to this article.

Data availability

All relevant data are available from the authors. The source data underlying all figures and supplementary figures are provided as a Source Data file.

Received: 18 December 2018; Accepted: 5 December 2019;
Published online: 24 January 2020

References

1. Barel, O. et al. Maternally inherited Birk Barel mental retardation dysmorphism syndrome caused by a mutation in the genomically imprinted potassium channel KCNK9. *Am. J. Hum. Genet.* 83, 193–199 (2008).
2. Graham, J. M. Jr. et al. KCNK9 imprinting syndrome-further delineation of a possible treatable disorder. *Am. J. Med. Genet. Part A* 170, 2632–2637 (2016).
3. Ruf, N. et al. Sequence-based bioinformatic prediction and QUASEP identify genomic imprinting of the KCNK9 potassium channel gene in mouse and human. *Hum. Mol. Genet.* 16, 2591–2599 (2007).
4. Court, F. et al. The PEG13-DMR and brain-specific enhancers dictate imprinted expression within the 8q24 intellectual disability risk locus. *Epigenetics Chromatin* 7, 5 (2014).
5. Fagerberg, L. et al. Analysis of the human tissue-specific expression by genome-wide integration of transcriptomics and antibody-based proteomics. *Mol. Cell. Proteom.* 13, 397–406 (2014).
6. Rusznak, Z. et al. Differential distribution of TASK-1, TASK-2 and TASK-3 immunoreactivities in the rat and human cerebellum. *Cell. Mol. Life Sci.* 61, 1532–1542 (2004).
7. Talley, E. M. & Bayliss, D. A. Modulation of TASK-1 (Kcnk3) and TASK-3 (Kcnk9) potassium channels: volatile anesthetics and neurotransmitters share a molecular site of action. *J. Biol. Chem.* 277, 17733–17742 (2002).
8. Marinc, C., Derst, C., Pruss, H. & Veh, R. W. Immunocytochemical localization of TASK-3 protein (K2P9.1) in the rat brain. *Cell. Mol. Neurobiol.* 34, 61–70 (2014).
9. Brickley, S. G. et al. TASK-3 two-pore domain potassium channels enable sustained high-frequency firing in cerebellar granule neurons. *J. Neurosci.* 27, 9329–9340 (2007).
10. Linden, A. M. et al. TASK-3 knockout mice exhibit exaggerated nocturnal activity, impairments in cognitive functions, and reduced sensitivity to inhalation anesthetics. *J. Pharmacol. Exp. Therapeutics* 323, 924–934 (2007).
11. Pang, D. S. et al. An unexpected role for TASK-3 potassium channels in network oscillations with implications for sleep mechanisms and anesthetic action. *Proc. Natl Acad. Sci. USA* 106, 17546–17551 (2009).
12. Gotter, A. L. et al. TASK-3 as a potential antidepressant target. *Brain Res.* 1416, 69–79 (2011).
13. Bando, Y., Hirano, T. & Tagawa, Y. Dysfunction of KCNK potassium channels impairs neuronal migration in the developing mouse cerebral cortex. *Cereb. Cortex* 24, 1017–1029 (2014).
14. Berger, S. L. Histone modifications in transcriptional regulation. *Curr. Opin. Genet. Dev.* 12, 142–148 (2002).
15. Weaver, J. R. & Bartolomei, M. S. Chromatin regulators of genomic imprinting. *Biochimica et. biophysica acta* 1839, 169–177 (2014).
16. Singh, P. et al. Chromosome-wide analysis of parental allele-specific chromatin and DNA methylation. *Mol. Cell. Biol.* 31, 1757–1770 (2011).
17. Xie, W. et al. Base-resolution analyses of sequence and parent-of-origin dependent DNA methylation in the mouse genome. *Cell* 148, 816–831 (2012).
18. Guyon, A. et al. Glucose inhibition persists in hypothalamic neurons lacking tandem-pore K+ channels. *J. Neurosci.* 29, 2528–2533 (2009).
19. Reppert, S. M. & Weaver, D. R. Coordination of circadian timing in mammals. *Nature* 418, 935–941 (2002).
20. Meuth, S. G. et al. Contribution of TWIK-related acid-sensitive K+ channel 1(TASK1) and TASK3 channels to the control of activity modes in thalamocortical neurons. *J. Neurosci.* 23, 6460–6469 (2003).

21. Samuels, E. R. & Szabadi, E. Functional neuroanatomy of the noradrenergic locus coeruleus: its roles in the regulation of arousal and autonomic function part II: physiological and pharmacological manipulations and pathological alterations of locus coeruleus activity in humans. *Curr. Neuropharmacol.* 6, 254–285 (2008).
22. Von Coelln, R. et al. Loss of locus coeruleus neurons and reduced startle in parkin null mice. *Proc. Natl Acad. Sci. USA* 101, 10744–10749 (2004).
23. Szabadi, E. Modulation of physiological reflexes by pain: role of the locus coeruleus. *Front. Integr. Neurosci.* 6, 94 (2012).
24. Carter, M. E. et al. Tuning arousal with optogenetic modulation of locus coeruleus neurons. *Nat. Neurosci.* 13, 1526–1533 (2010).
25. Beckers, T. et al. Distinct pharmacological properties of second generation HDAC inhibitors with the benzamide or hydroxamate head group. *Int. J. Cancer* 121, 1138–1148 (2007).
26. Graff, J. et al. Epigenetic priming of memory updating during reconsolidation to attenuate remote fear memories. *Cell* 156, 261–276 (2014).
27. Akhtar, J. et al. TAF-ChIP: an ultra-low input approach for genome-wide chromatin immunoprecipitation assay. *Life Sci. Alliance* 2,e201900318 (2019).
28. Scammell, T. E., Arrigoni, E. & Lipton, J. O. Neural circuitry of wakefulness and sleep. *Neuron* 93, 747–765 (2017).
29. Borodovitsyna, O., Flamini, M. & Chandler, D. Noradrenergic modulation of cognition in health and disease. *Neural Plasticity* 2017, 6031478 (2017).
30. Wersinger, S. R. & Martin, L. B. Optimization of laboratory conditions for the study of social behavior. *ILAR J.* 50, 64–80 (2009).
31. Kim, Y. et al. Targeting the histone methyltransferase G9a activates imprinted genes and improves survival of a mouse model of Prader-Willi syndrome. *Nat. Med.* 23, 213–222 (2017).
32. Sanchez, G. J. et al. Genome-wide dose-dependent inhibition of histone deacetylases studies reveal their roles in enhancer remodeling and suppression of oncogenic super-enhancers. *Nucleic Acids Res.* 46, 1756–1776 (2018).
33. Huang, P. H., Plass, C. & Chen, C. S. Effects of histone deacetylase inhibitors on modulating H3K4 methylation marks—a novel cross-talk mechanism between histone-modifying enzymes. *Mol. Cell. Pharmacol.* 3, 39–43 (2011).
34. Calo, E. & Wysocka, J. Modification of enhancer chromatin: what, how, and why? *Mol. Cell* 49, 825–837 (2013).
35. Tang, H. M. et al. An epithelial marker promoter induction screen identifies histone deacetylase inhibitors to restore epithelial differentiation and abolishes anchorage independence growth in cancers. *Cell Death Discov.* 2, 16041 (2016).
36. Zhang, S., Fujita, Y., Matsuzaki, R. & Yamashita, T. Class I histone deacetylase (HDAC) inhibitor CI-994 promotes functional recovery following spinal cord injury. *Cell Death Dis.* 9, 460 (2018).
37. Franklin, K. B. J. & Paxinos, G. *Paxinos and Franklin's The Mouse Brain in Stereotaxic Coordinates* (2008).
38. Christel, C. J. et al. Versatile viral vector strategies for postscreening target validation and RNAi ON-target control. *J. Biomolecular Screen.* 20, 976–984 (2015).
39. Livak, K. J. & Schmittgen, T. D. Analysis of relative gene expression data using real-time quantitative PCR and the 2(-Delta Delta C(T)) method. *Methods* 25, 402–408 (2001).
40. Radyushkin, K. et al. Genetic ablation of the mammillary bodies in the Foxb1 mutant mouse leads to selective deficit of spatial working memory. *Eur. J. Neurosci.* 21, 219–229 (2005).
41. Subramaniam, M. et al. Mutant alpha-synuclein enhances firing frequencies in dopamine substantia nigra neurons by oxidative impairment of A-type potassium channels. *J. Neurosci.* 34, 13586–13599 (2014).
42. Liss, B. et al. Tuning pacemaker frequency of individual dopaminergic neurons by Kv4.3L and KChip3.1 transcription. *EMBO J.* 20, 5715–5724 (2001).
43. Paxinos, G. & Franklin, K. B. J. *The Mouse Brain in Stereotaxic Coordinates* (Academic Press, 2008).

Acknowledgements

The work was supported by the Deutsche Forschungsgemeinschaft (CRC 1193 and CRC 1080). Alexis Cooper was funded by a fellowship of the Focus Program Translational Neurosciences Mainz.

Author contributions

A.C. carried out most experiments and wrote parts of the manuscript; J.R,. S.u.S. and U.Z. have designed the project, supervised the experiments and wrote the paper; J.W. supervised and helped with the ChIP experiments; T.B. conducted the ChIP experiments; N.H. did the AAV infusions into the LC; S.J. conducted in vitro brain slice patch-clamp recordings of LC neurons; D.L.F.G. and K.R. helped with the behavior experiments; J.A. has established the low-input ChIP, F.L. provided the *Kcnk9*KO animals, S.S. helped with microscopy.

Competing interests

The authors declare no competing interests.

Additional information

Supplementary information is available for this paper at https://doi.org/10.1038/s41467- 019-13918-4.

Correspondence and requests for materials should be addressed to U.Z. or S.S. Peer review information *Nature Communications* thanks Nihar Jana and the other, anonymous, reviewer(s) for their contribution to the peer review of this work.

Reprints and permission information is available at http://www.nature.com/reprints

Publisher's note Springer Nature remains neutral with regard to jurisdictional claims in published maps and institutional affiliations.

2.2 Fecal miRNAs association with bacterial genome regulation and host inflammatory response system following chronic social stress exposure

Authors: **Tamer Butto**, Anna Wierczeiko, Malena dos Santos Guilherme, Nicolas Ruffini, Francesco Valeri, Jennifer Winter, Kristina Endres and Susanne Gerber

Manuscript in preparation

My contributions to this article are listed in section 4.2 Contributions to individual publications.

Fecal miRNA association with bacterial genome regulation and host inflammatory response system following chronic social stress exposure

Tamer Butto[1], Malena dos Santos Guilherme[3],Anna Wierczeiko[1,2], Francesco Valeri[3], Nicolas Ruffini[1,2], Jennifer Winter[1,2], Kristina Endres[2,3]*and Susanne Gerber[1]*

[1]Institute for Human Genetics, University Medical Center of the Johannes Gutenberg-University Mainz, Mainz, Germany

[2] Leibniz Institute for Resilience Research (LIR), Mainz, Germany

[3]Department of Psychiatry and Psychotherapy, University Medical Center of the Johannes Gutenberg-University Mainz, Mainz, Germany

* contributed equally

Abstract

In recent years, several studies have shown a connection between the composition of the microbiota, the sum of all microbial populations in an organism, and the appearance of various neurological and mood-related disorders. The regulation of microRNAs (miR) was suggested to play a role in the interaction between the host and its gut microbiota; however, the means of communication between these two systems is still largely unknown. Here, we investigated this connection in relation to behavioral resilience to chronic social stress in female mice. Following behavioral assessment, we applied small RNA-seq to determine the level of fecal miRNA in each behavioral condition. We mapped all differentially expressed miRNAs to over 1500 bacterial genomes in order to determine possible connections between the host and the bacteria. From our analysis, we identified group-specific differentially expressed miRNAs (DEMs) associated with each behavioral group. Moreover, within the identified DEMs, six miRNAs (miR-194-2-5p, miR24-1-3p, miR200a-3p, miR215-5p, miR126a-3p, and let7f-1) showed robust sequence alignment correlation with multiple bacterial genomes. Interestingly, 4 of the six candidates, particularly miR-194-2-5p and miR200a-3p, have been associated to the miRNA-microbiota communication network and regulation of the inflammatory response system through the NF-kB pathway (i.e., IL1β, TNFα). These associations could provide a novel avenue in the understanding of miRNAs as building blocks for bacteria-host cross-talk as well as their probable involvement in the stress response system of the host.

Introduction

The gut microbiome comprises all microbial communities inhabiting the gut, living in a dynamic symbiotic relationship within and with the host (Chang and Kao 2019). Such communities produce and secrete a wide variety of metabolites including small molecules that ultimately may influence the host cellular activity and modulate various cellular systems such as neuroendocrine system and the immune system (Kim et al. 2017). This dynamic cross-talk provides an enormous potential for cellular regulation mediated by the gut microbiota's composition and the repertoire of secreted molecules (Rooks and Garret 2016).

In recent years, several studies have shown a strong connection between the composition of the gut microbiota and the appearance of various disorders that before have been seen as CNS-centered such as neurological and mood-related disorders (Jiang et al. 2015, Dinan and Cryan 2017, Rogers et al. 2016, Misiak et al. 2020). The gut microbiome influences the

regulation of key neurotransmitters such as serotonin (Yano et al. 2015, Kelly et al. 2015, Mittal et al. 2017), the inflammatory response system (Wong et al. 2016, Belkaid and Hand 2014, Lazar et al. 2018), and various behavioral phenotypes in response to stress (Palma et al. 2015, Zheng et al. 2016, Bridgewater et al. 2017). This connection links the gut-brain axis to a much broader extent of neurological and behavioral regulation through the enteric nervous system and the neuroendocrine systems.

The dynamic signal interchange between the host and the microbial community has raised several questions regarding the forms of communication between the bacteria and host cells. For instance, metabolites and small molecules released by the microbes interact with host cellular receptors leading to endogenous pathway motion followed by host cellular response and adaptation (Den Besten et al. 2013, Burokas et al. 2017). A more novel theory suggests that distinct forms of nucleic acids can be used as messengers between the host and the various bacterial species (Vojinovic et al. 2019). It has been proposed that miRNA and other small non-coding RNAs could mediate the connection between the bacteria and host transcriptional regulation (Williams et al. 2017).

miRNAs are known to influence gene expression in eukaryotic organisms (Gurtan and Sharp 2013) and to some extent, affect bacterial gene regulation (Liu et al. 2016, Zhou, Li and Wu 2018). Recent studies have shown the involvement of miRNAs in the regulation of mitochondria (Purohit and Saini 2020, Fan et al. 2019, Jeong et al. 2017, Indrieri et al. 2019) and chloroplasts (Ruwe and Schmitz-Linnweber 2012, Fang et al. 2019) suggesting an evolutionally conserved mechanism as part of the endosymbiont theory (Archibald 2015). However, the intersection between bacterial gene regulation and miRNAs (or miRNA-like molecules) is still poorly understood.

This study explores the connection between fecal small RNAs and their potential role in bacterial transcriptional regulation following stress exposure. Using small RNA-seq, we identified group-specific miRNAs associated with resilience or susceptibility to chronic social stress elicited by denial of a stable group hierarchy in female mice. Following a bacterial-miRNA alignment strategy (Hewel et al. 2019), we identified six miRNAs with large hit number with a variety of bacterial genomes. Interestingly, following a brief literature review we identified multiple studies connecting these candidates with regulation of several components of the inflammatory response system, which are also known to be altered by stress (Glaser and Kiecolt-Glaser 2005). Ultimately, we provide a novel connection between specific miRNAs and several bacterial cell population which could be induced by chronic social stress.

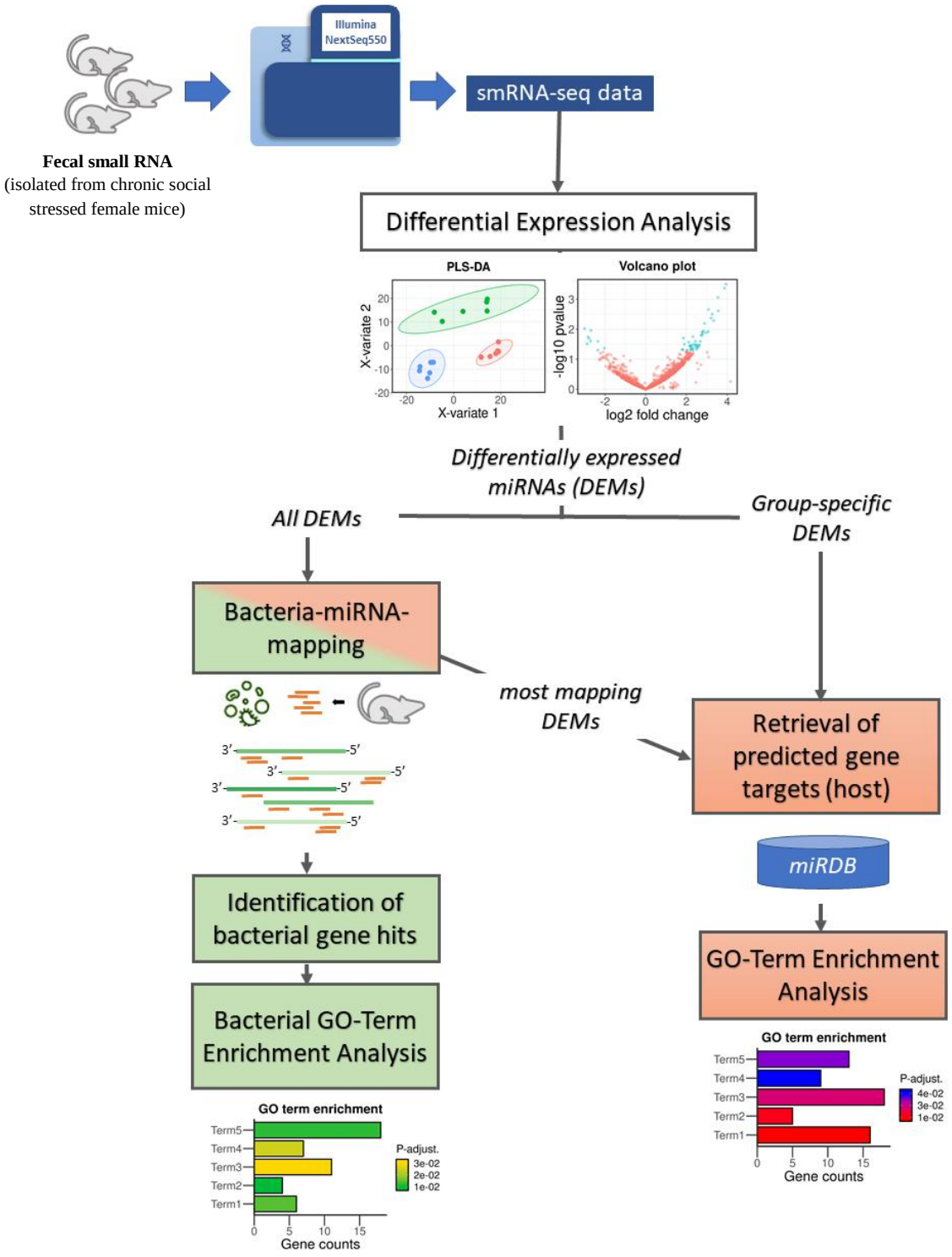

Graphical abstract. Strategy for miRNA association for both host and bacterial gene regulation following chronic social stress (CSS). Small RNA-seq used to identify faecal differential expressed miRNA (DEMs). We applied miRNA-bacterial association analyses to identify bacterial pathways affected by DEMs.

Results

3.1 Chronic social stress (CSS) elicits gastrointestinal effects in female mice

Female Arc-sGFP mice aged four weeks were group-housed in cages of four animals. The control mice were kept in this initial composition of individuals for another seven weeks, while the to be stressed animals received a two-time shuffling per week with the aim of only few repeated encounters of individuals as described previously (For an overview see Figure 1a).

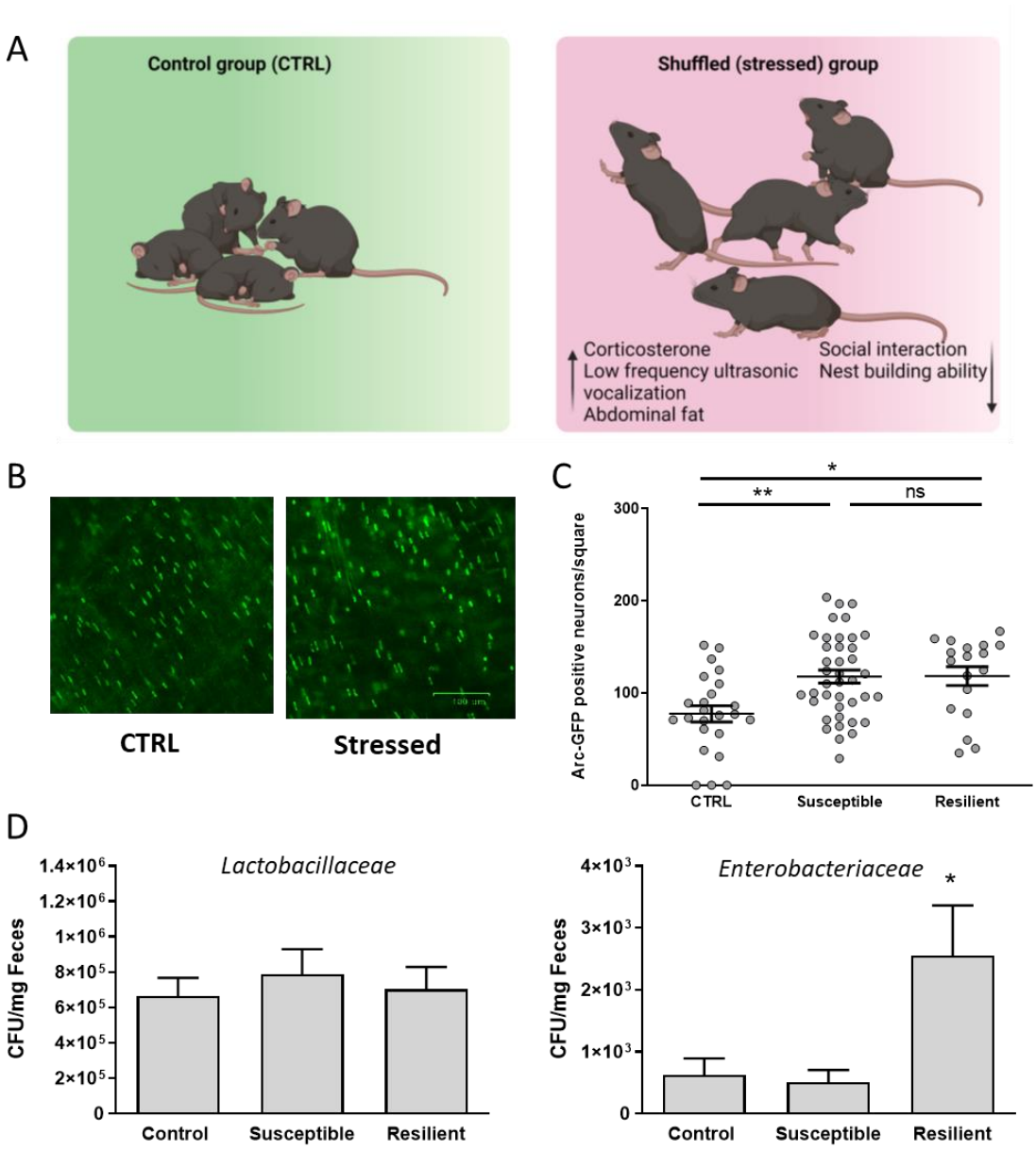

Figure 1. Effects of CSS on gut properties in female mice. A. Female Arc-sfGFP mice were subjected to chronic stress via group shuffling over seven weeks as described in (Ref). Thereby, animals displayed several signs of stress such as elevated serum corticosterone levels (Figure designed with Biorender). B. Animals were sacrificed about one week after the last shuffling. Tamoxifen was administered 9 h before the social interaction test was conducted to stratify for resilient and susceptible animals. This labels all neurons with Arc promoter activity via sGFP expression.

Continue of figure legends

Colonic longitudinal muscular layers with attached Myenteric plexus were prepared and sGFP visualized by green fluorescence. Scale bar: 100 µm. Exemplary specimen from a control and a stressed individual are shown. C. sGFP positive neurons were counted in three squares from two independent images per mouse (n=4 for resilient, 7 for susceptible and 5 for control). D. To assess potential changes in microbiota, viable individuals from two exemplary families – *Enterobacteriaceae* and *Lactobacillaceae* - were counted after plating fecal suspensions on respective selective plates (CFU: colony forming units). Six animals per group were used despite Enterobacteriaceae counting in susceptible animals (n=5). Statistical analysis was performed by one-way ANOVA with Dunnett's post-test.

Efficacy of the stress paradigm and the ability to stratify resilient and susceptible individuals via social interaction test has been described recently for the here used mouse strain (Ref.). Physiological parameters and behavioural response was comparable to similar approaches with other paradigms or other mouse strains (e.g. Schmitt et al., 2010). However, we here – to our knowledge – for the first time describe selective targeting of chronic social stress-induced activated neurons within the gut. In both, resilient and susceptible animals, social stress resulted in significantly enhanced Arc promoter activity in the Myenteric plexus, which was manifested as sGFP expression after Tamoxifen-injection (Figure 1 B and C). This indicates that social stress indeed evokes an altered enteric nervous system activity. Moreover, quantitative analysis of exemplary viable bacteria revealed that besides the host's own cells, changes in microbiota occur. Here, we identified an increase in viable fecal *Enterobacteriaceae* selectively in resilient individuals while *Lactobacillaceae* were not affected (Figure 1 D). By this, the question rises if host and microbiota might be independently affected by stress exposure or if a bilateral communication along the environmental challenge leads to these observations. One probable tool for the inter-species communication might be given by host-excreted miRNAs.

3.2 Small RNA-seq reveals group specific fecal miRNAs associated with stress resilience

To uncover whether the composition of fecal miRNAs changes upon stress exposure, we isolated RNA (small and large RNA fractions) from fecal samples of resilient and susceptible mice following chronic social stress (CSS) as well as control mice. Using the small RNA fractions, small RNA libraries were prepared, sequenced, and subsequently mapped to the mature miRNA sequences from miRBase (Kizinara, Birgaoanu and Griffiths-Jones 2019). After normalization and filtering the mapped reads, 1999 miRNAs revealed expression levels with nonzero total read counts. To determine the strength of the three groups' classification of mice (control, resilient, and susceptible) based on their miRNA expression, we performed a Partial Least Squared Discriminant Analysis, as visualized in Figure 2A. While the first component (x-axis) clearly separated the unstressed mice (control group) from the stressed animals, the behavioural difference between resilience and susceptibility was predominantly divided by the second component (y-axis).

A subsequent differential expression analyses revealed 78 differentially expressed miRNAs (DEMs) after performing all pairwise comparisons ($p < 0.05$, $|\text{fold change}| > 1.5$) (Supplementary Figure 1, Supplementary Table 1). Out of these miRNAs, 48were found to be differentially expressed in resilient vs. control animals (Figure 2B, Supplementary Figure 2A-C). Amongst these, six DEMs were downregulated and 42 upregulated. 25 DEMs were observed when comparing susceptible with control mice (7 downregulated; 18 upregulated) and 26 DEMs revealed significance in resilient vs. susceptible mice (5 downregulated; 21 upregulated).

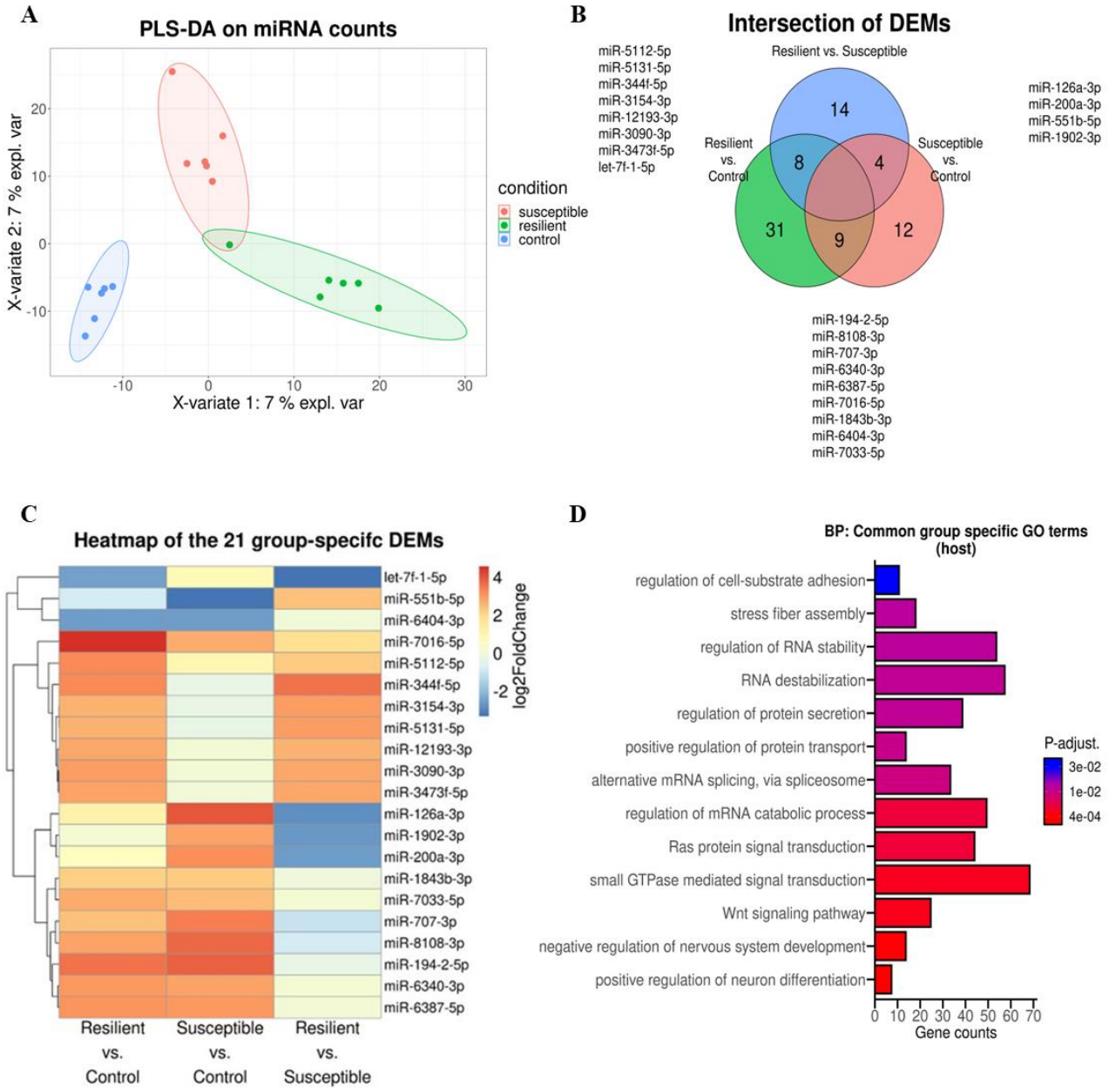

Figure 2. Fecal small RNA-seq following CSS in female mice. A. Partial Least Squared Discriminant Analysis (PLS-DA) on miRNA counts of control (blue; n=6), resilient (green; n=6) and susceptible (red; n=6) samples. B. Venn diagram of 78 differentially expressed miRNAs (DEMs) between resilient vs Control, susceptible vs control and resilience vs susceptible groups. C. Heatmap of the 21 group specific DEMs represented with log2FoldChange D. Common group specific GO term enrichment analysis. GO term highlights the biological processes enriched by predicted target genes associated with the identified fecal miRNAs

The intersection of DEMs from the different combinations indicated a group-specific miRNA regulation (Figure 2B). In other words, miRNAs found both in the comparison of resilient vs. susceptible as well as between resilient vs. control mice were classified as resilient-specific DEMs. Thus, the DEMs were subdivided into 8 resilient-specific (7 upregulated; 1 downregulated), 4 susceptible-specific (3 upregulated; 1 downregulated), and 9 stress-specific miRNAs (1 upregulated and 8 downregulated) (Figure 2C) and used for subsequent analyses (Figure 2B, Supplementary Figure 1).

In eukaryotic organisms, miRNAs are predominantly known for their role in transcriptional regulation. Therefore, we were interested in the predicted gene targets that might be affected by the group-specific miRNAs. Using the miRNA gene target database mirDB (Chen and Wang 2020), we identified mouse gene targets for each of our group-specific miRNAs derived from feces. Based on these genes, we subsequently performed a Gene Ontology (GO) term enrichment analysis to gain functional insights into the regulation of the group-specific miRNAs in the host's gut. The gene target prediction analysis yielded 1107 targets for resilient-specific, 697 target genes for susceptible- specific, and 2512 target genes for stress-specific miRNAs using the recommended minimum prediction score of 80 as suggested by Chen and Wang (2020). The resulting list of all targets is provided in the supplementary material (Supplementary Table 3).

The GO enrichment analysis of the predicted gene targets revealed unique and shared GO terms among the group-specific miRNAs (Supplementary Table 4). Notably, several overrepresented GO terms were enriched for mechanisms such as "regulation of RNA stability" (avg. p-adjust. = 0.0154) and "Small GTPase mediated signal transduction" (avg. p-adjust. = 2.17e-03) (Figure 2D, Supplementary Table 4). Interestingly, such mechanisms are shared by both host and bacteria and could be a potential source of interaction between the two systems (Popoff 2014, Wang et al. 2018, Spano and Galan 2018). Additionally, neuron-associated GO terms emerged in all three groups, which might reflect a possible role of the identified miRNAs in regulating parts of the nervous system (Supplementary Table 4).

Unique group-specific genes were significantly involved in immune-related mechanisms such as "lymphocyte differentiation" (p-adjust. = 1.18e-04, resilient specific), "negative regulation of I-kappaB kinase/NF-kappaB signaling" (p-adjust. = 0.038, susceptible specific) and "cellular response to extracellular stimulus" (p-adjust. = 8.49e-04, stress-specific) (Supplementary Figure 2D-F, Supplementary Table 4). This clearly indicates that the host's organism reacts to stress in general via a distinct miRNA pattern but also according to its behavioral classification. In order to unravel a potential association between the identified miRNAs and bacterial transcriptional regulation, we next investigated possible targets of differentially expressed miRNAs within bacterial genomes.

3.3 miRNA-bacterial genome alignment strategy reveals six miRNAs associated with bacterial genomes

Recently, specific miRNAs' association with neurodegenerative diseases such as Alzheimer's or Parkinson's disease and their potential role in bacterial transcriptional regulation has been reported (Hewel et al. 2019). Here, we investigated miRNA-bacterial interaction with those miRNAs found to be differentially expressed upon chronic social stress using a similar strategy (Figure 3A).

Following the miRNA-bacteria mapping, we were able to identify six miRNA candidates showing a high number of potential target sites on the bacterial genome (>4,000 hits) of over 300 distinct bacterial taxa (Figure 3B, Supplementary Table 5). These miRNAs include miR-194-2-5p, miR24-1-3p, miR200a-3p, miR215-5p, miR126a-3p and let7f-1-5p. The analysis of phyla distribution across the six candidates revealed that more than 65 % of the hits were located across Proteobacteria and Firmicutes (Figure 3C). Firmicutes contained the highest number of different species with miRNA hits (Supplementary Table 5, Figure 4A). Among the top hits, *Escherichia coli* (*E. coli*, Proteobacteria) revealed to be the species with the highest number of miRNA mappings across the six candidates (Figure 3D, Figure 4B).

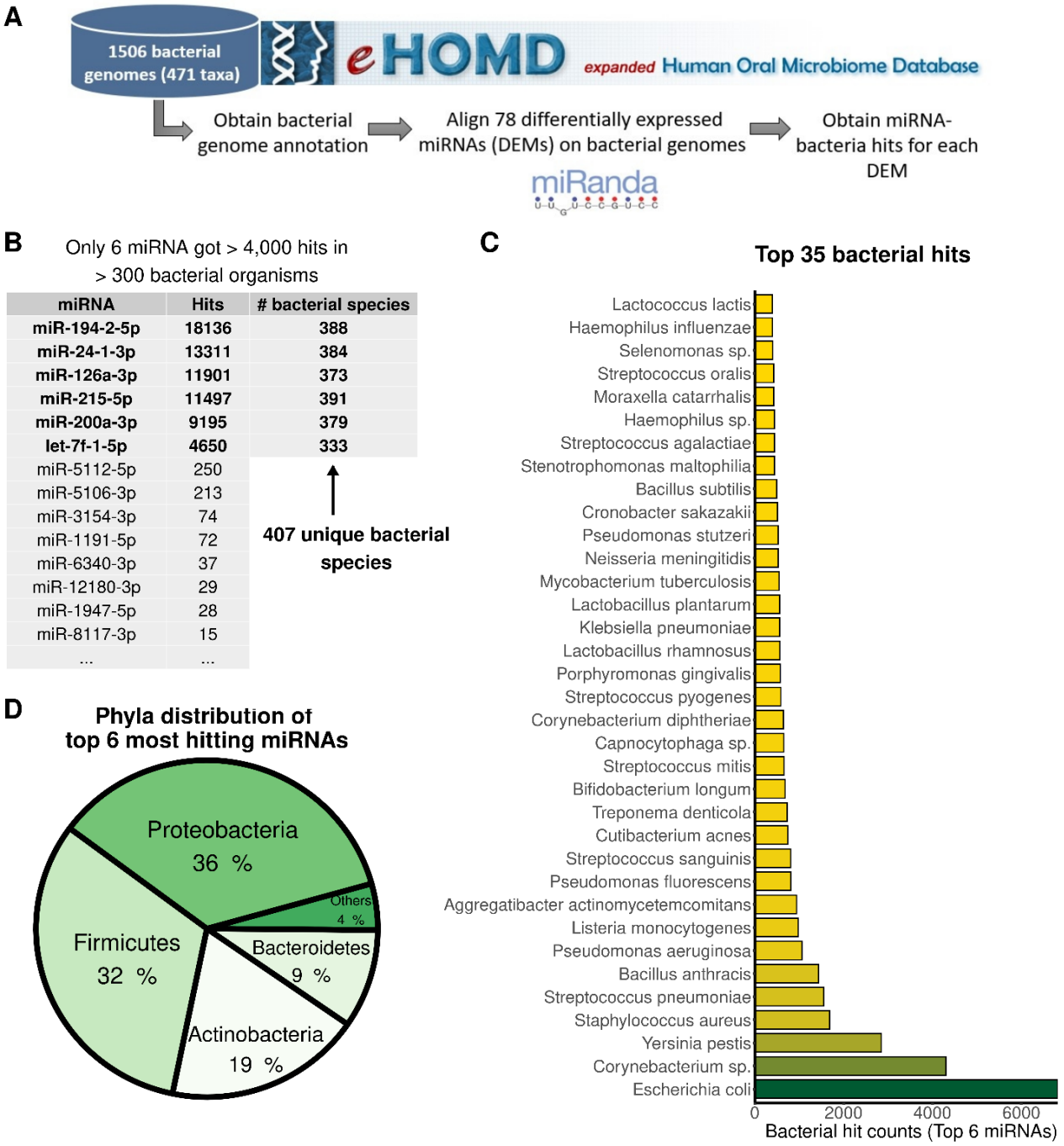

Figure 3. Retrieval of miRNA-bacteria aligned candidates. A. miRNA-bacterial genome alignment strategy. Bacterial genomes from the Human Oral Microbiome database following miRNA-bacteria alignment using miRanda. B. Six miRNA were identified to have >4,000 hits in several bacterial genomes. C. Phyla distribution of the top six miRNA candidates. D. Top 35 bacterial species with the most identified hit counts for the six miRNAs.

Subsequently, we examined the miRNA-bacteria hits for annotated genes by overlapping the matching positions with the respective bacterial gene annotations from NCBI (see material and methods). The miRNA-bacterial-gene target analysis revealed many genes located at the detected miRNA-bacteria mappings (Supplementary Table 6). Even though, Firmicutes had the largest number of taxa per phylum (Figure 4A), unique gene identifiers revealed a higher hit number among Proteobacteria (Figure 4C). This is probably due to their large number of annotations in general, especially for *E. coli* (Figure 4B).

To validate the levels of the six identified miRNAs that were mostly to be relevant in host-bacteria communication under stress condition, we performed qRT-PCR to quantify the relative expression of the fecal miRNA candidates. Of the six candidates, fecal miR200a revealed a significant upregulation between susceptible mice compared to control ($p = 0.0029$) while miR194-2 and miR24-1 revealed only an upregulation tendency between similar behavioral conditions (Figure 4D-I). To gain insight into the source of origin of the fecal miRNAs, we also investigated miRNA levels in the corresponding colonic tissue stretches from where the fecal pellets have been extracted. However, we did not detect similar tendencies or elevated amount as in the case of miR200a within the respective tissue (Supplementary Figure 3).

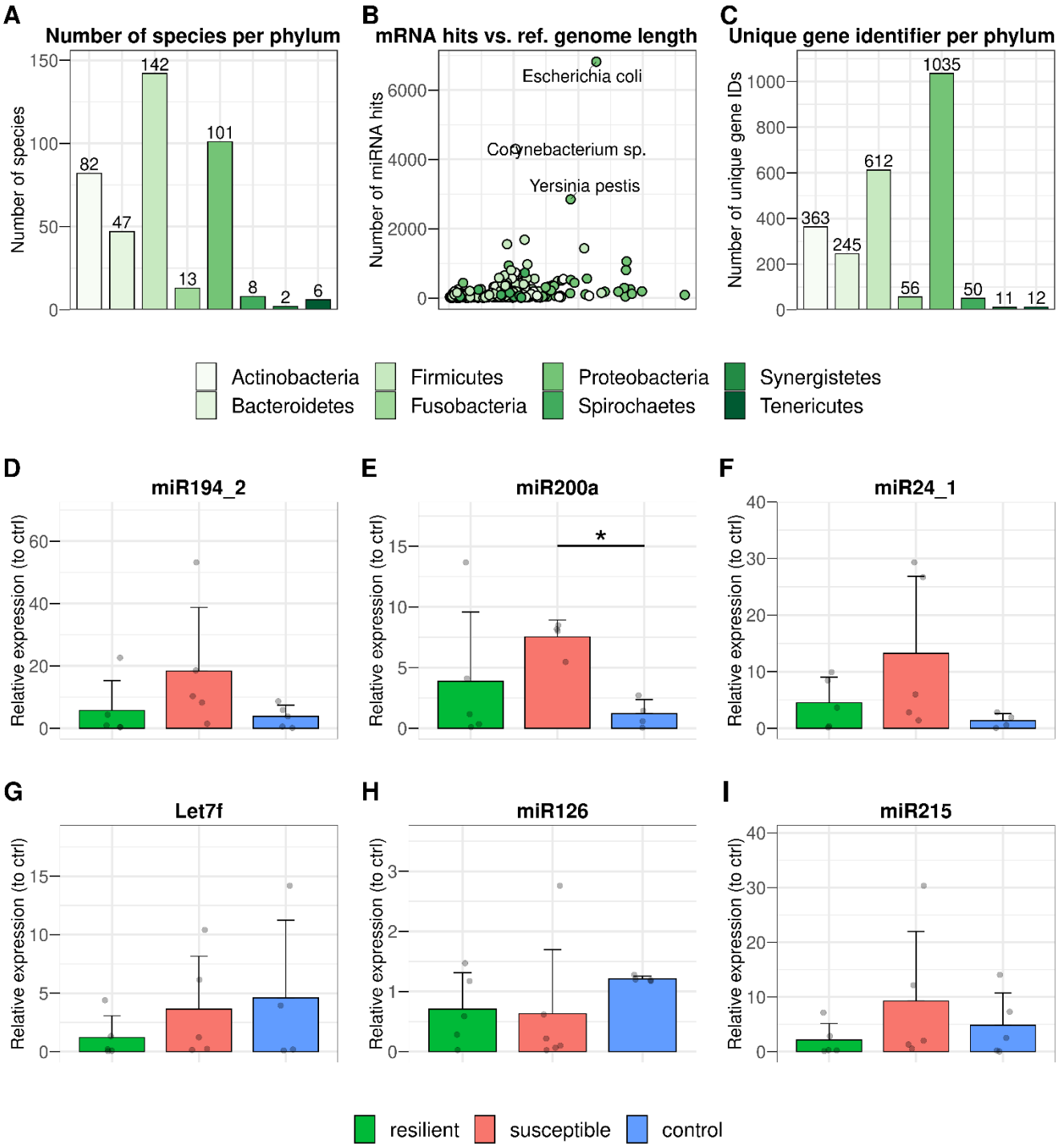

Figure 4. miRNA-bacterial gene hits per phyla and quantification of top six fecal miRNA using qPCR. A) Number of bacterial species per phylum. B) classification of miRNA hit per reference genome size C)Number of bacterial genes hit classified per phyla. Bacterial phyla legend is related to A, B and C. D-J. miRNA relative expression of identified candidates in fecal samples of resilient, susceptible and control mice. D. miR194-2 (Sus vs Con, pval=0.089, ns; Res vs Sus, 0.089, ns; n=5,5,5) E. miR200a (Sus vs Con, pval=0.029, *P<0.05; n=5,4,4) F. miR24-1 (Sus vs Con, pval=0.071, ns; n=5,5,5). G. Let7f (n=5,5,4) H. miR126 (Suc vs Con pval=0.054, ns; n=5,6,4) I. miR215 (n=5,5,5). Data represnsents mean values and error bars represent ±S.E.M

3.4 Predicted bacterial and host gene targets associated with fecal miRNA candidates and behavioral groups.

In order to identify functionalities possibly influenced by the binding of miRNA on bacterial gene sequences, we performed a global GO term enrichment analysis of bacterial species using the Uniprot database for available GO term annotations of bacterial genes. The bacterial gene targets of the top six most mapping miRNAs revealed significantly overrepresented GO terms of the Biological Process (BP) category including "regulation of transcription, DNA-templated" (p-adjust. = 3.53e-10), "response to antibiotic" (p-adjust. = 2.72e-07), and "SOS response" (p-adjust. = 3.46e-10) (Figure 5A, Supplementary Table 7). These findings suggest that the specific miRNAs could be involved in bacterial transcriptional regulation of cellular defense and adaptation mechanisms in response to environmental alterations.

We analyzed the predicted gene targets for the six candidate miRNAs in the host and identified their respective enriched GO terms (Supplementary Table 8). Here, we found host overrepresented GO terms involved in neuronal processes like "synapse organization" (p-adjust. = 1.64e-04), "negative regulation of neuron differentiation" (p-adjust. = 1.79e-03) and "signal release from synapse" (p-adjust. = 9.75e-04) (Figure 5B, Supplementary Table 9). Furthermore, "Ras protein signal transduction" (p-adjust. = 2.34e-05), "regulation of RNA stability" (p-adjust. = 2.49e-03) and "stress-activated MAPK cascade" (p-adjust. = 9.75e-04) revealed to be overrepresented for the predicted host target genes of the six miRNAs. These results indicate that the most mapping miRNAs derived from feces might be able to influence genes involved in host RNA processes as well as neuronal functionalities influenced by stress (Muller et al. 2020)

Additionally, we performed a GO-network analysis using ShinyGO (Ge, Jung and Yao 2020) to visualize the molecular network associations of selected bacterial GO terms and in order to identify potential shared mechanisms. For this, we used the gene targets of three selected GO terms including "response to antibiotic", "SOS response" and "carbohydrate derivative metabolic processes" which we termed as Modules I, II and III, respectively (Figure 5A,C). Following the generation of the ShinyGO network map, we identified one enriched GO term, "response to stimulus", from module I that contains gene targets that overlapped with the other modules. These results suggest that these gene sets are part of a pathway involved in bacterial cellular adaptation in response to external stimuli (Figure 5C).

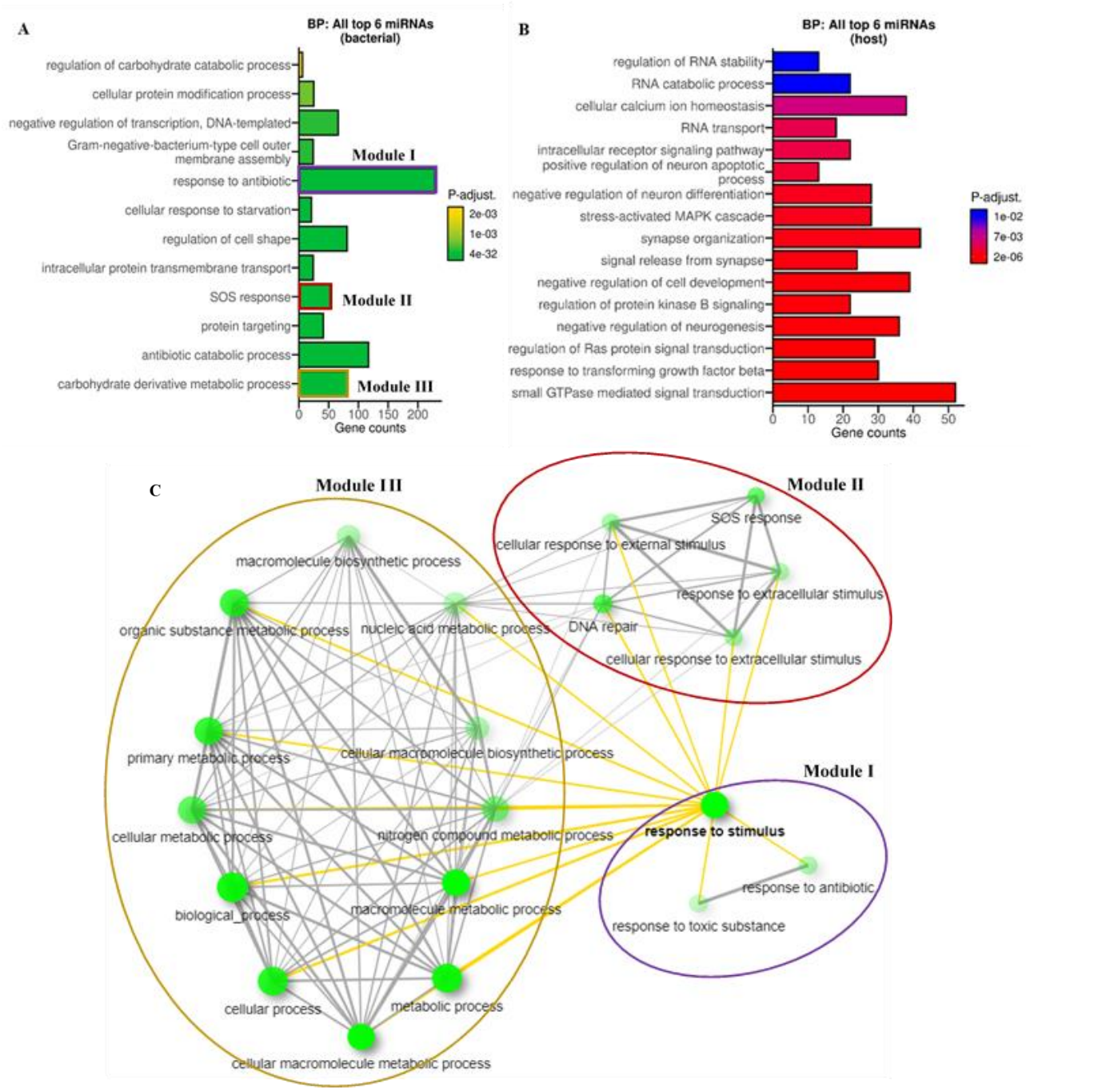

Figure 5. GO terms analysis of common predicted genes enriched for the top six miRNAs in host and bacteria. A. Bacterial GO term enrichment for the combined 6 miRNAs predicted-genes. B. Host GO term enrichment for the combined 6 miRNAs predicted-genes. C) ShinyGO network plot showing the relationship between enriched pathways within the three selected modules from bacterial GO terms in (A). Two pathways (nodes) are connected if they share 20% or more genes. Darker green nodes are more significantly enriched gene sets; bigger nodes represent larger gene sets; thicker edges represent more overlapped genes.

Next, we assessed the bacterial gene targets of the group-specific miRNAs to identify the mechanisms associated with each behavioral group among the bacterial populations (Supplementary Table 10). Here, we observed several bacterial cellular stress-related mechanisms within all group-specific BP terms, including "protein repair" (p-adjust. = 3.14e-17, resilient-specific), "response to antibiotic" (p-adjust. = 3.41e-30, susceptible-specific), and "regulation of transcription, DNA-templated" (p-adjust. = 9.23e-56, stress-specific) (Supplementary Table 11). Using ShinyGO analysis on group specific

enriched GO terms to identify the broader network of associated bacterial gene targets in each behavioral condition (Figure 6). Here, we used the target genes of the most significant and highest gene count of group-specific GO term as input in order to identify shared genes and additional mechanisms associated with selected GO term. The term "protein repair" (resilient-specific) revealed processes associated with "response to oxidative stress" (FDR = 0.0004) and more generally "response to stress" (FDR = 0.003) (Fig 6D) whereas the term "response antibiotic" (susceptible specific), revealed processes associated with "response to chemical" (FDR = 1.01E-19), "response to toxic substance" (FDR = 3.14E-21) and "response to stimulus" (FDR = 3.75E-15) (Fig 7E). The term "regulation of transcription-DNA templated" (stressed-specific) revealed processes associated with "regulation of RNA metabolic processes" (FDR = 1.09E-110) and "regulation of nucleobase-containing compound metabolic processes" (FDR = 7.48E-110) (Fig 6F).

Taken these observations together, our identified miRNA candidates are frequently associated with bacterial gene targets involved in "response to stimulus", "regulation of transcription", and defense mechanisms such as "SOS response" and "DNA repair". All these might suggest a possible pathway by which bacteria adapt to the cellular and environmental alteration occurring within the host. These alterations could be a result of host cells immune activation in response to stress where the bacterial populations attempt to adjust to the gut-related alterations and the identified miRNAs could mediate this communication.

3.5 miRNAs candidates involved in inflammation modulation

To uncover reported associations between the identified miRNAs, bacterial regulation, and potential shared mechanisms with stress-exposure we conducted a literature survey (Supplementary Table 1). We identified that a large number of studies linked these miRNAs with inflammatory response system mainly following exposure to bacterial lipopolysaccharides (LPS) (Supplementary table 1). Overall, most of the publications associated the candidate miRNAs with decreased inflammation through NF-kB inhibition or suppressing inflammatory cytokines such as IL1β and TNFα. Additionally, a previous study has demonstrated that commensal bacteria can induce the expression of IL1β mRNA leading to intestinal inflammation (Seo et al. 2015). Therefore, we opted to test the levels of IL1β in fecal RNA samples (large fragments including mRNA preparation) and included TNFα to assess the differences between the behavioral groups. We analyzed both, feces and colonic tissue RNA samples. Here we identified a significant elevation of fecal IL1β mRNA levels in the resilient group as compared to the susceptible (*$p<0.05$) and control group (*$p<0.05$). We did not detect similar tendencies of mRNA expression in the colon RNA samples (Supplementary Figure 4A).Similarly we did not detect significant difference in TNFα level in fecal and colon samples. These results suggest that stress exposure is associated with increased presence of IL1β mRNA in the feces, particularly of resilient mice.

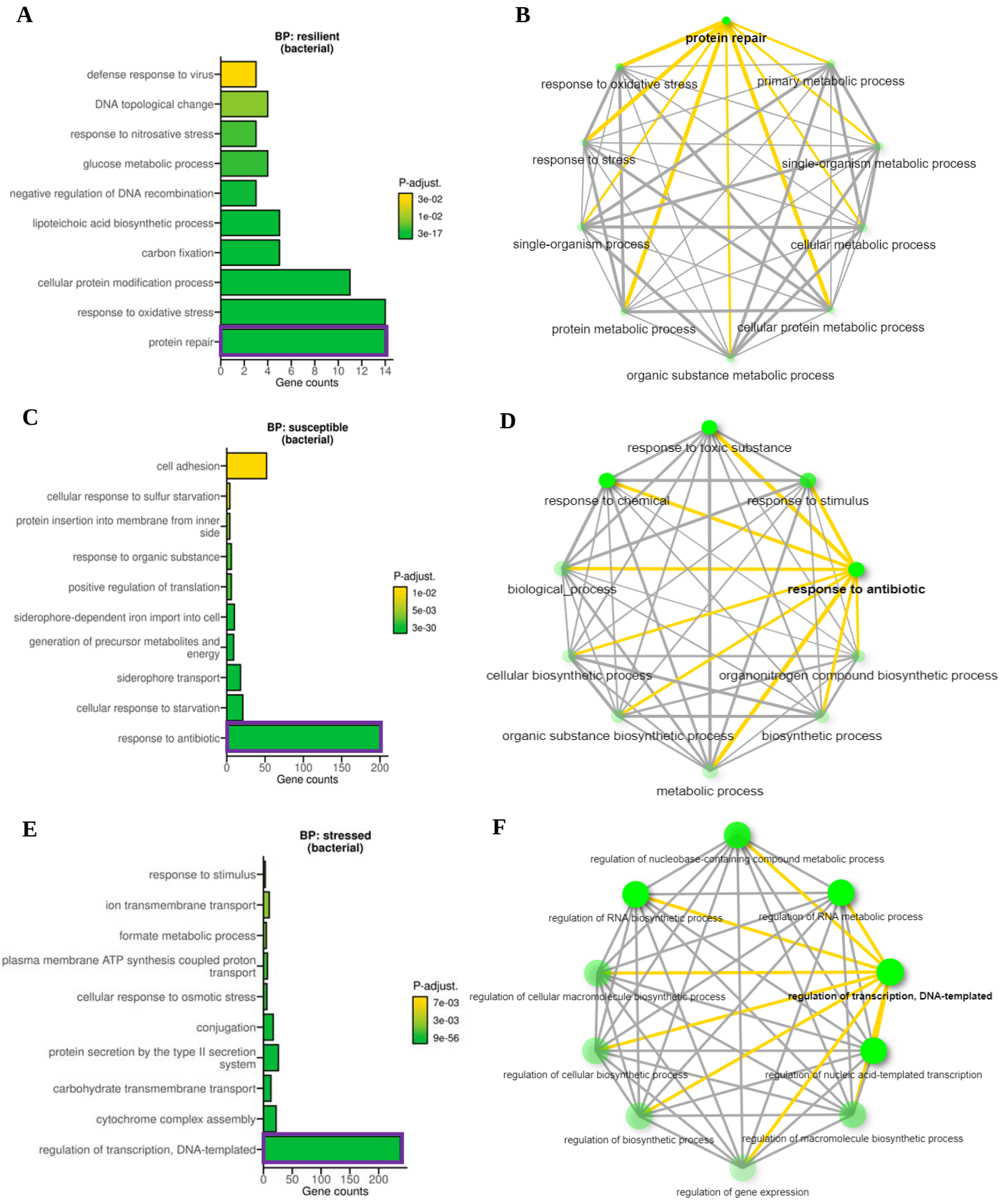

Figure 6. GO terms analysis of predicted genes enriched for group-specific in bacteria. A-B. Bacterial GO term enrichment for resilient-specific targeted genes (A) and associated network for "protein specific" term (B). **C-D.** Bacterial GO term enrichment for susceptible-specific targeted genes and associated network for "response to antibiotic" term (D). **E-F.** Bacterial GO term enrichment for stress-specific targeted genes (E) and associated network for "regulation of transcription, DNA-templated" term (F).

Previous studies had investigated the role of host miRNA processing machinery and microbiota composition on the reoccurrence of specific fecal miRNAs (Liu et al. 2016, Viennois et al. 2019). For instance, Liu and colleagues (2016) used miRNA-deficient mice (Dicer1(ΔIEC/ΔHopx)) to identify both, fecal miRNAs and bacterial composition alterations. In contrast, Viennois and colleagues (2019) investigated microbiota composition's role comparing fecal miRNA of wild-type and germ-free mice. For this, we obtained the relative miRNA levels detected in Dicer1fl/fl and Dicer1ΔIEC mice feces from Liu et al. 2016 and the differentially expressed miRNAs in GF vs. Conventional mice from Viennois et al. 2019. Following an intersection analysis of the differentially expressed miRNAs between the studies, four of our miRNA candidates (miR-194-5p, miR24-3p, miR200a-3p, and let-7f) were shown to be differentially expressed in at least one of the other data sets. At the same time, miR-194 and miR-200a were intersected in all data sets (Fig. 7C). More detailed information revealing the respective expression changes between our study and the reported studies is displayed in Table 2. The fact that these miRNAs were unexpectedly identified in our miRNA-bacterial-genome alignment strategy, as well as reported in miRNA machinery deficiency (Liu et al. 2016) and microbiota composition alterations (Viennois et al. 2019) suggests that these miRNAs might be involved in host-bacterial cell communication.

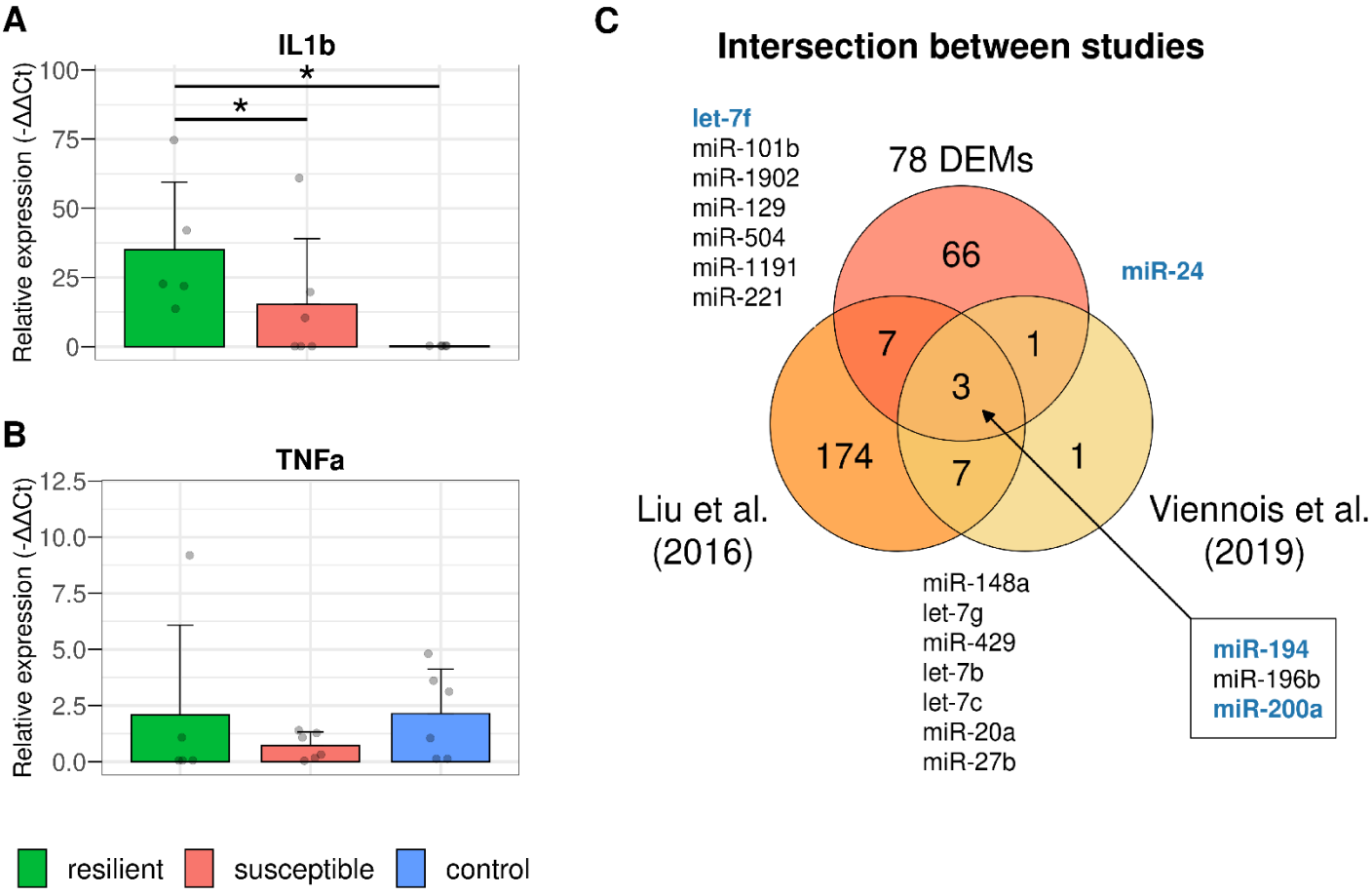

Figure 7. Association of identified fecal miRNAs with microbiota composition. A. qPCR quantification of TNFα transcript in fecal RNA from resilient, susceptible and control mice. B. qPCR quantification of IL1β transcript in fecal RNA from resilient, susceptible and control mice. C. Venn diagram of intersected DE miRNAs appearing in Liu et al. 2016, Viennois et al. 2019 and our study.

Discussion

An increasing number of studies is shifting the focus of investigation towards the brain-gut axis (Dinan and Cryan 2017, Fung, Olson and Hsiao 2017, Cussoto et al. 2018, Molina-Torres et al. 2019) and, more specifically, the relationship between gut microbiota and the manifestation of mood-related disorders (Zheng et al. 2016, Wong et al. 2016, Huang et al. 2019, Yang et al. 2019, Zhang et al. 2019). The gut microbiome composition has been shown to have an enormous potential to alternate behavioral and neurological phenotypes (Burokas et al. 2017, Yang et. al 2017, Huang et al. 2019, Lukić et al. 2019). However, the cross-talk between bacterial-host cells is still not fully understood, particularly in the context of stress exposure.

This study presents a link between gut microbiota and miRNA regulation concerning behavioral resilience to chronic social stress (CSS). Using small RNA-seq, we identified fecal miRNAs candidates associated with specific behavioral phenotypes. Unique group-specific GO term analysis revealed enrichment of genes involved in immune-related processes such as "lymphocyte differentiation" (resilient specific) and "negative regulation of I-kappaB kinase/NF-kappaB signaling" (susceptible specific). Such mechanisms reflect the influence of stress on immune response systems represented in the fecal miRNA predicted gene targets.

As part of our study, we were interested in the possible connection between miRNAs and bacterial transcriptional regulation using a previously reported miRNA-bacterial alignment strategy (Hewel et al. 2019). This strategy relies not only on miRNA-bacterial sequence complementation but also on free energy (ΔG) calculations to estimate the physical interaction between two complementary sequences, thus obtaining the most energetically favorable candidates. We reason that such features are essential for the potential role of miRNA-bacterial genome interaction, which relies on both, sequence complementation and kinetically favorable binding energy (Enright et al., 2003). Surprisingly, we identified six candidates (miR-194-2-5p, miR24-1-3p, miR200a-3p, miR215-5p, miR126a-3p, and let7f-1-5p) with a high number of hits within the bacterial genomes compared to all other hitting miRNAs. We were able to validate the expression of fecal miR200a in susceptible mice compared to controls via qPCR where miRNA194-2 and miR24-1 revealed only a tendency. However, at this stage, the individual potential role of each miRNA in bacterial gene regulation is still unknown.

Despite the notion that prokaryotic organisms are unlikely to possess miRNA regulation mechanisms (Watkins and Arya et al. 2019), the association between miRNAs and bacterial gene regulation is gradually being investigated (Liu et al. 2016, Williams et al. 2017, Zhou, Li, and Wu 2018, Hewel et al, 2019). We reasoned that miRNA-bacterial gene sequence complementation could provide valuable information about the role of specific miRNAs (or miRNA-like molecules) in bacterial gene regulation and activity. GO term analysis of miRNA-bacterial gene targets revealed enrichment of mechanisms such as "SOS response" and "response to antibiotic". Interestingly, such GO terms are part of the bacterial defense mechanisms often influenced by extracellular stimulus allowing them to adapt to fluctuating environments. For instance, SOS response system consists of various factors involved in error prone DNA repair mechanisms which induce phenotypic changes and ultimately allowing the survival of bacteria at a cost of elevated mutagenesis (Baharoglu and Mazel 2014, Maslowaska et al. 2018). Additionally, analysis of the group specific bacterial gene targets and enriched GO terms revealed mechanisms such as "regulation of transcription" and "nucleobase-containing compound metabolic processes" that could be altered by the presence of specific miRNAs candidates. This identified system could elucidate a dynamic network that is constantly influenced by the host cellular activity, and potentially mediated by small RNAs such miRNAs.

Interestingly, two of our miRNA candidates (miR200a-3p and miR-194-2-5p) were reported to be differentially expressed in both previously investigated fecal miRNA analyses (Liu et al. 2016, Viennois et al. 2019). Liu and colleagues (2016) demonstrated that manipulation of host miRNA processing machinery, using Dicer (ΔIEC , ΔHopx) mice, resulted in gut dysbiosis and thereby, indicating an unspecific role of miRNAs in regulating the gut microbiome (Liu et al. 2016). An additional study by Viennois and colleagues (2019) demonstrated how the presence of distinct gut microbiome of WT (Conventional) and germ-free (GF) mice resulted in numerous differentially expressed fecal miRNAs (Viennois et al. 2019). The fact that two of our identified candidates were intersected in both of these fecal miRNA analyses supports the idea that both the host miRNA machinery as well as the presence of bacterial populations influence these specific miRNAs. These findings present a novel view of such miRNAs and their potential reciprocal communication role between these two systems. However, some key features need to be addressed to understand the mechanistic role of miRNA-bacterial regulation. For instance, in those studies investigating fecal miRNA or other components' presence, such small RNAs' origin is unclear. Even though it is accepted that some sources of fecal miRNAs originate from exfoliated cells within the host gastrointestinal tract (Koga et al. 2010), the possibility that miRNAs could reach the gut from other sources should not be excluded. Such potential sources may include the circulatory system, released material from dead cells, or even an unknown bacterial mechanism. The latter's idea is becoming more probable as an increasing number of studies display bacterial sRNA secretion and interchange with the host cells.

In eukaryotic systems, the miRNA regulation pathway consists of several means by which the miRNA regulates a specific transcript. This is achieved either by transcript complementary binding (3’ or 5’ UTR of transcript) using RISC complex or miRNA-genome binding using RITS complex (Pratt and MacRae 2009). In both cases, miRNA binds a complementary region of a gene or transcript, thereby regulating its expression. However, in bacterial systems, these mechanisms are poorly understood. Generally, it is acknowledged that bacteria can produce small RNA (sRNAs) that ultimately regulate the expression of distinct transcripts within the bacteria (Storz, Vogel, and Wassarman 2012). Even though these sRNA are characterized by ~50-300 nucleotides, there is little evidence into how smaller RNA fragments such as miRNA (20-22nt) could regulate bacterial transcriptional expression. Nevertheless, it has been shown that bacteria can produce miRNA-like fragments that depend on the host miRNA processing machinery and ultimately alter the host transcriptional expression (Gu et al. 2017). Therefore, it is likely that bacteria could be responsible for producing a specific set of miRNA-like fragments, which regulate host activity.

This observation of trans-kingdom sRNA exchange was reported between bacteria and plants (Weiberg et al. 2013, Hudzik et al. 2020) and recently in animals such as *C. elegans* (Kaletsky et al. 2020), suggesting a potential evolutionary conserved mechanism. An additional indication of such trans-kindom miRNA regulation is observed in mitochondrial (Purohit and Saini 2020, Fan et al. 2019, Jeong et al. 2017, Indrieri et al. 2019) and chloroplast (Ruwe and Schmitz-Linnweber 2012, Fang et al. 2019) regulation, further suggesting an evolutionary conserved role of miRNA regulation between the host and the ancestral bacterial species. The uptake of host-related sRNA (e.g., miRNAs) by the bacteria was also shown to be mediated by direct uptake (Liu et al. 2016, Qin and Wade 2018) through extracellular vesicles (Lee 2019, Lecrivain and Beckmann 2020, O’brein et al. 2020), or through plant exosome-like nanoparticles (ELNs) (Teng et al. 2018).

All these mechanisms result in the internalization of sRNAs (including miRNAs), ultimately altering bacterial transcriptional expression. The interchange of sRNAs between bacteria and distinct host organisms is becoming more evident; however, further investigation is required to understand how this specific uptake mechanism is mediated and which cellular components, host and bacterial, are involved in the process.

A recent study has provided further evidence for the link between gut microbiota composition and host immune cell modulation (Schluter et al. 2020). Our literature search identified several reports that link our candidate miRNAs with a common role in the inflammatory response. More specifically, these candidates were shown to regulate immune factors such as IL1β and TNFα known to regulate the immune response through NF-kB regulation (Table 1). In our analysis, we identified an increase of IL1β transcript in fecal samples of stressed mice, and more specifically resilient compared to control mice. Interestingly, we detected a specific increase of *Enterobacteriaceae* species as well in resilient animals compared to susceptible and control animals which could link to the specific IL1β fecal mRNA level detected in resilient mice. However, both the origin of these immune factors fecal transcripts and the specific association of these bacterial species is still unclear as the fecal samples might contain several host and bacterial cells that release such transcripts. Future studies should focus on the source of release, as it might be crucial to determine their potential role in each system.

Overall, our findings support the notion that specific miRNA could interact with the gut microbiota (and vice versa) and alter the inflammatory response system, likely through the NF-kB pathway. Since both the host miRNA machinery and gut microbiota composition were shown to influence the stress response and adaptation mechanism, their interchange will likely affect the broader network system. Based on our data, we hypothesize that the inflammatory response regulation, both through the presence of specific miRNAs and bacterial composition, could influence the stress response and adaptation mechanisms. This provides a novel and broader view into the miRNA-microbiota regulation in response to stress, revealing a third link that could alter the network dynamics, which ultimately influences the stress adaptation mechanism. Future studies should deepen the relationship between identified miRNAs and gut microbiota to uncover their role in the host-microbiota communication network and their influence on stress adaptation mechanisms.

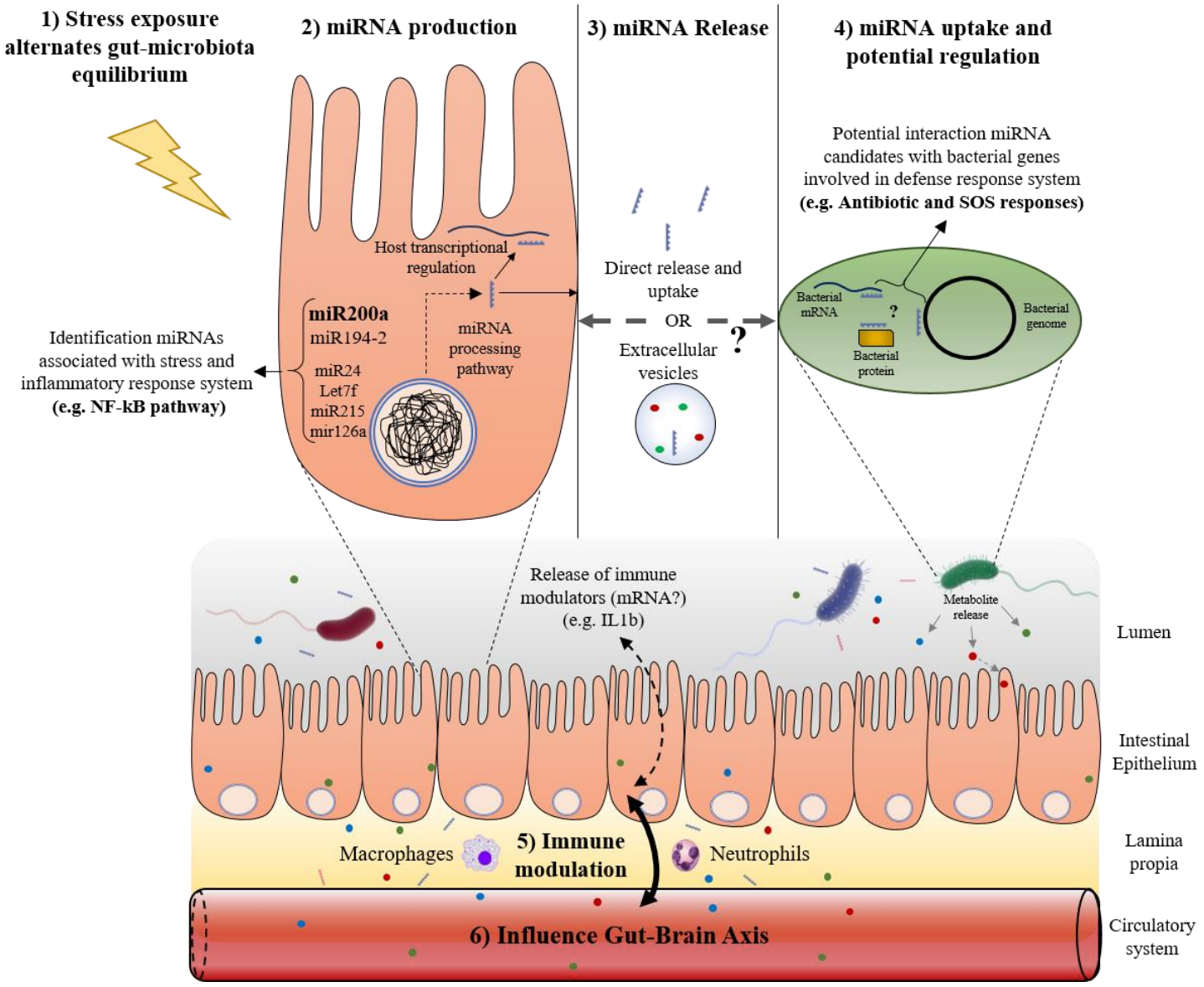

Figure 9. Working model of the miRNA-microbiota interaction network. Model of the broader dynamic network involving fecal miRNA (miRNA-like molecules), gut microbiota composition and its role in regulating the inflammatory response system which could affect the stress adaptation mechanisms.

Material and methods

Mice

Female Arc-GFP-Sun-Cre mice were obtained from the animal housing of the Johannes Gutenberg-University (TARC) and present F1 generation from breeding of Arc-GFP and Sun-Cre (both Jackson Lab, Bar Harbor, ME, USA; $ARC^{creERT2/+}R26^{CAG\text{-}LSL\text{-}Sun1\text{-}sfGFP\text{-}Myc/+}$). Mice were kept in groups of four with water and food (Ssniff Spezialdiäten GmbH, Soest, Germany) *ad libitum*. All animal procedures were performed in accordance with the European Guideline and were approved by local authorities (LUA Rhineland-Palatinate, G17-1-035).

Behavioral experiments

Female chronic social stress (CSS) paradigm has been performed as previously described (Santos Guilherme et al. 2021). Briefly, Female Arc-sGFP mice aged four weeks were group-housed in cages of four animals. The control mice were kept in this initial composition of individuals for another seven weeks, while the stressed animals received a two-time shuffling per week with the aim of only few repeated encounters of individuals. Mice designated control remained within the first established group of four until the end of the experiment. Additional behavioral test were performed to assess animals behavioral states (resilient or susceptible compared to control). Such tests include ultrasonic vocalization recording, Huddling behavioral test, novelty-induced repression of feeding, nesting test and social interaction test.

RNA extraction

Fecal or colonic samples were ruptured using a tissue disruptor (Machine) and RNA was isolated using NucleoSpin miRNA (Isolation of small and large RNA) (Machery-Nagel, Ref 740971.50) following the manufacturer's instruction with minor modifications by collecting the small and large RNA samples separately. Briefly, small and large RNA samples were collected independently by using two distinct "blue ring columns" to elute the large (original "blue ring column"), and small RNA (additional "blue ring column"). Samples from six resilient, six susceptible, and six control animals were prepared, quantified using Nanodrop and submitted to the Genomics Core Facility in the Institute of Molecular Biology (IMB, Mainz) for library preparation.

Small RNA library preparation and sequencing

NGS library prep was performed with NEXTflex Small RNA-Seq Kit V3 following Step A to Step G of Bioo Scientific`s standard protocol (V16.06). Libraries were prepared with a starting amount of 266ng and amplified in 16 PCR cycles. Amplified libraries were purified by running an 8% TBE gel and size-selected for 18 – 40nt. Libraries were profiled in a High Sensitivity DNA on a 2100 Bioanalyzer (Agilent Technologies) and quantified using the Qubit dsDNA HS Assay Kit in a Qubit 2.0 Fluorometer (Life technologies). All 18 samples were pooled in equimolar ratio and sequenced on 1 NextSeq 500/550 Flowcell, SR for 1x 75 cycles plus 7 cycles for the index read.

miRNA annotation

For the quantification of miRNA abundance, unitas 1.75 (Gebert, Hewel and Rosenkranz, 2017) was used with the settings -species mus_musculus, and the most recent version of miRNA sequences from the miRBase database was used for annotation (Griffiths-Jones, 2006) and (Kozomara, Birgaoanu and Griffinths-Jones 2019).

Differentially Expression Analysis

The raw count data was used for a supervised clustering analysis using the Partial Least Squares Discriminant Analysis (PLS-DA) offered in the mixOmics R package (version 6.14.0) with the condition, control, resilient and susceptible, as a label for training (Rohart F et al. 2017). The Differentially Expression Analysis (DEA) of the miRNA counts was performed between all pairwise combinations of resilient, susceptible and control mice using the R package DESeq2 (version 1.30.0) (Love, Huber and Anders, 2014). The p values derived from the DEA were adjusted for multiple testing using the Benjamini-Hochberg (BH) correction (Benjamini and Hochberg, 1995). However, as none of the miRNAs reached an adjusted p-value < 5 %, we considered the uncorrected p-value by setting our cutoff to p-value ≤ 0.05 and absolute log2 fold change > 1.5. All plots were done using the R packages ggplot2 (version 3.3.2) or Venn (version 1.9) (Wickham 2016, Dusa 2020).

Gene Target Prediction of miRNAs and GO term enrichment analysis

For interesting miRNA subgroups, mouse gene targets were predicted using the most recent version of the miRNA gene target database mirDB (v6.0, updated July 2019, Lui and Wang 2019, Chen and Wang 2020). Subsequently, we conducted a Gene Ontology (GO) enrichment analysis for the predicted target genes using the R packages clusterProfiler (version 3.18.0, G. Yu et al. 2012). The p values were adjusted by BH correction and the cutoff for significantly overrepresented terms was set to adjusted p-value < 5 %.

For the ShinyGO analysis, genes target of selected GO terms were uploaded on the online tool (http://bioinformatics.sdstate.edu/go/) as described in Ge, Jung and Yao (2020). We used the following features for the analysis: Species used- *Escherichia coli* K12 DH10B STRINGdb; GO- Biological process; P-val cutoff (FDR)- 0.005; number of most significant terms to show- 10 (group-specific) or 30 (top 6).

Bacterial Target Scan Analysis

For the Bacterial Target Scan Analysis, multiple sequences per miRNA were used, based on all sequences that matched the respective miRNA in the unitas annotation step. For each miRNA that showed a p-value < 0.05 and absolute log2FC > 1.5 in the DEA, all these sequences were used to scan for potential targets in the human gut microbiome with miRanda (Enright *et al.*, 2003). The procedure followed those of (Hewel *et al.*, 2019) using miRanda with the parameters -strict -go -2 -ge 8 -sc 150.00 -en 25.00 -scale 3.00. The database was created based on the Human Oral Microbiome Database (Escapa *et al.*, 2018) using only species with a complete available annotation in NCBI RefSeq (O'Leary *et al.*, 2016).

Functional Annotation of Bacteria-miRNA-hits

The bacteria-miRNA-hit regions on the bacterial species were investigated for bacterial target genes using all RefSeq annotation files for bacteria provided by NCBI Assembly (https://www.ncbi.nlm.nih.gov/assembly/). The R package GenomicRanges (version 1.42.0) was used to find those genes lying in the bacteria-miRNA-hit region (Lawrence et al. 2013). All results with known gene names were used for further analyses.

For the functional annotation of the predicted bacterial target genes, the Gene Ontology (GO) terms of all bacteria were extracted from the Uniprot database (Uniprot 2020). For all different gene subsets, those GO terms annotated to the input species were used for the GO term enrichment analysis using the Fisher's Exact test function implemented in R (R Core Team 2020). P values were adjusted by the BH method and filtered by being < 5 %.

cDNA synthesis and qRT-PCR

Small RNA. Reverse transcription for small RNA samples was performed using the miScript II RT kit (Qiagen, 218161) according to the manufacturer's instructions. Briefly, a master mix was prepared on ice containing 2 µl of 5x HiSpec Buffer, 1 µl of 10x Nucleics Mix, and 1 µl of Reverse Transcriptase. 75ng of small RNA were taken per reaction, and RNase-free water was filled to a total volume of 10 µl. Each reaction was incubated in a thermo cycler using the following conditions: 37 °C for 60 minutes, followed by 95 °C for 5 minutes to inactivate the reverse transcriptase. cDNA was kept and stored at -80 °C until use. For small RNA quantification, qPCR was performed using miScript SYBR Green PCR kit (Qiagen, 218073) according to the manufacturer's instructions. A master mix was briefly prepared on ice containing 5 µl of 2x QuantiTect SYBR Green PCR Master Mix, 1 µl of 10x miScript Universal primer, 1 µl of 10x miScript primer assay, or 250mM of designed primer. miScript primer assay (Qiagen) were used to quantify fecal miR24-1-3p, miR200a-3p, miR215-5p, miR126a-3p and let7f-1-5p (Material Table 1). The primers for miR-194-2-5p were designed as described in Busk et al.

2014. cDNA was diluted 1/10 µl using RNase-free water and were quantified using relative expression to control samples using ViiA7 PCR machine (Life Technologies) with the cycling conditions described in miScript SYBR Green PCR kit (Qiagen, 218073). qPCR was performed with 4-7 biological replicates for each group.

Large RNA (mRNA). Reverse transcription for mRNA quantification was performed using First Strand cDNA Synthesis Kit (Thermo Scientific, K1612) according to the manufacturer's instructions. Briefly, 100ng of RNA was taken from each sample to a final volume of 8ul. A mater mix of 1 µl of 10x DNase Buffer and 1 µl of 10x DNase (NEB) was added to each reaction and incubated in a thermal cycler using the following conditions: 37 °C for 10 minutes, followed by 75 °C for 10 minutes to inactivate the DNAse. 1 µl of random hexamer primer was added to each reaction and incubated at 65 °C for 5 min., An additional master mix was prepared on ice containing 4 µl of 5x Buffer, 1 µl of Ribo Lock, 2 µl of dNTP and 2 µl MuLv Reverse Transcriptase and H_2O was added to each sample to a final volume of 20 µl. Samples were incubated for 5 minutes in RT followed by a thermo cycler incubation using the following conditions: 42 °C for 60 minutes, followed by 70 °C for 5 minutes. cDNA was kept and stored at -80 °C until use. For transcript qPCR quantification, cDNA was diluted 1/10 µl using RNase-free water and were quantified using standard -ΔΔCT using ViiA7 PCR machine (Life Technologies). qPCR was performed with 5-7 biological replicates for each group.

miRNA and mRNA primer assays		
miRNAs primers		
Target Mature miRNA	**Catalog # or Sequence (5'=>3')**	**Source**
Mm_miR-200a	MS00001813	miScript primer assays (Qiagen)
Mm_miR-24_1	MS00005922	miScript primer assays (Qiagen)
Mm_let-7f_1	MS00005866	miScript primer assays (Qiagen)
Mm_miR-126-3p_1	MS00005999	miScript primer assays (Qiagen)
Mm_miR-215_1	MS00001918	miScript primer assays (Qiagen)
miR194-2_for	CTGTAACAGCAACTCCATGT	Designed as in Busk et al. 2014
miR194-2_rev	CCAGTTTTTTTTTTTTTTTGCACTTC	Designed as in Busk et al. 2014
mRNA primers		
Primer Annotation	**Sequence (5'=>3')**	**Source**
Tnfa_F	GGTGCCTATGTCTCAGCCTCTT (Cat# MP217748)	Origene
Tnfa_R	GCCATAGAACTGATGAGAGGGAG (Cat# MP217748)	Origene
IL1b_F	TGGACCTTCCAGGATGAGGACA (Cat# MP206724)	Origene
IL1b_R	GTTCATCTCGGAGCCTGTAGTG (Cat# MP206724)	Origene
RPL19_F	CTCGTTGCCGGAAAAACA	Meyer-Schaller et al. 2019
RPL19_R	TCATCCAGGTCACCTTCTCA	Meyer-Schaller et al. 2019

Acknowledgments

We would like to thank the Institute of the Molecular Biology (Mainz) and particularly flow cytometry, and genomics core facilities for their assistance and support throughout the study. The use of GCF's NextSeq500 (INST 247/870-1 FUGG) is gratefully acknowledged. We also extend our sincere thanks to the Mouse Behavioral Unit of the Leibniz Institute of Resilience Research.

References

1. Apweiler, R. *et al.* UniProt: The universal protein knowledgebase. *Nucleic Acids Res.* **32**, 2699 (2004).
2. Belkaid, Y. & Hand, T. W. Role of the microbiota in immunity and inflammation. *Cell* **157**, 121–141 (2014).
3. Bravo, J. A. *et al.* Ingestion of Lactobacillus strain regulates emotional behavior and central GABA receptor expression in a mouse via the vagus nerve. *Proc. Natl. Acad. Sci. U. S. A.* **108**, 16050–16055 (2011).
4. Bridgewater, L. C. *et al.* Gender-based differences in host behavior and gut microbiota composition in response to high fat diet and stress in a mouse model. *Sci. Rep.* **7**, 1–12 (2017).
5. Burokas, A. *et al.* Targeting the Microbiota-Gut-Brain Axis: Prebiotics Have Anxiolytic and Antidepressant-like Effects and Reverse the Impact of Chronic Stress in Mice. *Biol. Psychiatry* **82**, 472–487 (2017).
6. Chang, C. S. & Kao, C. Y. Current understanding of the gut microbiota shaping mechanisms. *J. Biomed. Sci.* **26**, 1–11 (2019).
7. Chen, R. J. *et al.* MicroRNAs as biomarkers of resilience or vulnerability to stress. *Neuroscience* **305**, 36–48 (2015).
8. Chen, Y. & Wang, X. MiRDB: An online database for prediction of functional microRNA targets. *Nucleic Acids Res.* **48**, D127–D131 (2020).
9. Chen, Z. *et al.* Inflammation-dependent downregulation of miR-194-5p contributes to human intervertebral disc degeneration by targeting CUL4A and CUL4B. *J. Cell. Physiol.* **234**, 19977–19989 (2019).
10. Cussotto, S., Sandhu, K. V., Dinan, T. G. & Cryan, J. F. The Neuroendocrinology of the Microbiota-Gut-Brain Axis: A Behavioural Perspective. *Front. Neuroendocrinol.* **51**, 80–101 (2018).
11. De Palma, G. *et al.* Microbiota and host determinants of behavioural phenotype in maternally separated mice. *Nat. Commun.* **6**, (2015).
12. Den Besten, G. *et al.* The role of short-chain fatty acids in the interplay between diet, gut microbiota, and host energy metabolism. *J. Lipid Res.* **54**, 2325–2340 (2013).
13. Dinan, T. G. & Cryan, J. F. Mood by microbe: Towards clinical translation. *Genome Med.* **8**, 36–38 (2016).
14. Dinan, T. G. & Cryan, J. F. Gut instincts: microbiota as a key regulator of brain development, ageing and neurodegeneration. *J. Physiol.* **595**, 489–503 (2017).
15. Duan, X. J., Zhang, X., Li, L. R., Zhang, J. Y. & Chen, Y. P. MiR-200a and miR-200b restrain inflammation by targeting ORMDL3 to regulate the ERK/MMP-9 pathway in asthma. *Exp. Lung Res.* **46**, 321–331 (2020).
16. Fordham, J. B., Naqvi, A. R. & Nares, S. Regulation of miR-24, miR-30b, and miR-142-3p during macrophage and dendritic cell differentiation potentiates innate immunity. *J. Leukoc. Biol.* **98**, 195–207 (2015).
17. Fung, T. C., Olson, C. A. & Hsiao, E. Y. Interactions between the microbiota, immune and nervous systems in health and disease. *Nat. Neurosci.* **20**, 145–155 (2017).
18. Geng, L. *et al.* Reduced Let-7f in Bone Marrow-Derived Mesenchymal Stem Cells Triggers Treg/Th17 Imbalance in Patients With Systemic Lupus Erythematosus. *Front. Immunol.* **11**, (2020).
19. Gu, H. *et al.* Salmonella produce microRNA-like RNA fragment Sal-1 in the infected cells to facilitate intracellular survival. *Sci. Rep.* **7**, 1–12 (2017).
20. Gurtan, A. M. & Sharp, P. A. The role of miRNAs in regulating gene expression networks. *J. Mol. Biol.* **425**, 3582–3600 (2013).
21. Hewel, C. *et al.* Common miRNA Patterns of Alzheimer's Disease and Parkinson's Disease and Their Putative Impact on Commensal Gut Microbiota. *Front. Neurosci.* **13**, 1–13 (2019).
22. Huang, H. L. *et al.* Relief of irritable bowel syndrome by fecal microbiota transplantation is associated with changes in diversity and composition of the gut microbiota. *J. Dig. Dis.* **20**, 401–408 (2019).
23. Huang, T. T. *et al.* Current understanding of gut microbiota in mood disorders: An update of human studies. *Front. Genet.* **10**, 1–12 (2019).
24. Hudzik, C., Hou, Y., Ma, W. & Axtell, M. J. Exchange of small regulatory rnas between plants and their pests. *Plant Physiol.* **182**, 51–62 (2020).
25. Jiang, H. *et al.* Altered fecal microbiota composition in patients with major depressive disorder. *Brain. Behav. Immun.* **48**, 186–194 (2015).

26. Jingjing, Z. *et al.* MicroRNA-24 Modulates Staphylococcus aureus-Induced Macrophage Polarization by Suppressing CHI3L1. *Inflammation* **40**, 995–1005 (2017).
27. Kaletsky, R. *et al.* C. elegans interprets bacterial non-coding RNAs to learn pathogenic avoidance. *Nature* **586**, 445–451 (2020).
28. Kelly, J. R. *et al.* Breaking down the barriers: The gut microbiome, intestinal permeability and stress-related psychiatric disorders. *Front. Cell. Neurosci.* **9**, (2015).
29. Kim, D., Zeng, M. Y. & Núñez, G. The interplay between host immune cells and gut microbiota in chronic inflammatory diseases. *Exp. Mol. Med.* **49**, (2017).
30. Koga, Y. *et al.* MicroRNA expression profiling of exfoliated colonocytes isolated from feces for colorectal cancer screening. *Cancer Prev. Res.* **3**, 1435–1442 (2010).
31. Kong, L., Sun, M., Jiang, Z., Li, L. & Lu, B. MicroRNA-194 inhibits lipopolysaccharide-induced inflammatory response in nucleus pulposus cells of the intervertebral disc by targeting TNF receptor-associated factor 6 (TRAF6). *Med. Sci. Monit.* **24**, 3056–3067 (2018).
32. Kozomara, A., Birgaoanu, M. & Griffiths-Jones, S. MiRBase: From microRNA sequences to function. *Nucleic Acids Res.* **47**, D155–D162 (2019).
33. Kumar, M. *et al.* MicroRNA let-7 modulates the immune response to mycobacterium tuberculosis infection via control of A20, an inhibitor of the NF-κB pathway. *Cell Host Microbe* **17**, 345–356 (2015).
34. Lawrence, M. *et al.* Software for Computing and Annotating Genomic Ranges. *PLoS Comput. Biol.* **9**, 1–10 (2013).
35. Lazar, V. *et al.* Aspects of gut microbiota and immune system interactions in infectious diseases, immunopathology, and cancer. *Front. Immunol.* **9**, 1–18 (2018).
36. Lécrivain, A. L. & Beckmann, B. M. Bacterial RNA in extracellular vesicles: A new regulator of host-pathogen interactions? *Biochim. Biophys. Acta - Gene Regul. Mech.* **1863**, 194519 (2020).
37. Lee, H. J. Microbial extracellular RNAs and their roles in human diseases. *Exp. Biol. Med.* **245**, 845–850 (2020).
38. Li, M. *et al.* MiR-200a contributes to the migration of BMSCs induced by the secretions of E. faecalis via FOXJ1/NFκB/MMPs axis. *Stem Cell Res. Ther.* **11**, 1–12 (2020).
39. Liang, Y. *et al.* Genetic variants in the promoters of let-7 family are associated with an increased risk of major depressive disorder. *J. Affect. Disord.* **183**, 295–299 (2015).
40. Liu, S. *et al.* The Host Shapes the Gut Microbiota via Fecal MicroRNA. *Cell Host Microbe* **19**, 32–43 (2016).
41. Liu, W. & Wang, X. Prediction of functional microRNA targets by integrative modeling of microRNA binding and target expression data. *Genome Biol.* **20**, 1–10 (2019).
42. Liu, Y. Z., Wang, Y. X. & Jiang, C. L. Inflammation: The common pathway of stress-related diseases. *Front. Hum. Neurosci.* **11**, 1–11 (2017).
43. Lo, W. Y., Yang, W. K., Peng, C. T., Pai, W. Y. & Wang, H. J. MicroRNA-200a/200b modulate high glucose-induced endothelial inflammation by targeting O-linked n-acetylglucosamine transferase expression. *Front. Physiol.* **9**, 1–13 (2018).
44. Lopizzo, N., Zonca, V., Cattane, N., Pariante, C. M. & Cattaneo, A. miRNAs in depression vulnerability and resilience: novel targets for preventive strategies. *J. Neural Transm.* **126**, 1241–1258 (2019).
45. Love, M. I., Huber, W. & Anders, S. Moderated estimation of fold change and dispersion for RNA-seq data with DESeq2. *Genome Biol.* **15**, 1–21 (2014).
46. Lukić, I. *et al.* Antidepressants affect gut microbiota and Ruminococcus flavefaciens is able to abolish their effects on depressive-like behavior. *Transl. Psychiatry* **9**, (2019).
47. Misiak, B. *et al.* The HPA axis dysregulation in severe mental illness: Can we shift the blame to gut microbiota? *Prog. Neuro-Psychopharmacology Biol. Psychiatry* **102**, (2020).
48. Mittal, R. *et al.* Neurotransmitters: The Critical Modulators Regulating Gut–Brain Axis. *J. Cell. Physiol.* **232**, 2359–2372 (2017).
49. Molina-Torres, G., Rodriguez-Arrastia, M., Roman, P., Sanchez-Labraca, N. & Cardona, D. Stress and the gut microbiota-brain axis. *Behav. Pharmacol.* **30**, 187–200 (2019).
50. Naqvi, A. R., Fordham, J. B., Ganesh, B. & Nares, S. MiR-24, miR-30b and miR-142-3p interfere with antigen processing and presentation by primary macrophages and dendritic cells. *Sci. Rep.* **6**, 1–12 (2016).
51. Nie, H. *et al.* MicroRNA-194 inhibition improves dietary-induced non-alcoholic fatty liver disease in mice through targeting on FXR. *Biochim. Biophys. Acta - Mol. Basis Dis.* **1863**, 3087–3094 (2017).
52. O'Brien, K., Breyne, K., Ughetto, S., Laurent, L. C. & Breakefield, X. O. RNA delivery by extracellular vesicles in mammalian cells and its applications. *Nat. Rev. Mol. Cell Biol.* **21**, 585–606 (2020).
53. Parker, M. I. & Palladino, M. A. MicroRNAs downregulated following immune activation of rat testis. *Am. J. Reprod. Immunol.* **77**, 1–4 (2017).
54. Pekow, J. *et al.* Increased mucosal expression of miR-215 precedes the development of neoplasia in patients with long-standing ulcerative colitis. *Oncotarget* **9**, 20709–20720 (2018).

55. Popoff, M. R. Bacterial factors exploit eukaryotic Rho GTPase signaling cascades to promote invasion and proliferation within their host. *Small GTPases* **5**, (2014).
56. Prashar, A., Schnettger, L., Bernard, E. M. & Gutierrez, M. G. Rab GTPases in immunity and inflammation. *Front. Cell. Infect. Microbiol.* **7**, 1–11 (2017).
57. Pratt, A. J. & MacRae, I. J. The RNA-induced silencing complex: A versatile gene-silencing machine. *J. Biol. Chem.* **284**, 17897–17901 (2009).
58. Pua, H. H. *et al.* production. **44**, 821–832 (2017).
59. Qin, Y. & Wade, P. A. Crosstalk between the microbiome and epigenome: Messages from bugs. *J. Biochem.* **163**, 105–112 (2018).
60. Rogers, G. B. *et al.* From gut dysbiosis to altered brain function and mental illness: Mechanisms and pathways. *Mol. Psychiatry* **21**, 738–748 (2016).
61. Rohart, F., Gautier, B., Singh, A. & Lê Cao, K. A. mixOmics: An R package for 'omics feature selection and multiple data integration. *PLoS Comput. Biol.* **13**, 1–19 (2017).
62. Rooks, M. G. & Garrett, W. S. Gut microbiota, metabolites and host immunity. *Nat. Rev. Immunol.* **16**, 341–352 (2016).
63. Schluter, J. *et al.* The gut microbiota is associated with immune cell dynamics in humans. *Nature* (2020). doi:10.1038/s41586-020-2971-8
64. Spanò, S. & Galán, J. E. Taking control: Hijacking of Rab GTPases by intracellular bacterial pathogens. *Small GTPases* **9**, 182–191 (2018).
65. Storz, G., Vogel, J. & Wassarman, K. M. Regulation by Small RNAs in Bacteria: Expanding Frontiers. *Mol. Cell* **43**, 880–891 (2011).
66. Tan, W. *et al.* Let-7f-5p ameliorates inflammation by targeting NLRP3 in bone marrow-derived mesenchymal stem cells in patients with systemic lupus erythematosus. *Biomed. Pharmacother.* **118**, 109313 (2019).
67. Tang, S. tao, Wang, F., Shao, M., Wang, Y. & Zhu, H. qing. MicroRNA-126 suppresses inflammation in endothelial cells under hyperglycemic condition by targeting HMGB1. *Vascul. Pharmacol.* **88**, 48–55 (2017).
68. Teng, Y. *et al.* Plant-Derived Exosomal MicroRNAs Shape the Gut Microbiota. *Cell Host Microbe* **24**, 637-652.e8 (2018).
69. Vojinovic, D. *et al.* Relationship between gut microbiota and circulating metabolites in population-based cohorts. *Nat. Commun.* **10**, 1–7 (2019).
70. Wang, J., Li, P., Xu, X., Zhang, B. & Zhang, J. MicroRNA-200a Inhibits Inflammation and Atherosclerotic Lesion Formation by Disrupting EZH2-Mediated Methylation of STAT3. *Front. Immunol.* **11**, 1–13 (2020).
71. Wang, K. *et al.* miR-194 inhibits innate antiviral immunity by targeting FGF2 in influenza H1N1 virus infection. *Front. Microbiol.* **8**, 1–10 (2017).
72. Wang, Y., Xu, G., Han, J. & Xu, T. MiR-200a-3p regulates TLR1 expression in bacterial challenged miiuy croaker. *Dev. Comp. Immunol.* **63**, 181–186 (2016).
73. Wang, Z. *et al.* Regulation of the small GTPase Rab1 function by a bacterial glucosyltransferase. *Cell Discov.* **4**, (2018).
74. Watkins, D. & Arya, D. P. Regulatory roles of small RNAs in prokaryotes: parallels and contrast with eukaryotic miRNA. *Non-coding RNA Investig.* **3**, 28–28 (2019).
75. Wei, Y. B. *et al.* Elevation of Il6 is associated with disturbed let-7 biogenesis in a genetic model of depression. *Transl. Psychiatry* **6**, e869 (2016).
76. Weiberg, A. *et al.* Fungal small RNAs suppress plant immunity by hijacking host RNA interference pathways. *Science (80-.).* **342**, 118–123 (2013).
77. Williams, M. R., Stedtfeld, R. D., Tiedje, J. M. & Hashsham, S. A. MicroRNAs-based inter-domain communication between the host and members of the gut microbiome. *Front. Microbiol.* **8**, 1–10 (2017).
78. Wong, M. L. *et al.* Inflammasome signaling affects anxiety- and depressive-like behavior and gut microbiome composition. *Mol. Psychiatry* **21**, 797–805 (2016).
79. Wu, Y. *et al.* MicroRNA-126 Regulates Inflammatory Cytokine Secretion in Human Gingival Fibroblasts Under High Glucose via Targeting Tumor Necrosis Factor Receptor Associated Factor 6. *J. Periodontol.* **88**, e179–e187 (2017).
80. Xie, F., Yang, L., Han, L. & Yue, B. MicroRNA-194 Regulates Lipopolysaccharide-Induced Cell Viability by Inactivation of Nuclear Factor-κ B Pathway. *Cell. Physiol. Biochem.* **43**, 2470–2478 (2017).
81. Yan, Y. *et al.* Deletion of miR-126a Promotes Hepatic Aging and Inflammation in a Mouse Model of Cholestasis. *Mol. Ther. - Nucleic Acids* **16**, 494–504 (2019).
82. Yang, C. *et al.* Bifidobacterium in the gut microbiota confer resilience to chronic social defeat stress in mice. *Sci. Rep.* **7**, 1–7 (2017).
83. Yang, C. *et al.* Possible role of the gut microbiota-brain axis in the antidepressant effects of (R)-ketamine in a social defeat stress model. *Transl. Psychiatry* **7**, (2017).

84. Yang, Q. *et al.* Longitudinal development of the gut microbiota in healthy and diarrheic piglets induced by age-related dietary changes. *Microbiologyopen* **8**, 1–17 (2019).
85. Yano, J. M. *et al.* Indigenous bacteria from the gut microbiota regulate host serotonin biosynthesis. *Cell* **161**, 264–276 (2015).
86. Yao, Y. *et al.* MiR-215-5p inhibits the inflammation injury in septic H9c2 by regulating ILF3 and LRRFIP1. *Int. Immunopharmacol.* **78**, 106000 (2020).
87. Yu, C. D., Miao, W. H., Zhang, Y. Y., Zou, M. J. & Yan, X. F. Inhibition of miR-126 protects chondrocytes from IL-1β induced inflammation via upregulation of Bcl-2. *Bone Jt. Res.* **7**, 414–421 (2018).
88. Yu, J., Chen, J., Yang, H., Chen, S. & Wang, Z. Overexpression of MIR-200a-3p promoted inflammation in sepsis-induced brain injury through ROS-induced NLRP3. *Int. J. Mol. Med.* **44**, 1811–1823 (2019).
89. Zhang, K. *et al.* Abnormal composition of gut microbiota is associated with resilience versus susceptibility to inescapable electric stress. *Transl. Psychiatry* **9**, (2019).
90. Zhang, X. *et al.* miR-194 relieve neuropathic pain and prevent neuroinflammation via targeting FOXA1. *J. Cell. Biochem.* **121**, 3278–3285 (2020).
91. Zheng, P. *et al.* Gut microbiome remodeling induces depressive-like behaviors through a pathway mediated by the host's metabolism. *Mol. Psychiatry* **21**, 786–796 (2016).
92. Zheng, Y., Li, Y., Liu, G., Qi, X. & Cao, X. MicroRNA-24 inhibits the proliferation and migration of endothelial cells in patients with atherosclerosis by targeting importin-α3 and regulating inflammatory responses. *Exp. Ther. Med.* **15**, 338–344 (2018).
93. Zhou, X., Li, X. & Wu, M. miRNAs reshape immunity and inflammatory responses in bacterial infection. *Signal Transduct. Target. Ther.* **3**, 1–13 (2018).

2.2.1 Supplementary material

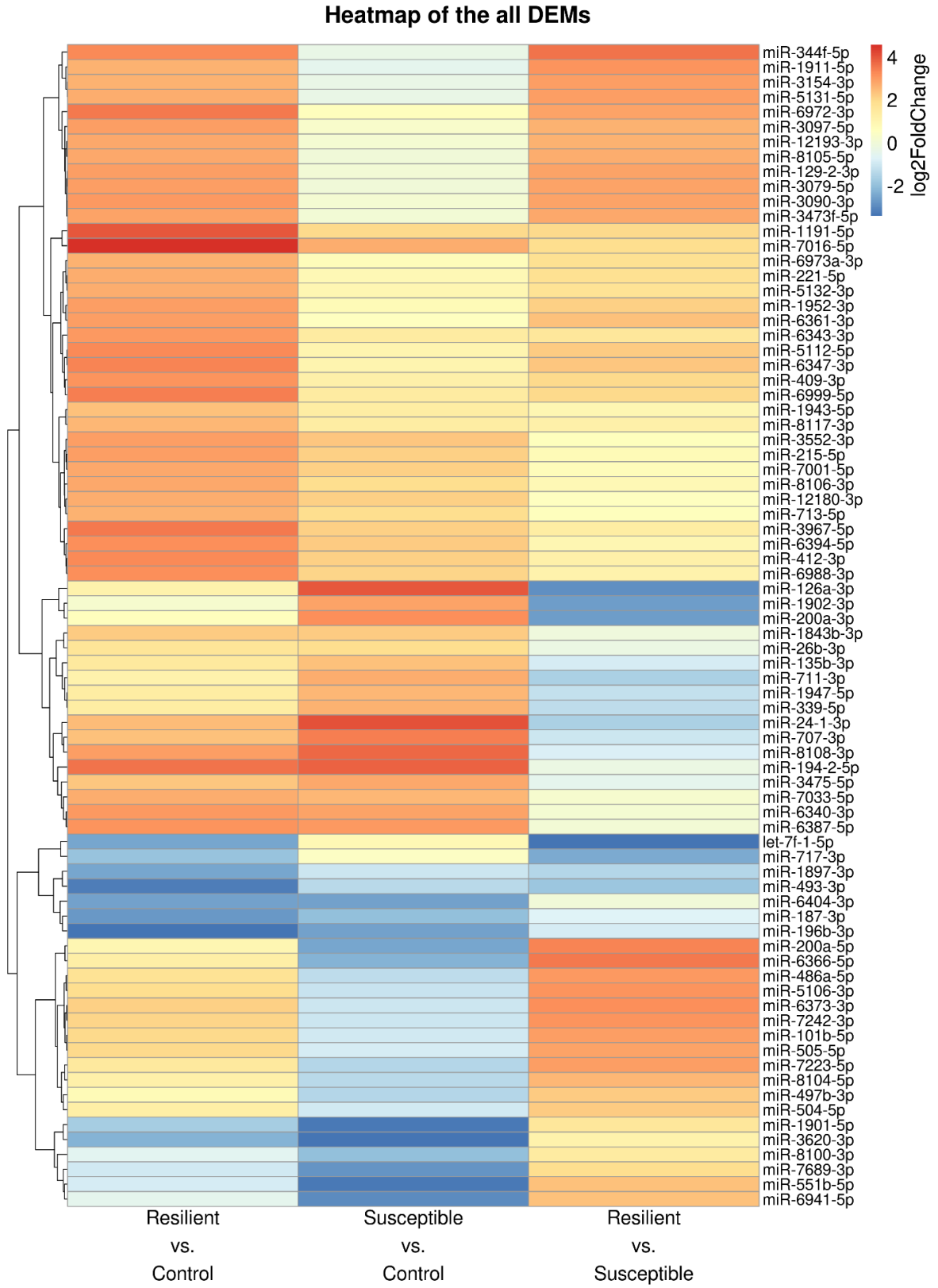

Supplementary Figure 1. Heat-map representing the 78 differentially expressed miRNAs.

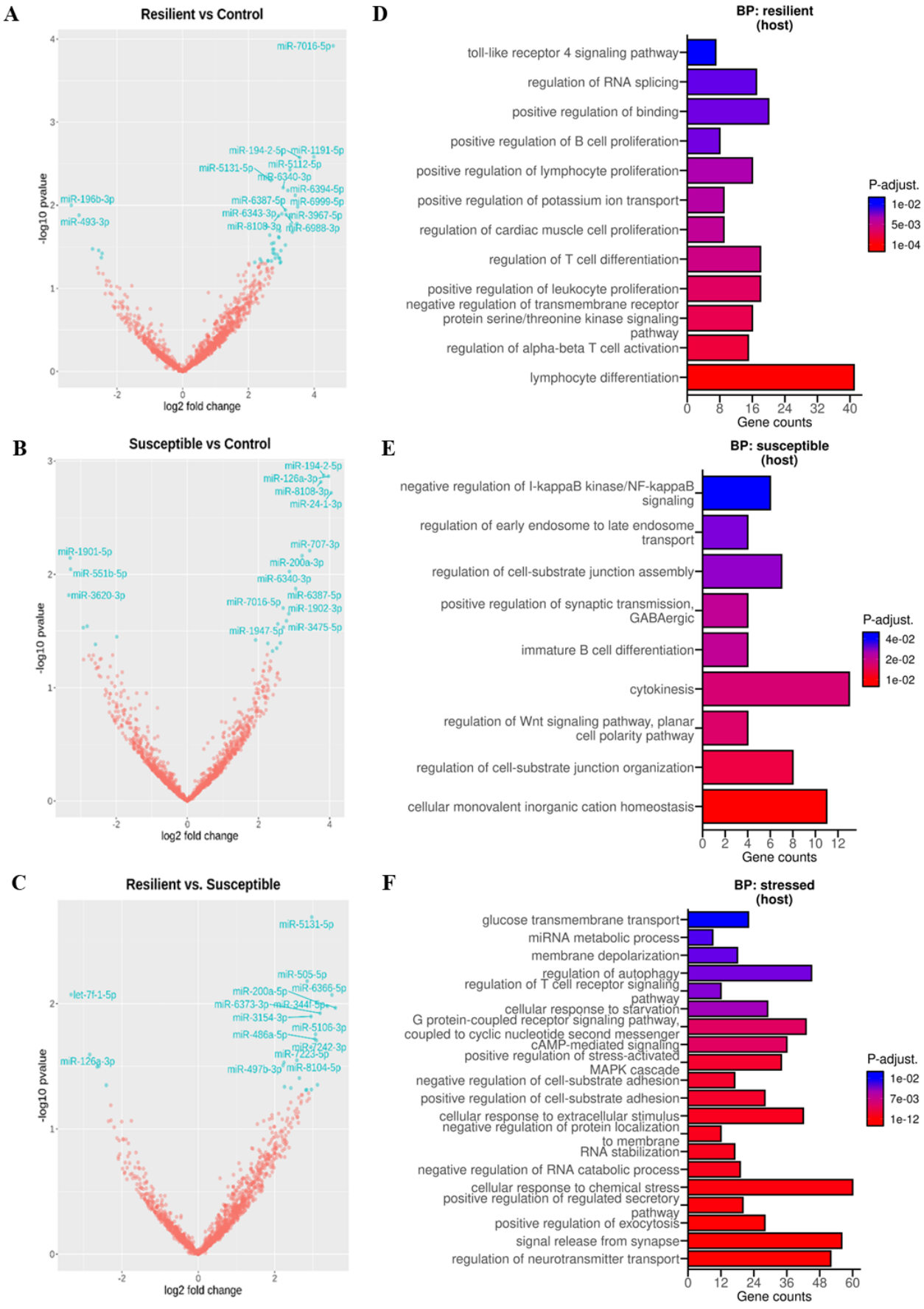

Supplementary Figure 2. Differnetially expressed miRNAs between the different conditions (A-C) and group-specific unique GO terms (D-F)

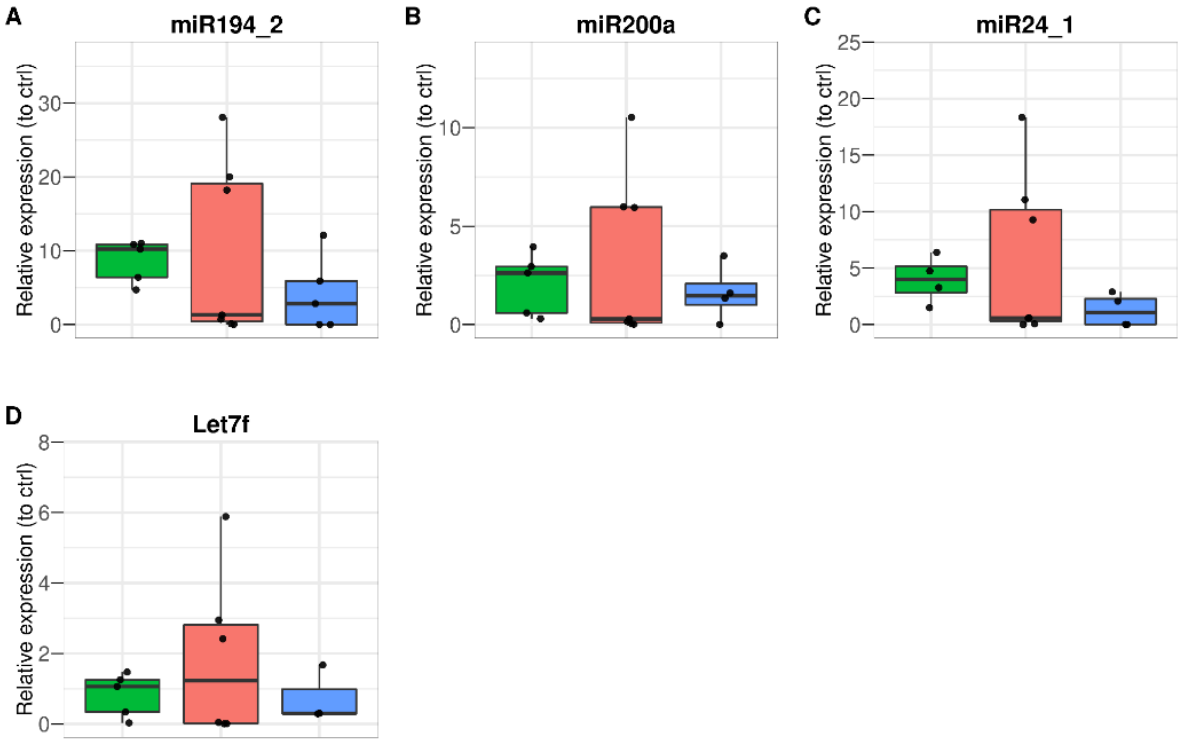

Supplementary Figure 3. qPCR of Colon miRNA candidates. D-J. miRNA expression of identified candidates in colon samples of resilient, susceptible and control mice. D. miR194-2, n=5,5,5 E. miR200a n=5,4,4 F. miR24-1, n=5,5,5. G. Let7f, n=5,5,4 H. miR126, n=5,6,4) I. miR215, n=5,5,5. Data represnsents mean values and error bars represent ±S.E.M

Table 1. Summary of candidate miRNA associated with bacterial and inflammatory response				
microRNA	**principal finding in relation to inflammation**	**(Potential) Gene targets**	**Presence of miR associated with inflammation**	**Reference**
miR-194-5p	LPS-induced Inhibition of NF-κB pathway	p-65 and Bcl-3	↓	Xie et al. 2017
	Down regulation of inflammatory cytokines such as IL6 and IL10	FoxA1	↓	Zhang et al. 2020
	miR-194 negatively regulate type I IFN production	TBK1, IRF3	↓	Wang et al. 2017
	Protects Palmititc acid-induced inflammatory response	FXR, Nr1h4	↓	Nie et al. 2017
	Treatment with IL-6 and TNF-α lead to the repression of miR-194-5p (cell line)	Cul4A and Cul4B	↓?	Chen et al. 2019
	miR194 LPS-induced Inhibition of inflammatory cytokines (TNF-α, IL-1, IL-6, PGE2)	TRAF6	↓	Kong et al. 2018
miR-24	Overexpression of miR-24 attenutes secretion of inflammatory mediators TNF-a, IL-6, and IL12p40	/	↓	Naqvi et al. 2015
	Limit IL-4 production in asthma mouse model	IL-4	↓	Pua et al. 2016
	miR24 decreases M1 markers such as IL-6, iNOS and TNF-α in S.aureus-stimulated macrophages	CHI3L1	↓	Jingjing et al. 2017
	miR24 inhibted cytokine secretion in response to LPS.	TLR4/CD14/MD-1 ?	↓	Fordham, Naqvi and Nares 2015
	miR24 blocks NF-κB pathway in atherosclerosis	KPNA4,TNF-α	↓?	Zheng et al. 2018
miR-200a-3p	Reduced levels of miR200a/200b increased inflammatory cytokines (TNF-α, IL-4, IL-5, IL-13 and IL-1β) in A549 cells	ORMDL3	↓	Duan et al. 2020
	miR200a overexpression promoted inflammation in sepsis-induced brain injury	NLRP3	↑	Yu et al. 2019
	miR200a has anti-inflammatory activity dependnet on EZH2/STAT3 signaling cascade.	EZH2	↓	Wang et al. 2020
	miR200a-3p regulates TLR1 which could modulate NF-κB activity	TLR1	?	Wang et al. 2016
	miR200a-3p negative regulator of pro-inflammatory chemocike ligand 9 (CXCL9)	CXCL9	↓	Wu et al. 2019
	miR-200a/200b are involved in modulating HG-induced endothelial inflammation	OGT, ICAM-1, VCAM-1, and E-selectin	↓	Lo et al. 2018
	miR200a contributes to BMSC migration via FOXJ1/NFκB/MMPs axis	/	?	Li et al. 2020
let7f-5p	M. tuberculosis suppresses let-7f-5p resulting in NF-kB signaling inhibition	A20	↓	Kumar et al. 2015
	High levels of let-7f-5p alleviated inflammation cytokine secretion	NLRP3	↓	Tan et al. 2019
	Let7f impared proliferation of BM-MSC and promoting apoptosis through IL6 targeting	IL-6	↓	Geng et al. 2020
	let7f-5p is downregulated upon LPS-induction	/	↓	Parker and Palladino 2017

Table continuation

Table continuation

miR-126a-3p	miRNA126a overexpression abrogates secretion of pro-inflammatory cytokines (IL-6, TNF-α, and CCL2)	TRAF6	↓	Wu et al. 2017
	miR-126 suppresses inflammation and ROS production in human endothelial cells	HMGB1	↓	Tang et al. 2017
	miR-126a suppresses ingplamation in BMSCs	VCAN	↓	Yan et al. 2019
	Inhibition of miR-126 decreased IL-1β-induced inflammation and cell apoptosis	Bcl-2	↑	Yu et al. 2018
miR-215-5p	miR-215-5p overexpression could suppress the inflammation injury.	LRRFIP1, ILF3	↓	Yao et al. 2020
	miR-215 expression increases in Ulcerative Colitis-associated colon cancers and non-dysplastic UC tissue	/	?	Pekow et al. 2018

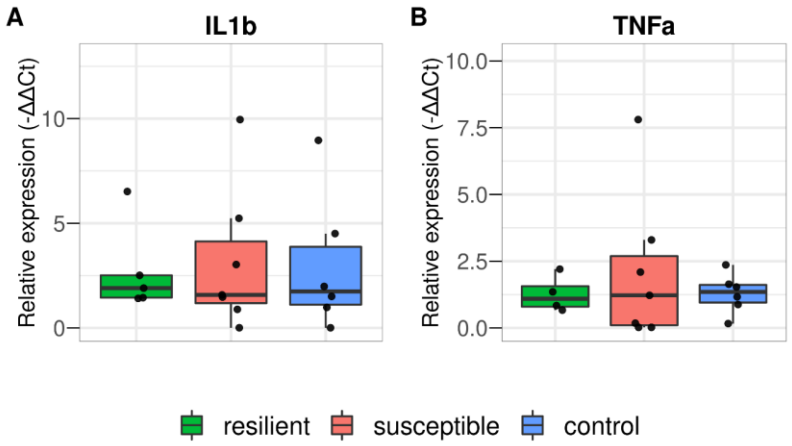

Supplementary Fig. 4- qPCR for Colon mRNA IL1b and Tnfa and study-intersection table. A-B mRNA expression of IL1β and TNFα in colon samples of resilient, susceptible and control mice. A. IL1β, n=5,6,5 B. TNFα n=5,6,6. Data represnsents mean values and error bars represent ±S.E.M.

Table 2. miRNA intersrction between selected studies and expression change

miRNA	miRNA annotation	Condition compared	Expression change	Pvalue	Study
miR-200a	miR-200a-5p	Resilient vs. Susceptible	Up ↑	0.010484	This study
	miR-200a-3p	Resilient vs. Susceptible	Down ↓	0.03151	This study
	miR-200a-3p	Susceptible vs. Control	Up ↑	0.006847	This study
	miR-200a	miRNA-deficient (IEC) vs. Control	Down ↓	0.000312	Liu et al. 2016
	miR-200a	miRNA-deficient (Hopx-expressing cells) vs. Control	Down ↓	0.037379	
	miR-200a-3p	Germ-free vs. Control	Down ↓	0.01565	Viennois et al. 2019
miR-24	miR-24-1-3p	Susceptible vs. Control	Up ↑	0.001907	This study
	miR-24-3p	Germ-free vs. Control	Down ↓	0.006076	Viennois et al. 2019
miR-194	miR-194-2-5p	Resilient vs. Control	Up ↑	0.002663	This study
	miR-194-2-5p	Susceptible vs. Control	Up ↑	0.001338	
	miR-194	miRNA-deficient (IEC) vs. Control	Down ↓	0.00016	Liu et al. 2016
	miR-194	miRNA-deficient (Hopx-expressing cells) vs. Control	Down ↓	0.005135	
	miR-194-5p	Germ-free vs. Control	Up ↑	0.039871	Viennois et al. 2019
let-7f	let-7f-1-5p	Resilient vs. Control	Down ↓	0.042694	This study
	let-7f-1-5p	Resilient vs. Susceptible	Down ↓	0.008463	
	let-7f	miRNA-deficient (IEC) vs. Control	Down ↓	0.000702	Liu et al. 2016
	let-7f	miRNA-deficient (Hopx-expressing cells) vs. Control	Down ↓	0.041755	

2.3 Association of transcriptional and epigenetic changes in active neuronal populations with stress-resilience behavior

Authors: **Tamer Butto**† , Monika C. Chongtham †, Kanak Mungikar †, Dewi Sri, Matthias Linke, Nicolas Ruffini, Marija Milic , Konstantin Radyushkin, Susann Scweiger, Jennifer Winter†, Susanne Gerber †

(† These authors contributed equally to this work)

Manuscript in preparation

Supplmentary Statement: The manuscript presented here is a section of a broader collaborative project titled "Deciphering the epigenetic basis of resilience" (CRC1193 A05). The results presented here relate mainly to my work within the larger collaborative project.

My contributions to this study are listed in section 4.2 Contributions to individual publications.

Association of transcriptional and epigenetic changes in active neuronal populations with stress-resilience behavior

Tamer Butto[1,†] , Monika C. Chongtham[1,2, †], Kanak Mungikar[1, †], Dewi Sri[1], Matthias Linke[1], Nicolas Ruffini[1], Marija Milic[2] , Konstantin Radyushkin[2], Susann Scweiger[1,2], Jennifer Winter[1,2*], Susanne Gerber[2*]

[1] Institute of Human Genetics, University Medical Center of the Johannes Gutenberg University Mainz, Langenbeckstr 1, 55131 Mainz, Germany
[2] Leibniz Institute of Resilience Research, Wallstr 7, 55122 Mainz, Germany

Abstract

Chronic stress can have a significant impact on mood-related behavior. Despite being exposed to similar stressful cues, some individuals develop mood-related disorders, whereas others adapt to the stressor and become resilient. Although many behavioral studies attempted to understand the effects of chronic stress on behavior, there is still little understanding of the molecular mechanisms such as transcriptional and epigenetic modulation occurring in activated neuronal population in response to chronic stress. In the study presented, we performed nuclear RNA-seq, and ATAC-seq on FANS-sorted activated neuronal populations using the mouse model Arc$^{creERT2/+}$/R26$^{CAG\text{-}LSL\text{-}Sun1\text{-}sfGFP\text{-}Myc/+}$ (Arc-TRAP) following chronic social defeat stress exposure. We performed an in-depth transcriptome analysis associated with resilience or susceptible behaviors (and controls), and distinct enriched mechanisms were identified as being associated with PFC and vHIP brain regions. Upregulated genes in PFC of resilient mice were enriched for "neurogenesis" and "synaptic signaling" mechanisms. Notably, multiple synaptotagmin genes were upregulated in resilient mice compared to susceptible and control mice. In vHIP samples, upregulated transcripts in resilient mice were enriched for "regulation of neuron differentiation mechanism" while downregulated resilient-associated genes were enriched for "cell-cell adhesion". Overall, our study revealed various gene targets that appear to be involved in synaptic signaling and regulation in activated neuronal populations. These findings might offer a better understanding of molecular mechanisms underlying stress-adaptation and its influence on the resilience of susceptibility to chronic stress.

Introduction

It is increasingly evident that stress-induced modulation of gene expression is mediated via a various of epigenetic mechanisms (Stankiewicz et al., 2013). Studies in mice repeatedly exposed to aggressive conspecifics have already linked stress resilience to differential gene expression and epigenetic alterations in brain regions known to be involved in reward processing. These observationshave supported the hypothesis that the reward system is involved in stress resilience (Covington et al. 2011; LaPlant et al. 2010; Wilkinson et al. 2009).

Using a validated mouse model of stress-resilience such as chronic social defeat (Berton et al., 2006, Krishnan et al., 2007) coupled with genome-wide transcriptional and epigenetic methodologies, provides a valuable opportunity to uncover further the molecular properties underlying stress adaptation mechanisms. An example of such studies includes genome-wide transcriptional profiling, which shed light on the molecular network that could be affected following continuous stress exposure (Bagot et al. 2016). Additionally, several studies had explored the functional and transcriptional alterations of distinct brain regions such as the prefrontal cortex (PFC) and ventral hippocampus (vHIP) (Bagot et al. 2015, Covington et al. 2010, Ding et al. 2015, Sequeria et al. 2009, Vialou et al. 2014). However, the global transcriptional profiles of distinct brain regions have yielded relevant data, a more targeted approach of cell-type specific investigation may offer a fundamentally better understanding of the cellular population's individual role in processing of stress.

Immediately early genes (IEGs) had been previously used as indicators of neuronal activity, providing a connection between gene expression and neuronal synaptic activity (Guenther et al. 2013, Bagot et al. 2015). As their name denotes, IEGs are rapidly activated and transiently expressed following exposure to external stimuli. This leads to a rapid alterations in chromatin accessibility states (Su et al. 2017) and overall gene expression, leading to cellular adaptation following stress stimulation (Senba and Ueyma 1997, Saunderson et al. 2016, Bahrami and Drablos 2016). IEGs such as *Fos* and *Arc*, are frequently studied marker genes used to monitor neuronal activity following stimulation and used in a number of methods for studying activity-dependent neuronal circuits (Minatoharam akiyoshi and Okuno 2016, Clayton et al. 2020). One such example includes the genetic manipulation of transiently active neurons using targeted recombination in active populations (TRAP) (Guenther et al. 2013). This experimental setup allows genetic access to transiently active neurons by inducing tamoxifen-dependent recombinase CreERT2 exclusively in IEG-expression cells and tissues including stimulated neurons. Activated neurons express fusion nuclear membrane and superfold green-fluorescence protein (Sun1sfGFP) which can be monitored and sorted using fluorescence-activated nuclei sorting (FANS). Since its development, the TRAP strategy has been used in various of studies to uncover the unique molecular properties of activated neuronal populations (Mo et al. 2015, Fernandez-Albert et al. 2019, Marco et al. 2020, Chongtham et al. 2021).

In this study, we employ the TRAP method using the mouse model ($Arc^{creERT2(TG/WT)}$.$R26^{CAG\text{-}Sun1\text{-}sfGFP\text{-}Myc(M/WT\ or\ M/M)}$) to identify the transcriptional and chromatin accessibility alterations occurring in active neuronal populations of resilient and susceptible mice exposed to chronic social defeat. Nuclei were isolated from selected brain regions, including vHIP and PFC, and processed for nuclear RNA-seq and assay for transposase accessible chromatin (ATAC-seq). Using such analyses, we aim to detect stressor-induced transcriptional and epigenetic alterations and identify interesting candidate genes associated with resilient behavior.

Results

The use of Arc-TRAP mice to isolate active neuronal populations in association with chronic social defeat (CSD) paradigm.

To investigate the transcriptional and chromatin accessibility changes occurring in active neuronal populations, we used Arc$^{creERT2(TG/WT)}$.R26$^{CAG\text{-}Sun1\text{-}sfGFP\text{-}Myc(M/WT\ or\ M/M)}$ mice to genetically mark Arc-dependent neuronal activation (Fig. 1). In the presence of tamoxifen, Cre-ERT2 translocates to the nucleus allowing loxp cassette recombination and expression of the fusion nuclear membrane protein SUN1GFP (Fig. 1A). To assess the distinct behavioral outputs, we used a modified version of the chronic social defeat stress paradigm (CSDS) followed by social interaction (SI) test to screen the resilient animals against the susceptible animals (Krishnan et al., 2007). The behavioral paradigm consisted of 10 days of social defeat (daily 3x15sec exposure) followed by seven days of rest (Fig 1A). Tamoxifen (TAM) injection was given to the animals 5 hours before SI to trap active neuronal populations expressing *Arc* during the SI test. Following behavioral classification, animals were sacrificed, and nuclei were isolated from selected brain regions (PFC and vHIP) and sorted for active neuronal population (SUN1GFP^{+}) using FANS (Fluorescence-activated nuclei sorting) (Fig. 1B). The sorted nuclei were used for molecular applications such as nuclear RNA-seq (nucRNA-seq) and assay for transposase-accessible chromatin (ATAC-seq) to uncover the transcriptional and chromatin accessibility alterations associated with the behavioral outputs (resilience and susceptible compared to control) (Fig. 1B). Using FANS, activated neurons (GFP+) were discriminated from non-activated neurons (GFP-) (Fig. 1C). Initial analysis of activated GFP+ neuronal populations revealed an increased tendency of neuronal activation in susceptible animals compared to resilient and control animals, however, the changes were non-significant (Fig. 1D).

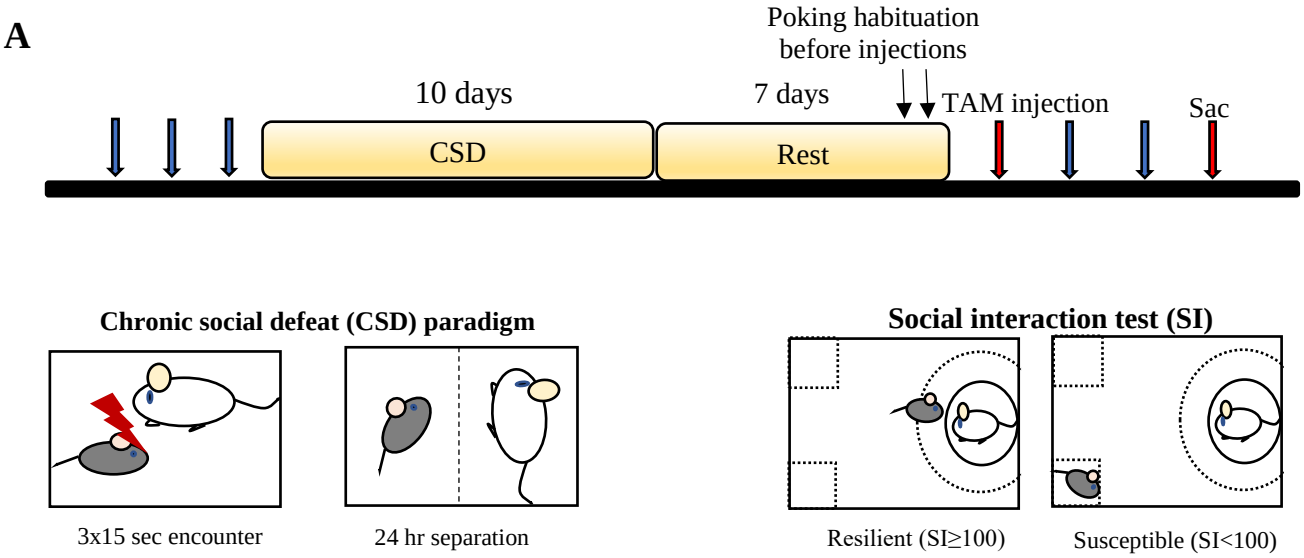

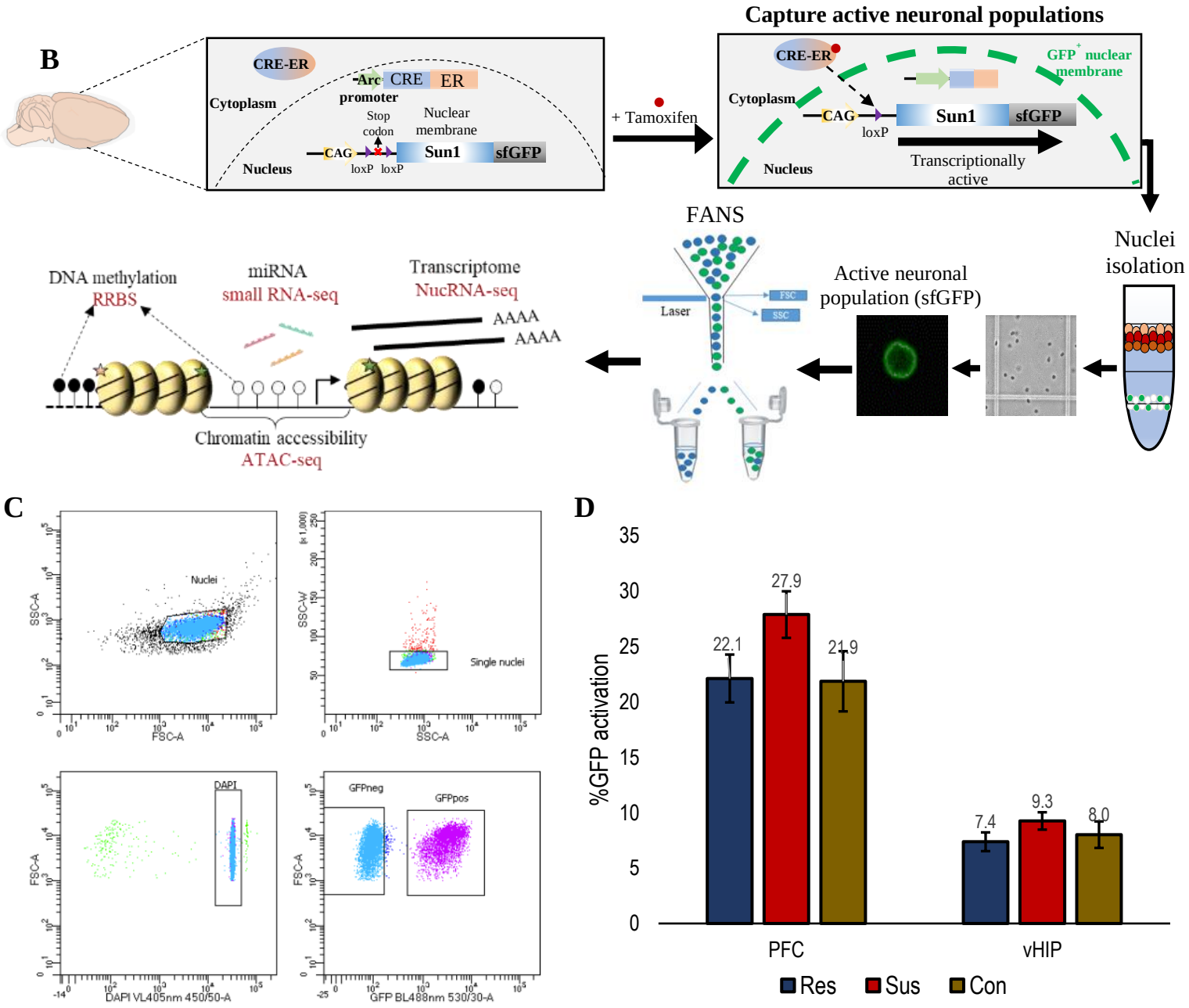

Figure 1. Behavioral paradigm to select resilient animals against susceptible animals. A. CSD is performed for 10 days followed by seven days of rest. A larger and more aggressive mouse strain (CD1) is placed with the tested mouse and defeated three times (15 seconds) followed by 24h barrier separation (sensory stimulation). TAM injection is given to the animals 5 hours before SI to trap active neuronal populations expressing *Arc* during the SI. **B.** Arc-CreERT2/R26-CAG-LSL-Sun1-sfGFP mice display activity-dependent expression of the tamoxifen-dependent recombinase CreERT2 from the endogenous locus of the immediate early gene *Arc*. In the presence of tamoxifen (TAM), recombination occurs (removal of the upstream loxP-STOP-loxP cassette) exclusively in Arc-expressing cells and tissues, including neurons. As a result, the expression of mouse SUN1sfGFP occurs. Activated neuronal populations are sorted using FANS and processed for molecular analyses such as nuclear RNA-seq and ATAC-seq **C.** Representative flow-cytometry analysis of GFP+ and GFP- nuclei. Isolated nuclei are gated according to their forward-and side-scatter properties (FSC-A/SSC-A), followed by doublet exclusion using

SSC-A and SSC-W. Nuclei are then gated according to their DAPI expression, and lastly, GFP expression is used as a sorting gate. D. % GFP expression of resilient, susceptible, and control mice. Data represent the average of 9-13 biological replicates. (PFC samples n=13,13,9; vHIP data: n=11,12,9). Error bars represent ±SD

Transcriptional and chromatin accessibility analyses reveal resilience-associated changes involved in synaptic regulation.

For the transcriptional analyses, nuclear RNA was isolated from 10,000 GFP+ and GFP- nuclei to ensure that the transcriptional differences between these isolated nuclei are distinct in each brain region tested. First, using principal component analysis (PCA), we compared the transcriptional states of GFP+ and GFP- sorted nuclei both in PFC and vHIP to ensure that the samples originated from distinct cellular populations and thus comprised of different transcriptional states. As expected, we identified two distinct clusters of the GFP+ and GFP- populations (Fig.2A-B). Gene ontology (GO) term analysis both in PFC and vHIP revealed similarly enriched termed for "cell adhesion", "extracellular matrix organization", and "cell migration" for the GFP+ population (Fig. 2B, D) (Data of GFP+ upregulated is represented in blue for downregulated in GFP- compared to GFP+). Interestingly, upregulated GFP- samples in vHip were enriched for glial-asssociated mechanisms such as "glial cell development" and "oligodendrocyte development", whereas upregulated GFP- in the PFC were enriched predominantly for neuronal-associated mechanisms such as "neurogenesis", "synapse organization" and "axonogenesis". These results suggest that the GFP- populations captured in vHIP and PFC might be different. Nevertheless, clear discrimination between the GFP+ and GFP- populations was observed, and thus we proceeded with chromatin accessibility and in-depth transcriptional analyses with the GFP+ population between the different behavioral groups.

Next, we performed low input-ATAC-seq on 5,000 isolated GFP+ nuclei to assess the chromatin accessibility alteration occurring in activated neuronal population between the distinct conditions states. Following the initial analysis, we retained the samples with an alignment rate >60% (Supplementary figure 1A). Additionally, we observed a varying number of peaks called between the distinct brain regions (Supplementary figure 1B). Peak distribution analysis across distinct genomic regions reveales a high percentage of peaks distributed across intergenic regions followed by intron and promoters regions (Supplementary Figure 1C). Next, we performed differential peak analysis between different conditions in the distinct brain regions. Here, we found a low number of differential accessible regions (DARs) in PFC samples (Supplementary Figure 2A; C vs. R 19 ; C vs. S 18 ; in R vs. S 24) compared to vHIP samples (Supplementary Figure 2B; C vs. R 114 ; C vs. S 41 ; R vs. S 348) with the majority of DARs located at intergenic regions (Supplementary Figure 2C, Table 1).

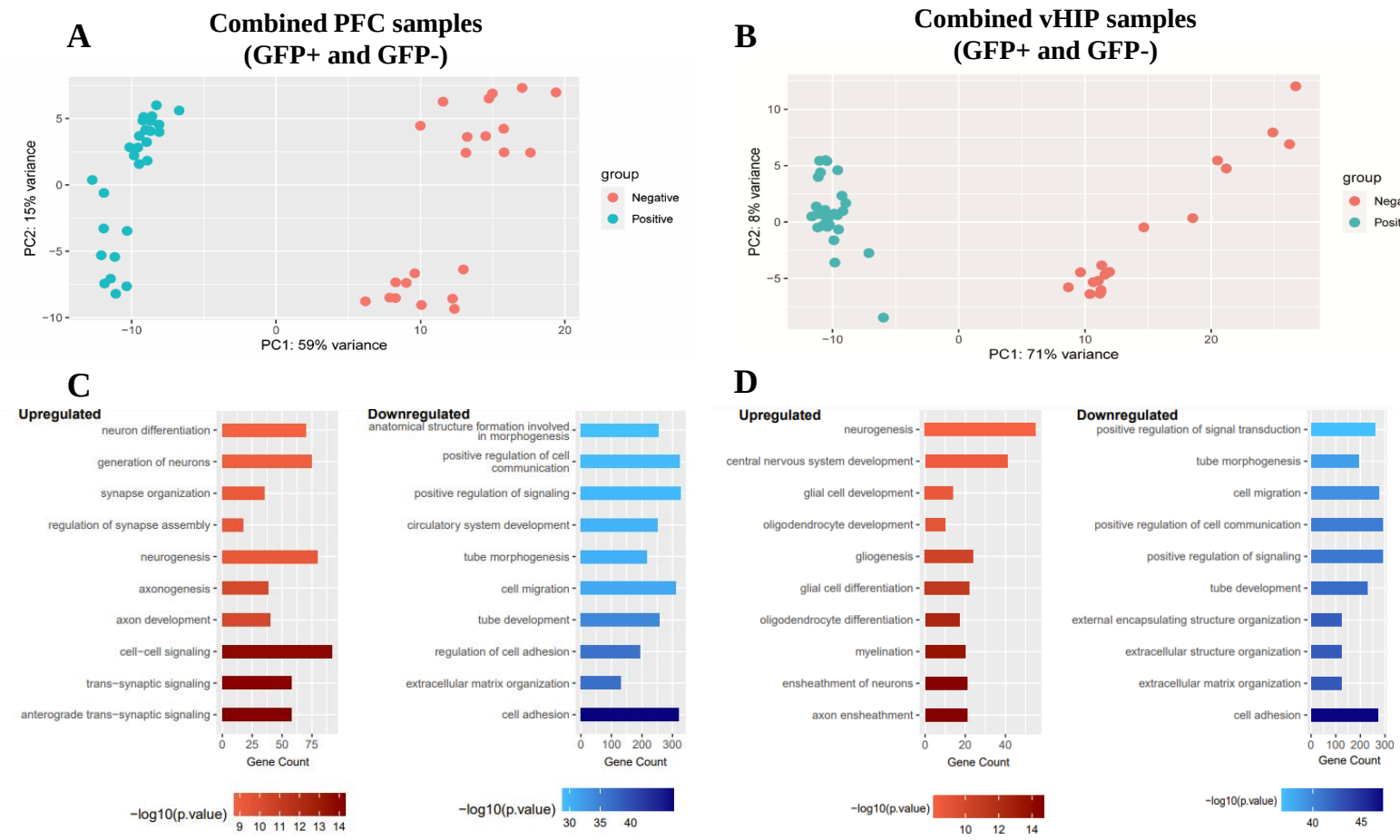

Figure 2. Classification of GFP+ and GFP+ cellular population isolated from PFC (A,C) or vHIP (B-D). A. PCA clustering analysis of all of GFP+ and GFP- samples from PFC (A, n=27, 22) and vHIP (B, (n=41, 20). C. GO term enrichment analysis of GFP- upregulated and downregulated samples compared to GFP+ in the PFC (D) and vHIP (D).

To further examine the potential candidates associated with resilient and susceptible conditions, we profiled the differential gene expression (DEGs) between the different behavioral groups both in PFC and vHIP brain regions. These analyses included the following conditions: resilient vs. control [R vs. C], susceptible vs. control [S vs. C], and resilient vs. susceptible [R vs. S]. An overall representation of all of the condition comparisons is presented in supplementary Figures 3-8. Analyzing of the samples isolated from the PFC, we identified overall more downregulated DEGs when comparing the R vs. S group (405 downregulated genes) than in all other conditions (Fig 3A). On the contrary, the number of upregulated DEGs was higher in C vs. R group (282 upregulated) compared to the other groups (Fig 3B). Interestingly, several DEGs overlapped between distinct conditions revealing group-specific transcriptional expression. For instance, 194 DEGs were identified as downregulated in C vs. R and upregulated in R vs S (Fig. 3C, Supplementary Figure 9A-C). Most notably, multiple synaptotagmin proteins (*Syt1*, *Syt5*, *Syt11*, *Syt13*) were downregulated in resilient and upregulated in susceptible, as well as additional candidates such as *Gabra1*, *Gabbr1*, and *Kcnk1* (Fig. 3C).

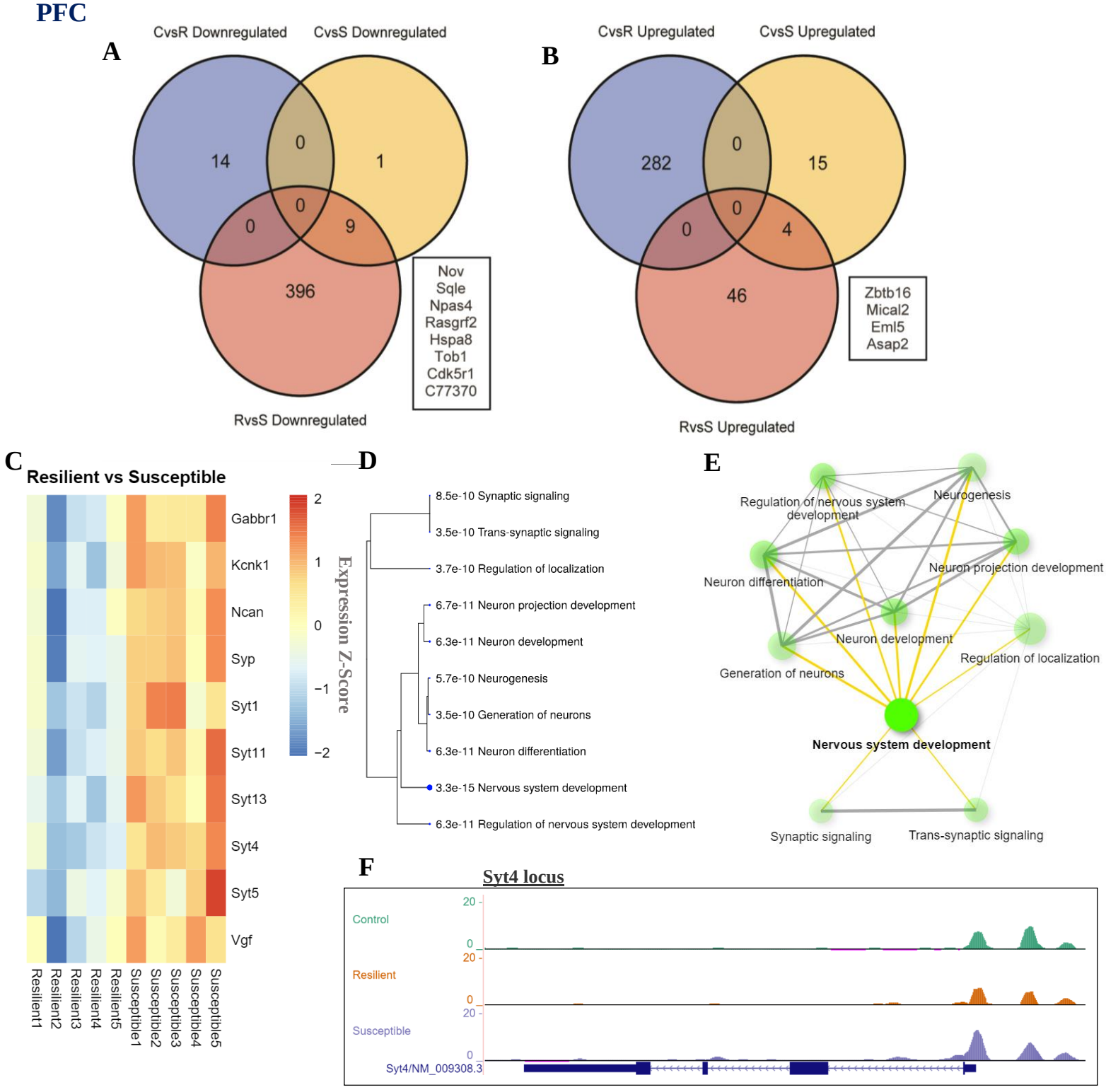

Figure 3. Overlapping DEGs (down- and upregulated) in the PFC between distinct behavioral groups. A-B. Venn diagram displaying the unique and overlapping DEGs in downregulated (A) and upregulated (B) genes. C. Heat map of nuclear RNA-seq expression z-scores computed for selected DEGs in R vs. S comparison in PFC. D. ShinyGO term analysis of the 194 gene list showing a hierarchical clustering tree summarizing the correlation among significant pathways. E. Pathways with many shared genes are clustered together where bigger dots indicate more significant P-values (Edge cutoff=0.2). F. ATAC-seq bowser track of *Syt4* locus. *Syt4* was the only DEG downregulated C vs R AND upregulated in C vs S AND upregulated in R vs S groups

GO term network analysis revealed several genes enrichment in mechanisms such as "Synaptic signaling" (p-value = 8.5e-10) and "Neuron differentiation" (p-value= 8.5e-10) (Fig 3D,E). Interestingly, *Syt4*, an additional protein from synaptotagmin family, was shown to be downregulated in C vs. R, upregulated in C vs. S, and upregulated R vs. S, suggesting a reduced expression of such protein in the resilient animals compared to control and susceptible. A representative genome browser ATAC-seq track of Syt4 locus is shown in figure 3F.

Analysis of the vHIP region, revealed more alternate DEGs numbers between the distinct conditions. C vs. R comprised 204 downregulated and 237 upregulated genes, C vs. S 184 downregulated and 156 upregulated whereas R vs .S revealed 197 downregulated and 335 upregulated genes (Fig. 4A- B). Overlapping DEGs between different groups revealed 22 combined-susceptible upregulated genes, including the transcription factor *Nfia*, which could be an interesting transcriptional regulator influenced by stress exposure (Fig 4A,C). On the contrary, 55 combined-susceptible downregulated genes included *Klf5, Satb1, Satb2, Slc17a6, and Camk2d* (Fig 5B, C). Interestingly, 10 DEGs, including *Kat2a, Neurod2 and Sox8*, were shown to be both downregulated in C vs. R and upregulated in R vs. S (Fig. 4C, F, Supplementar Figure 7D-G). A representative genome browser ATAC-seq track of *Neurod2* locus is shown in figure 4F. Targeted GO term analysis revealed these gene to be enriched for "Regulation of neurogenesis" (p-value = 2.7e-03) and "negative regulation of nervous system development" (p-value = 2.7e-03) (Fig. D, E). On the contrary, 20 DEGs, including multiple proteocadherin family members (*pcdhga12, pcdhga6, pcdhgb8, pcdha12, pcdhgb4*) were upregulated in C vs. R and downregulated R vs. S (Fig. 4C, G-H). Proteocadherin genes are known to be involved in the regulation of cellular adhesion properties, and indeed, targeted GO term analysis revealed that these genes were enriched for "Cell-cell adhesion" (p-value =1.8e-06).

Discussion

Chronic stress has become a predominant factor associated with a variety of disorders (Mariotti 2015). Therefore, it is essential to explore the molecular mechanisms associated with the behavioral alterations to chronic stress. Here, we applied Arc-TRAP mice which allowed us to capture the neuronal activated population linked to the behavioral stimulation applied using chronic social defeat. Recent studies used similar strategies to identify the chromatin structure dynamics underlying neuronal activation during epileptic seizures (Fernandez-Albert 2019) and during engram memory formation (Marco et al. 2020). Studying the individual role of the stimulated neuronal populations is arguably a better strategy to comprehend further the influence of investigated cellular population on the overall behavioral phenotypes.

Our study investigated the transcriptional and epigenetic alterations occurring in the PFC and vHIP, two highly studied brain regions shown to be involved in the mechanisms of stress-adaptation and reward circuitry (Krishnan and Nestler 2008, Russo and Nestler 2013). Overall, we identified distinct DEGs between the different behavioral conditions associated specifically with the PFC and vHIP.

vHip

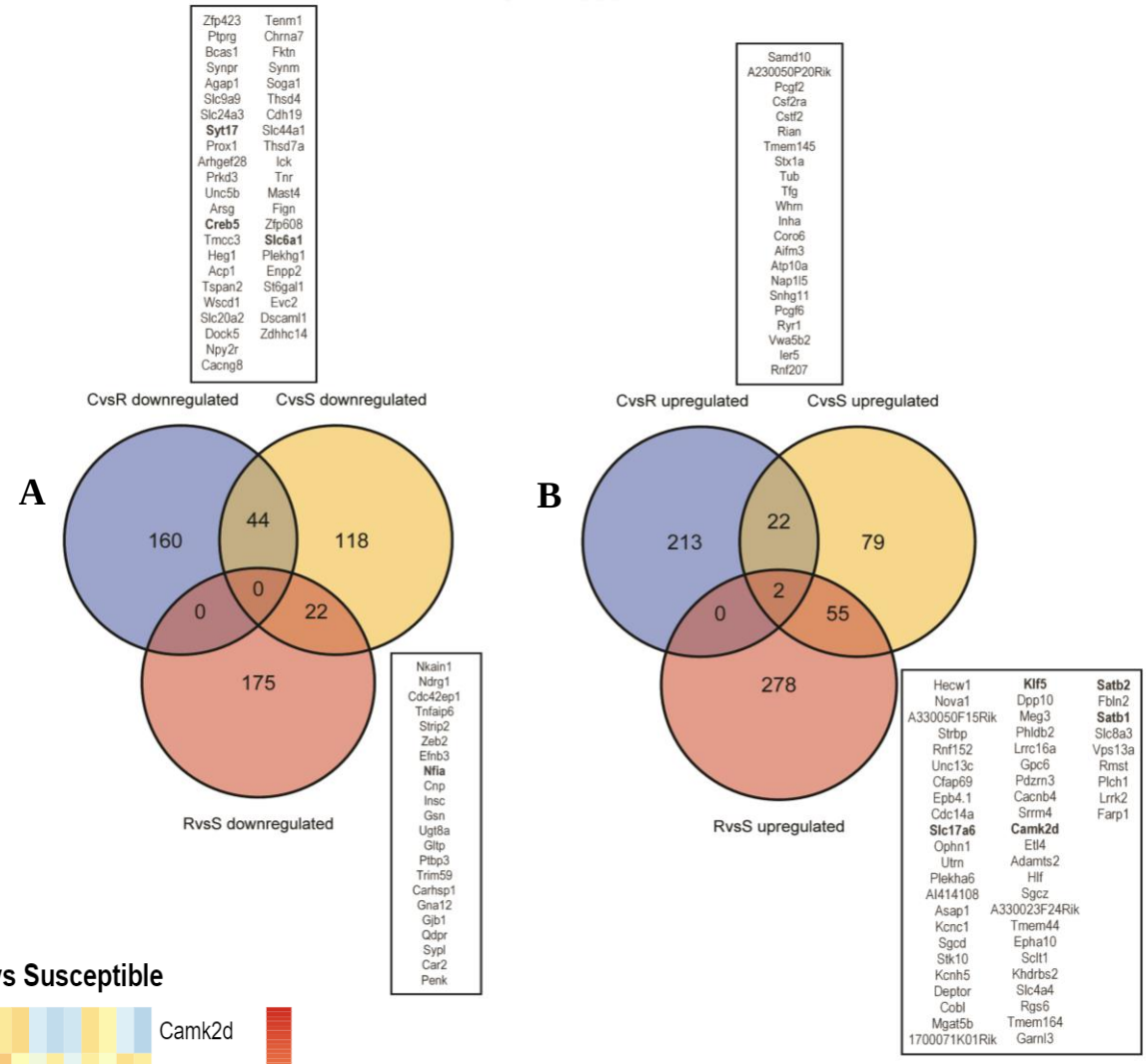

C
Resilient vs Susceptible

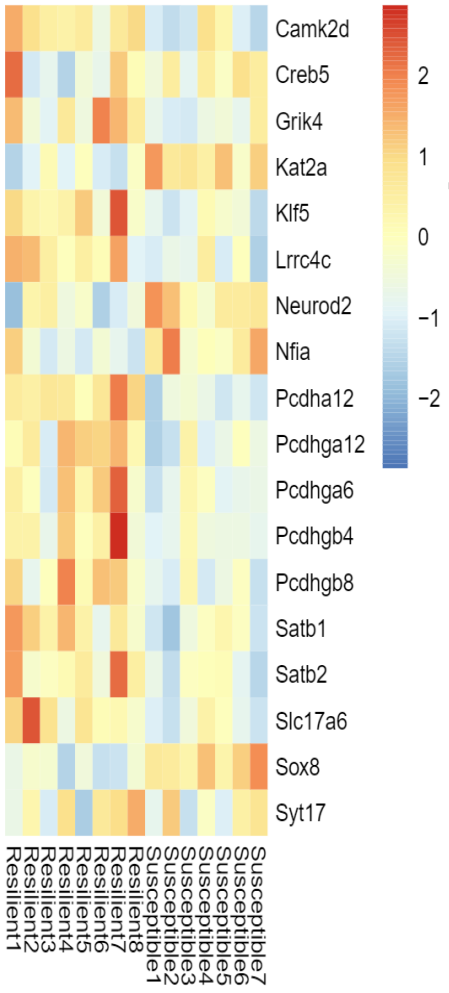

D

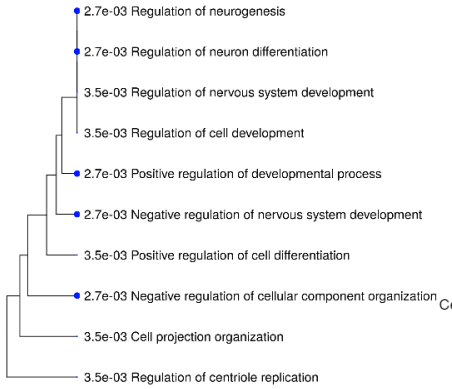

E

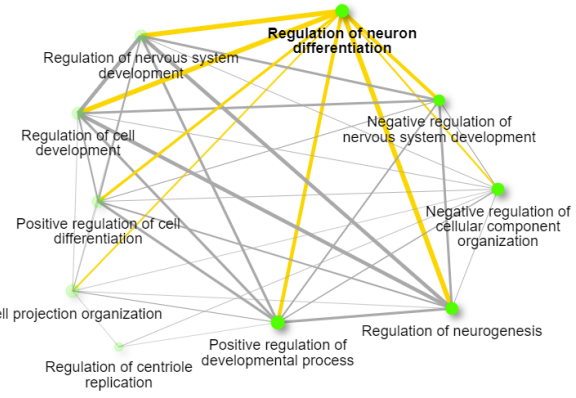

F
Neurod2 locus

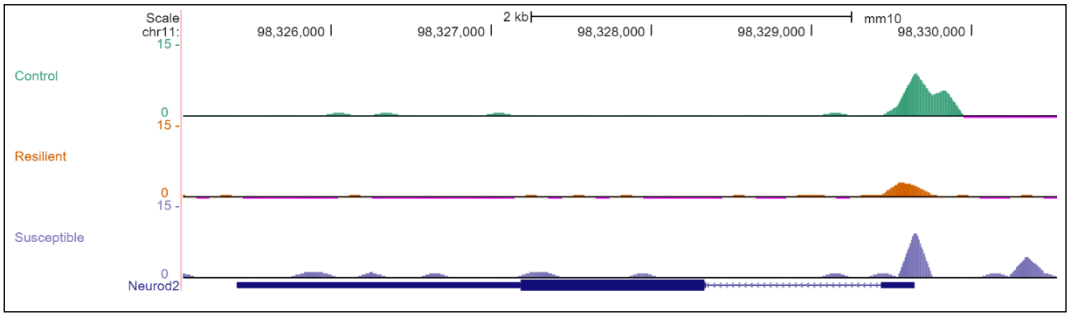

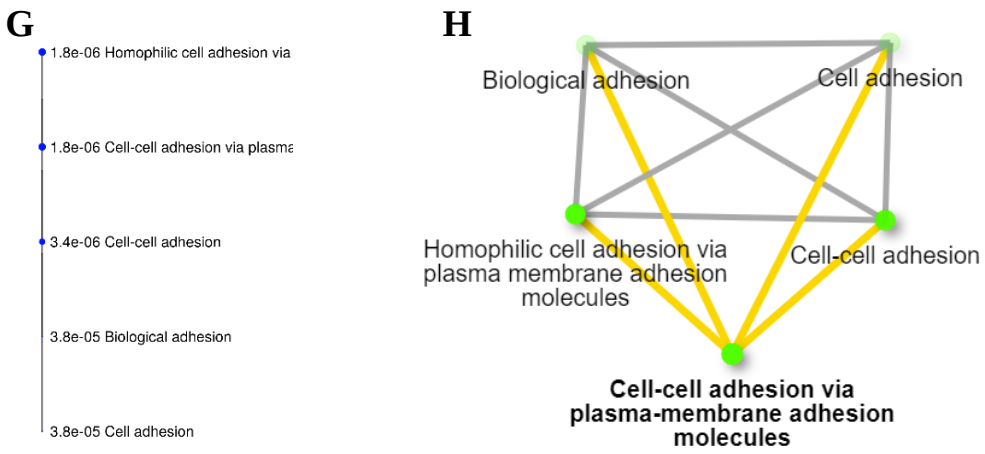

Figure 4. Overlapping DEGs (down- and upregulated) in the vHIP between distinct behavioral groups. A-B. Venn diagram displaying the unique and overlapping DEGs in downregulated (A) and upregulated (B) genes. C. Heat map of nuclear RNA-seq expression z-scores computed for selected DEGs in R vs. S comparison in vHip. D. ShinyGO term analysis showing a hierarchical clustering tree summarizing the correlation among significant pathways. E. Pathways with many shared genes are clustered together where bigger dots indicate more significant P-values (Edge cutoff=0.2). F. Representative ATAC-seq bowser track of *Neurod*2 locus. G. ShinyGO term analysis showing a hierarchical clustering tree summarizing the correlation among significant pathways. H. Pathways with many shared genes are clustered together where bigger dots indicate more significant P-values (Edge cutoff=0.2).

However, it seems that different target genes are involved in synaptic regulation and neuronal differentiation, as several downregulated resilience-associated genes were enriched for "synaptic signaling" and "regulation of neurogenesis", such as synaptotagmins (*Syt*) genes, known to be involved in calcium-dependent synaptic regulation (Bornschein and Schmidt 2019). This observation was detected both in the PFC and vHIP resilient upregulated target, suggesting a potential parallel mechanism that regulates neuronal activation, possibly through the regulation of several synaptic mechanisms. Interestingly, when we analyzed the combined % of GFP for the behavioral group, we observed an increased tendency of activation in the susceptible group compared to resilient and control groups, indicating reduced neuronal reactivity of resilience compared to susceptible animals. Further studies should aim to comprehend such relationship between neuronal reactivation and stress, particularly in association with synaptic regulation and its influence on behavior.

Upon resilient-upregulated target analysis, we identified a clear enrichment in "cell-cell adhesion" with various proteocadherins (*Pcdh*) genes. The relationship between cell-adhesion and neuron development and differentiation has gained further support (Scuderi et al. 2019, Lv et al. 2019, Kozlova et al. 2020). More specifically, the role of distinct proteocaherins has been linked to both synaptic regulation and overall neuronal differentiation (Light and Jontes 2017, Mancini, Bassani and Passafaro et al. 2020), both mechanisms of which we observed in our data.

Taken together, the study of activated neurons could provide valuable detailed information regarding the specific role of such population in processing the external stimulation, particularly in association with chronic social defeat. The identification of resilient-associated changes, particularly in such populations, provides a novel perspective into the altered mechanisms influenced by stress exposure. An increasing number of studies suggest that the mechanisms of cellular adhesion, synaptic regulation and neuronal activity could be intertwined, creating broader networks that influence one another and may a crucial role in cellular and behavioral adaptation to stress.

Material and methods

Animals

Seven to Eight week old male Arc$^{creERT2(TG/WT)}$.R26$^{CAG\text{-}Sun1\text{-}sfGFP\text{-}Myc(M/WT\ or\ M/M)}$ and CD1 retired breeders were used for this study [10,29]. Habituation in the experimental environment lasted for a week before performing tamoxifen (TAM) injections. All behavioral experiments were performed in accordance with the institutional animal welfare guidelines approved by the ethical committee of the state government of Rhineland-Palatinate, Germany, approved on 2 March 2017 (G-17-1-021)

Behavioral experiments and tamoxifen injection

Chronic social defeat was performed as previously described (Krishnan et al., 2007) with minor modification. Briefly, tested mice (Arc-Sun1GFP) was introduced to a cage of an aggressive CD1 mouse, during which they were attacked for 15 seconds (3 times per day) and displayed subordinate posturing. The paradigm consisted of 10 days of social defeat followed by 7 days of rest. For the social interaction (SI), Test mice were allowed to explore an open field box (40 cm wide × 40 cm depth × 40 cm length) that had an empty cylindrical cage, at one side for 150 S in the habituation phase. Then, the CD1 mouse was placed in the cylindrical cage and the test mouse was allowed to explore again in the test phase for another 150 seconds. Tamoxifen (Sigma–Aldrich, St. Louis, MI, USA, T5648-1G) was dissolved in corn oil:ethanol mixture (9:1) ratio at 42 °C with constant shaking at 500 rpm in light protected Eppendorf tubes (Amber). Animals were injected with tamoxifen at a dosage of 150 mg/kg 5 h before social interaction experiments to activate nuclei sfGFP expression under the control of the Arc promoter. Mice were sacrificed on the third day following tamoxifen injections and SI to allow for optimal sfGFP expression on the nuclear membrane.

Nuclei Isolation

Following behavioral experiments, the brain regions—prefrontal cortex (PFC) and ventral hippocampus (vHIP) were dissected according to region specifications in the Allen Brain Atlas for mouse. Nuclei were isolated using the iodixanol-based gradient ultracentrifugation protocol for isolation of micro-dissected brain regions as described in Chongtham et al. 2021. After the ultracentrifugation process, nuclei were collected from the 30–40% iodixanol layer interface.

FANS

Flow cytometry analysis and FANS were performed using a BD FACSAria III SORP (Becton Dickinson, Franklin Lakes, NJ, USA) equipped with four lasers (405 nm, 488 nm, 561 nm, and 640 nm) and a 70 µm nozzle. GFP expression was detected using the blue laser and a 530/30 BP filter, whereas DAPI was detected using the violet laser and a 450/50 BP filter. Prior sort, 10,000 total events were recorded, and a gating strategy was applied. First, nuclei were gated according to their forward-and side-scatter properties (FSC-A/SSC-A), followed by doublet exclusion using SSC-A and SSC-W. Nuclei were then gated according to their DAPI expression. GFP expression was used as a sorting gate. Sorted nuclei were collected in 1.5 mL Eppendorf tubes containing the optimal buffers for downstream analyses.

RNA Isolation and nucRNA-Seq Library Preparation

Ten thousand GFP+ or GFP- FANS-sorted nuclei were collected in 100 µL of RLT buffer followed by flash freezing. RNA was purified using the RNeasy Micro kit (Qiagen 74004, Hilden, Germany) following the manufacturer's instructions. For the nuclear RNA-seq library preparation, we used a ribo-depletion based method, using the Ovation® SoLo RNA-Seq System (NuGEN M01406v2, Redwood City, CA, USA). NGS library preparation was performed following NuGEN's standard protocol (M01406v2). Libraries were prepared with a starting amount of 1.5 ng and amplified in 14 PCR cycles. The resulting cDNA were sheared using an S2 focused ultrasonicator (Covaris, Woburn, MA, USA) with the following parameters: 20% duty cycle; 0.5 intensity; 50 cycles/burst; 20 °C; 60 s. The NGS library preparation was performed with 3.16 ng of sheared cDNA with NuGEN's Ovation Ultralow System V2 M01379 v5. Libraries were amplified in 11 PCR cycles. NGS libraries were profiled in a High Sensitivity DNA Chip on a 2100 Bioanalyzer (Agilent Technologies, Santa Clara, CA, USA) and quantified using the Qubit dsDNA HS Assay Kit, in a Qubit 2.0 Fluorometer (Life Technologies, Carlsbad, CA, USA). Samples were sequenced on NextSeq 500 Highoutput Flowcells, single-read aiming for a total of 60M reads. All RNA-seq library preparations and sequencing were performed by the Genomic Core Facility from the Institute of Molecular Biology (IMB, Mainz, Germany).

Nuclear RNA-seq Data analysis

Sequenced data quality assessment was performed using FASTQC (v. 0.11.8). Read alignment was done using STAR aligner (v2.7.1a) (Dobin et al. 2013) to the *Mus musculus* genome (mm10) UCSC annotations with default parameter. Further, duplicates were removed using UMI (Unique Molecular Identifier) introduced by Nugen Ovation RNA Solo library. Uniquely mapped reads were retained in the output BAM file. Samtools(v1.7) (Li et al. 2009) was used to sort, and index mapped files. Read count per gene was calculated using HTSeq (v0.11.1) (Andres et al. 2015). Normalization and differential expression analysis were conducted using the DESeq2 (Love et al. 2014) Bioconductor package with an FDR rate of 0.05. The ToppGEne database was used for gene ontology analysis.

ATAC-Seq Library Preparation

ATAC-seq was performed as previously described (Buenrostro et al. 2013**)** with minor modifications. Briefly, 5,000 FANS-sorted nuclei were collected in 50 µL cold lysis buffer (10 mM Tris-HCl, pH 7.4, 10 mM NaCl, 3 mM $MgCl_2$, and 0.1% IGEPAL CA-630) and centrifuged at 750× *g* for 15 min using a cold centrifuge (4 °C). Immediately after centrifugation, the pellet was resuspended in the transposase reaction mix (2.5 µL 2× TD buffer, 1 µL transposase (Illumina FC-121–1030, San Diego, CA, USA) and 1.5 µL nuclease-free water). The transposition reaction was carried out for 30 min at 37 °C. Following transposition, the sample was purified using a Qiagen MinElute kit (Qiagen, 28006, Hilden, Germany) following the manufacturer's instructions. After purification, the library was amplified using 1× NEBnext PCR master mix (NEB M0541, Ipswich, MA, USA) and 1.25 µM of custom Nextera PCR primers 1 and 2 (See Buenrostro et al. 2013). An optimization qPCR quantification was performed as described in Buenrostro et al. 2013. The following PCR conditions were used: 72 °C for 5 min; 98 °C for 30 s; thermocycling at 98 °C for 10 s, 63 °C for 30 s, and 72 °C for 1 min. After 18-21 cycles of PCR amplification, samples were further purified using Qiagen MinElute kit. To remove primer dimers, samples were further purified using purified by running an 8% TBE gel and size-selected for >200nt. The purified samples were then analyzed in bioanalyzer (Agilent) and sequenced on NextSeq 500 Highoutput Flowcell (150-cycles PE for 2 × 75bp). Sequencing was performed by the Genomic Core Facility from the Institute of Molecular Biology (IMB, Mainz, Germany).

ATAC-Seq Data Analysis

The ATAC-seq data quality check was performed using FASTQC (v. 0.11.8). Further, adaptors were removed using Trimmomatic (v0.39) (Bolger et al. 214). Paired-end ATAC-seq reads were mapped to *Mus musculus* genome (mm10) UCSC annotations using Bowtie2 (v2.3.5.1) with default parameters. Properly paired end reads with high mapping quality (MAPQ ≥ 10) were retained in analysis with the help of Samtools (v1.7). Next, using Picard tools MarkDuplicates utility, duplicates were removed. ATAC-seq peaks were called using MACS2 (v2.1.1.20160309) (Zhang et al. 2008) and visualized with UCSC genome browser. Peaks that were reproducible in all samples were considered for differential accessible region analysis. Differential accessible region analysis was performed using DESeq (*p*-value cutoff of 0.05). Further, peaks were annotated using the annotatePeaks.pl utility of HOMER.

Acknowledgments

We would like to thank the Institute of the Molecular Biology (Mainz) and particularly the microscopy, flow cytometry, and genomics core facilities for their assistance and support throughout the study. The use of GCF's NextSeq500 (INST 247/870-1 FUGG) is gratefully acknowledged. We also extend our sincere thanks to the Mouse Behavioral Unit of the Leibniz Institute of Resilience Research. We are grateful to the CRC1193 (DFG) for funding our work.

References

Bagot, Rosemary C., Eric M. Parise, Catherine J. Peña, Hong Xing Zhang, Ian Maze, Dipesh Chaudhury, Brianna Persaud, Roger Cachope, Carlos A. Bolaños-Guzmán, Joseph Cheer, Karl Deisseroth, Ming Hu Han, and Eric J. Nestler. 2015. "Ventral Hippocampal Afferents to the Nucleus Accumbens Regulate Susceptibility to Depression." *Nature Communications* 6(1):1–9.

Bagot, Rosemary C. C., Hannah M. M. Cates, Immanuel Purushothaman, Zachary S. S. Lorsch, Deena M. M. Walker, Junshi Wang, Xiaojie Huang, Oliver M. M. Schlüter, Ian Maze, Catherine J. J. Peña, Elizabeth A. A. Heller, Orna Issler, Minghui Wang, Won min Song, Jason L. Stein, Xiaochuan Liu, Marie A. A. Doyle, Kimberly N. N. Scobie, Hao Sheng S. Sun, Rachael L. L. Neve, Daniel Geschwind, Yan Dong, Li Shen, Bin Zhang, and Eric J. J. Nestler. 2016. "Circuit-Wide Transcriptional Profiling Reveals Brain Region-Specific Gene Networks Regulating Depression Susceptibility." *Neuron* 90(5):969–83.

Bahrami, Shahram and Finn Drabløs. 2016. "Gene Regulation in the Immediate-Early Response Process." *Advances in Biological Regulation* 62:37–49.

Berton, Olivier, Colleen A. McClung, Ralph J. DiLeone, Vaishnav Krishnan, William Renthal, Scott J. Russo, Danielle Graham, Nadia M. Tsankova, Carlos A. Bolanos, Maribel Rios, Lisa M. Monteggia, David W. Self, and Eric J. Nestler. 2006. "Essential Role of BDNF in the Mesolimbic Dopamine Pathway in Social Defeat Stress." *Science* 311(5762):864–68.

Chongtham, Monika Chanu, Tamer Butto, Kanak Mungikar, Susanne Gerber, and Jennifer Winter. 2021. "Intact vs. Fans for Cell-Type-Specific Nuclei Sorting: A Comprehensive Qualitative and Quantitative Comparison." *International Journal of Molecular Sciences* 22(10):5335.

Covington, Herbert E., Mary Kay Lobo, Ian Maze, Vincent Vialou, James M. Hyman, Samir Zaman, Quincey LaPlant, Ezekiel Mouzon, Subroto Ghose, Carol A. Tamminga, Rachael L. Neve, Karl Deisseroth, and Eric J. Nestler. 2010. "Antidepressant Effect of Optogenetic Stimulation of the Medial Prefrontal Cortex." *Journal of Neuroscience* 30(48):16082–90.

Covington, Herbert E., Ian Maze, Hao Sheng Sun, Howard M. Bomze, Kristine D. DeMaio, Emma Y. Wu, David M. Dietz, Mary Kay Lobo, Subroto Ghose, Ezekiel Mouzon, Rachael L. Neve, Carol A. Tamminga, and Eric J. Nestler. 2011. "A Role for Repressive Histone Methylation in Cocaine-Induced Vulnerability to Stress." *Neuron* 71(4):656–70.

Fernandez-Albert, Jordi, Michal Lipinski, María T. Lopez-Cascales, M. Jordan Rowley, Ana M. Martin-Gonzalez, Beatriz del Blanco, Victor G. Corces, and Angel Barco. 2019. "Immediate and Deferred Epigenomic Signatures of in Vivo Neuronal Activation in Mouse Hippocampus." *Nature Neuroscience* 22(10):1718–30.

Gaiteri, C., Y. Ding, B. French, G. C. Tseng, and E. Sibille. 2014. "Beyond Modules and Hubs: The Potential of Gene Coexpression Networks for Investigating Molecular Mechanisms of Complex Brain Disorders." *Genes, Brain and Behavior* 13(1):13–24.

Guenthner, Casey J., Kazunari Miyamichi, Helen H. Yang, H. Craig Heller, and Liqun Luo. 2013. "Permanent Genetic Access to Transiently Active Neurons via TRAP: Targeted Recombination in Active Populations." *Neuron* 78(5):773–84.

Kozlova, Irina, Saroj Sah, Ryan Keable, Iryna Leshchyns'ka, Michael Janitz, and Vladimir Sytnyk. 2020. "Cell Adhesion Molecules and Protein Synthesis Regulation in Neurons." *Frontiers in Molecular Neuroscience* 13:12.

Krishnan, Vaishnav and Eric J. Nestler. 2008. "The Molecular Neurobiology of Depression." *Nature* 455(7215):894–902.

Laplant, Quincey, Vincent Vialou, Herbert E. Covington, Dani Dumitriu, Jian Feng, Brandon L. Warren, Ian Maze, David M. Dietz, Emily L. Watts, Sergio D. Iñiguez, Ja Wook Koo, Ezekiell Mouzon, William Renthal, Fiona Hollis, Hui Wang, Michele A. Noonan, Yanhua Ren, Amelia J. Eisch, Carlos A. Bolaños, Mohamed Kabbaj, Guanghua Xiao,

Rachael L. Neve, Yasmin L. Hurd, Ronald S. Oosting, Gouping Fan, John H. Morrison, and Eric J. Nestler. 2010. "Dnmt3a Regulates Emotional Behavior and Spine Plasticity in the Nucleus Accumbens." *Nature Neuroscience* 13(9):1137–43.

Light, Sarah E. W. and James D. Jontes. 2017. "δ-Protocadherins: Organizers of Neural Circuit Assembly." *Seminars in Cell and Developmental Biology* 69:83–90.

Lv, Xiaohui, Si Qiang Ren, Xin Jun Zhang, Zhongfu Shen, Tanay Ghosh, Anjin Xianyu, Peng Gao, Zhizhong Li, Susan Lin, Yang Yu, Qiangqiang Zhang, Matthias Groszer, and Song Hai Shi. 2019. "TBR2 Coordinates Neurogenesis Expansion and Precise Microcircuit Organization via Protocadherin 19 in the Mammalian Cortex." *Nature Communications* 10(1):1–15.

Mancini, Maria, Silvia Bassani, and Maria Passafaro. 2020. "Right Place at the Right Time: How Changes in Protocadherins Affect Synaptic Connections Contributing to the Etiology of Neurodevelopmental Disorders." *Cells* 9(12).

Mariotti, Agnese. 2015. "The Effects of Chronic Stress on Health: New Insights into the Molecular Mechanisms of Brain-Body Communication." *Future Science OA* 1(3).

Minatohara, Keiichiro, Mika Akiyoshi, and Hiroyuki Okuno. 2016. "Role of Immediate-Early Genes in Synaptic Plasticity and Neuronal Ensembles Underlying the Memory Trace." *Frontiers in Molecular Neuroscience* 8(JAN2016):78.

Mo, Alisa, Eran A. Mukamel, Fred P. Davis, Chongyuan Luo, Gilbert L. Henry, Serge Picard, Mark A. Urich, Joseph R. Nery, Terrence J. Sejnowski, Ryan Lister, Sean R. Eddy, Joseph R. Ecker, and Jeremy Nathans. 2015. "Epigenomic Signatures of Neuronal Diversity in the Mammalian Brain." *Neuron* 86(6):1369–84.

Russo, Scott J. and Eric J. Nestler. 2013. "The Brain Reward Circuitry in Mood Disorders." *Nature Reviews Neuroscience* 14(9):609–25.

Saunderson, Emily A., Helen Spiers, Karen R. Mifsud, Maria Gutierrez-Mecinas, Alexandra F. Trollope, Abeera Shaikh, Jonathan Mill, and Johannes M. H. M. Reul. 2016. "Stress-Induced Gene Expression and Behavior Are Controlled by DNA Methylation and Methyl Donor Availability in the Dentate Gyrus." *Proceedings of the National Academy of Sciences of the United States of America* 113(17):4830–35.

Scuderi, Soraya, Giovanna G. Altobelli, Vincenzo Cimini, Gianfilippo Coppola, and Flora M. Vaccarino. 2021. "Cell-to-Cell Adhesion and Neurogenesis in Human Cortical Development: A Study Comparing 2D Monolayers with 3D Organoid Cultures." *Stem Cell Reports* 16(2):264–80.

Senba, Emiko and Takashi Ueyama. 1997. "Stress-Induced Expression of Immediate Early Genes in the Brain and Peripheral Organs of the Rat." *Neuroscience Research* 29(3):183–207.

Sequeira, Adolfo, Firoza Mamdani, Carl Ernst, Marquis P. Vawter, William E. Bunney, Veronique Lebel, Sonia Rehal, Tim Klempan, Alain Gratton, Chawki Benkelfat, Guy A. Rouleau, Naguib Mechawar, and Gustavo Turecki. 2009. "Global Brain Gene Expression Analysis Links Glutamatergic and GABAergic Alterations to Suicide and Major Depression." *PLoS ONE* 4(8):e6585.

Stankiewicz, Adrian M., Artur H. Swiergiel, and Pawel Lisowski. 2013. "Epigenetics of Stress Adaptations in the Brain." *Brain Research Bulletin* 98:76–92.

Su, Yijing, Jaehoon Shin, Chun Zhong, Sabrina Wang, Prith Roychowdhury, Jongseuk Lim, David Kim, Guo Li Ming, and Hongjun Song. 2017. "Neuronal Activity Modifies the Chromatin Accessibility Landscape in the Adult Brain." *Nature Neuroscience* 20(3):476–83.

Vialou, Vincent, Rosemary C. Bagot, Michael E. Cahill, Deveroux Ferguson, Alfred J. Robison, David M. Dietz, Barbara Fallon, Michelle Mazei-Robison, Stacy M. Ku, Eileen Harrigan, Catherine A. Winstanley, Tej Joshi, Jian Feng,

Olivier Berton, and Eric J. Nestler. 2014. “Prefrontal Cortical Circuit for Depression- and Anxiety-Related Behaviors Mediated by Cholecystokinin: Role of ΔFosB.” *Journal of Neuroscience* 34(11):3878–87.

Wilkinson, Matthew B., Guanghua Xiao, Arvind Kumar, Quincey LaPlant, William Renthal, Devanjan Sikder, Thomas J. Kodadek, and Eric J. Nestler. 2009. “Imipramine Treatment and Resiliency Exhibit Similar Chromatin Regulation in the Mouse Nucleus Accumbens in Depression Models.” *Journal of Neuroscience* 29(24):7820–32.

2.3.1 Supplementary material

A

		Sample name	Alignment after Trimming	Peak calling
PFC	Resilient	JGU_Gerber_2020_03_01_R1P	79.03%	9311
		jgu_gerber_2020_04_butto_ATAC_6_R13P	90.17%	36654
		jgu_gerber_2020_07_1_R2PFC	74.57%	13074
	Suceptible	JGU_Gerber_2020_03_02_S1P	84.29%	34679
		JGU_Gerber_2020_03_06_S4PFC	79.74%	31818
		jgu_gerber_2020_06_butto_ATAC_02_S7P	78.78%	9018
		jgu_gerber_2020_06_butto_ATAC_03_S8P	88.21%	13904
	Control	JGU_Gerber_2020_03_03_C1P	78.04%	7862
		jgu_gerber_2020_05_butto_ATAC_2_C18P	90.16%	23323
		jgu_gerber_2020_05_butto_ATAC_3_C13P	92.35%	22784
vHIP	Resilient	JGU_Gerber_2020_03_05_R2vH	61.18%	10645
		jgu_gerber_2020_04_butto_ATAC_1_R3vH	71.52%	39741
		jgu_gerber_2020_06_butto_ATAC_06_R7vH	73.88%	20897
	Suceptible	jgu_gerber_2020_04_butto_ATAC_2_S3vH	68.57%	10838
		jgu_gerber_2020_06_butto_ATAC_05_S8vH	58.83%	11427
		jgu_gerber_2020_07_3_S1vHIP	75.24%	7139
	Control	JGU_Gerber_2020_03_04_C1vH	77.81%	6617
		jgu_gerber_2020_04_butto_ATAC_3_C3vH	71.14%	50500

B

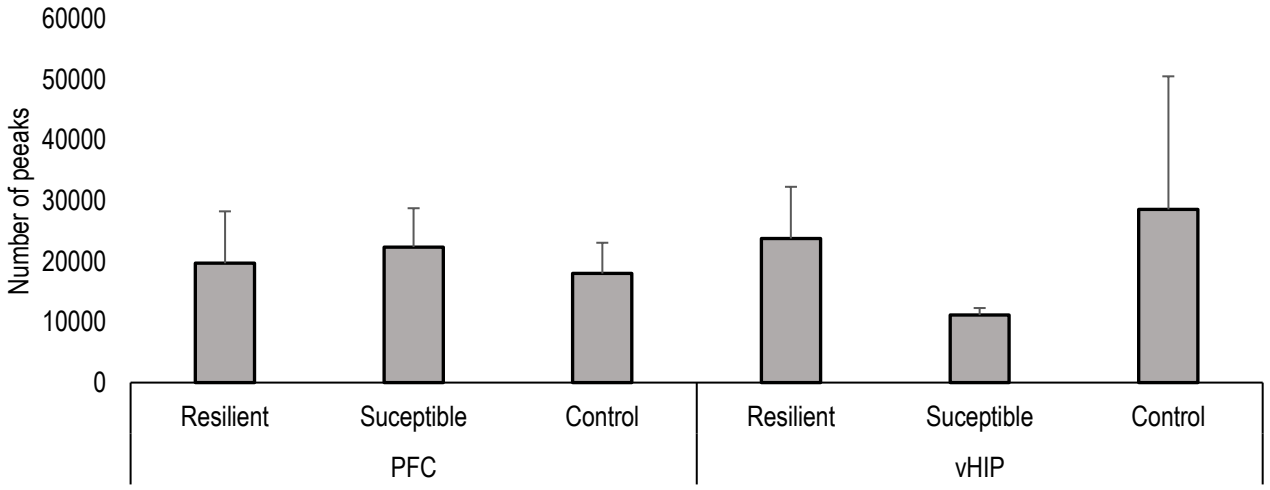

Continue next page

C

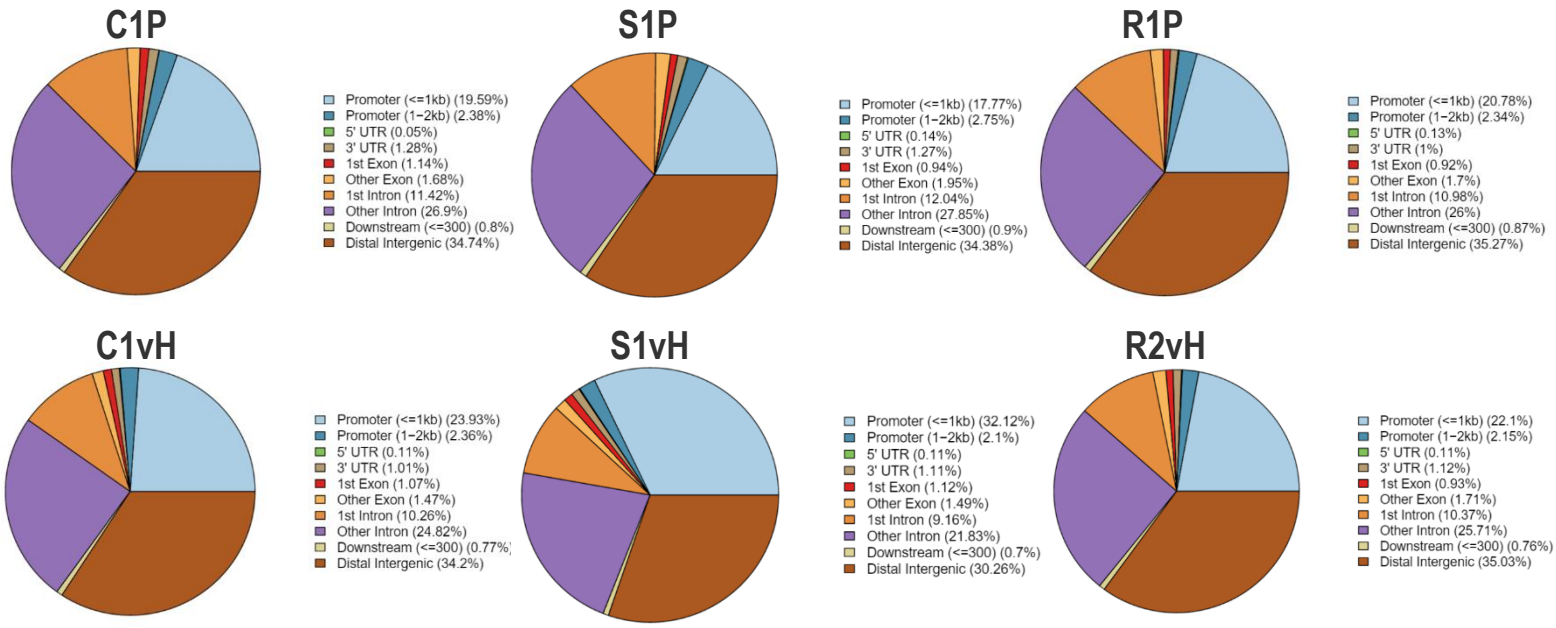

Supplementary figure 1: Low input ATAC-seq % of alignment and number of peaks detected. A. Table biological replicates sequencing properties including % of alignment and number of peaks detected. B. Average peaks number per condition (res, sus, con) per brain region (PFC and vHIP). Error bars represent ±S.E.M. C. Representative images of peaks distribution across distinct genomic regions.

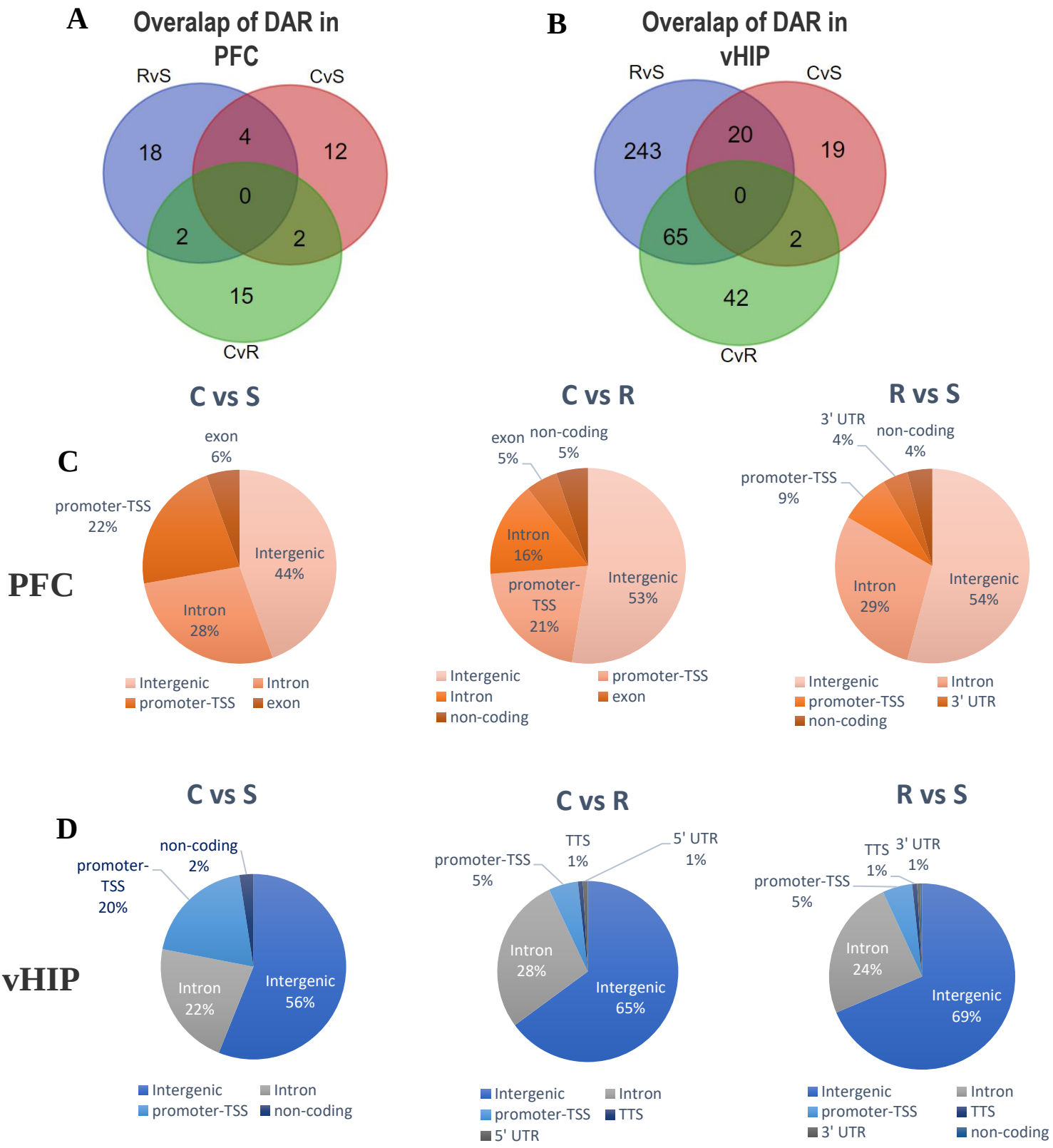

Supplementary figure 2: Differentially accessible regions analysis. A-B. Venn diagrams displaying the overlapping DARs in the PFC (A) and vHIP (B). C-D. Distribution of DARs across distinct genomic regions in PFC (C) and vHIP (D), in Con vs Sus, Con vs Res and Res vs Sus. (PFC material- DARs in C vs R 19 ; DARs in C vs S 18 ; DARs in R vs S 24; vHIP material- DARs in C vs R 114 ; DARs in C vs S 41 ; DARs in R vs S 348

Table 1. Overlapping genes across the different behavioral conditions in PFC and vHIP						
PFC			vHIP			
CvS AND RvS	CvR AND RvS	CvR AND CvS	CvS AND RvS	CvR AND RvS		CvR AND CvS
4	2	2	20	65		2
Ppp3r1	Limk2	2610301B20Rik	Cox7c	Scgb2b2	Nedd4	G6pd2
Gpr55	Fyn	Mettl4	Gm30214	Dlgap2	6530403H02Rik	Shcbp1
AF366264			2700054A10Rik	Siglech	Rpap2	
Tada1			Tex14	Kif18a	Col3a1	
			Pex2	Gm4788	Fbxw17	
			1700008C04Rik	**Npy**	Mir5624	
			Rpl31-ps12	Gm12171	Zfp352	
			Ube3a	AA536875	G530011O06Rik	
			Tmem200c	Cldn34d	Gm29089	
			Zmym2	Gpr22	Cldn34c4	
			Gsdmc	Defb41	Gm39774	
			Zc2hc1a	2610316D01Rik	Vwa8	
			Olfr845	Vmn2r9	Fam135b	
			Saxo1	Mir1904	Tbx18	
			Unc80	Gm28590	Olfr371	
			Arx	Ube2e2	Etv4	
			Mir101c	Samt1	**Syncrip**	
			Dpf3	Pom121l2	Axin2	
			1700017L05Rik	Cfap126	Api5	
			Prame	Serpinb1b	Ssty1	
				Tlr4	1700020D14Rik	
				Pqlc1	Olfr1295	
				Slitrk6	Col22a1	
				Timm8a1	2900052N01Rik	
				Esp1	Mir3963	
				Shisal2b	Sulf2	
				4930503H13Rik	Mir6336	
				Adgrb3	LOC100125594	
				Ndc80	4930509J09Rik	
				Zmynd11	**Hist2h2ac**	
				Mir1902	Malrd1	
				Fahd2a	Ccng1	
				Rad51b		

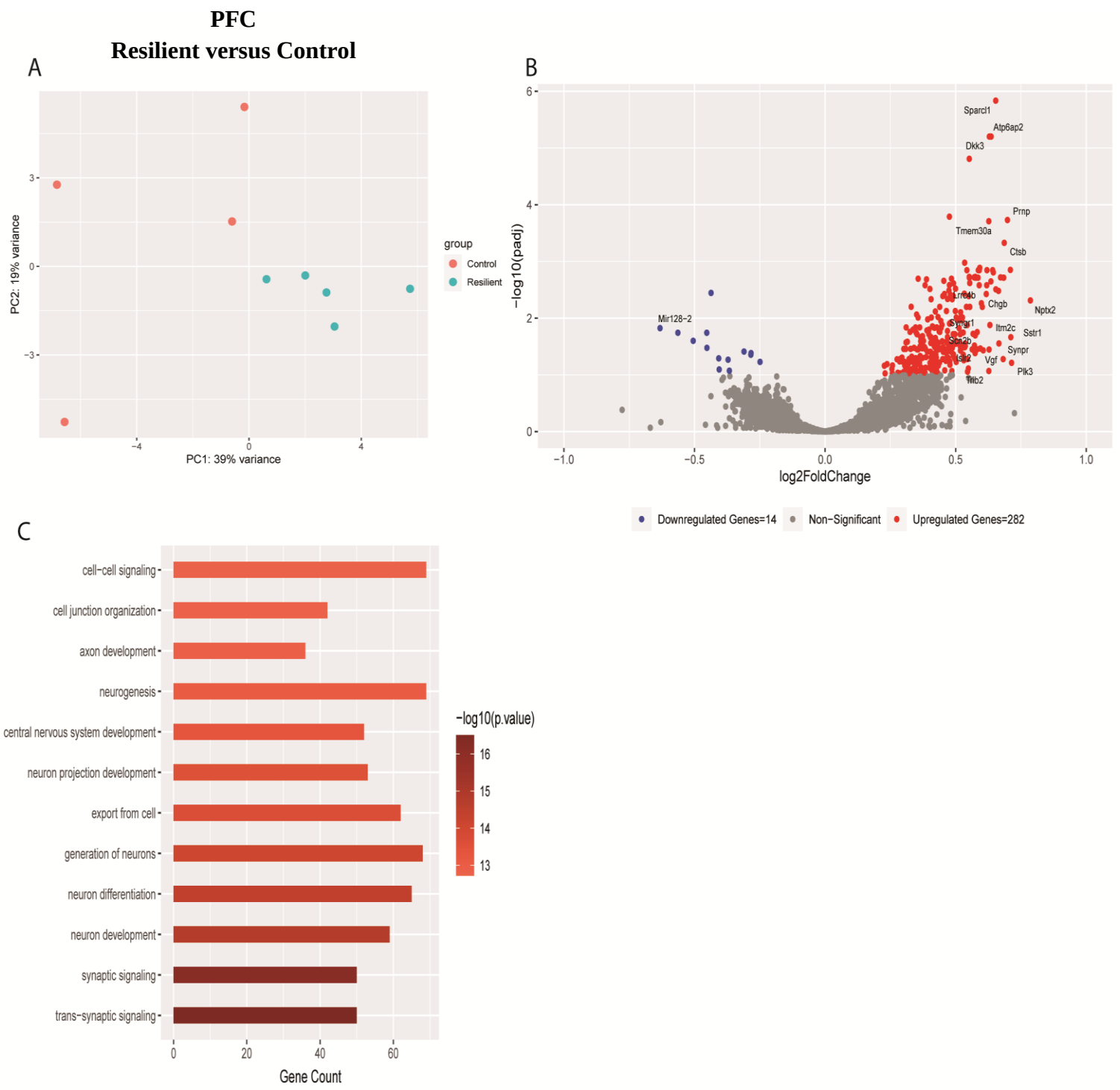

Supplementary Figure 3: Resilient versus control transcriptional comparison in PFC. A. PCA clustering analysis of resilient samples compared to control. B. Volcano Plot representing the DEGs of resilient samples compared to control. GO term enrichment analysis of upregulated transcripts in resilient compared to control.

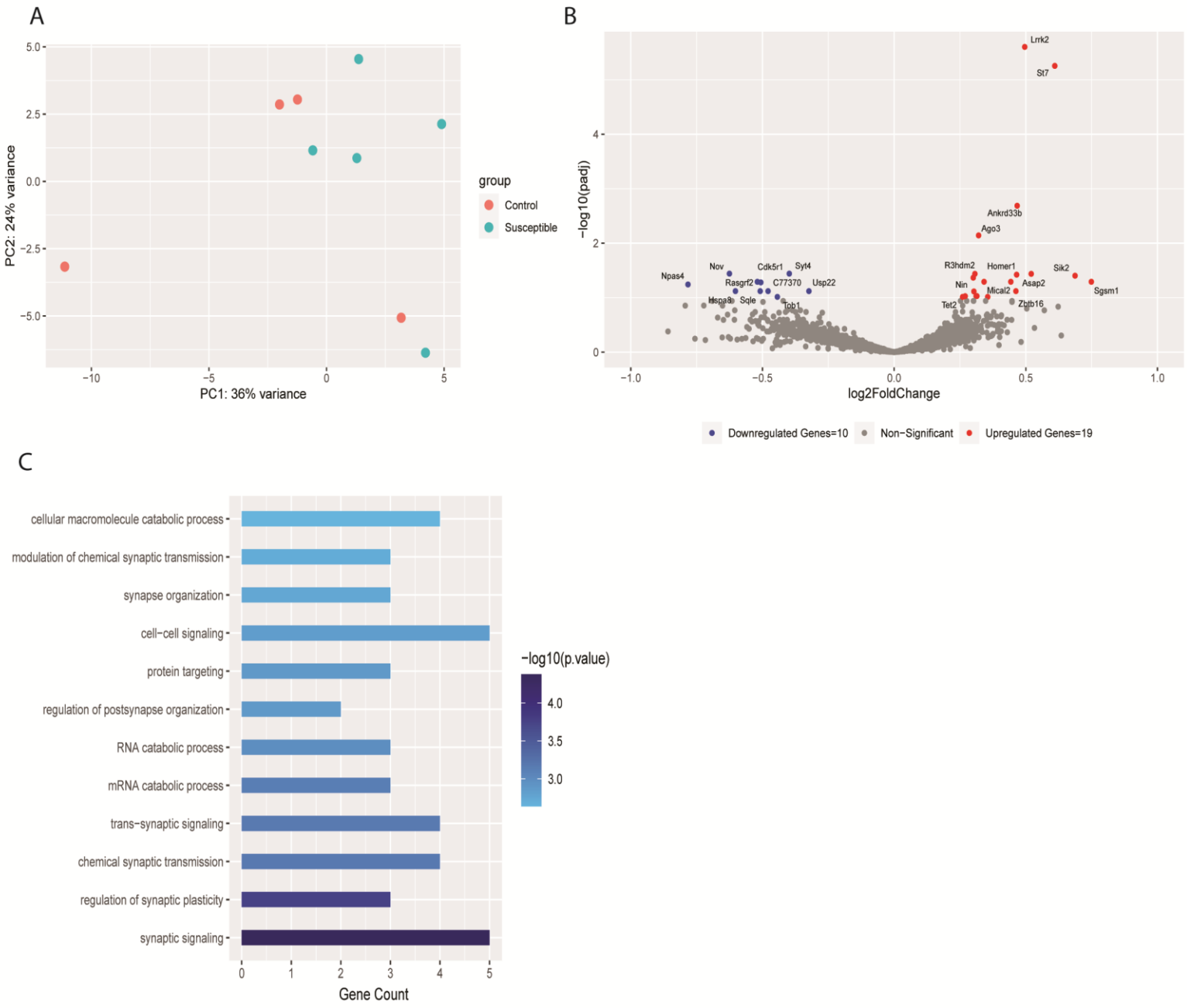

Supplementary figure 4: Susceptible versus control transcriptional comparison in PFC. A. PCA clustering analysis of susceptible samples compared to control. B. Volcano Plot representing the DEGs of susceptible samples compared to control. GO term enrichment analysis of upregulated transcripts in susceptible compared to control.

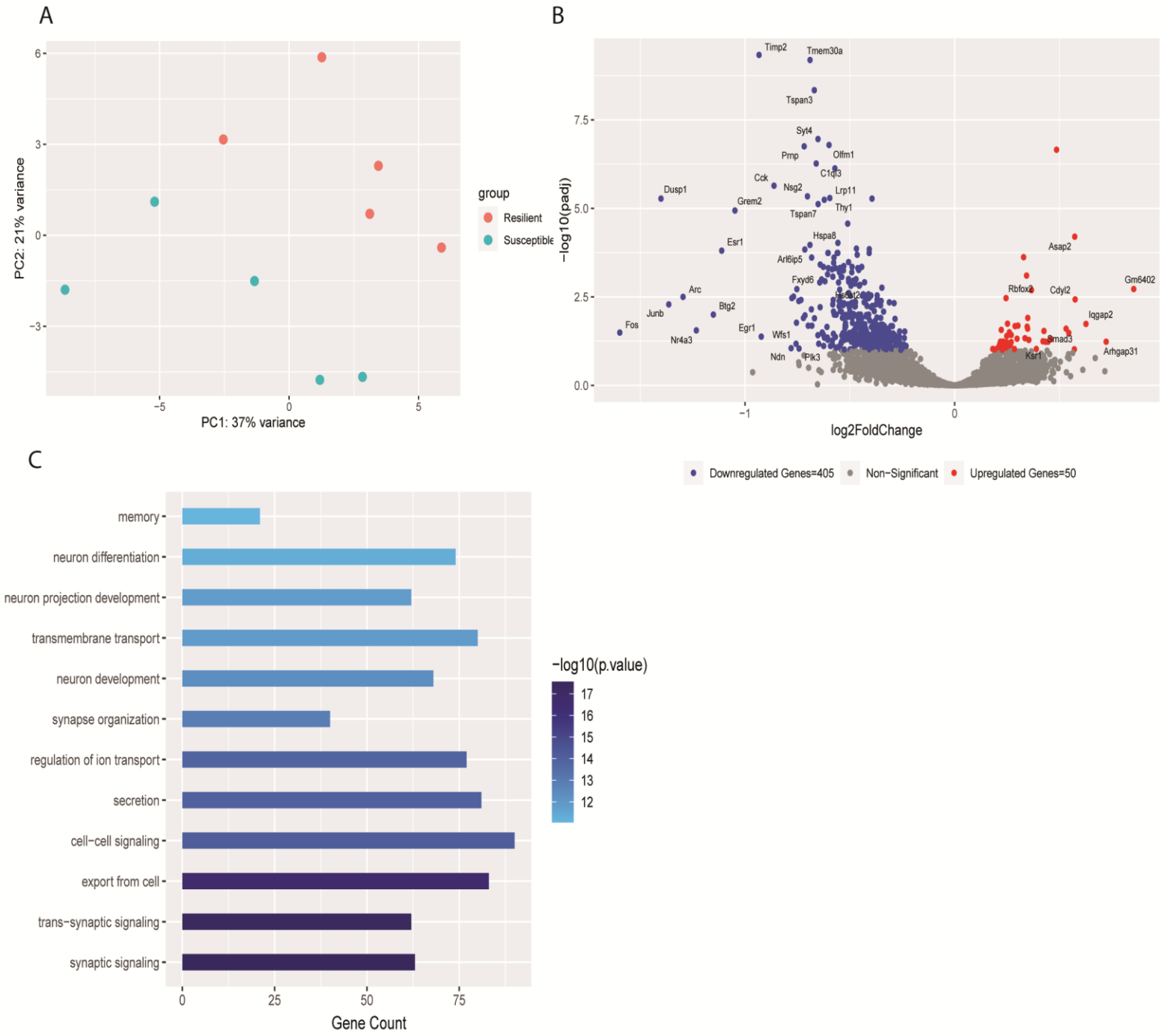

Supplementary figure 5: Susceptible versus resilient transcriptional comparison in PFC. A. PCA clustering analysis of susceptible samples compared to resilient. B. Volcano Plot representing the DEGs of susceptible samples compared to resilient. GO term enrichment analysis of upregulated transcripts in susceptible compared to resilient.

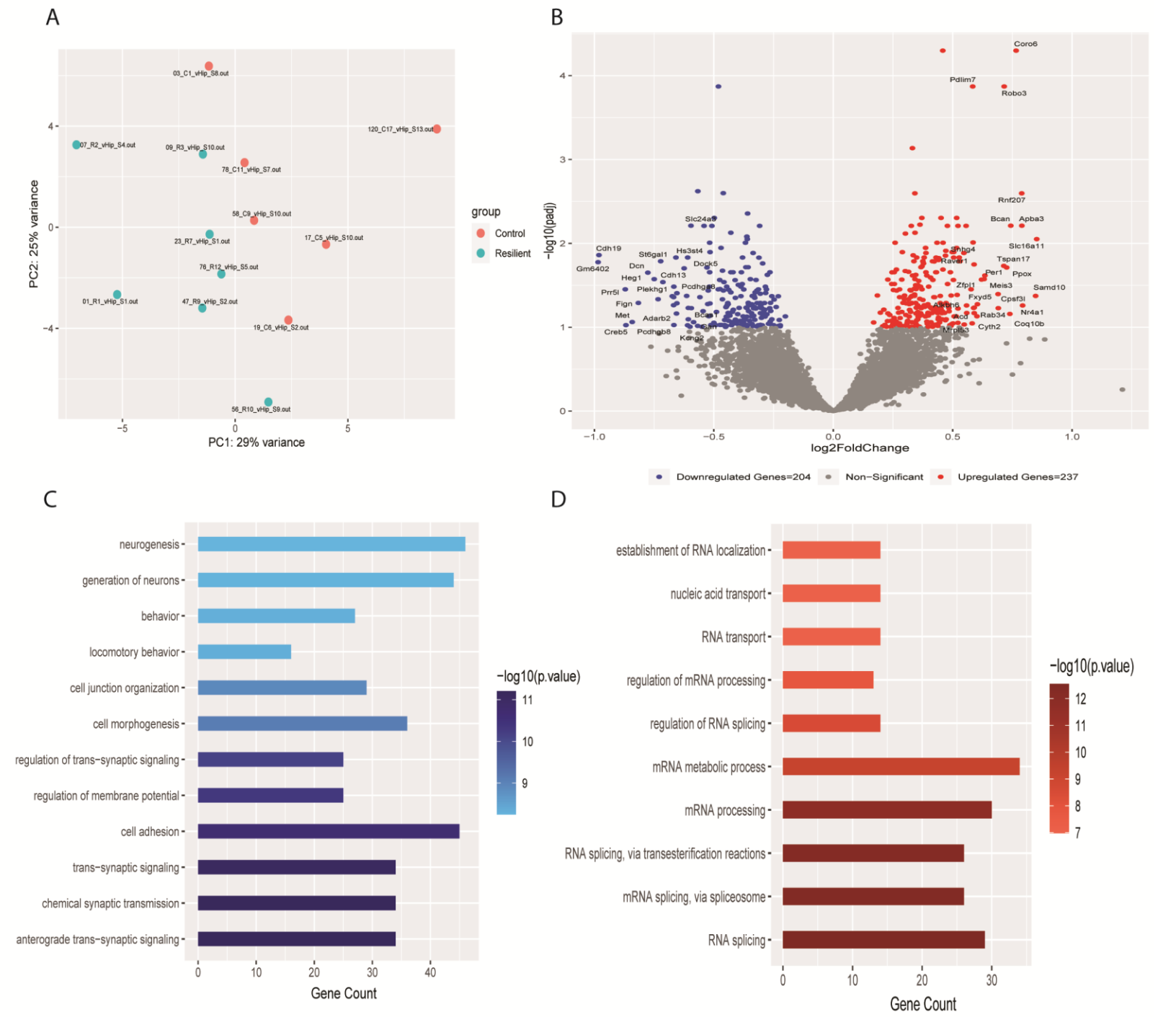

Supplementary figure 6: Resilient versus control transcriptional comparison in vHIP. A. PCA clustering analysis of resilient samples compared to control. B. Volcano Plot representing the DEGs of resilient samples compared to control. GO term enrichment analysis of upregulated transcripts in resilient compared to control.

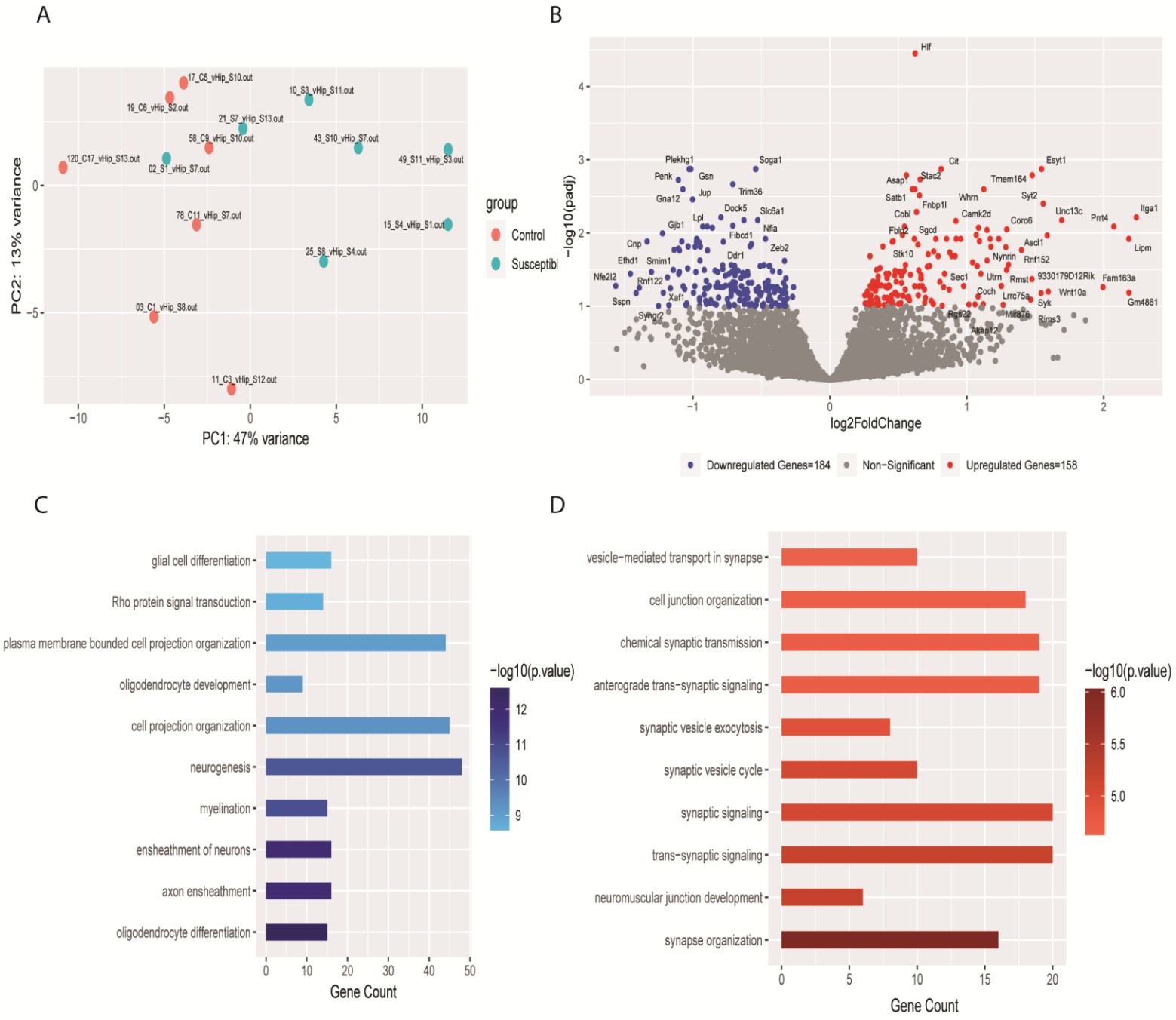

Supplementary figure 7: Susceptible versus control transcriptional comparison in vHIP. A. PCA clustering analysis of susceptible samples compared to control. B. Volcano Plot representing the DEGs of susceptible samples compared to control. GO term enrichment analysis of upregulated transcripts in susceptible compared to control.

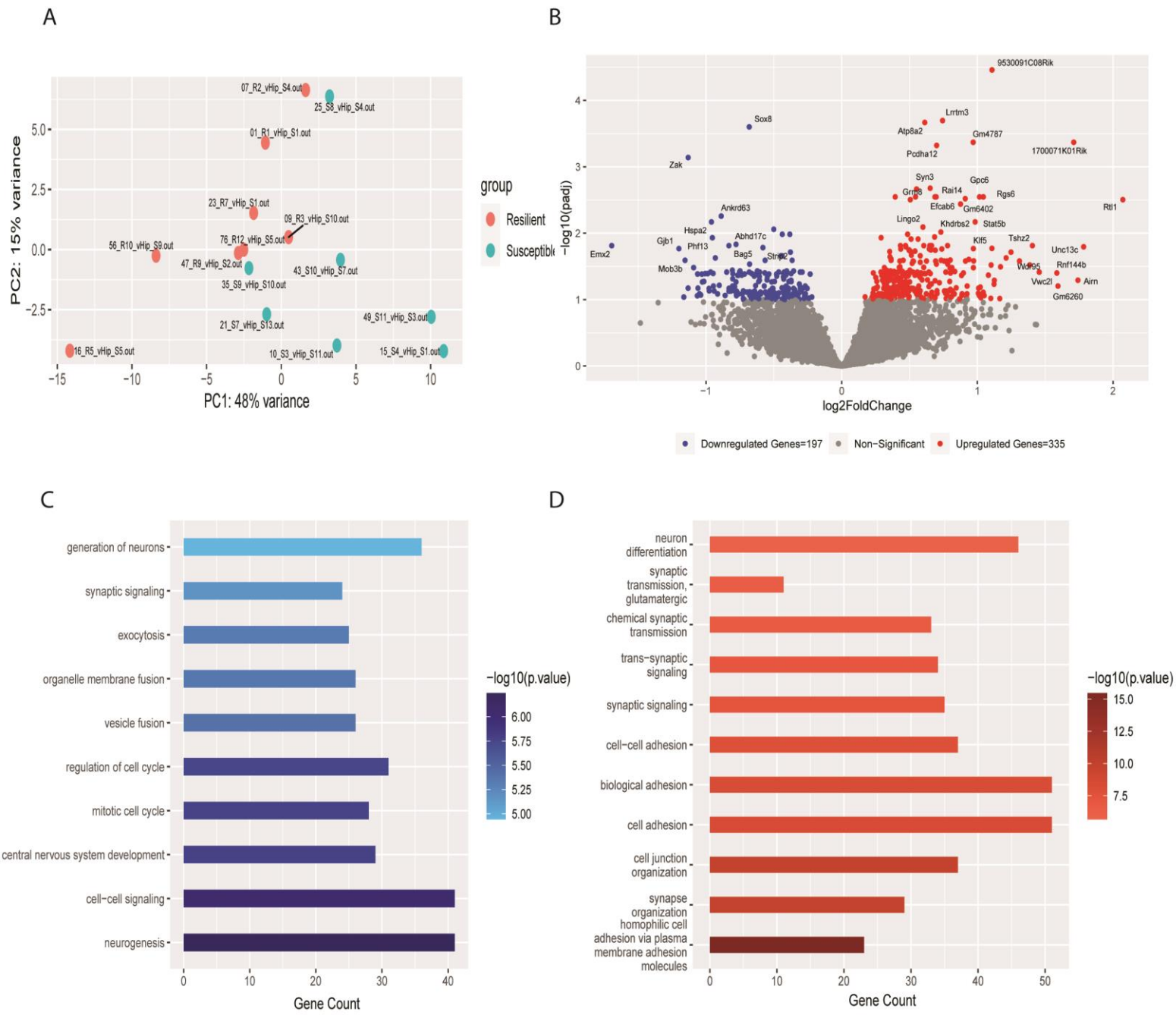

Supplementary figure 8: Susceptible versus resilient transcriptional comparison in vHIP. A. PCA clustering analysis of susceptible samples compared to resilient. B. Volcano Plot representing the DEGs of susceptible samples compared to resilient. GO term enrichment analysis of upregulated transcripts in susceptible compared to resilient.

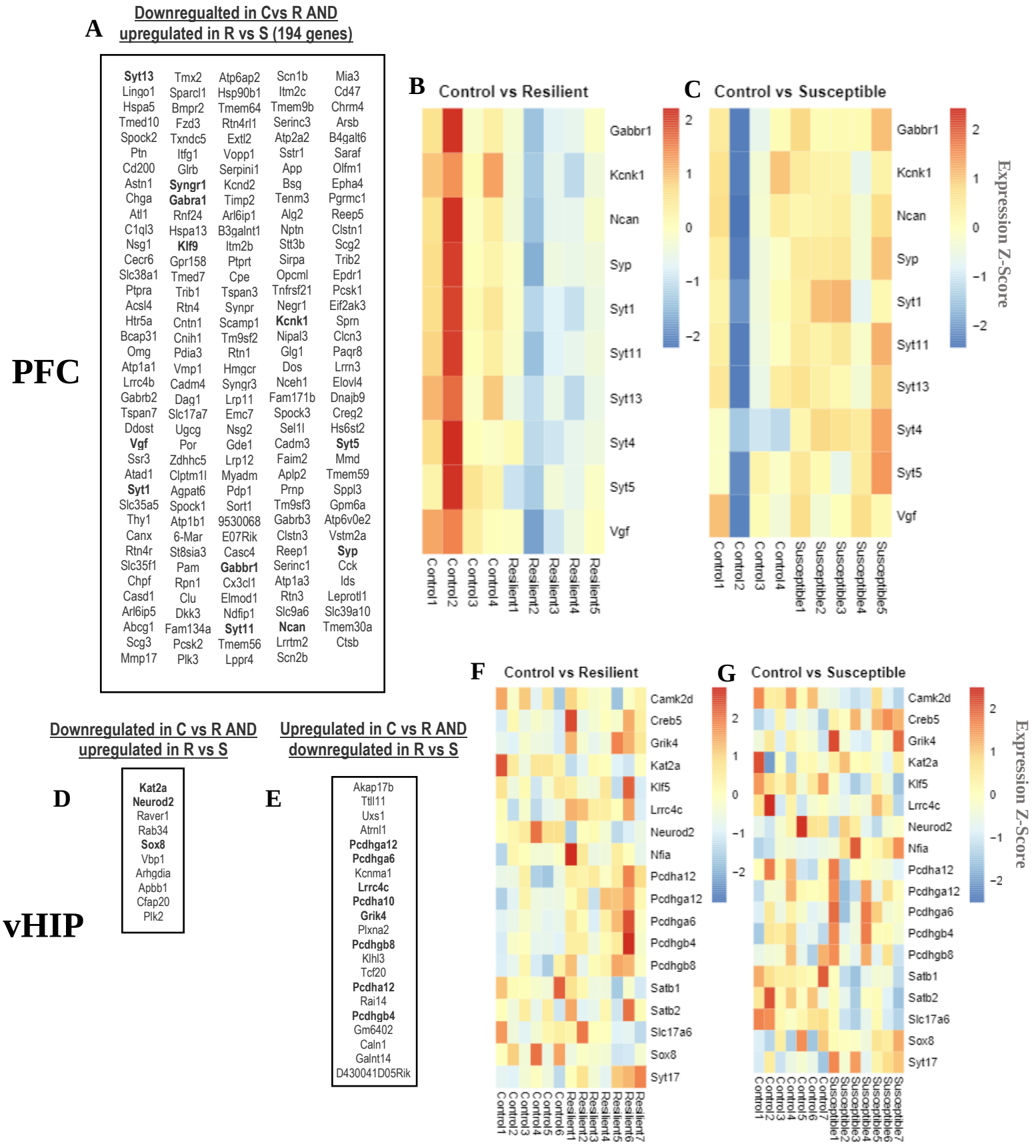

Supplementary figure 9: Overlapping DEGs between different conditions in the PFC (A-C) and vHIP (D-G). A. List of overlapping DEGs between downregulated C vs R AND upregulated in R vs S groups. B-C. Heat map of nuclear RNA-seq expression z-scores computed for selected DEGs in C vs R (B) and C vs S (C). D. List of overlapping DEGs between downregulated C vs R AND upregulated in R vs S groups. E. List of overlapping DEGs between upregulated C vs R AND downregulated in R vs S groups. F-G. Heat map of nuclear RNA-seq expression z-scores computed for selected DEGs in C vs R (F) and C vs S (G).

2.4 mTOR Driven Gene Transcription Is Required for Cholesterol Production in Neurons of the Developing Cerebral Cortex

Authors: Martin Schüle, **Tamer Butto**, Sri Dewi, Laura Schlichtholz, Susanne Strand, Susanne Gerber, Kristina Endres, Susann Schweiger and Jennifer Winter

This article is published in *International journal of Molecular Science.* 2021, *22*(11), 6034; https://doi.org/10.3390/ijms22116034

My contributions to this article are listed in section 4.2 Contributions to individual publications.

International Journal of Molecular Sciences

MDPI

Article

mTOR Driven Gene Transcription Is Required for Cholesterol Production in Neurons of the Developing Cerebral Cortex

Martin Schüle [1,2], Tamer Butto [1], Sri Dewi [1], Laura Schlichtholz [1,2], Susanne Strand [3], Susanne Gerber [1], Kristina Endres [4], Susann Schweiger [1,2,5] and Jennifer Winter [1,2,5,*]

1 Institute of Human Genetics, University Medical Center Mainz Johannes Gutenberg-University, 55131 Mainz, Germany; mschuele@students.uni-mainz.de (M.S.); T.Butto@imb-mainz.de (T.B.); Dewi.Hartwich@unimedizin-mainz.de (S.D.); lschlich@uni-mainz.de (L.S.); sugerber@uni-mainz.de (S.G.); susann.schweiger@unimedizin-mainz.de (S.S.)
2 Focus Program of Translational Neurosciences, University Medical Center Mainz, 55131 Mainz, Germany
3 First Department of Internal Medicine, University Medical Center Mainz, 55131 Mainz, Germany; sstrand@uni-mainz.de
4 Department of Psychiatry and Psychotherapy, University Medical Center Johannes Gutenberg-University, 55131 Mainz, Germany; Kristina.Endres@unimedizin-mainz.de
5 German Resilience Centre, University Medical Center Mainz, 55131 Mainz, Germany
* Correspondence: jewinter@uni-mainz.de

Citation: Schüle, M.; Butto, T.; Dewi, S. Schlichtholz, L.; Strand, S.; Gerber, S.; Endres, K.; Schweiger, S.; Winter, J. mTOR Driven Gene Transcription Is Required for Cholesterol Production in Neurons of the Developing Cerebral Cortex. *Int. J. Mol. Sci.* **2021**, *22*, 6034.https://doi.org/10.3390/ijms22116034

Academic Editor: Anindita Das

Received: 21 April 2021
Accepted: 28 May 2021
Published: 3 June 2021

Abstract: Dysregulated mammalian target of rapamycin (mTOR) activity is associated with vari- ous neurodevelopmental disorders ranging from idiopathic autism spectrum disorders (ASD) to syndromes caused by single gene defects. This suggests that maintaining mTOR activity levels in a physiological range is essential for brain development and functioning. Upon activation, mTOR regulates a variety of cellular processes such as cell growth, autophagy, and metabolism. On a molecular level, however, the consequences of mTOR activation in the brain are not well understood. Low levels of cholesterol are associated with a wide variety of neurodevelopmental disorders. We here describe numerous genes of the sterol/cholesterol biosynthesis pathway to be transcriptionally regulated by mTOR complex 1 (mTORC1) signaling in vitro in primary neurons and in vivo in the developing cerebral cortex of the mouse. We find that these genes are shared targets of the transcription factors SREBP, SP1, and NF-Y. Prenatal as well as postnatal mTORC1 inhibition downregulated expression of these genes which directly translated into reduced cholesterol levels, pointing towards a substantial metabolic function of the mTORC1 signaling cascade. Altogether, our results indicate that mTORC1 is an essential transcriptional regulator of the expression of sterol/cholesterol biosynthesis genes in the developing brain. Altered expression of these genes may be an important factor contributing to the pathogenesis of neurodevelopmental disorders associated with dysregulated mTOR signaling.

Keywords: mTOR; mTORC1; cholesterol; neurogenesis; SREBP; SP1; NF-Y

1. Introduction

Although changes in the activity of the mTOR pathway are associated with numerous neurodevelopmental disorders, the molecular basis of disease development remains poorly understood. The mTOR pathway is a central cellular signaling pathway that controls gene expression at multiple levels. While mTOR is well known for its role in regulating the translation of specific target mRNAs, it also governs RNA stability and gene transcription [1–7]. The evolutionarily conserved mTOR kinase comprises the core of two protein complexes, mTORC1 and mTOR complex 2 (mTORC2) [8]. In proliferating cells such as mouse embryonic fibroblasts (MEFs) and cancer cells, mTORC1 controls transcription of glycolysis, lipid and lysosome biogenesis, and mitochondrial metabolism genes [1,3] and also activates several transcription factors involved in metabolic processes including sterol regulatory element-binding proteins (SREBPs) and hypoxia-inducible factor-1α(HIF1α) [1,9–11].

The dysregulation of transcriptional processes most likely contributes to disease development in neurodevelopmental disorders associated with changes in mTOR activity —yet mTOR-mediated transcriptional regulation in the brain has been poorly investigated. In the brain, the mTOR signaling pathway controls various cellular processes such as neuronal differentiation, neuronal cell size determination, axon guidance, dendritogenesis, and synaptic plasticity [12]. Dysregulation of the mTOR pathway has been associated with epilepsy, ASD, and intellectual disability (ID). In this context, both hyper- and hypoactive mTOR signaling are connected to disease. mTOR hyperactivity was observed for example in fragile X syndrome (FXS), neurofibromatosis 1 (NF1), tuberous sclerosis, and Opitz BBB/G syndrome. mTOR hypoactivity was one characteristic of a mouse model for Rett syndrome. It was also observed in neurons that were derived from human embryonic stem cells (hESC) and carried a *MECP2* loss-of-function allele [13–18].

mTOR activity is regulated intracellularly by nutrients, energy level, and stress factors (e.g., hypoxia) and extracellularly by growth factors (e.g., brain-derived neurotrophic factor (BDNF)), hormones (e.g., insulin), neurotransmitters, and cytokines. Upon activation, mTORC1 phosphorylates eukaryotic translation initiation factor 4E (eIF4E) binding proteins (4E-BP1 and 4E-BP2) and S6 kinases (S6K1 and S6K2) which influence different steps of translation [8,19]. Two studies showed that, rather than having a global effect on protein translation, mTOR inhibition specifically affects translation of mRNAs containing a 5′- terminal oligopyrimidine tract (5′TOP) or a pyrimidine-rich translational element (PRTE), in their 5′-untranslated regions (5′UTRs) [20,21]. While protein translation regulation by mTOR has been studied extensively in the brain, much less is known about mTOR- mediated transcriptional regulation.

Here, we used 3′mRNA sequencing (3′mRNA-Seq) to identify mTOR-dependent genes, the expression of which is changed upon mTOR inhibition in murine neurons. We found that using the mTOR inhibitor temsirolimus [22] numerous genes of the sterol/ cholesterol biosynthesis pathway were downregulated, which resulted in decreased choles- terol levels. Injection of rapamycin into pregnant dams confirmed our results in vivo, in the developing pre- and postnatal cerebral cortex. In summary, our findings strongly suggest an important role for the mTOR pathway in regulating the expression of genes involved in lipid metabolism in neurons and the developing brain.

2. Results

2.1. Transcriptional Targets Downstream of mTOR in Neurons

To identify mTOR-dependent transcriptional changes, we treated primary cortical neurons with the mTOR inhibitor temsirolimus. Temsirolimus treatment had a strong effect on mTOR activity as measured by the ratio of the mTOR downstream effector pS6/S6 (Figure1A). With the mock-treated, and the 5 h and 24 h treated cells, we carried out 3′mRNA-Seq and identified a total of 522 differentially expressed genes (DEGs) at 5 h and 1090 DEGs at 24 h of temsirolimus treatment with an overlap of 241 DEGs between the two time points (0.5 log2 fold change and adjusted *p*-value < 0.05). Of all DEGs 315 and 564 were upregulated at 5 and 24 h, respectively, and 207 and 526 were downregulated (Figure1B,C, Supplementary Table S2).

Because mTOR is best known for its function in gene activation, we decided to focus on the set of genes downregulated upon mTOR inhibition in subsequent analyses. mRNA expression changes can be mediated at the epigenetic level, by changes in chromatin ac- cessibility, at the transcriptional level, by changes in transcription factor binding, or at the posttranscriptional level, by changes in mRNA stability. It was demonstrated before that mTOR activation can both enhance transcription of metabolic genes and increase their mRNA stability [1,6]. To test for possible mRNA stability changes we treated primary neu- rons with the transcriptional inhibitor Actinomycin D in combination with temsirolimus or DMSO and measured the mRNA decay rate of three downregulated targets, Ldlr, Osc, and Nsdhl. None of the three mRNAs underwent a decrease in stability upon mTOR inhibition, which suggests that posttranscriptional regulation of the mRNA amount is not a general mechanism of gene regulation under these experimental conditions (Supplementary Figure S1A–C).

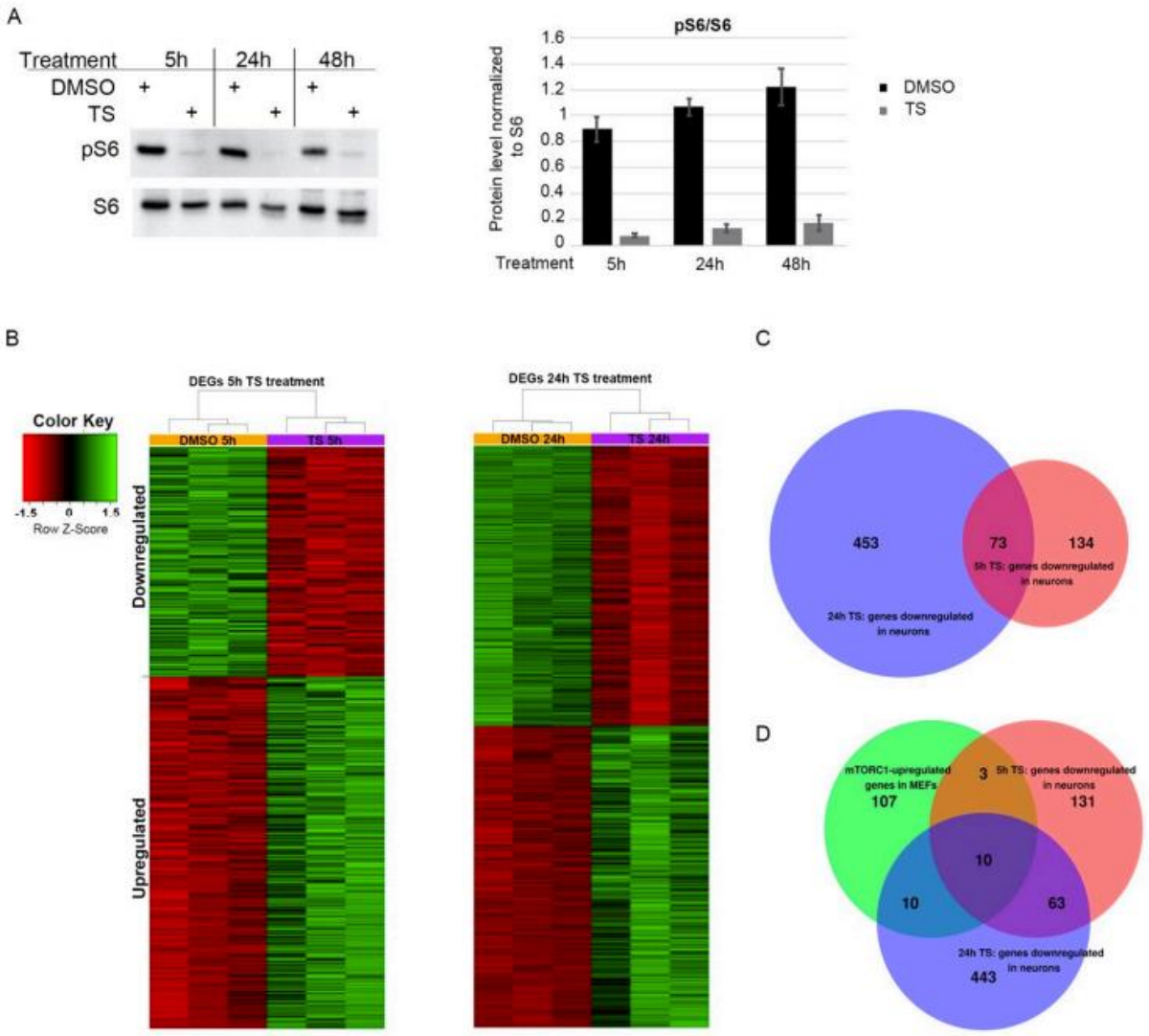

Figure 1. Temsirolimus treatment leads to widespread gene expression changes in primary neurons. Primary cortical neurons at days in vitro (DIV) 6 were treated with temsirolimus (10 μM) or vehicle (DMSO) and subjected to Western blot analysis (**A**) or RNA-Seq (**B**,**C**). (**A**) The cells were lysed at the indicated time points and subjected to immunoblot analysis with pS6 and S6 specific antibodies. Bands were quantified using ChemiDoc software (Image Lab V5. Version 5.2.1.). (**B**–**D**) For RNA-Seq analysis, total RNA was extracted from DMSO and temsirolimus-treated neurons from three different biological replicates each and converted into cDNA using a QuantSeq 3′mRNA-Seq Reverse (REV) Library Prep Kit (Lexogen, Vienna, Austria). (**B**) Heat maps indicating differentially expressed genes (DEGs) between neurons treated with DMSO or temsirolimus for 5 or 24 h. (**C**) Venn diagram of genes downregulated after 5 or 24 h of temsirolimus treatment.(**D**) Venn diagram showing the overlap between genes downregulated in neurons after 5 and 24 h of temsirolimus treatment and upregulated in mTOR hyperactive MEFs [1].

To test for mTOR-mediated chromatin accessibility changes, we employed an assay for Transposase-Accessible Chromatin with high-throughput sequencing (ATAC-seq) on biological replicates ($n = 2$ for each condition) from cortical neurons treated with tem- sirolimus or DMSO for 5 h. We identified 62,225 and 53,051 (Replicate 1) and 119,339 and 90,435 (Replicate 2) open chromatin regions in DMSO- and temsirolimus-treated neurons, respectively ($p < 0.05$; Supplementary Table S3). The majority of open chromatin regions mapped to promoters, introns, and intergenic regions of annotated genes (Supplementary Figure S1D). When comparing open chromatin regions of DMSO- and temsirolimus-treated neurons, we could, however, not identify major differences, especially not in those regions associated with genes involved in cholesterol

biosynthesis (Supplementary Figure S1E). This suggests that modifications in chromatin accessibility do not play a major role in mediating gene expression changes after temsirolimus treatment. Rather, this suggests that mTOR-mediated activation of gene expression in neurons occurs directly at the level of transcription factor regulation. Several studies have reported mTOR-regulated tran- scriptional changes in non-neuronal cells. For instance, Duvel et al. [1] Tsc1−/− and Tsc2−/− MEFs, which exhibit growth factor independent activation of mTORC1 in combination with rapamycin treatment. The authors found that mTORC1 activates the expression of numerous genes involved in glycolysis, the pentose phosphate pathway, and lipid/sterol biosynthesis. We used this dataset to identify mTOR-dependent transcriptional changes shared between MEFs and neurons. Surprisingly, when we compared our set of downregulated genes with the 130 genes found to be upregulated by mTORC1 in MEFs, only 13 genes overlapped between both sets after 5 h of temsirolimus treatment and only 20 genes after 24 h (Figure1D, Supplementary Table S2).

2.2. mTOR Regulates the Expression of Genes of the Cholesterol Pathway in Primary Neurons

Among the genes overlapping in neurons and MEFs were genes of the cholesterol synthesis pathway. Gene ontology analysis of our neuronal data set revealed that genes downregulated after 5 or 24 h of temsirolimus treatment were enriched for metabolic terms (Figure2A). These terms comprised sterol/lipid biosynthesis/metabolism processes including the cholesterol biosynthesis pathway (Figure2A). Other metabolic pathways previously described to be dependent on mTOR signaling such as the glycolysis and pentose phosphate pathway [1] were, however, not enriched. By qRT-PCR analysis of gene expression changes, we could confirm a general downregulation of sterol/cholesterol pathway genes. Genes of the glycolysis pathway, however, remained unaltered in their expression (Figure2B). A 40–60% downregulation of genes involved in the cholesterol biosynthesis process was found after 5 h of temsirolimus treatment (Figure2C). Western blot experiments confirmed significant downregulation of Ldlr and Osc proteins after 24 h of temsirolimus treatment and for Mvd a trend of downregulation was seen (p = 0.13; Figure2D, pS6/S6 ratio served as proof of efficacy of treatment). In contrast to genes of the cholesterol biosynthesis pathway, genes of the glycolysis pathway (*Pfkp*, *Pgm2*, and *Pdk1*) remained unaltered (Figure2C). Temsirolimus is a derivative of rapamycin, an interaction partner of FK506-binding protein-12 (FKBP-12) and allosteric partial inhibitor of the mTORC1 kinase [22]. In contrast to rapamycin (and temsirolimus), ATP-competitive inhibitors such as Torin 1 inhibit the phosphorylation of all mTORC1 substrates. The observed effect that temsirolimus treatment caused inhibition of the genes of some, but not all metabolic pathways previously described to be dependent on mTOR activity, could theoretically be due to temsirolimus being only a partial mTORC1 inhibitor. Therefore, we treated neurons with Torin 1 for 5 h. As expected, Torin 1 treatment not only caused a strong reduction of pS6, but also of p4EBP (Supplementary Figure S2A). Like temsirolimus treatment, the cholesterol biosynthesis pathway genes *Ldlr* and *Dhcr7* were significantly downregulated after 5 h of Torin 1 treatment (Supplementary Figure S2B). In contrast to temsirolimus treatment; however, the glycolysis pathway genes *Pfkp*, *Pgm2*, and *Pdk1* were also significantly downregulated (Supplementary Figure S2C).

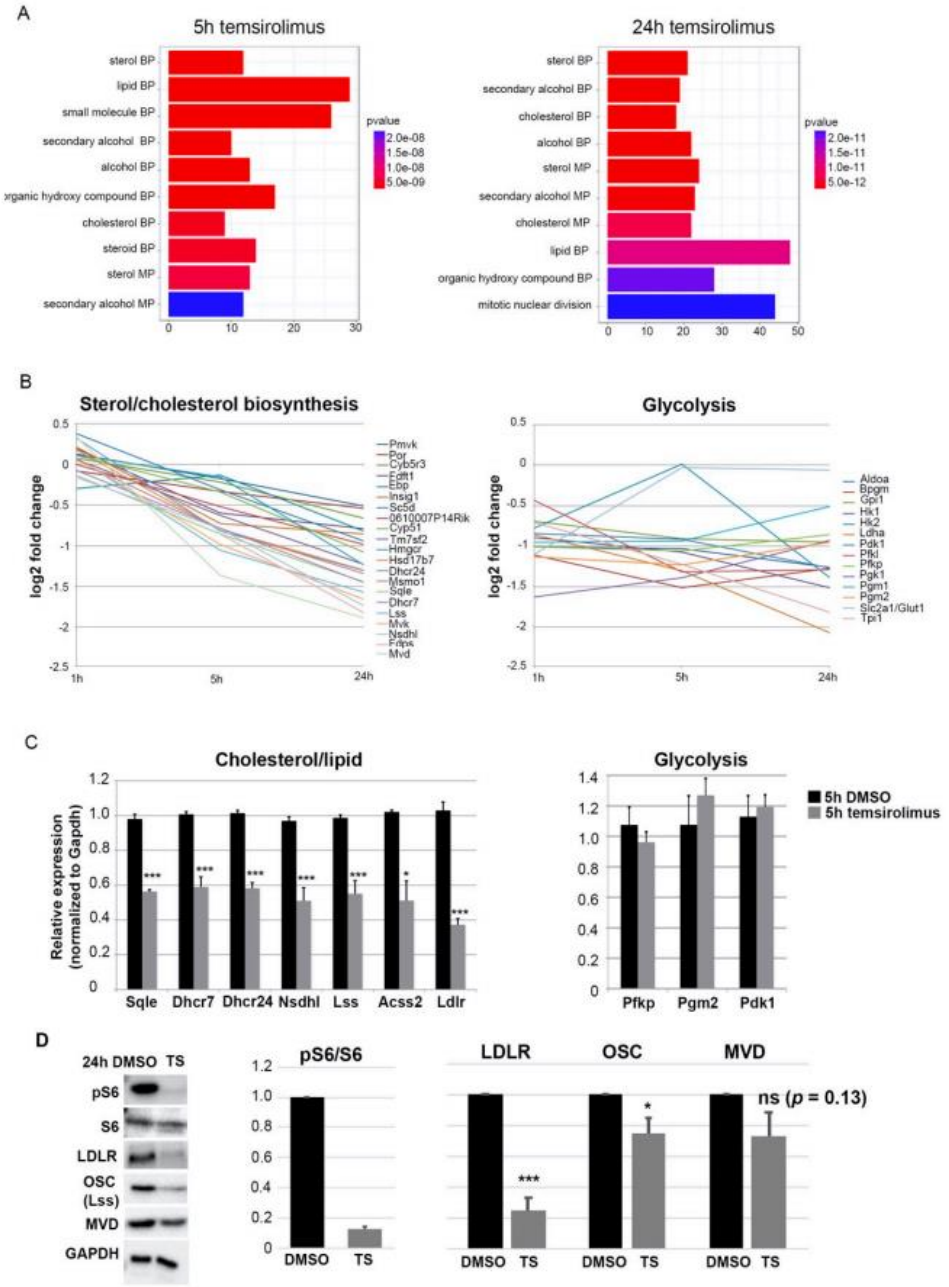

Figure 2. Temsirolimus treatment causes downregulation of genes of the sterol/cholesterol biosyn- thesis pathway. (**A**) Barplots of the top 10 GO enriched terms of downregulated genes after 5 h (left) and 24 h (right) of temsirolimus treatment. Both plots show a high enrichment for metabolic pathways shown on the *y*-axis and the number of gene counts on the *x*-axis. Enrichment scores are depicted in the colored bar. (**B**) Inhibition of mTORC1 by temsirolimus treatment downregulates the sterol and cholesterol biosynthesis pathway genes but does not change expression of glycolysis genes.(**C**) Confirmation of changes in the expression of cholesterol/glycolysis genes by RT-qPCR. Cells were lysed after 5 h of temsirolimus/DMSO treatment and subjected to total RNA extraction and RT-qPCR; mRNA expression was normalized to the housekeeping gene *GAPDH* (**D**) Western blot ex- periments in primary neurons after treatment with DMSO or temsirolimus for 24 h. Reduction in pS6 in relation to S6 confirms mTORC1 inhibition. Expression pattern of proteins involved in cholesterol biosynthesis. Data represent the average of three biological replicates (from three independent donor litters). For statistical analyses, Student's *t*-test was used. * $p < 0.05$; *** $p < 0.001$.

2.3. mTOR Activity Is Essential for Proper Expression of Cholesterol Pathway Genes in the Embryonic and Postnatal Cerebral Cortex

Having shown that mTOR promotes the expression of cholesterol pathway genes in primary neurons in vitro we next wanted to validate this in the brain in vivo. While

neurons of the adult brain rely mainly on astrocytes for cholesterol, in a critical time window

during development, neuronal cholesterol synthesis is essential for neurons to differentiate normally [23]. To analyze if mTOR activity is required for the expression of cholesterol pathway genes we, therefore, chose to inhibit mTOR prenatally starting at E16.5, by injecting rapamycin which has the same mechanism of action as temsirolimus intraperitoneally into pregnant mice. Twenty-four hours after a single rapamycin injection we observed a strong inhibition of the mTOR pathway as shown by Western blot analysis of the mTOR downstream effector pS6 (Figure3A). Already at this time point, RT-qPCR showed that all four tested cholesterol pathway genes (*Ldlr*, *Osc*, *Mvd*, *Dhcr7*) were reduced in their mRNA expression by about 50% (Figure3B). In contrast, only *Ldlr* was significantly reduced by about 20% at the protein level at this time point (Figure3C). Because the low effect on protein level could be due to high protein stability, we subsequently injected rapamycin on three consecutive days. Surprisingly, after three days of injection, mRNA levels of the four tested genes had returned to their normal levels which might be due to compensatory effects (Figure3D). Protein expression of Ldlr, Mvd, and Nsdhl was, however, significantly reduced by 45, 30, and 25%, respectively (Figure3E).

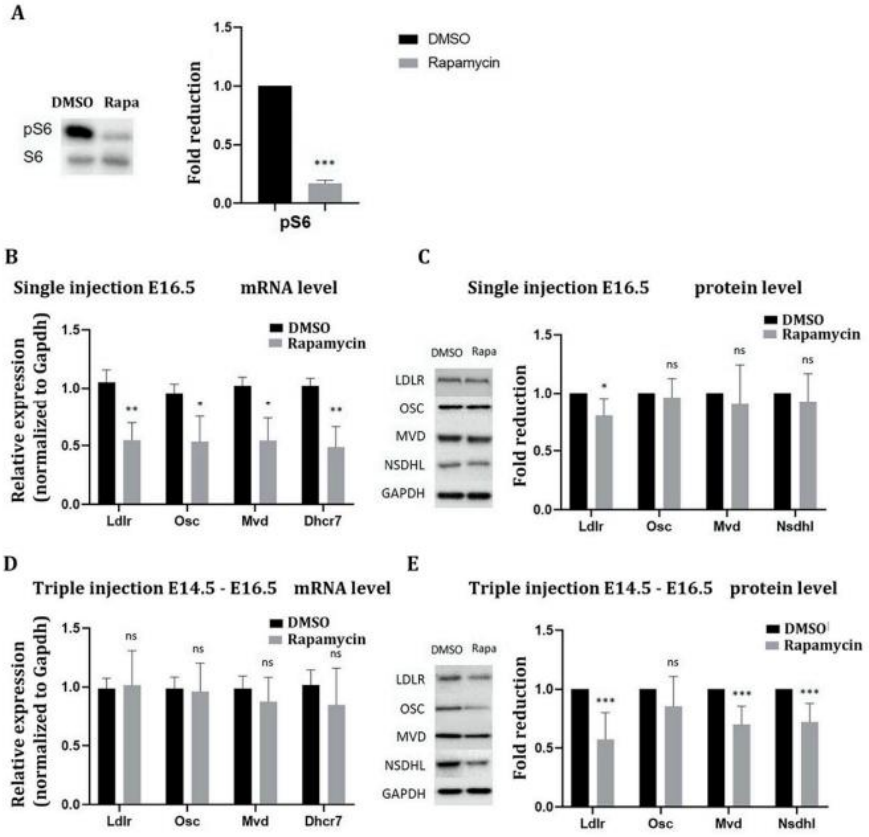

Figure 3. mTORC1 inhibition in the embryonic cerebral cortex downregulates cholesterol biosynthesis genes in vivo. Pregnant mice received either a single injection according to E16.5 of the offspring or were injected on three consecutive days (E14.5-E16.5) once per day with DMSO or rapamycin at a dose of 1 mg/kg. Subsequently, total RNA and protein were extracted from the cerebral cortex and RT-qPCR and Western blot experiments were performed. (**A**) Inhibition of mTORC1 activity was confirmed by Western blot analysis of the mTORC1 downstream effector pS6 (compared to S6) 24 h after a single rapamycin injection. (**B**,**D**) RT-qPCR to detect RNA expression of the four genes *Ldlr*, *Osc*, *Mvd*, and *Dhcr7* after one day (**B**) or three days (**D**) of i. p. injection of rapamycin compared to DMSO; mRNA expression was normalized to Gapdh. (**C**,**E**) Immunoblot analysis to detect Ldlr, Osc, Mvd, and Dhcr7 protein expression after one day (**C**) or three days (**E**) of i. p. injection of rapamycin compared to DMSO and normalized to Gapdh. Data represent the average of six biological replicates. For statistical analyses, Student's *t*-test was used. * $p < 0.05$; ** $p < 0.01$; *** $p < 0.001$

To further corroborate our data, we repeated the i. p. injections of DMSO and rapamycin at early postnatal stages starting at postnatal day two (P2). A single injection of rapamycin at this stage led to similar results as a single injection at prenatal stage E16.5 (Figure4A–C). Twenty-four hours after rapamycin injection, the mTOR pathway was strongly inhibited and all three genes analyzed, *Ldlr*, *Osc*, and *Mvd* were significantly downregulated at the mRNA level (Figure4B). As seen after a single prenatal rapamycin injection, only *Ldlr* was also downregulated at the protein level under these conditions (Figure4C). To test for a delayed reduction in protein levels, we injected rapamycin twice (on P2 and P4) and analyzed the mice at P6. Such a prolonged mTOR inhibition caused overall growth retardation in the rapamycin-injected mice when compared to DMSO-injected mice. Thus, rapamycin-injected mice were smaller and weighed less than DMSO-injected mice—an effect that was highly significant (Figure4D). Similar to three days of prenatal rapamycin injection, mRNA levels of Ldlr, Osc, and Mvd had returned to normal levels, and instead, protein levels of Ldlr, Mvd, and Nsdhl were significantly reduced by about 40–50% (Figure4E,F).

2.4. mTOR Inhibition Reduces Cholesterol Production In Vitro and In Vivo

After 5 and 24 h of temsirolimus treatment, eight and fifteen genes of the cholesterol biosynthesis pathway, respectively, were significantly downregulated in their expression (Figure5A, Supplementary Figure S3). The cholesterol biosynthesis pathway can be separated into three sections according to the type of compounds that are produced—mevalonate, isoprenoids, and sterols. After 24 h of temsirolimus treatment, genes of all three sections were downregulated in their expression, including the gene encoding Hmgcr which catalyzes the rate-limiting step in cholesterol biosynthesis; the reduction of HMG-CoA to mevalonate.

We, therefore, expected impaired cholesterol biosynthesis in neurons treated with temsirolimus. To test for this, we treated cortical neurons with temsirolimus for two days and performed Amplex Red cholesterol assays. Compared with DMSO treated neurons, cholesterol levels were significantly reduced in temsirolimus-treated neurons as well as in neurons treated with cyclodextrin, a cholesterol-depleting reagent which served as a positive control (Figure5B).

To further corroborate our data and to test for their in vivo relevance we measured cholesterol levels in the brains of rapamycin-injected mouse embryos. In agreement with the results obtained in neurons, we saw a significant decrease in cholesterol production in the embryonic cerebral cortex after injection of the mTOR inhibitor (Figure5C).

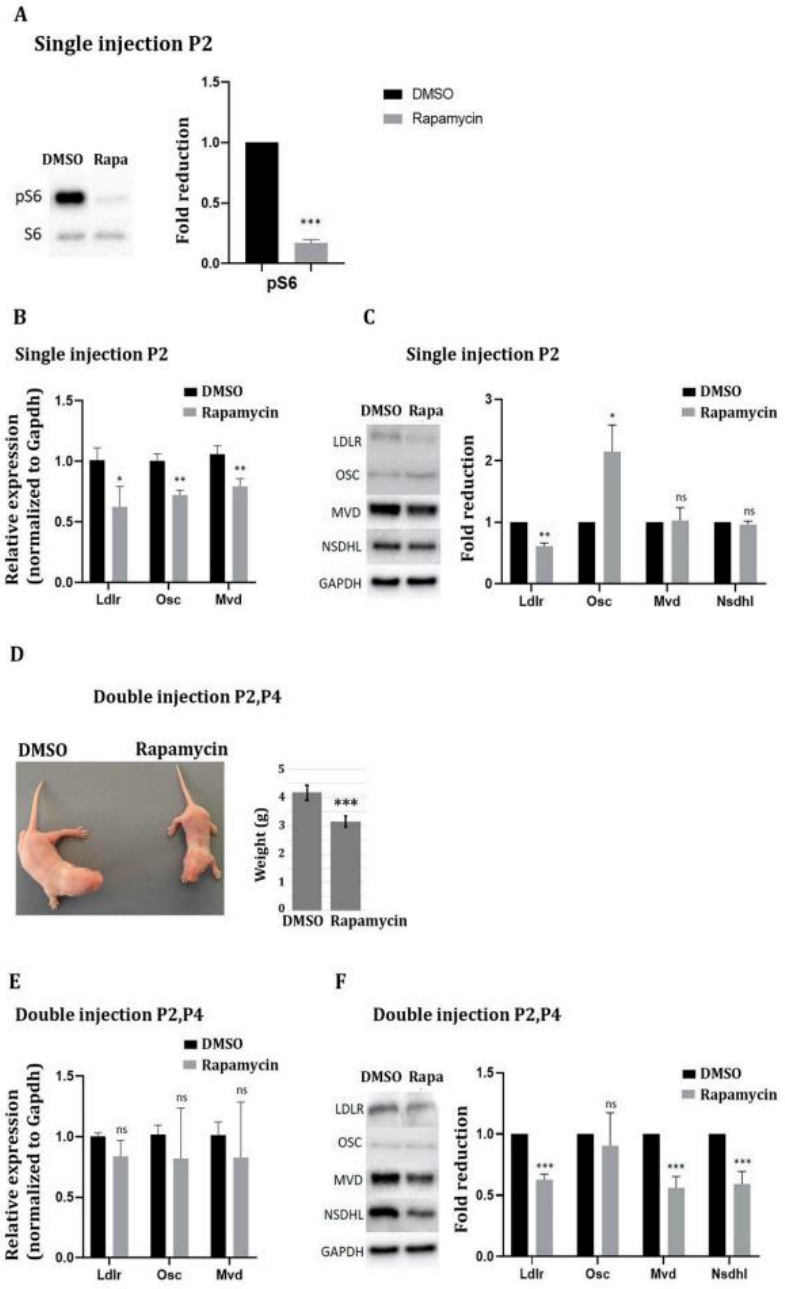

Figure 4. mTORC1 inhibition in the postnatal cerebral cortex downregulates cholesterol biosynthesis genes in vivo. Mice at P2 received either a single injection or received a total of two injections of DMSO or rapamycin at a dose of 1 mg/kg every two days (P2 and P4). Twenty-four hours after the single injection and 48 h after the double injection, total RNA and protein were extracted from the cerebral cortex and RT-qPCR and Western blot experiments were performed. (**A**) Inhibition of mTORC1 activity was confirmed by Western blot analysis of the mTORC1 downstream effector pS6 (compared to S6) 24 h after a single rapamycin injection. The DMSO and rapamycin treated samples were not loaded on adjacent lanes but were derived from the same gel. (**B**,**E**) RT-qPCR to detect RNA expression of the three genes *Ldlr*, *Osc*, and *Mvd* after single (**B**) or double (**E**) i. p. injections of rapamycin compared to DMSO; mRNA expression was normalized to Gapdh. (**C**,**F**) Immunoblot analysis to detect Ldlr, Osc, Mvd, and Nsdhl protein expression after one (**C**) or two (**F**) i. p. injections of rapamycin compared to DMSO and normalized to GAPDH. (**D**) Mice that had received a double injection of rapamycin at P2 and P4 were smaller than control mice at P6 and weighed less. Data represent the average of six biological replicates. For statistical analyses, Student's *t*-test was used. * $p < 0.05$; ** $p < 0.01$; *** $p < 0.001$.

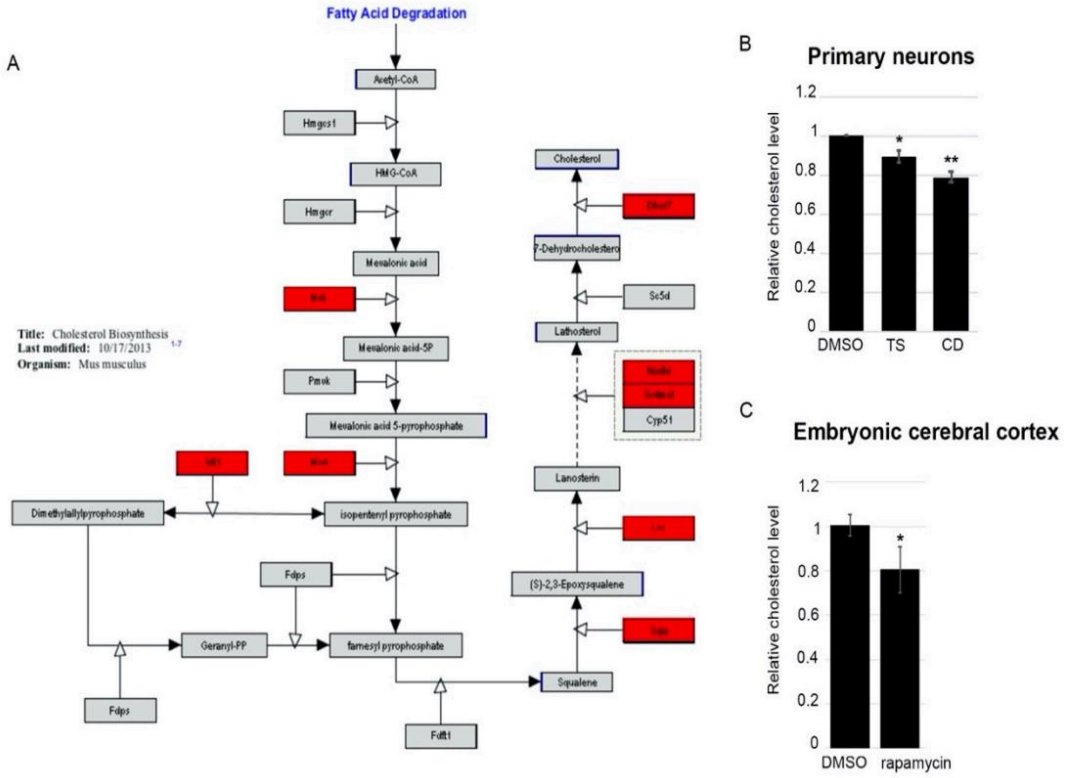

Figure 5. mTOR inhibition reduces cholesterol levels in primary neurons and the developing cerebral cortex. (**A**) Schematic overview of the cholesterol synthesis pathway in the mouse. Genes identified as being downregulated in the RNA-Seq experiment after 5 h of temsirolimus treatment are marked in red. (**B**) Changes in cholesterol levels were identified in DIV 6 primary cortical neurons treated with DMSO, temsirolimus (both for 48 h), or cyclodextrin (for one hour) using an Amplex Red Cholesterol Assay Kit. TS, temsirolimus; CD, cyclodextrin. (**C**) Changes in cholesterol levels after i.p. injection of 1 mg/kg rapamycin or DMSO on three consecutive days (E14.5–E16.5). * $p < 0.05$; ** $p < 0.01$.

2.5. mTOR Dependent Genes Contain SREBP, NF-YA, and SP1 Binding Sites in Their Promoter Regions

Düvel and colleagues [1] showed that in MEFs the binding site for SREBPs is over-represented in the promoters of mTOR-regulated targets. It is also known that mTORC1 regulates the nuclear abundance of SREBP1 and that SREBP transcription factors are required for mTOR-induced expression of metabolic genes [1,9]. When using the software findM [24] to screen the promoter regions of the genes downregulated in neurons treated with temsirolimus for 5 h we found that 44.9% of them contained at least one such binding site (Figure6A).

We applied the software Homer [25] on 5 h temsirolimus vs. DMSO downregulated genes to identify additional transcription factor binding sites in an unbiased manner. This analysis revealed that the binding sites for the transcription factors SP1 and NF-Y,respec- tively, occurred in 56 and 52% of the promoters of the downregulated genes (Figure6B,C). SREBPs, which are weak transcriptional activators on their own [26], cooperate with other transcription factors on their target promoters. Two key interaction partners of SREBP1 are SP1 and NF-Y [27]. In our data, we found that of the 93 downregulated genes that contained an SREBP binding motif in their promoters, 83 (89.2%) also contained an SP1 motif and 38 (40.9%) an NF-Y motif (Figure6D). Interestingly, the majority (36 out of 38) of downregulated genes containing both an SREBP and an NF-Y binding site also had an SP1 motif in their promoters (Figure6D).

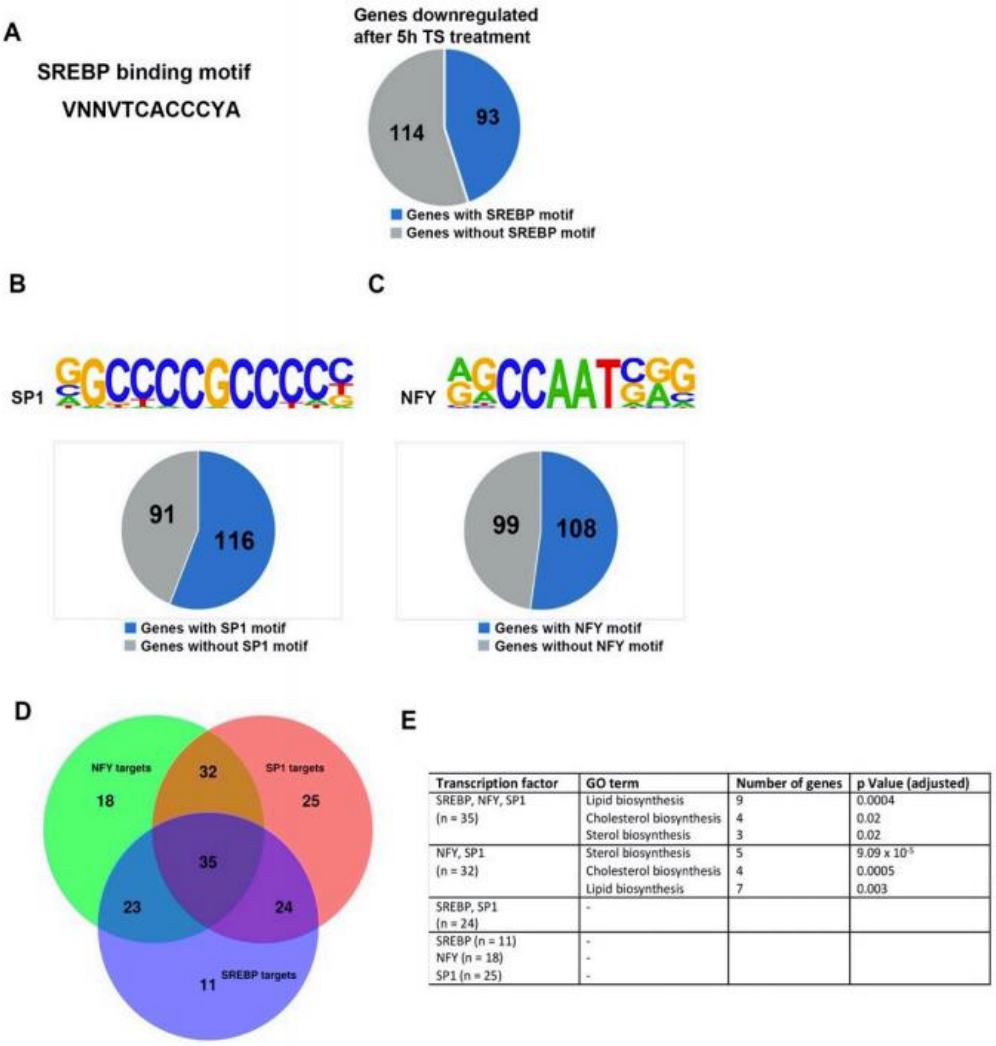

Transcription factor	GO term	Number of genes	p Value (adjusted)
SREBP, NFY, SP1 (n = 35)	Lipid biosynthesis	9	0.0004
	Cholesterol biosynthesis	4	0.02
	Sterol biosynthesis	3	0.02
NFY, SP1 (n = 32)	Sterol biosynthesis	5	9.09×10^{-5}
	Cholesterol biosynthesis	4	0.0005
	Lipid biosynthesis	7	0.003
SREBP, SP1 (n = 24)	-		
SREBP (n = 11)	-		
NFY (n = 18)	-		
SP1 (n = 25)	-		

Figure 6. Analysis of transcription factor binding in mTORC1 inhibited neurons. (**A**) Pie chart of the genes downregulated after 5 h temsirolimus treatment, which contain SREBP binding sites in their promoters. For SREBP binding site identification, the software findM was used. (**B**,**C**) Pie charts of the genes which were downregulated after 5 h temsirolimus treatment and contained SP1 (**B**) or NF-Y (**C**) binding sites in their promoters. The software HOMER v4.9 was used to screen the promoters of the downregulated genes for the presence of transcription factor binding sites. (**D**) Venn diagram depicting downregulated genes that share binding sites for two or three of the transcription factors SREBP, SP1, and NF-Y in their promoters. (**E**) GO term analysis of the genes which contain different combinations of transcription factor binding sites in their promoters.

Identification of enriched GO terms revealed that genes involved in the sterol/cholesterol biosynthesis pathway preferentially contained binding sites for all three (SREBP, NF-Y, SP1) or two (NF-Y, SP1) of the three factors in their promoters (Figure6E).

3. Discussion

Surprisingly, it has not yet been investigated whether mTOR controls the transcription of metabolic genes in neuronal cells in the brain.

Previously, it was shown that the mTOR kinase is an important transcriptional activator of metabolic genes in non-neuronal cellular systems such as MEFs, regulatory T cells, and cancer cell lines [1,3,5]. Having in mind that mTOR signaling is an essential pathway during brain development and that mTOR dysregulation causes various neurodevelopmental disorders, dysregulation of metabolic gene expression may well contribute to neurological symptoms in mTOR-associated disorders. Here we show that mTOR drives

the expression of metabolic genes of the sterol/cholesterol pathway in primary cortical neurons in vitro and in the developing cerebral cortex in vivo.

Although in neurons like in non-neuronal cells the mTOR kinase promotes the ex- pression of metabolic genes, we observed a major difference between the different cell types: in neurons treated with temsirolimus, we found downregulation of the cholesterol biosynthesis pathway genes but not of the glycolysis and pentose phosphate pathways which were both affected in MEFs [1]. One explanation for this discrepancy might be the different experimental conditions. Indeed, when we treated cortical neurons with the mTOR inhibitor, Torin 1, which inhibits the phosphorylation of mTORC1 substrates more completely than rapamycin and temsirolimus, we not only observed downregulation of genes of the cholesterol biosynthesis pathway, but also of the glycolysis pathway. Because Torin 1 does not cross the blood-brain barrier we could not test for this effect in vivo in the same way as we did in vitro. Besides, prior studies suggest that cell type-specific effects exist which are likely to contribute to the differences observed between non-neuronal cell types and neurons. For example, depending on the cell type, mTOR activates specific transcription factors such as HIF1α, SREBPs, and TFEB in MEFs and IRF4 and GATA3 in regulatory T cells [1,3,28]. Even nuclear localization and binding of mTOR itself to DNA were reported [5,10,29]. Which mechanisms contribute to the regulation of cholesterol gene expression by mTOR in neurons is still unclear. We found a significant enrichment of binding sites for the transcription factors SP1, SREBPs, and NF-Y in the promoters of mTOR-regulated genes in neurons. To our knowledge, a binding sites' enrichment for NF-Y has not yet been described in promoters that respond to mTOR activity. NF-Y regulates an increasingly identified number of genes and is ubiquitously expressed, so it is likely to have different roles depending on the cellular context. The NF-YA knockout in mice for example, causes early embryonic lethality [30], underpinning its importance for physiolog- ical functions. In proliferating cells such as MEFs and hematopoietic stem cells, NF-Y is involved in cell cycle regulation [31–34]. While it is downregulated in most tissues during differentiation [35,36], NF-Y is active in mature neurons of the adult mouse brain where its deletion causes neurodegeneration [37,38]. NF-Y co-localizes with other transcription factors such as Fos proto-oncogene (FOS) at genomic sites [39]. In differentiating neurons and HEK293 cells, NF-YA and c-Jun N-terminal kinase (JNK) were found to bind to the same genomic sites and NF-YA recruits JNK to these sites [40]. It was also shown that NF-Y interacts at target gene promoters in cooperation with SREBP1 or SREBP2 and SP1 and activates genes of metabolic pathways [26,41,42].

Downregulation of mTOR activity is thought to play an essential role in the pathogen- esis of neurodevelopmental disorders such as Rett syndrome and Cyclin-Dependent Kinase Like 5 (CDKL5) deficiency disorder [14,43,44]. How reduced mTOR activity contributes to disease development in these disorders is, however, not entirely clear. Defects in the cholesterol pathway may be a contributing mechanism. This is supported by the observa- tion that even small perturbations in cholesterol metabolism can primarily affect neuronal development [45–48]. Low levels of cholesterol have been associated with a variety of neurodevelopmental disorders. Cholesterol biosynthesis is a multistep process divided into a pre- and post-squalene pathway. Low levels of cholesterol have been associated with a variety of neurodevelopmental disorders and several genes of the cholesterol biosynthe- sis pathway have been found to carry mutations. The most common genetic syndrome associated with defects in cholesterol biosynthesis is the autosomal recessive Smith Lemli Opitz syndrome (SLOS; OMIM# 270400) which is caused by mutations in *DHCR7* encoding the enzyme 7-dehydrocholesterol D7reductase [49,50]. The neurological symptoms of SLOS include epilepsy, ID, and behavioral problems, among others. Mutations in NAD(P) steroid dependent dehydrogenase-like (*NSDHL*) gene are associated with the X-linked dominant disorder CHILD syndrome (OMIM #308050; [51]) and the X-linked recessive disorder CK syndrome (OMIM #300831; [52]), and mutations in mevalonate kinase (*MVK*) with the autosomal recessive disorder Mevalonic Aciduria (OMIM #610377; [53]). All three syndromes are characterized by structural brain abnormalities and/or neurological symptoms including ID. The gene product of *NSDHL*, 3β-hydroxysteroid dehydrogenase, is

involved in one of the later steps in cholesterol biosynthesis, and the gene product of *MVK*, mevalonate kinase, is a peroxisomal enzyme involved in cholesterol biosynthe- sis in the pre-squalene pathway. Expression of all three genes, *Dhcr7*, *Nsdhl*, and *Mvk* were found downregulated in temsirolimus-treated neurons. Although these results sug- gest that perturbations in cholesterol biosynthesis in disorders associated with mTOR downregulation may contribute to disease development, it is still unclear whether mTOR downregulation leads to a long-lasting reduction of cholesterol levels in the brain. In the in vivo experiments, we observed that 24 h after injecting a single dose of rapamycin the mRNA expression of all tested genes was decreased. After three days (prenatal) or four days (postnatal) of mTOR inhibition, however, it had returned to normal levels. In contrast, protein levels of most tested genes only decreased significantly after three (prenatal) or four days (postnatal) of mTOR inhibition. Even more surprising, OSC protein expression did not change when a single dose of rapamycin was injected prenatally but increased significantly when a single dose of rapamycin was injected postnatally. The delayed reduction at the protein level could possibly be caused by enhanced protein stability. In addition, these observations hint at feedback and compensatory mechanisms, which is confirmed in a study by Buchovecky and colleagues [54] who found that in the brains of a mouse model for Rett syndrome (*Mecp2* null mice) total cholesterol was increased at P56 when mutant males had developed severe symptoms. At a later age (P70), however, brain cholesterol levels were comparable to wildtype levels which reflected reduced cholesterol synthesis. Likely, the overproduction of cholesterol had fed back to a decreased cholesterol synthesis later. Genetic or pharmacologic inhibition of cholesterol synthesis ameliorated some of the symptoms in these mice. This suggests a critical window during brain development when neuronal tissue depends particularly on neuronal cholesterol biosynthesis.

Our studies were focused on mTOR-mediated regulation of cholesterol biosynthesis in cortical neurons. Because the brain needs to synthesize its own cholesterol even during development when the blood-brain barrier has not fully formed yet, neuronal cholesterol synthesis is most important during a critical developmental time window [23]. Neurons in the adult brain rely mainly on astrocytes for providing cholesterol. Also, during myelination oligodendrocytes synthesize vast amounts of cholesterol. It was already shown in zebrafish that cholesterol is needed for mTOR activity in oligodendrocyte precursor cells and that mTOR regulates cholesterol-dependent myelin gene expression [55]. Therefore, an open question is whether mTOR signaling in astrocytes and oligodendrocytes is equally essential for cholesterol biosynthesis as it is in neurons.

4. Materials and Methods

4.1. Mice, Cell Culture, and Drug Treatment

NMRI mice (8–12 weeks old) were obtained from Janvier labs (Saint Berthevin, France) and sacrificed by cervical dislocation. For neuron culture, primary cortical neurons were isolated from E14.5 embryos from pregnant NMRI mice. After the collection of brains, cortices were dissected and mechanically separated into single cells via resuspension. The neurons were plated on Poly-L-Ornithine (Sigma, St. Louis, MO, USA) and Laminin (Sigma St. Louis, MO, USA)-coated plates, and cultured in Neurobasal medium (Gibco, Carlsbad, CA, USA), supplemented with 2% B-27 plus vitamin A (Gibco, Carlsbad, CA, USA) and 1% GlutaMAX (Gibco, Carlsbad, CA, USA), in a humidified incubator at 37 °C and 8% CO_2. For drug treatment, primary cortical neurons were cultured for six days in 6-well- plates followed by treatment with the mTOR inhibitor temsirolimus (10 μM in DMSO; Sigma, St. Louis, MO, USA) or Torin 1 (500 nM in DMSO; LC Laboratories, Woburn, MA, USA) diluted in culture medium for the indicated periods. For measuring RNA stability, neurons were treated with the transcriptional blocker Actinomycin D (Sigma, St. Louis, MO, USA; 5 μg/mL). For further analyses, cells were harvested in PBS using cell scrapers. For in vivo experiments in prenatal mice 8–12 weeks old, pregnant NMRI mice received a single intraperitoneal (i. p.) injection at stage E16.5 or were injected i. p. once daily with

rapamycin (LC Laboratories, Woburn, MA, USA) or DMSO (control vehicle) on three consecutive days. For in vivo experiments in postnatal mice, two day old mice received a single i. p. injection or were injected i. p. twice at P2 and P4. A single injection contained either 10 µL DMSO or 10 µL rapamycin (1 mg/kg) dissolved in 100% DMSO. Twenty-four to 48 h after the last injection, embryonic cortices were isolated and stored either in lysis buffer (48% Urea, 14 mM Tris pH 7.5, 8.7% Glycerol, 1% SDS, protease inhibitor cocktail (Roche, Basel, CH, Switzerland)) or RNAlater (Sigma, St. Louis, MO, USA) for further analysis at −80 °C.

4.2. Immunoblotting

Antibodies for immunoblotting were as follows: phospho-S6, S6 (Cell Signaling Technology, Danvers, MA, USA), Osc, Mvd (Santa Cruz Biotechnology, Santa Cruz, CA, USA), Ldlr, Nsdhl (Novus Biologicals, Centennial, WY, USA), GAPDH (Abcam, Cambridge, UK). Western blot analysis was performed by standard methods using enhanced chemiluminescence.

4.3. RNA Isolation, cDNA Synthesis, RT-qPCR, and RNA Sequencing

Total RNA extraction with TRIzol reagent from brain tissue was performed as recommended by Invitrogen Life Technologies (Carlsbad, CA, USA). A High Pure RNA Isolation Kit (Roche, Basel, CH, Switzerland) was used to extract total RNA from cell samples us- ing spin columns. The purity, quantity, and integrity of the RNA were measured with a NanoDrop One spectrophotometer (Thermo Fisher Scientific, Waltham, MA, USA). Accord- ing to the manufacturer's instructions, the cDNA samples were synthesized from 500 to 1000 ng total RNA using the PrimeScriptTM RT Master Mix cDNA (Takara, Kyoto, Japan). Quantitative real-time PCR (qRT-PCR) was carried out using SYBR® Premix Ex Taq™ II (Tli RNaseH Plus) and 10 µM primers (final concentration), according to the manufacturer's instructions. RT-qPCR reactions were performed on an ABI StepOnePlus Real-Time PCR System using intron spanning primers with the following conditions: 95 °C/30 s, 40 cycles of 95 °C/5 s, 60 °C/30 s, 72 °C/30 s. For primer sequences see Supplementary Table S1. All reactions were measured in triplicate, and median cycles to threshold (Ct) values were used for analysis. The housekeeping gene *GAPDH* was used for normalization, and relative gene expression was determined using the 2 ΔΔCT method.

For RNA sequencing, RNA purity and integrity were measured using the Agilent 2100 bioanalyzer (Agilent Technologies, Santa Clara, CA, USA). RNA was converted into cDNA by using a QuantSeq 3′mRNA-Seq Reverse (REV) Library Prep Kit (Lexogen, Vienna, Austria) according to the manufacturer's instruction to generate a compatible library (2.5 pM) for Illumina sequencing. RNA sequencing was performed using a high output reagent cartridge v2 (75 cycles; Illumina, San Diego, CA, USA) with a custom primer (0.3 µM) provided by Lexogen on an Illumina NextSeq 500 device.

4.4. RNA-Seq Data Analysis

After the sequencing, bcl2fastq v2.17.1.14 conversion software (Illumina, San Diego, CA, USA) was used to demultiplex sequence data and convert base call (BCL) files into Fastq files. Sequencing adapters (AGATCGGAAGAG) were trimmed and reads shorter than six nucleotides were removed from further analysis using Cutadapt v1.11 [56]. Qual- ity control checks were performed on the trimmed data with FastQC v0.11.4 [57]. Read mapping of the trimmed data against the mouse reference genome and transcriptome (mm9) was conducted using STAR aligner v2.5.3 [58]. To estimate each transcript's ex- pression levels the mapped reads were assigned to annotated features using the Subread tool featureCounts v1.5.2 [59]. The output of the raw read counts from featureCounts was used as an input for the differential expression analysis using the combination of DESeq2 v1.16.1 [60] and edgeR v3.26.8 [61] packages. Pairwise comparison analysis of two different conditions was carried out with edgeR to normalize the expression levels of known genes. Only genes with CPM

(counts per million) > 10 were further analyzed. The differentially expressed gene analysis was performed on the normalized genes' expression using DESeq2 with |log2FoldChange| > 0.5 and padj (adjusted *p*-value) > 0.05. Overlapping DEGs were visualized using VennDiagram package v1.6 [62] in R. Heatmaps of up- and downregulated genes was created using ComplexHeatmap package v2.7 [63] in R.

1.1. ATAC-Seq

ATAC-seq was done as previously described [64]. Briefly, 50,000 DMSO- or temsirolimus-treated cells were resuspended in cold lysis buffer (10 mM Tris-HCl, pH 7.4, 10 mM NaCl, 3 mM $MgCl_2$ and 0.1% IGEPAL CA-630) and centrifuged at 750 g for 30 min at 4 °C. Immediately following the cell preparation, the pellet was resuspended in the transposase reaction mix (25 µL 2× TD buffer, 2.5 µL transposase (Illumina, San Diego, CA, USA) and 22.5 µL nuclease-free water). The transposition reaction was carried out for 30 min at 37 °C. Following transposition, the sample was purified using a Qiagen MinElute kit (Qiagen, Hilden, Germany). Following purification, the library was amplified using 1 NEBnext PCR master mix and 1.25 µM of custom Nextera PCR primers 1 and 2 [64], using the following PCR conditions: 72 °C for 5 min; 98 °C for 30 s; and thermocycling at 98 °C for 10 s, 63 °C for 30 s and 72 °C for 1 min. After 11–12 cycles of PCR amplification, the sample was further purified using Qiagen MinElute kit (Qiagen, Hilden, Germany). To remove primer dimers from the samples they were further purified using AMPure beads XP (Beckman Coulter, Brea, CA, USA) with a ratio of x0.9 of beads to samples. Samples were then analyzed in a bioanalyzer (Agilent Technologies, Santa Clara, CA, USA) and sequenced on an Illumina NextSeq 500 Illumina, San Diego, CA, USA.

1.2. ATAC-Seq Data Analysis

ATAC-Seq data quality check was performed using reads FASTQC v0.11.8 [56]. Further, adaptors were removed using Trimmomatic v0.39 [65]. Paired-end ATAC-Seq reads were mapped to Mus musculus genome (mm10) UCSC annotations using Bowtie2 v2.3.5.1 [66] with default parameters. Properly paired-end reads with high mapping quality (MAPQ ≥ 10) were retained in analysis with Samtools v1.7 [67]. Next, using Picard tools MarkDuplicates [68] utility duplicates were removed. ATAC-Seq peaks were called using MACS2 v2.1.1.20160309 [69] and were visualized with the USCS genome browser [70].

1.3. Cholesterol Assay

Primary cortical neurons were treated with DMSO or temsirolimus at 4 days in vitro (DIV4) for 48 h and with Cyclodextrin (Sigma, St. Louis, MO, USA) for one hour before cholesterol measurement. The cells were harvested using cell scrapers in a volume of 500 µL DPBS. The AmplexTM Red Cholesterol Assay (Thermo Fisher Scientific, Waltham, MA, USA) was performed in a black 96 well plate by the reaction of 50 µL of Amplex Red working solution with 50 µL of assay sample. A 5 mL volume of working solution, prepared before the analysis, contained 75 µL of the Amplex Red reagent (300 µM) and 2 U/mL of HRP (horseradish peroxidase), 2 U/mL cholesterol oxidase, and 0.2 U/mL cholesterol esterase. The working solution volume was adjusted to 5 mL with reaction buffer, which contained 25 mM potassium phosphate, pH 7.4, 12.5 mM NaCl, 1.25 mM cholic acid, and 0.025% TritonX-100. The reactions were incubated for 30 min at 37 °C, protected from light. After incubation, fluorescence was measured in a fluorescence microplate reader FLUOstar Optima (BMG Labtech, Ortenberg, Germany) using an excitation wavelength of 560 nm and emission detection at 590 nm.

For in vivo cholesterol measurement, cortex samples were isolated after three injections on three consecutive days (E14.5–E16.5) of DMSO or rapamycin (1 mg/kg) and collected in cholesterol lysis buffer (50 mM Tris-HCl pH 7.5, 150 mM NaCl, 1% Nonidet-P40, 0.5% deoxycholic acid, Protease Inhibitor Cocktail). The AmplexTM Red Cholesterol Assay (Thermo Fisher Scientific, Waltham, MA, USA) was performed in Qubit tubes using the

Qubit 2.0 Fluorometer. Cortex samples were diluted by using 20 µL cortex samples and 80 µL 1 reaction buffer and transferred into Qubit tubes. After adding 100 µL Amplex Red working solution (see above) to each tube the samples were incubated for 15 min at

room temperature, protected from light. Subsequently, the reaction was stopped using AmplexTM Red/UltraRed Stop Reagent (Thermo Fisher Scientific, Waltham, MA, USA) and fluorescence was measured using a Qubit 2.0 Fluorometer.

4.5. Statistical Analyses

All statistical analyses except for NGS analyses were done with GraphPad Prism 5 or Microsoft Office Excel version 16.49. Data are shown as mean + standard error of the mean. Statistical analyses were done using Student's *t*-test. p values < 0.05 were considered statistically significant.

4.6. Gene Ontology Analysis and KEGG Pathway Analysis

For differentially up- and down-regulated expressed genes of each pairwise comparison as well as overlapping genes for SREBP, NFY, and SP1 motifs, an overrepresentation analysis (ORA) was carried out with clusterProfiler v3.4.4 [71]. All expressed genes within the pairwise comparison samples with CPM > 10 served as a background for the analy- sis. The Bioconductor org.Mm.eg.db v 3.8.2 mouse annotation package [72] and mouse KEGG.db [73] were used for the gene ontology analysis and KEGG analysis, respectively. The default parameters were used for all over-representation tests.

4.7. Motif Identification

Motif discovery analysis within promoter sequences was performed using HOMER (Hypergeometric Optimization of Motif EnRichment) Software v4.9 [25]. ATAC-Seq sequencing data from 186 genes in FASTA format served as input for the findMotif.pl function. Scrambled input sequences (randomized) were created automatically by HOMER and used as a background for the motif analysis.

Supplementary Materials: The following are available online at https://www.mdpi.com/article/10.3390/ijms22116034/s1.

Author Contributions: M.S. designed and performed experiments, analyzed the data, and wrote the manuscript, and T.B. and L.S. designed and performed experiments and analyzed the data. S.S. (Susanne Strand), S.G., and K.E. designed experiments and analyzed the data. S.D. analyzed the data. S.S. (Susann Schweiger) supervised the project. J.W. planned experiments, analyzed the data, supervised the project and wrote the manuscript. All authors have read and agreed to the published version of the manuscript.

Funding: This work was funded by the Deutsche Forschungsgemeinschaft (CRC 1193).

Institutional Review Board Statement: The study was conducted according to the guidelines of the Declaration of Helsinki, and approved by the local ethical committee (Landesuntersuchungsamt Rheinland-Pfalz G-19-1-098, 20.08.2020).

Informed Consent Statement: Not applicable.

Data Availability Statement: The FASTQ files from the RNA-Seq and ATAC-Seq data were deposited in the NCBI Sequence Read Archive (SRA) under the BioProject accession number PRJNA719973.

Acknowledgments: Martin Schüle was supported by stipends from the Focus Program of Transla- tional Neurosciences of the Johannes Gutenberg-University Mainz. This work was supported by the Deutsche Forschungsgemeinschaft (CRC 1193).

Conflicts of Interest: The authors declare no conflict of interest.

References

1. Düvel, K.; Yecies, J.L.; Menon, S.; Raman, P.; Lipovsky, A.I.; Souza, A.L.; Triantafellow, E.; Ma, Q.; Gorski, R.; Cleaver, S.; et al. Activation of a Metabolic Gene Regulatory Network Downstream of mTOR Complex 1. *Mol. Cell* **2010**, *39*, 171–183. [CrossRef]
2. Avet-Rochex, A.; Carvajal, N.; Christoforou, C.P.; Yeung, K.; Maierbrugger, K.T.; Hobbs, C.; Lalli, G.; Cagin, U.; Plachot, C.; McNeill, H.; et al. Unkempt Is Negatively Regulated by mTOR and Uncouples Neuronal Differentiation from Growth Control. *PLoS Genet.* **2014**, *10*, e1004624. [CrossRef] [PubMed]
3. Chapman, N.M.; Zeng, H.; Nguyen, T.-L.M.; Wang, Y.; Vogel, P.; Dhungana, Y.; Liu, X.; Neale, G.; Locasale, J.W.; Chi, H. mTOR coordinates transcriptional programs and mitochondrial metabolism of activated Treg subsets to protect tissue homeostasis. *Nat. Commun.* **2018**, *9*, 1–15. [CrossRef]
4. Guertin, D.A.; Guntur, K.V.; Bell, G.W.; Thoreen, C.C.; Sabatini, D.M. Functional genomics identifies TOR-regulated genes that control growth and division. *Curr. Biol.* **2006**, *16*, 958–970. [CrossRef]
5. Audet-Walsh, É.; Dufour, C.R.; Yee, T.; Zouanat, F.Z.; Yan, M.; Kalloghlian, G.; Vernier, M.; Caron, M.; Bourque, G.; Scarlata, E.; et al. Nuclear mTOR acts as a transcriptional integrator of the androgen signaling pathway in prostate cancer. *Genes Dev.* **2017**, *31*, 1228–1242. [CrossRef] [PubMed]
6. Lee, G.; Zheng, Y.; Cho, S.; Jang, C.; England, C.; Dempsey, J.M.; Yu, Y.; Liu, X.; He, L.; Cavaliere, P.M.; et al. Post-transcriptional Regulation of De Novo Lipogenesis by mTORC1-S6K1-SRPK2 Signaling. *Cell* **2017**, *171*, 1545–1558.e18. [CrossRef] [PubMed]
7. Peng, T.; Golub, T.R.; Sabatini, D.M. The Immunosuppressant Rapamycin Mimics a Starvation-Like Signal Distinct from Amino Acid and Glucose Deprivation. *Mol. Cell. Biol.* **2002**, *22*, 5575–5584. [CrossRef] [PubMed]
8. Switon, K.; Kotulska, K.; Janusz-Kaminska, A.; Zmorzynska, J.; Jaworski, J. Molecular neurobiology of mTOR. *Neuroscience* **2017**, *341*, 112–153. [CrossRef]
9. Peterson, T.R.; Sengupta, S.S.; Harris, T.E.; Carmack, A.E.; Kang, S.A.; Balderas, E.; Guertin, D.A.; Madden, K.L.; Carpenter, A.E.; Finck, B.N.; et al. mTOR Complex 1 Regulates Lipin 1 Localization to Control the SREBP Pathway. *Cell* **2011**, *146*, 408–420. [CrossRef] [PubMed]
10. Bernardi, R.; Guernah, I.; Jin, D.; Grisendi, S.; Alimonti, A.; Teruya-Feldstein, J.; Cordon-Cardo, C.; Simon, M.C.; Rafii, S.; Pandolfi, P.P. PML inhibits HIF-1α translation and neoangiogenesis through repression of mTOR. *Nat. Cell Biol.* **2006**, *442*, 779–785. [CrossRef] [PubMed]
11. Kelsey, I.; Zbinden, M.; Byles, V.; Torrence, M.; Manning, B.D. mTORC1 suppresses PIM3 expression via miR-33 encoded by the SREBP loci. *Sci. Rep.* **2017**, *7*, 1–11. [CrossRef]
12. Garza-Lombó, C.; Gonsebatt, M.E. Mammalian Target of Rapamycin: Its Role in Early Neural Development and in Adult and Aged Brain Function. Front. Cell. Neurosci. 2016, 10, 157. [CrossRef]
13. Lee, D.Y. Roles of mTOR Signaling in Brain Development. Exp. Neurobiol. 2015, 24, 177–185. [CrossRef]
14. Li, Y.; Wang, H.; Muffat, J.; Cheng, A.W.; Orlando, D.A.; Lovén, J.; Kwok, S.-M.; Feldman, D.A.; Bateup, H.S.; Gao, Q.; et al. Global Transcriptional and Translational Repression in Human-Embryonic-Stem-Cell-Derived Rett Syndrome Neurons. Cell Stem Cell 2013, 13, 446–458. [CrossRef]
15. Ricciardi, S.; Boggio, E.M.; Grosso, S.; Lonetti, G.; Forlani, G.; Stefanelli, G.; Calcagno, E.; Morello, N.; Landsberger, N.; Biffo, S.; et al. Reduced AKT/mTOR signaling and protein synthesis dysregulation in a Rett syndrome animal model. *Hum. Mol. Genet.* **2011**, *20*, 1182–1196. [CrossRef] [PubMed]
16. Hoeffer, C.A.; Sanchez, E.; Hagerman, R.J.; Mu, Y.; Nguyen, D.V.; Wong, H.; Whelan, A.M.; Zukin, R.S.; Klann, E.; Tassone, F. Altered mTOR signaling and enhanced CYFIP2 expression levels in subjects with fragile X syndrome. *Genes Brain Behav.* **2012**, *11*, 332–341. [CrossRef] [PubMed]
17. Sharma, A.; Hoeffer, C.A.; Takayasu, Y.; Miyawaki, T.; McBride, S.M.; Klann, E.; Zukin, R.S. Dysregulation of mTOR Signaling in Fragile X Syndrome. *J. Neurosci.* **2010**, *30*, 694–702. [CrossRef] [PubMed]
18. Liu, E.; Knutzen, C.A.; Krauss, S.; Schweiger, S.; Chiang, G.G. Control of mTORC1 signaling by the Opitz syndrome protein MID1. *Proc. Natl. Acad. Sci. USA* **2011**, *108*, 8680–8685. [CrossRef] [PubMed]
19. Burnett, P.E.; Barrow, R.K.; Cohen, N.A.; Snyder, S.H.; Sabatini, D.M. RAFT1 phosphorylation of the translational regulators p70 S6 kinase and 4E-BP1. *Proc. Natl. Acad. Sci. USA* **1998**, *95*, 1432–1437. [CrossRef] [PubMed]
20. Thoreen, C.C.; Chantranupong, L.; Keys, H.R.; Wang, T.; Gray, N.S.; Sabatini, D.M. A unifying model for mTORC1-mediated regulation of mRNA translation. *Nat. Cell Biol.* **2012**, *485*, 109–113. [CrossRef]
21. Hsieh, A.C.; Liu, Y.; Edlind, M.P.; Ingolia, N.T.; Janes, M.R.; Sher, A.; Shi, E.Y.; Stumpf, C.R.; Christensen, C.; Bonham, M.J.; et al. The translational landscape of mTOR signalling steers cancer initiation and metastasis. *Nat. Cell Biol.* **2012**, *485*,

55–61. [CrossRef] [PubMed]
22. Hidalgo, M.; Rowinsky, E.K. The rapamycin-sensitive signal transduction pathway as a target for cancer therapy. *Oncogene* **2000**,
19, 6680–6686. [CrossRef] [PubMed]
23. Fünfschilling, U.; Jockusch, W.J.; Sivakumar, N.; Möbius, W.; Corthals, K.; Li, S.; Quintes, S.; Kim, Y.; Schaap, I.; Rhee, J.-S.; et al. Critical Time Window of Neuronal Cholesterol Synthesis during Neurite Outgrowth. *J. Neurosci.* **2012**, *32*, 7632–7645. [CrossRef] [PubMed]
24. Ambrosini, G.; Praz, V.; Jagannathan, V.; Bucher, P. Signal search analysis server. *Nucleic Acids Res.* **2003**, *31*, 3618–3620. [CrossRef]
25. Heinz, S.; Benner, C.; Spann, N.; Bertolino, E.; Lin, Y.C.; Laslo, P.; Cheng, J.X.; Murre, C.; Singh, H.; Glass, C.K. Simple Combinations of Lineage-Determining Transcription Factors Prime cis-Regulatory Elements Required for Macrophage and B Cell Identities. *Mol. Cell* **2010**, *38*, 576–589. [CrossRef] [PubMed]
26. Sanchez, H.B.; Yieh, L.; Osborne, T.F. Cooperation by Sterol Regulatory Element-binding Protein and Sp1 in Sterol Regulation of Low Density Lipoprotein Receptor Gene. *J. Biol. Chem.* **1995**, *270*, 1161–1169. [CrossRef]
27. Reed, B.D.; Charos, A.E.; Szekely, A.M.; Weissman, S.M.; Snyder, M. Genome-Wide Occupancy of SREBP1 and Its Partners NFY and SP1 Reveals Novel Functional Roles and Combinatorial Regulation of Distinct Classes of Genes. *PLoS Genet.* **2008**, *4*, e1000133. [CrossRef]
28. Peña-Llopis, S.; Vega-Rubin-De-Celis, S.; Schwartz, J.C.; Wolff, N.C.; Tran, T.A.T.; Zou, L.; Xie, X.-J.; Corey, D.R.; Brugarolas, J. Regulation of TFEB and V-ATPases by mTORC1. *EMBO J.* **2011**, *30*, 3242–3258. [CrossRef]
29. Rosner, M.; Hengstschläger, M. Cytoplasmic and nuclear distribution of the protein complexes mTORC1 and mTORC2: Ra- pamycin triggers dephosphorylation and delocalization of the mTORC2 components rictor and sin1. *Hum. Mol. Genet.* **2008**, *17*, 2934–2948. [CrossRef]
30. Bhattacharya, A.; Deng, J.M.; Zhang, Z.; Behringer, R.; De Crombrugghe, B.; Maity, S.N. The B subunit of the CCAAT box binding transcription factor complex (CBF/NF-Y) is essential for early mouse development and cell proliferation. *Cancer Res.* **2003**, *63*, 8167–8172.
31. Gurtner, A.; Fuschi, P.; Magi, F.; Colussi, C.; Gaetano, C.; Dobbelstein, M.; Sacchi, A.; Piaggio, G. NF-Y Dependent Epigenetic Modifications Discriminate between Proliferating and Postmitotic Tissue. *PLoS ONE* **2008**, *3*, e2047. [CrossRef]
32. Benatti, P.; Dolfini, D.; Viganò, A.; Ravo, M.; Weisz, A.; Imbriano, C. Specific inhibition of NF-Y subunits triggers different cell proliferation defects. *Nucleic Acids Res.* **2011**, *39*, 5356–5368. [CrossRef]
33. Di Agostino, S.; Strano, S.; Emiliozzi, V.; Zerbini, V.; Mottolese, M.; Sacchi, A.; Blandino, G.; Piaggio, G. Gain of function of mutant p53: The mutant p53/NF-Y protein complex reveals an aberrant transcriptional mechanism of cell cycle regulation. *Cancer Cell* **2006**, *10*, 191–202. [CrossRef] [PubMed]
34. Imbriano, C.; Gnesutta, N.; Mantovani, R. The NF-Y/p53 liaison: Well beyond repression. *Biochim. Biophys. Acta* **2012**, *1825*, 131–139. [CrossRef] [PubMed]
35. Gurtner, A.; Manni, I.; Fuschi, P.; Mantovani, R.; Guadagni, F.; Sacchi, A.; Piaggio, G. Requirement for Down-Regulation of the CCAAT-binding Activity of the NF-Y Transcription Factor during Skeletal Muscle Differentiation. *Mol. Biol. Cell* **2003**, *14*, 2706–2715. [CrossRef]
36. Farina, A.; Manni, I.; Fontemaggi, G.; Tiainen, M.; Cenciarelli, C.; Bellorini, M.; Mantovani, R.; Sacchi, A.; Piaggio, G. Down- regulation of cyclin B1 gene transcription in terminally differentiated skeletal muscle cells is associated with loss of functional CCAAT-binding NF-Y complex. *Oncogene* **1999**, *18*, 2818–2827. [CrossRef] [PubMed]
37. Yamanaka, T.; Miyazaki, H.; Oyama, F.; Kurosawa, M.; Washizu, C.; Doi, H.; Nukina, N. Mutant Huntingtin reduces HSP70 expression through the sequestration of NF-Y transcription factor. *EMBO J.* **2008**, *27*, 827–839. [CrossRef] [PubMed]
38. Yamanaka, T.; Tosaki, A.; Kurosawa, M.; Matsumoto, G.; Koike, M.; Uchiyama, Y.; Maity, S.N.; Shimogori, T.; Hattori, N.; Nukina,
N. NF-Y inactivation causes atypical neurodegeneration characterized by ubiquitin and p62 accumulation and endoplasmic reticulum disorganization. *Nat. Commun.* **2014**, *5*, 3354. [CrossRef]
39. Fleming, J.D.; Pavesi, G.; Benatti, P.; Imbriano, C.; Mantovani, R.; Struhl, K. NF-Y coassociates with FOS at promoters, enhancers, repetitive elements, and inactive chromatin regions, and is stereo-positioned with growth-controlling transcription factors. *Genome Res.* **2013**, *23*, 1195–1209. [CrossRef]
40. Tiwari, V.K.; Stadler, M.B.; Wirbelauer, C.; Paro, R.; Schübeler, D.; Beisel, C. A chromatin-modifying function of JNK during stem cell differentiation. *Nat. Genet.* **2011**, *44*, 94–100. [CrossRef]
41. Benatti, P.; Chiaramonte, M.L.; Lorenzo, M.; Hartley, J.A.; Hochhauser, D.; Gnesutta, N.; Mantovani, R.; Imbriano, C.; Dolfini, D. NF-Y activates genes of metabolic pathways altered in cancer cells. *Oncotarget* **2016**, *7*, 1633–1650. [CrossRef]
42. Schiavoni, G.; Bennati, A.M.; Castelli, M.; Della Fazia, M.A.; Beccari, T.; Servillo, G.; Roberti, R. Activation of TM7SF2 promoter by SREBP-2 depends on a new sterol regulatory element, a GC-box, and an inverted CCAAT-box. *Biochim. Biophys. Acta* **2010**, *1801*, 587–592. [CrossRef]

43. Della Sala, G.; Putignano, E.; Chelini, G.; Melani, R.; Calcagno, E.; Ratto, G.M.; Amendola, E.; Gross, C.T.; Giustetto, M.; Pizzorusso, T. Dendritic Spine Instability in a Mouse Model of CDKL5 Disorder Is Rescued by Insulin-like Growth Factor 1. *Biol. Psychiatry* **2016**, *80*, 302–311. [CrossRef]
44. Wang, I.-T.J.; Allen, M.; Goffin, D.; Zhu, X.; Fairless, A.H.; Brodkin, E.S.; Siegel, S.J.; Marsh, E.D.; Blendy, J.A.; Zhou, Z. Loss of CDKL5 disrupts kinome profile and event-related potentials leading to autistic-like phenotypes in mice. *Proc. Natl. Acad. Sci. USA* **2012**, *109*, 21516–21521. [CrossRef] [PubMed]
45. Keber, R.; Motaln, H.; Wagner, K.D.; Debeljak, N.; Rassoulzadegan, M.; Ačimovič, J.; Rozman, D.; Horvat, S. Mouse Knockout of the Cholesterogenic Cytochrome P450 Lanosterol 14α-Demethylase (Cyp51) Resembles Antley-Bixler Syndrome. *J. Biol. Chem.* **2011**, *286*, 29086–29097. [CrossRef] [PubMed]
46. Waterham, H.R. Defects of cholesterol biosynthesis. *FEBS Lett.* **2006**, *580*, 5442–5449. [CrossRef]
47. Zhang, J.; Liu, Q. Cholesterol metabolism and homeostasis in the brain. *Protein Cell* **2015**, *6*, 254–264. [CrossRef] [PubMed]
48. Driver, A.M.; Kratz, L.E.; Kelley, R.I.; Stottmann, R.W. Altered cholesterol biosynthesis causes precocious neurogenesis in the developing mouse forebrain. *Neurobiol. Dis.* **2016**, *91*, 69–82. [CrossRef]
49. Wassif, C.A.; Maslen, C.; Kachilele-Linjewile, S.; Lin, D.; Linck, L.M.; Connor, W.E.; Steiner, R.D.; Porter, F.D. Mutations in the Human Sterol Δ7-Reductase Gene at 11q12-13 Cause Smith-Lemli-Opitz Syndrome. *Am. J. Hum. Genet.* **1998**, *63*, 55–62. [CrossRef]
50. Fitzky, B.U.; Witsch-Baumgartner, M.; Erdel, M.; Lee, J.N.; Paik, Y.-K.; Glossmann, H.; Utermann, G.; Moebius, F.F. Mutations in the 7-sterol reductase gene in patients with the Smith-Lemli-Opitz syndrome. *Proc. Natl. Acad. Sci. USA* **1998**, *95*, 8181–8186. [CrossRef]
51. König, A.; Happle, R.; Bornholdt, D.; Engel, H.; Grzeschik, K.H. Mutations in the NSDHL gene, encoding a 3beta-hydroxysteroid dehydrogenase, cause CHILD syndrome. *Am. J. Med Genet.* **2000**, *90*, 339–346. [CrossRef]
52. McLarren, K.W.; Severson, T.M.; Du Souich, C.; Stockton, D.W.; Kratz, L.E.; Cunningham, D.; Hendson, G.; Morin, R.D.; Wu, D.; Paul, J.E.; et al. Hypomorphic Temperature-Sensitive Alleles of NSDHL Cause CK Syndrome. *Am. J. Hum. Genet.* **2010**, *87*, 905–914. [CrossRef] [PubMed]
53. Schafer, B.L.; Bishop, R.W.; Kratunis, V.J.; Kalinowski, S.S.; Mosley, S.T.; Gibson, K.M.; Tanaka, R.D. Molecular cloning of human mevalonate kinase and identification of a missense mutation in the genetic disease mevalonic aciduria. *J. Biol. Chem.* **1992**, *267*, 13229–13238. [CrossRef]
54. Ahmad, F.; Sun, Q.; Patel, D.; Stommel, J.M. Cholesterol Metabolism: A Potential Therapeutic Target in Glioblastoma. *Cancers* **2019**, *11*, 146. [CrossRef] [PubMed]
55. Mathews, E.S.; Appel, B. Cholesterol Biosynthesis Supports Myelin Gene Expression and Axon Ensheathment through Modulation of P13K/Akt/mTor Signaling. *J. Neurosci.* **2016**, *36*, 7628–7639. [CrossRef] [PubMed]
56. Martin, M. Cutadapt removes adapter sequences from high-throughput sequencing reads. *EMBnet. J.* **2011**, *17*, 10–12. [CrossRef]
57. Andrew, S. Fast QC: A Quality Control Tool for High Throughput Sequence Data. Available online:http://www.bioinformatics. babraham.ac.uk/projects/fastqc(accessed on 30 January 2018).
58. Dobin, A.; Davis, C.A.; Schlesinger, F.; Drenkow, J.; Zaleski, C.; Jha, S.; Batut, P.; Chaisson, M.; Gingeras, T.R. STAR: Ultrafast universal RNA-seq aligner. *Bioinformatics* **2013**, *29*, 15–21. [CrossRef]
59. Liao, Y.; Smyth, G.K.; Shi, W. featureCounts: An efficient general purpose program for assigning sequence reads to genomic features. *Bioinformatics* **2013**, *30*, 923–930. [CrossRef]
60. Love, M.I.; Huber, W.; Anders, S. Moderated estimation of fold change and dispersion for RNA-seq data with DESeq2. *Genome Biol.* **2014**, *15*, 550. [CrossRef]
61. Robinson, M.D.; McCarthy, D.J.; Smyth, G.K. edgeR: A Bioconductor package for differential expression analysis of digital gene expression data. *Bioinformatics* **2009**, *26*, 139–140. [CrossRef]
62. Chen, H.; Boutros, P.C. VennDiagram: A package for the generation of highly-customizable Venn and Euler diagrams in R. *BMC Bioinformatics* **2011**, *12*, 35. [CrossRef] [PubMed]
63. Gu, Z.; Eils, R.; Schlesner, M. Complex heatmaps reveal patterns and correlations in multidimensional genomic data. *Bioinformatics* **2016**, *32*, 2847–2849. [CrossRef] [PubMed]
64. Buenrostro, J.D.; Giresi, P.G.; Zaba, L.C.; Chang, H.Y.; Greenleaf, W.J. Transposition of native chromatin for fast and sensitive epigenomic profiling of open chromatin, DNA-binding proteins and nucleosome position. *Nat. Methods.* **2013**, *10*, 1213–1218. [CrossRef] [PubMed]
65. Bolger, A.M.; Lohse, M.; Usadel, B. Trimmomatic: A flexible trimmer for Illumina sequence data. *Bioinformatics* **2014**, *30*, 2114–2120. [CrossRef]
66. Langmead, B.; Salzberg, S.L. Fast gapped-read alignment with Bowtie 2. *Nat. Methods* **2012**, *9*, 357–359. [CrossRef]
67. Li, H.; Handsaker, B.; Wysoker, A.; Fennell, T.; Ruan, J.; Homer, N.; Marth, G.; Abecasis, G.; Durbin, R. The Sequence Alignment/Map Format and SAMtools. *Bioinformatics* **2009**, *25*, 2078–2079. [CrossRef]
68. Broad Institute GR. Picard Toolkit. Available online:http://broadinstitutegithubio/picard/(accessed on 6 September 2018).
69. Zhang, Y.; Liu, T.; Meyer, C.; Eeckhoute, J.; Johnson, D.S.; Bernstein, B.; Nussbaum, C.; Myers, R.M.; Brown, M.; Li, W.;

et al. Model-based Analysis of ChIP-Seq (MACS). *Genome Biol.* **2008**, *9*, R137. [CrossRef]
70. Kent, W.J.; Sugnet, C.W.; Furey, T.S.; Roskin, K.M.; Pringle, T.H.; Zahler, A.M.; Haussler, A.D. The Human Genome Browser at UCSC. *Genome Res.* **2002**, *12*, 996–1006. [CrossRef]
71. Yu, G.; Wang, L.-G.; Han, Y.; He, Q.-Y. clusterProfiler: An R Package for Comparing Biological Themes Among Gene Clusters.
OMICS **2012**, *16*, 284–287. [CrossRef]
72. Carlson, M. Org.Mm.eg.db: Genome Wide Annotation for Mouse. R Package Version 3.8.2. Available online:https://bioconductor. org/packages/release/data/annotation/html/org.Mm.eg.db.html.xs(accessed on 28 May 2021).
73. Kanehisa, M.; Sato, Y.; Kawashima, M.; Furumichi, M.; Tanabe, M. KEGG as a reference resource for gene and protein annotation.
Nucleic Acids Res. **2016**, *44*, D457–D462. [CrossRef]

2.4.1 Supplementary material

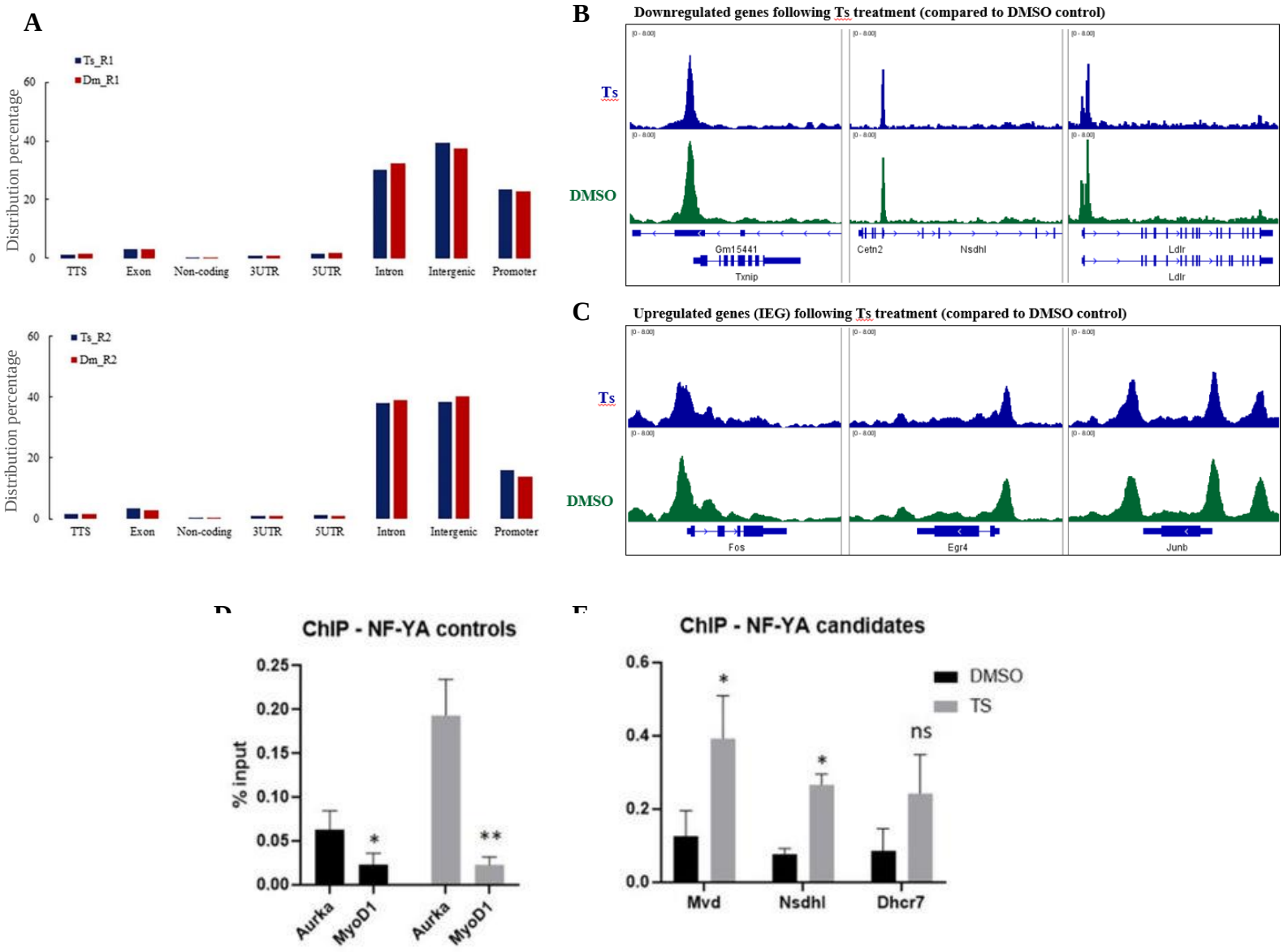

ATAC-seq and ChIP-qPCR for NF-YA binding. Primary cortical neurons were treated with DMSO or Temsirolimus (10 µM) for 5 hours followed by cell lysis and ATAC-Seq. **A** Genomic features of two biological replicates of the following temsirolimus or DMSO treatment. B-C Representative pictures of ATAC-Seq peaks at the promoters of (B) downregulated genes cholesterol biosynthesis genes (Txnip, NSdhl and Ldlr) and (D) upregulated IEGs (Fos, Egr4 and Junb). D-E. ChIP was performed with NF-YA specific antibodies in neruons treated for 5 hours with DMSO or temsirolimus followed bu qPCR of positive control Aurka and negative control MyoD (D) or the down regulated targets Mvd, Nsdhl and Dhcr7 (D). Data represent the average of three biological replicates. For statistical analyses, Student's t-test was used. *p<0.05. Error bars represent ±S.E.M.

2.5 INTACT vs. FANS for Cell-Type-Specific Nuclei Sorting: A Comprehensive Qualitative and Quantitative Comparison

Authors: Monika Chanu Chongtham [1,†], **Tamer Butto** [2,†], Kanak Mungikar [2,†], Susanne Gerber [2,*] and Jennifer Winter [1,2,*] († These authors contributed equally to this work)

This article is published in *International journal of Molecular Sciences* 22(10), 5335; https://doi.org/10.3390/ijms22105335

My contributions to this article are listed in section 4.2 Contributions to individual publication

International Journal of Molecular Sciences

MDPI

Article

INTACT vs. FANS for Cell-Type-Specific Nuclei Sorting: A Comprehensive Qualitative and Quantitative Comparison

Monika Chanu Chongtham [1,†], Tamer Butto [2,†], Kanak Mungikar [2,†], Susanne Gerber [2,*] and Jennifer Winter [1,2,*]

[1] Leibniz Institute of Resilience Research, Wallstr 7, 55122 Mainz, Germany; mchongth@uni-mainz.de
[2] Institute of Human Genetics, University Medical Center of the Johannes Gutenberg University Mainz, Langenbeckstr. 1, 55131 Mainz, Germany; T.Butto@imb-mainz.de (T.B.); kamungik@uni-mainz.de (K.M.)
* Correspondence: sugerber@uni-mainz.de (S.G.); jewinter@uni-mainz.de (J.W.)
† These authors contributed equally to this work.

Abstract: Increasing numbers of studies seek to characterize the different cellular sub-populations present in mammalian tissues. The techniques "Isolation of Nuclei Tagged in Specific Cell Types" (INTACT) or "Fluorescence-Activated Nuclei Sorting" (FANS) are frequently used for isolating nuclei of specific cellular subtypes. These nuclei are then used for molecular characterization of the cellular sub-populations. Despite the increasing popularity of both techniques, little is known about their isolation efficiency, advantages, and disadvantages or downstream molecular effects. In our study, we compared the physical and molecular attributes of sfGFP+ nuclei isolated by the two methods—INTACT and FANS—from the neocortices of Arc-CreERT2 × CAG-Sun1/sfGFP animals. We identified differences in efficiency of sfGFP+ nuclei isolation, nuclear size as well as transcriptional (RNA-seq) and chromatin accessibility (ATAC-seq) states. Therefore, our study presents a comprehensive comparison between the two widely used nuclei sorting techniques, identifying the advantages and disadvantages for both INTACT and FANS. Our conclusions are summarized in a table to guide researchers in selecting the most suitable methodology for their individual experimental design.

Keywords: FANS; INTACT; nuclei sorting; neuronal nuclei; ATAC-Seq; RNA-Seq

Citation: Chongtham, M.C.; Butto, T.; Mungikar, K.; Gerber, S.; Winter, J. INTACT vs. FANS for Cell-Type-Specific Nuclei Sorting: A Comprehensive Qualitative and Quantitative Comparison. Int. J. Mol. Sci. 2021, 22, 5335. https://doi.org/ 10.3390/ijms22105335

Academic Editor: Luca Agnelli

Received: 6 March 2021
Accepted: 14 May 2021
Published: 19 May 2021

1. Introduction

The mammalian system consists of distinct and highly specific cell types that contribute to a given tissue's function and, ultimately, promote the organism's survival. Therefore, cell-specific studies have become highly relevant in uncovering such specific mechanisms. In recent years, many studies focused on developing different techniques to investigate the cells' molecular properties, ranging from bulk to single-cell populations [1,2]. Fluorescence-activated cell sorting (FACS) has been widely used in a variety of molecular studies as a method to isolate populations using endogenous or external fluorescence tagging [3,4] since its introduction in the 1970s [5]. With the increasing interest in the genomic and epigenetic properties of specific cell types, the research focus has shifted to nuclei isolation techniques. Therefore, a variant of FACS was adapted, "fluorescence-activated nuclei sorting" (FANS), to isolate specific nuclei populations using nuclear fluorescence tags [6,7].

Although flow cytometry is a widely used technique to separate specific cells/nuclei populations, certain disadvantages have been associated with it. For instance, FACS/FANS requires high-cost equipment and specially trained people. These requirements can be an unaffordable obstacle, particularly for smaller labs. Additionally, it is challenging to sort morphologically complex cells such as cells from the central nervous system [8,9]. The high hydrodynamic stress forms one of the major challenges [10,11], as this could trigger cellular stress responses leading to a subsequent modification of different molecular profiles [8,12–

14]. Apart from this, FACS/FANS also comes with a high time–cost factor to isolate rare cell populations at a multiscale level [1,9,15].

As an alternative, Deal and Henikoff [15] demonstrated a proof of principle for magnetic sorting of nuclei using genetically modified plants with the technique "isolation of nuclei tagged in specific cell types" (INTACT). Since then, this method has been adapted to model organisms such as *C. elegans, D. melanogaster* [16,17], and other mammalian systems [18,19]. Mo and colleagues introduced INTACT to sort activated neuronal (sfGFP+) populations in the mammalian brain [10,20]. Since then, the use of INTACT has been extended to distinct neuronal cells [18,19,21,22], cardiomyocytes [23–25], and hepatocytes [26,27]. INTACT and flow cytometry-based techniques from multiple literature data have already been reviewed in [1]. However, data of a systematic comparison, displaying the physical differences in the sorted nuclei, the overall efficiency of isolation, and subsequent molecular analyses between these two techniques are still lacking. Additionally, neither method has been tested or optimized for sorting small nuclei numbers, which are important for distinguishing between the numerous cellular subtypes' expression profiles in the brain. For simplicity, FANS will be utilized as the default term to describe the work presented unless mentioned otherwise.

In this study, we used a transgenic mouse model ($Arc^{creERT2(TG/WT)}$.$R26^{CAG\text{-}Sun1\text{-}sfGFP\text{-}Myc(M/WT\ or\ M/M)}$) to establish and compare the two techniques—INTACT and FANS—for the isolation of activated neuronal nuclei from small as well as bulk tissue samples. Using a modified protocol for nuclei isolation from small tissues [28], first, we examined the sorting processes' speed and efficiency using different tissue types and sfGFP+ nuclei percentage. Then, we selected the neocortex (i.e., bulk tissue) to compare the physical (i.e., nuclei shape and intensity) and molecular (i.e., transcriptional profile and chromatin accessibility) aspects using low-input nuclei from the different sorting methods. We observed differences in the techniques in terms of both physical and molecular attributes. These observations are summarized in a simple informative overview to guide researchers towards a better experimental design for using cell-type-specific populations (to uncover unique cellular properties).

2. Results

2.1. Literature Review of INTACT and FANS/FACS Studies

To compare the methodologies of INTACT and FANS for cell-type-specific isolation, we first conducted a literature review to identify and summarize shared and distinct features of both techniques. We decided to limit the range of studies and focus on Mo et al.'s [10] citations, since we based our experimental comparisons on the same reporter line ($R26^{CAG\text{-}Sun1\text{-}sfGFP\text{-}Myc}$). Additionally, this publication reports the first use of INTACT in the mammalian system, providing an essential landmark in the field. In the review, we included all studies that used INTACT/FANS (or both) regardless of the organismal system. We noticed that several studies used the term FACS while describing nuclei sorting and, therefore, we included them in the summary as FANS. The literature review comprised four stages including identification, screening, eligibility, and analysis (Figure 1A). We found that 31 publications used FANS, 18 used INTACT, and nine used both (Figure 1A). To track each technique's dynamic use over time, we plotted the individual publications obtained from 2016 until 2020. Overall, we observed increased use of both methods each year (Supplementary Materials Table S1 and Figure S1A,B). Of the studies under consideration, ~53% (31 out of 58) used FANS, ~31% used INTACT (18 out of 58), and ~16% used both (9 out of 58).

Next, we looked at the subsequent molecular analyses used in conjugation with the investigated techniques. The four main fields of interest included RNA-seq, ATAC-seq, ChIP-seq, and DNA methylation analyses (Supplementary Materials Table S1). Overall, we observed that FANS was applied more often than INTACT in combination with subsequent methodologies (Figure 1C). However, this was expected, as the use of flow- cytometry techniques precedes the application of techniques such as INTACT. Additionally, we observed an increase in the use of the molecular technique considered per year, most notably in RNA-

seq and ATAC-seq, followed by a slight rise in ChIP-seq and DNA methylation analyses (Supplementary Materials Figure S1B).

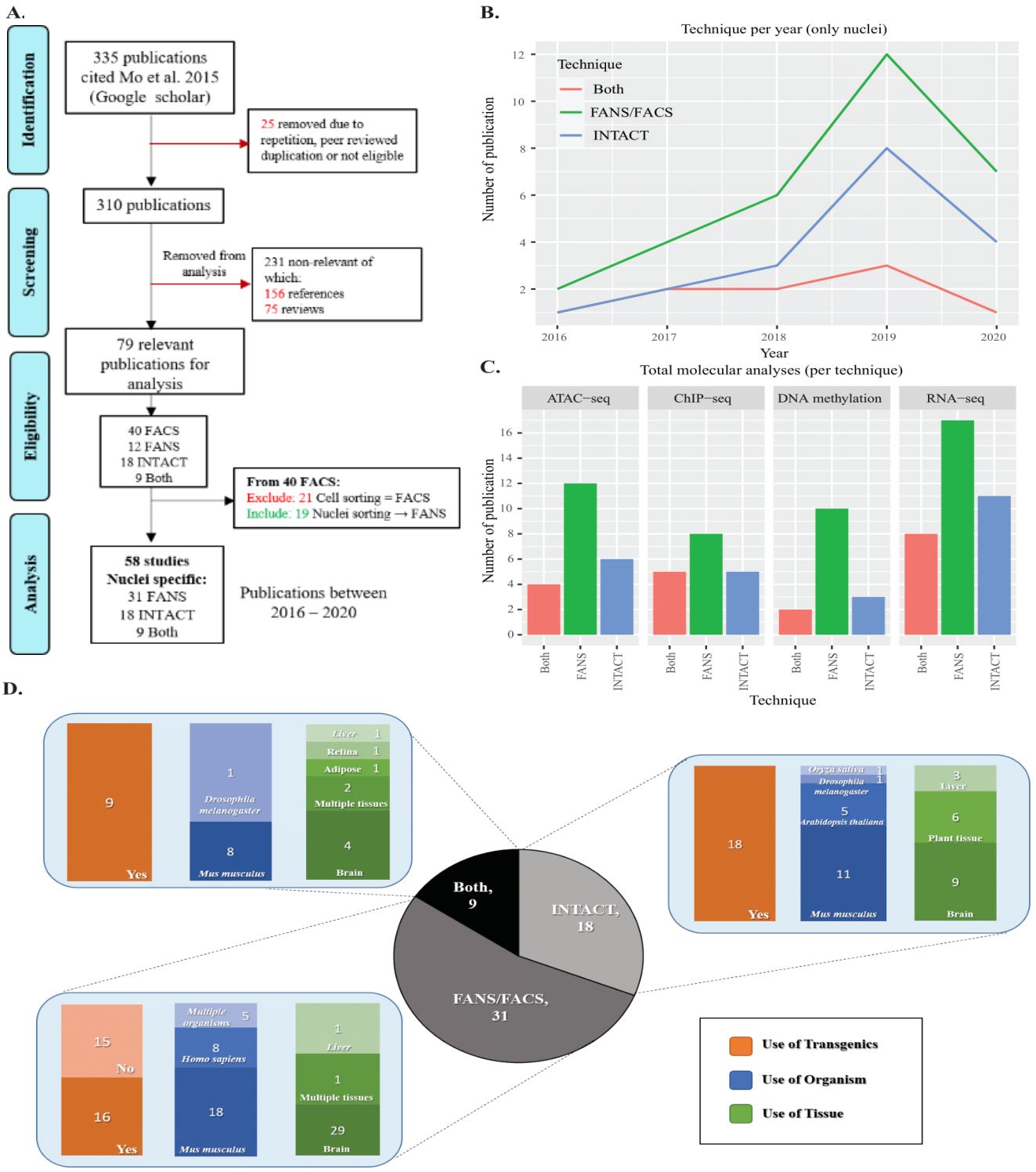

Figure 1. Literature review of Mo et al.'s (2015) citations: (**A**) literature review workflow for assessing the usage of INTACT and FANS; (**B**) publication trend of individual techniques per year; (**C**) use of subsequent sequencing techniques per year of publications for INTACT, FANS or both; (**D**) overview of the use of transgenics, organism, and tissue per technique (see Supplementary Materials Table S1 for additional information).

We further performed an analysis based on features such as the use of transgenics, tissue type, and organism. Due to the variability in data description, we opted to provide generalized information on the material used. For additional details of the specific tissues and quantities used, see Supplementary Materials Table S1. In our results, we observed that the "brain" was the most frequently investigated tissue with 62% of all of the citations, followed by "plant tissue" (6%), "heart" (3.5%), and "liver" (2.4%) (Figure 1D, Supplementary Materials Figure S1C,D). On the other hand, "*mus musculus*" was the most frequently used organism in the selected studies with 42% of the citations along with "*Homo sapiens*" (12%), "*Arabidopsis thaliana*" (5.8%), and "*Drosophila melanogaster*" (2.3%) (Figure 1D, Supplementary Materials Figure S1E,F). The frequently used tissue and organisms are not surprising, as Mo et al. [10] investigated epigenetic signature changes occurring in mature neurons of transgenic mice.

From our literature review, we observed an increased use of FANS and INTACT for cell-type-specific nuclei isolation. In terms of application and subsequent molecular analysis, FANS was used more frequently than INTACT. However, a comparative analysis of the two techniques concerning their suitability for downstream molecular analysis was lacking. Therefore, we decided to carry out such a comparative analysis starting with sorting efficiency using different brain sub-regions with varying amounts of nuclei and sfGFP+ percentages.

2.2. Assessing Differences in Speed and Sorting Efficiency between FANS and INTACT

To provide a comprehensive comparison between INTACT- and FANS-isolated nuclei, we used the tamoxifen (TAM)-dependent $Arc^{creERT2\ (TG/WT)}.R26^{CAG\text{-}Sun1\text{-}sfGFP\text{-}Myc\ (M/WT\ or\ M/M)}$ mouse line [10,29]. The mouse line expresses sfGFP on the nuclear membrane of specific stimulus-activated cells (expressing Arc) upon TAM injection. In our experiments, we used the "social interaction test" (SI, [30]) as the intended behavioral stimulus to obtain populations of sfGFP-positive (sfGFP+) nuclei, following TAM injection. Nuclei were isolated from the neocortices of 13–16 week old transgenic mice using the protocol from Chongtham et al. [28] (Figure 2A). Following isolation, nuclei were diluted with wash buffer and aliquoted into equal volumes to isolate the sfGFP+ nuclei using either INTACT or FANS (Figure 2B,C). Depending on the technique used, the sorted sfGFP+ nuclei were termed as INTACT-nuclei or FANS-nuclei.

It has been shown that INTACT is more efficient at processing larger amounts of samples compared to FANS because it requires less processing time [1]. Therefore, we first analyzed the speed of sfGFP+ nuclei isolation using INTACT or FANS under different conditions. We chose specific micro-dissected brain regions, which provided different nuclei yield and sfGFP+ nuclei percentages, in this experimental design (Table 1, Yield: sfGFP%; 73 × 10^4/mL: 18.95; 60 × 10^4/mL: 12.8; 140 × 10^4/mL: 47.45, 136 × 10^4/mL: 23, 200 × 10^4/mL: 29.3 for nucleus accumbens, hypothalamus, pituitary, hippocampus, and neocortex, respectively). The regions were selected to represent diverse sample populations.

The experiment was performed in a parallel run for all brain regions analyzed (technical duplicates). First, we noted the time required to obtain 5000 sfGFP+ nuclei from a single sample using FANS or INTACT. Next, the theoretical time needed to obtain large numbers (for example, 50k) was calculated using the unitary method. Here, we observed that a single sample's processing speed was faster using FANS (Table 1, 1–3 min for FANS as compared to INTACT—35 min). However, when multiple samples were considered and the theoretical time was calculated, the FANS technique could be more time-consuming (100–200 min for FANS compared to INTACT—about 60 min).

Additionally, when using INTACT, despite the high overall purity of the separation, we observed differences in sorting efficiency, which was dependent on nuclei yield and sfGFP+ percentages. For example, for nucleus accumbens, where the nuclei yield was low, the yield of sfGFP+ nuclei was only 15%. In contrast, for pituitary with high nuclei yield and high sfGFP+ percentage, the extraction efficiency was approximately 40% (see Table 1, "yield"). However, when we applied the same protocol to the neocortex (high nuclei concentration

and sfGFP+ percentage), the yield was approximately 86–90% (Table 1). The efficiency of nuclei extraction in FANS did not vary under these different conditions.

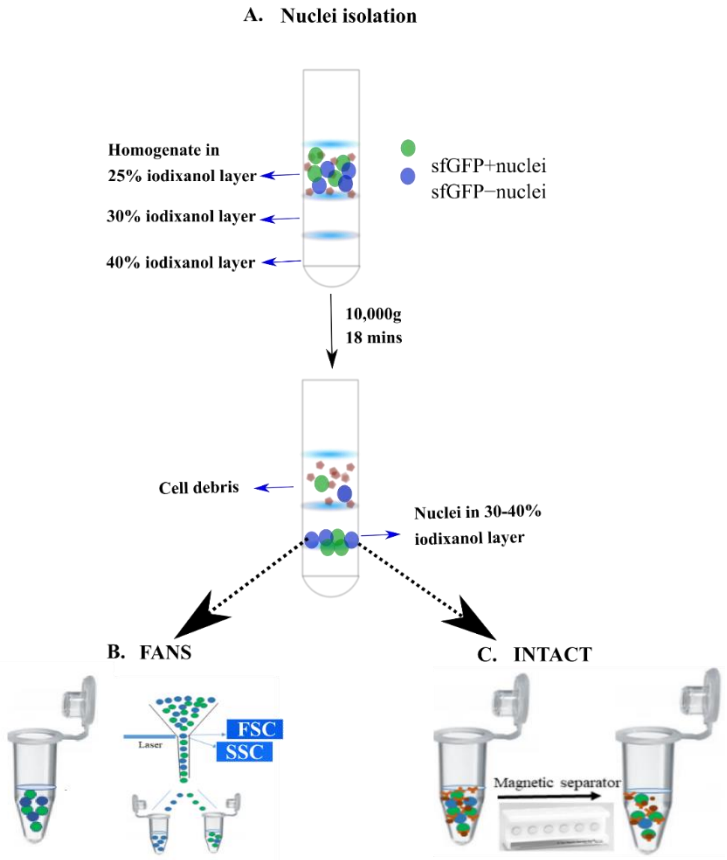

Figure 2. FANS vs. INTACT: Procedural differences and purity estimation: (**A**) nuclei extraction via ultracentrifugation (adapted from Chongtham et al. (2020)); (**B**) nuclei sorting using FANS; (**C**) magnetic separation of bead-bound nuclei using INTACT.

Table 1. Processing speed of sfGFP+ nuclei separation using FANS and INTACT (mean of biological replicates).

Brain Region\Property Tested	Nuclei Yield (×10⁴/mL)	Total Volume (µL)	Input Nuclei sfGFP+%	Actual 5k Nuclei/Sample (mins)		Theoretical 50k Nuclei/10 Samples (mins)		sfGFP+ Nuclei Yield from INTACT		
				FANS	INTACT	FANS	INTACT	GFP% Supernatant	Yield %	Purity
Small–medium brain regions										
Nucleus accumbens	73	300	18.95	2	35	200	60	16.5	15	98.5
Hypothalamus	60	400	12.8	3	35	300	60	7.6	44	98.2
Pituitary	140	400	47.45	1	35	100	60	28.9	40	99.1
Hippocampus	136	400	23	1.5	35	150	60	12.3	50	99.8
Large brain regions										
Neocortex 1	>200	900	29.3	-	-	-	-	3.6	87	98.5
Neocortex 2	>200	900	26.7	-	-	-	-	3.7	86	93.6

Overall, our results indicate that the INTACT method might be preferable in cases of large sample numbers, where fast processing of nuclei is required. When rather accurate nuclei numbers are required for downstream processing, FANS may be better suited.

2.3. Quantification of Morphological Attributes: FANS- and INTACT-Nuclei in Comparison to INPUT-Nuclei

As in the previous section, 13–16 week old mice were subjected to an SI test 5 h after TAM injection to induce sfGFP expression on activated nuclei. Neocortices were dissected and nuclei were isolated. The experiments were repeated a total of three times on different experimental days using different biological replicates.

2.4. Structural and Optical Modifications Observed under Phase-Contrast Microscopy and Fluorescence Microscopy

Upon verifying the purity of the separated sfGFP+ populations (Supplementary Materials Figure S2), the nuclei morphology of FANS-nuclei and INTACT-nuclei were compared to unsorted nuclei (INPUT-nuclei) using phase-contrast microscopy and to sfGFP+ populations (INPUT-sfGFP nuclei) using fluorescence microscopy. For investigating structural modifications, we used phase-contrast microscopy to measure the "area" of FANS- and INTACT-nuclei in comparison to INPUT-nuclei (n = 100–200 nuclei; Figure 3A,B) from three different biological replicates. After sorting (<3 h), we detected a slight increase in the area and perimeter of FANS-nuclei compared to the INPUT-nuclei ($p < 0.05$, $p < 0.0001$), while INTACT-nuclei did not show a detectable change (Figure 3B, Supplementary Materials Figure S3A,B)

Next, we quantified the "optical density" using the Trypan blue staining intensity, as the optical properties of a nucleus convey important information about the nucleus (including nuclear membrane integrity). Since the INTACT-nuclei beads affected the optical light transmission, we could only perform this analysis on FANS-nuclei compared to INPUT-nuclei. There was no significant difference between FANS-nuclei and INPUT-nuclei <3 h after sorting ($p = 0.5397$, n.s., Supplementary Materials Figure S3C).

Using phase contrast microscopy, we could only compare sfGFP+ FANS- and INTACT-nuclei to a pool of sfGFP− and sfGFP+ INPUT-nuclei. This was suboptimal because most sfGFP+ nuclei from the neocortices are likely to be nuclei from excitatory neurons where Arc expression is abundant, whereas sfGFP− nuclei contain a mixture of all different cell types of the neocortex. Therefore, we used fluorescence microscopy for the next step to compare the sfGFP+ FANS- and INTACT-nuclei to sfGFP+ INPUT-nuclei. For these experiments, nuclei were embedded in the wells of a chambered coverglass (IBIDI) within 3 h or 4–6 h after sorting. Representative images of the INPUT-, FANS-, and INTACT-nuclei (<3 h) are shown in Figure 3C. Upon quantification, we observed a significant increase ($p < 0.0001$, $p < 0.0001$, n = 100–200 nuclei) in the size (area and perimeter) of sfGFP+ FANS-nuclei compared to that of sfGFP+ INPUT-nuclei (Figure 3D). The size of the INTACT-nuclei did not change significantly when compared to sfGFP+ INPUT-nuclei. The observations remain similar to that in phase-contrast microscopy. Thereafter, the increase in the size of FANS-nuclei was validated over a larger sample size using a macroscript [28] for faster processing ($p < 0.0001$, n = 300–400 nuclei, Supplementary Materials Figure S3D, <3 h after sorting (A)). Already, 4–6 h after sorting the size of FANS-nuclei again decreased as shown in the Supplementary Materials Figure S3D, $p < 0.001$. Interestingly, the increase in size (<3 h) was accompanied by a significant shift in the optical density of FANS-nuclei (only sfGFP+ populations considered) that showed a brighter pattern in the brightfield image (Supplementary Materials Figure S3E, $p < 0.0001$ (NB: * these nuclei were without Trypan blue staining and, hence, exhibited the opposite pattern of that in Supplementary Materials Figure S3C)). This finding suggests a possible change in FANS-nuclei's osmotic pressure within a few hours of sorting, followed by subsequent shrinkage.

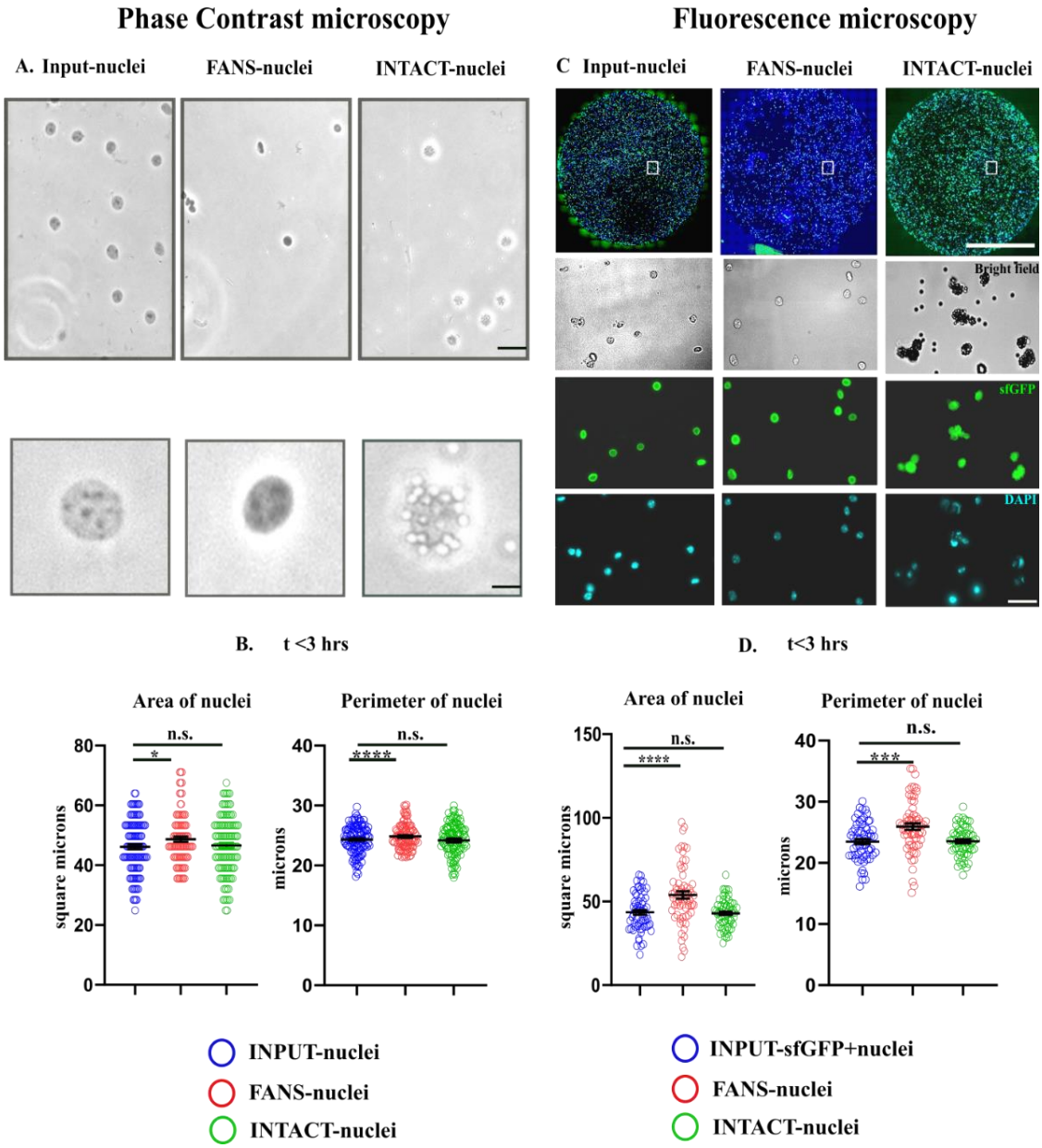

Figure 3. Morphological comparisons between FANS- and INTACT-sorted nuclei. Nuclei were isolated from the neocortices of 13–16 week old mice and sfGFP+ nuclei were sorted using FANS or INTACT. (**A**) For phase contrast microscopy, sorted nuclei were observed within 2–3 h of the sort. Representative images of INPUT-, FANS- and INTACT-nuclei. Scalebar: 25 μm. (**B**) Nuclei area and perimeter after sorting with FANS or INTACT. Both parameters in FANS- but not INTACT nuclei (n.s. ($p > 0.05$) increased significantly compared to the INPUT-nuclei ($p < 0.05$ (*), $n = 100–200$ nuclei). Scalebar: 5 μm, Air Objective, 40×. (**C**) For fluorescence microscopy, sorted nuclei were embedded in IBIDI chambers within 3 h or within 4–6 h of the sort. Representative images of INPUT-, FANS- and INTACT-nuclei (within 3 h of the sort) in the wells of IBIDI chambers and the representative enlarged images showing brightfield, GFP, and DAPI fluorescence along with the magnetic beads (2.8 μm diameter) showing a green autofluorescence (for INTACT) are shown. Scale bar: 2 mm (inset), scale bar—25 μm, water objective, 20× and 40×. (**D**) Analysis of nuclei area embedded in the IBIDI chambers within 3 h after sorting manually. Significant increase in the size of FANS-nuclei <3 h of sorting (nuclei area and perimeter) compared to the sfGFP+ INPUT-nuclei ($p < 0.001$ (***), $p < 0.0001$ (****), $n = 100–200$ nuclei) while no significant changes in INTACT-nuclei.

Conclusively, the results indicate that FANS but not INTACT induces morphological changes in the sorted nuclei. The change in shape and optical density of FANS-nuclei, compared to INTACT-

nuclei/INPUT-nuclei, could portray changes in chromatin dynamics and gene expression [31–35]. Therefore, we investigated the transcriptome and chromatin accessibility status in FANS- and INTACT-nuclei.

2.5. Transcriptional Differences of Low-Input RNA-Seq from FANS-Nuclei vs. INTACT-Nuclei

Following the qualitative assessment of INTACT and FANS on isolated nuclei, we focused on the sorted nuclei's transcriptomic signatures. First, we examined two different RNA library preparation kits in order to select the most suitable one for nuclear RNA. The first was a polyA-based cDNA amplification kit (Clontech, *Mountain View, CA, USA*), while the second was a ribo depletion-based library preparation kit (NuGen Ovation Solo RNA-seq). Both kits dealt with low concentrations of RNA typically obtained from rare cell types or limited cell numbers. In this experimental design, RNA samples were isolated from 10,000 nuclei sorted with either INTACT or FANS using hippocampal sfGFP+ nuclei (RIN > 7) (Supplementary Materials Figure S4A). Amplified cDNA libraries revealed similar cDNA distribution according to library preparation strategy (Supplementary Materials Figure S4B). Following sequencing, we performed read alignment analysis to observe the distribution of mapped reads across the gene body. The read distribution was uniform across the gene body for Nugen compared to Clontech library preparation (Figure 4A). Additionally, 3'UTR distribution bias was observed in the Clontech library preparation as previously reported in poly(A) based strategies [3]. Using principal component analysis (PCA) [36], we observed that all samples clustered according to their isolation technique and library preparation strategy (Supplementary Materials Figure S4C). To avoid 3'UTR distribution bias and since we were using low-input material isolated from the selected neuronal populations, we decided to use the Nugen Ovation Solo as our library preparation strategy for the following transcriptional analyses.

A.

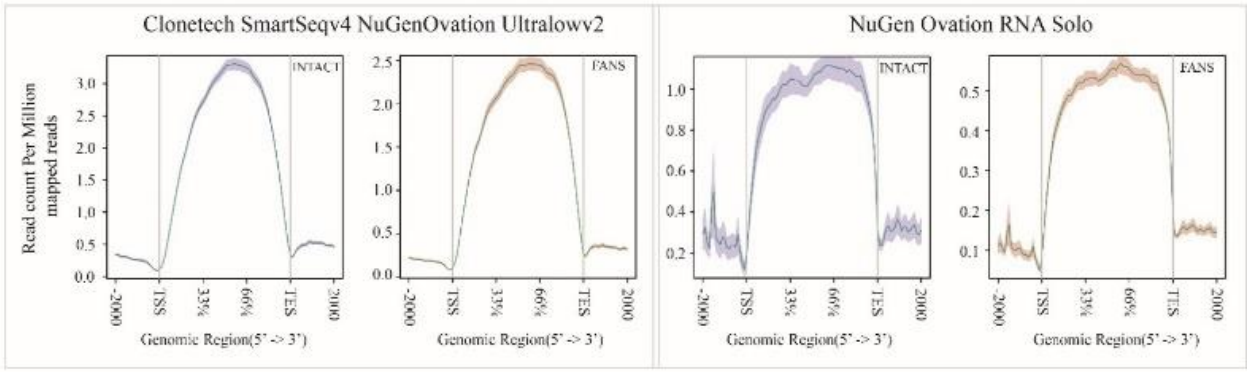

B

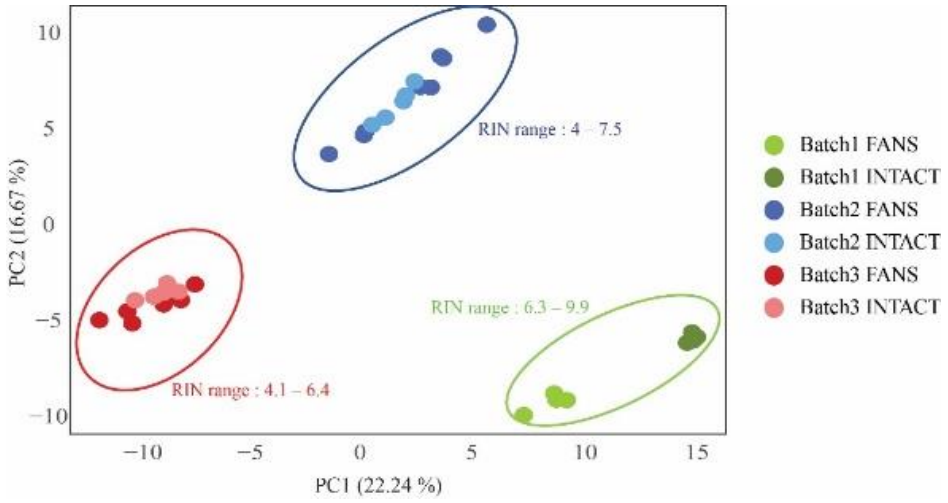

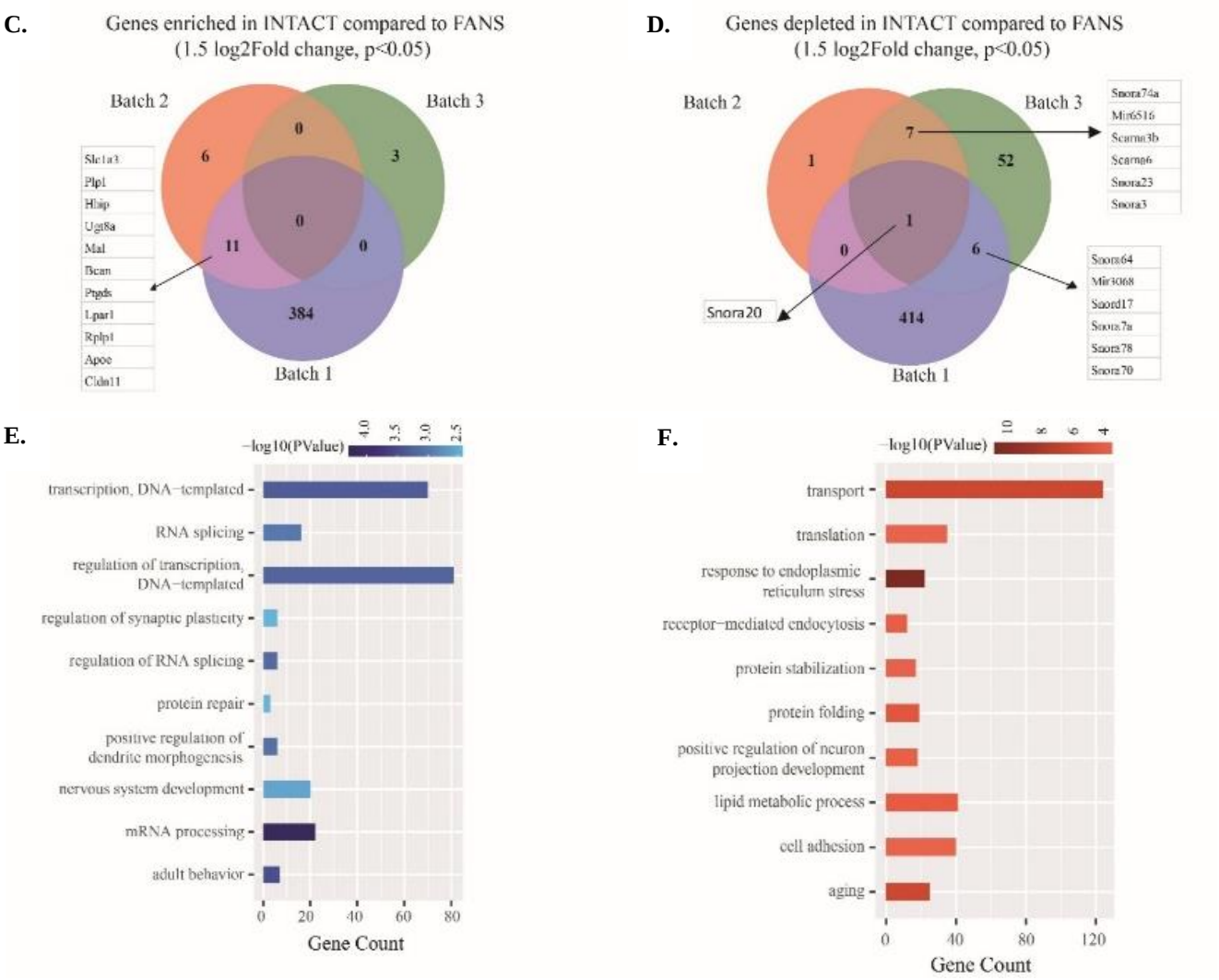

Figure 4. Transcriptional comparison between FANS- and INTACT-nuclei with distinct RIN values: (**A**) FANS/INTACT-mapped reads across the gene body based on library preparation strategy; (**B**) combined PCA from the three batches with distinct RIN values; (**C**) Venn diagrams of shared upregulated genes in INTACT compared to FANS among the 3 batches (1.5-fold change, $p < 0.05$); (**D**) Venn diagrams of shared downregulated genes in INTACT compared to FANS among the 3 batches (1.5-fold change, $p < 0.05$); (**E**,**F**) GO term enrichment analysis of INTACT-depleted (**E**) genes and enriched (**F**) compared to FANS. (Data represent depleted and enriched in INTACT compared to FANS).

Next, we examined the transcriptome differences between INTACT- and FANS-nuclei. For this comparison, we isolated RNA from neocortical sfGFP+ nuclei. We used the neocortex due to the ease of dissection and availability of higher number of isolated nuclei and sfGFP+ RNA quality was determined by the RNA integrity number (RIN). Isolation of RNA from low-input material results in variable RIN values that often do not reach the accepted RIN of ≥7 [3]. Therefore, we examined how RNA quality isolated from low-input nuclei influence the RNA-seq analysis of INTACT- and FANS-nuclei in order to identify potential transcriptional changes influenced by RIN values. Overall, we compared 14 replicates per technique deriving from three distinct biological sources (batch 1: $n = 4$ per technique; batch 2: $n = 5–7$ per technique; batch 3: $n = 5–7$ per technique) (Supplementary Materials Figure S5A). Batch 1 contained samples with high RIN values ranging from 6.3–9.9, whereas batch 2 and 3 comprised samples with RIN values ranging from 4 to 7.5 (Supplementary Materials Figure S5A). First, we evaluated alignment statistics to identify changes among the different batches (Supplementary Materials Figure S5B). We observed

no significant mapping variations between the samples with varying RIN values of both FANS and INTACT. Next, we compared the different batches and analyzed the samples according to the isolation technique. The PCA of all the samples discriminated the samples according to the batch of isolation (Figure 4B). When all batches were combined in PCA, only the high RIN batch (batch 1) separated the samples according to the isolation technique suggesting that the technique's clustering became more evident with increasing RIN values (Figure 4B). Batch-specific PCA, revealed similar separation between INTACT and FANS samples within batch 1, whereas the discrimination within the lower RIN value batches (batches 2 and 3) was present but less distinct than in batch 1 (Supplementary Materials Figure S6A–C).

To identify significant transcriptional differences between the techniques, we looked at differentially expressed genes (DEGs) between FANS and INTACT in each batch as well as among all the three batches. Within the high RIN value batch (batch 1), we identified 395 enriched and 422 depleted genes in INTACT compared to FANS, whereas 17 significantly enriched and nine depleted genes were identified in batch 2 and 3 enriched, and 66 depleted genes were identified in batch 3 (1.5 log2fold-change and p-value < 0.05; Supplementary Materials Figure S7A–F). Using the obtained DEGs, we tested if the enriched and depleted genes were shared across the three distinct batches. In the INTACT-enriched genes, only 11 genes were shared across batches 1 and 2 (Figure 4C), whereas in the INTACT-depleted DEGs, we identified seven genes shared between batches 2 and 3, and six genes were shared between batches 1 and 3 (Figure 4D). The INTACT-depleted genes comprised various small nucleolar RNA (snoRNAs) (Figure 4D). Interestingly, Snora20 was the only significantly depleted gene in INTACT compared to FANS in all batches.

Finally, using batch 1 DEGs, we performed GO term enrichment analysis to identify potentially altered mechanisms between INTACT and FANS samples (Supplementary Table S2). Interestingly, the GO term for biological processes in INTACT-depleted genes were enriched for "regulation of transcription—DNA templated" (p-value = 5.25×10^{-4}) and "mRNA processing" (p-value = 4.83×10^{-5}) (Figure 4D), whereas INTACT-enriched genes were enriched for "transport" (p-value = 3.60×10^{-7}) and "response to endoplasmic reticulum stress" (p-value = 5.59×10^{-12}) (Figure 4E).

Overall, we did not observe major differences between INTACT and FANS when we compared the three distinct batches. However, batch-specific analysis revealed numerous DEGs between INTACT and FANS, especially for the high RIN value batch, which were associated with "transcriptional regulation" in FANS and "regulation of protein-related mechanisms" in INTACT. When comparing the distinct batches together, several Snor genes were depleted in INTACT compared to FANS, which reflects the possible changes in nuclear membrane integrity as observed in our qualitative assessment section. Following these observations, we next investigated whether nuclei sorting by INTACT or FANS leads to significant differences in the nuclei's chromatin accessibility state.

2.6. ATAC-Seq Reveals Differences in Chromatin Accessibility State between FANS- and INTACT-Nuclei

Finally, to determine potentially significant differences in chromatin accessibility states between INTACT and FANS samples, we used an assay of transposable accessible chromatin coupled with high throughput sequencing (ATAC-seq) [37]. This technique allowed us to identify and compare the accessible chromatin region differences between these two techniques. We used three technical replicates from the same biological source to monitor the differences and similarities between the techniques. Following the initial analysis, we observed that all FANS and INTACT samples' alignment rates were comparable. FANS samples had an average of 127,531 peaks (SD ± 3458), while INTACT samples had an average of 112,211 peaks (SD ± 12,222) (Figure 5A). Using a read distribution plot, we observed that the peak heights (i.e., reads assigned to particular peaks) at promoter/transcription start sites (TSS) were reduced in INTACT samples compared to

FANS samples (Figure 5B). Similarly, peak distribution analysis showed a minor difference between FANS and INTACT, notably in peaks mapped to intergenic region and promoters of INTACT (33.76% and 21%, respectively) compared to FANS (30.17% and 22.23%, respectively) (Figure 5C,D). Additionally, we observed a large number of reads from INTACT samples mapped to the X-chromosome compared to FANS (Supplementary Materials Figure S8A,B). Next, we performed differential peak analysis between FANS and INTACT samples. Here, we found 24,315 differential accessible regions (DARs) out of which 2578 DARs were at promoter/TSS sites of INTACT samples compared to FANS (Figure 5E and Supplementary Table S3). Gene browser tracks were used to illustrate the peak annotation and DARs between FANS and INTACT of selected gene promoter regions (Figure 5F). Further, selected promoter DAR were assigned to the nearest genes, and Gene Ontology (GO) analysis was performed to decipher the difference in biological processes between the DARs of the two techniques. INTACT gained-accessibility genes did not have significant enriched GO terms. On the contrary, INTACT loss-accessibility gene GO terms revealed multiple enriched GO-terms for biological processes, such as "transport" (p-value = 4.68×10^{-5}) and "transcription—DNA templated" (p-value = 8.45×10^{-7}), compared to FANS. Lastly, we performed motif enrichment analysis on the promoter regions of INTACT-loss and gained DARs (compared to FANS) in order to identify potential transcription factor motifs associated with technique-specific chromatin accessibility changes. For this analysis, we considered only promoter-associated motifs; however, the complete list of enriched motifs is presented in Supplementary Materials Table S4. INTACT-gained accessibility revealed only the TATA-Box motif (p-value = 1×10^{-2}) (Supplementary Materials Figure S9A), whereas INTACT-reduced accessibility revealed six enriched motifs including: NRF (p-value = 1×10^{-10}), ETS (p-value = 1×10^{-9}), YY1 (p-value = 1×10^{-8}), SP1 (p-value = 1×10^{-7}), NFY (p-value = 1×10^{-5}), and GFY-staf (p-value = 1×10^{-2}) (Supplementary Materials Figure S9B and Table S4). These six motifs associated with INTACT-reduced accessibility (i.e., FANS-gained) have been previously labeled as "cardinal cis-regulatory motifs" suggested to be involved in regulation of chromatin structure by recruitment of secondary co-factors [38].

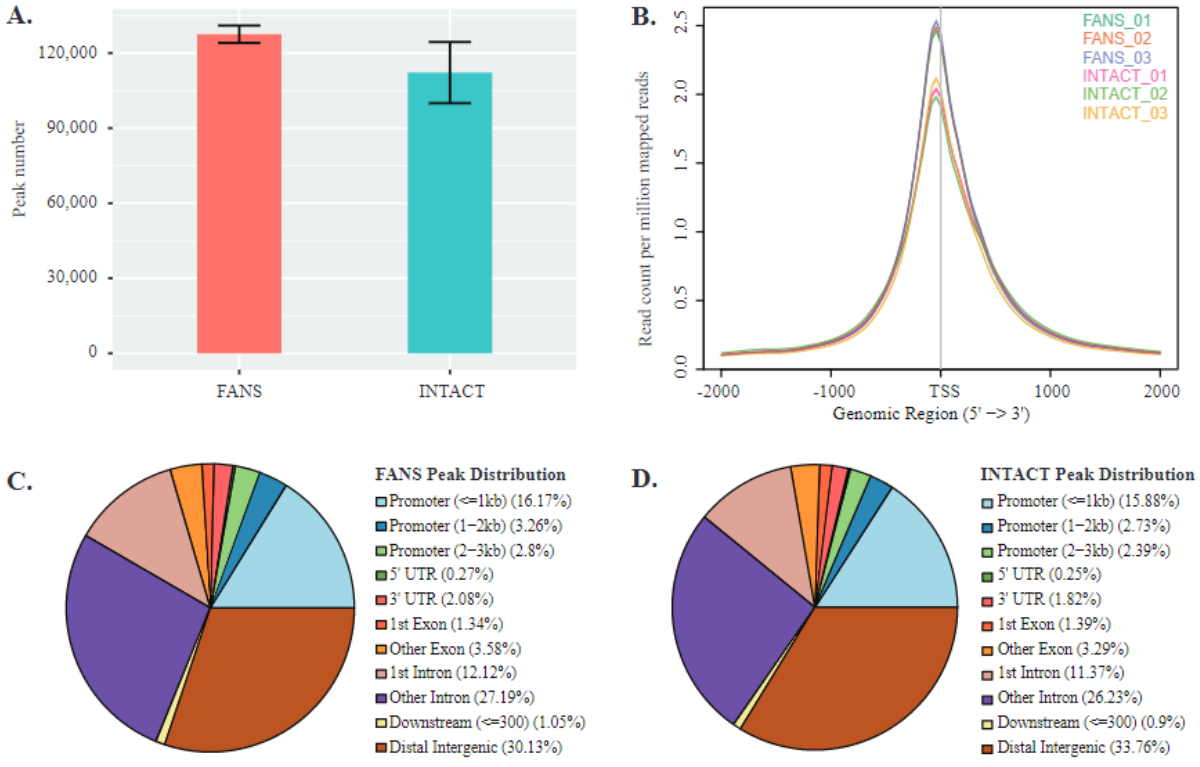

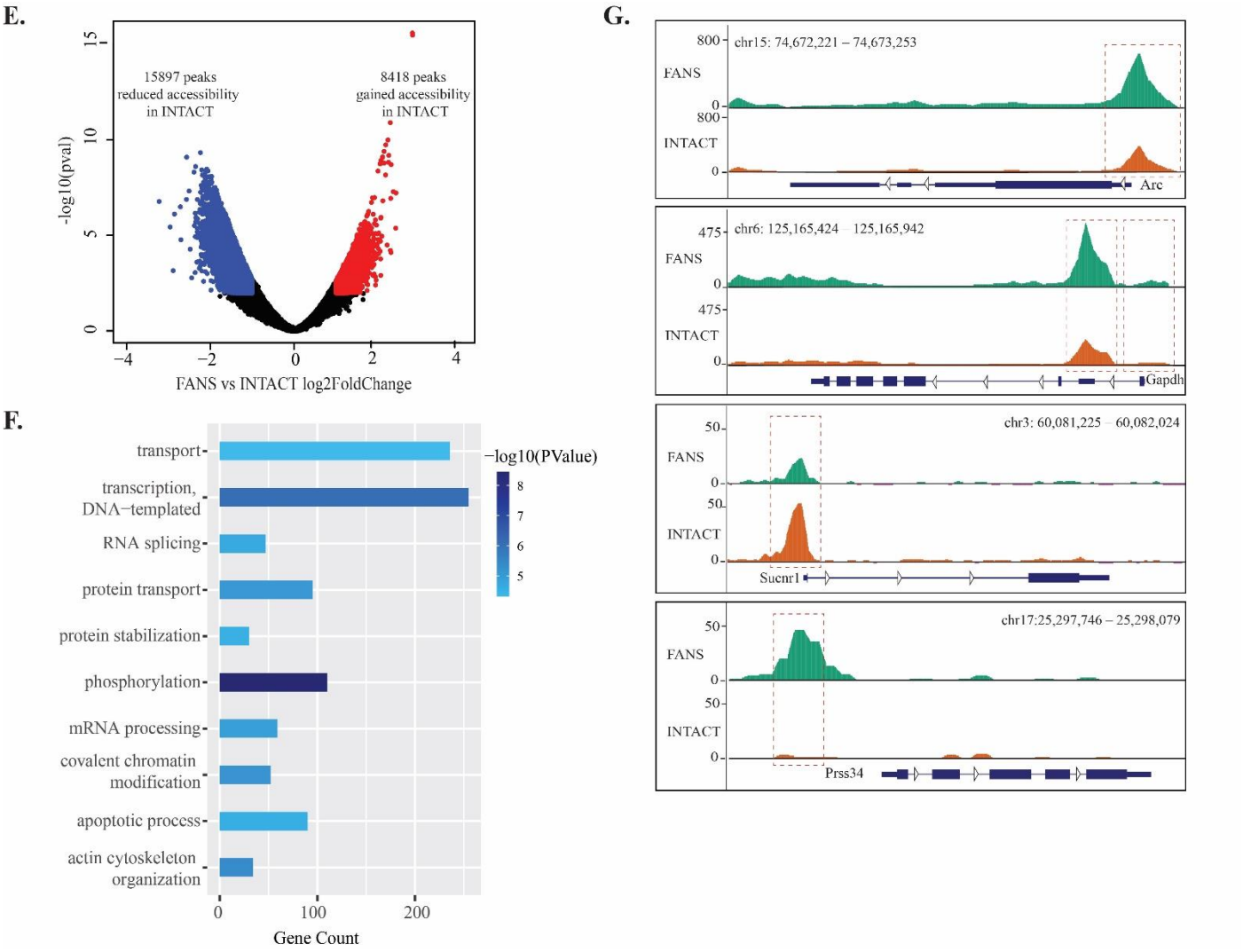

Figure 5. Chromatin accessibility comparison between FANS- and INTACT-nuclei: (**A**) average peak number in FANS and INTACT; (**B**) mapped reads coverage at transcriptional start site (TSS) in FANS and INTACT; (**C**,**D**) peak distribution across distinct genomic regions of FANS (**C**) and INTACT (**D**); (**E**) volcano-plot of differentially accessible regions (DARs) between INTACT and FANS; (**F**) GO term enrichment analysis for INTACT loss-accessibility genes compared to FANS; (**G**) genome browser tracks of selected genes Arc (IEGs), Gapdh (positive control), Sucnr1 (Gained accessibility in INTACT), and Prss34 (Gained accessibility in FANS).

Overall, these results suggest that increased promoter accessibility of genes associated with transcriptional regulation is associated with FANS samples compared to INTACT. These observations agree with the transcriptional changes observed in the nucRNA-seq. It supports the hypothesis that changes in the physical properties of the sorted nuclei could lead to downstream molecular alterations.

3. Discussion

Increasing amounts of studies seek to characterize distinct cellular and rare sub-cellular populations. With the increasing interest in cell-type-specific epigenetic studies, novel techniques have evolved to isolate cell-type-specific populations with a shift of focus towards using nuclei [1]. Of these techniques, FANS has commonly been used to isolate cell-type-specific nuclei. Other methods, based on magnetic-based isolation principles, such as INTACT, have also been increasingly used. Although these two techniques have been

interchangeably used, no study has performed an in-depth comparison of the two methods. This study provided a detailed qualitative and quantitative comparison between the two techniques, INTACT and FANS, using sfGFP+ nuclei.

Our results from the literature review indicate a gradual increase in the use of both techniques within the past four years. The trend shows an increased interest in cell-type-specific studies (Figure 1). Additionally, we observed a common use of the organism "M*us musculus*" and "brain-related" tissue in the cited publications. These observations are not surprising, as [10] investigated epigenetic changes occurring in mature neurons using transgenic mice. We noticed several studies used the term FACS while describing nuclei sorting (i.e., FANS) [39–43]. It is reasonable that FACS will remain as general term for flow cytometry sorting; however, it is important to emphasize the material sorted and use appropriate terminology when required (e.g., FANS for nuclei sorting). Additionally, nine out of the 58 analyzed studies used both INTACT and FANS within the same study. Based on our results, we identified both physiological and molecular differences between the two techniques. Therefore, we recommend using only one method in the same study to avoid specific biases attributed by each technique.

3.1. Physiological Differences between INTACT- and FANS-Nuclei

We observed that flow cytometry techniques (FACS/FANS) were the method of choice to isolate specific cells/nuclei. However, these techniques use high hydrodynamic pressure that could adversely affect the cells/nuclei [1,15,25]. Certain studies have reported adverse effects on cells' viability and structure while using flow cytometry techniques [8,13]. Therefore, alternative methods of sorting, such as affinity purification methods, have been presented, such as magnetic bead sorting of astroglia/microglia for cell sorting [9,11]. INTACT has been introduced to separate cell-type-specific nuclei using magnetic beads. Another advantage of INTACT is the ease with which the sorted bead-bound nuclei can be concentrated into smaller buffer volumes compared to FANS [10]. Therefore, in our study, INTACT- and FANS-nuclei were compared in terms of nuclei structure/integrity and optical density.

In our results, FANS-nuclei showed a significant increase in size compared to the INPUT nuclei, while INTACT-nuclei did not change significantly within 3 h of sorting. We hypothesize that the increase in FANS-nuclei size could be due to the high hydrodynamic pressure, shearing stress [8], or PBS-induced destabilization of membrane integrity during the sort [28,44]. Destabilized membrane integrity has been associated with flow cytometry as stated in previous studies [8,13]. We reason that the change in membrane integrity results in osmotic pressure alteration, which leads to an initial increase, followed by a size reduction after 4 h for FANS nuclei. Although Trypan staining did not reveal significant changes between Input-nuclei and FANS-nuclei within our recorded time, we speculate that differences might be observed if a longer incubation is performed. Accumulation of Trypan blue in nuclei has been associated with compromised membrane integrity [45–47], and the level of staining could indicate the extent of membrane permeability.

Though Trypan blue staining showed no significant changes under phase-contrast microscopy, when FANS-nuclei were compared to the sfGFP+ nuclei population of the INPUT nuclei under AF7000 fluorescence microscope, a substantial change in optical density was observed in the brightfield. This could be due to the differences in nuclei properties of different cell types. The fluorescence microscopy data also revealed that reversal in the size of FANS-nuclei already occurs prominently after 4 h of the sort. All these structural and optical changes could portray possible molecular changes occurring in the FANS-nuclei compared to INTACT-nuclei.

3.2. Molecular Differences between FANS- and INTACT-Nuclei

We assessed the transcriptional and chromatin accessibility signatures following the microscopy observations, comparing FANS- to INTACT- nuclei. In order to get the best coverage of the nuclei contents, we examined different library preparation strategies for nuclear transcriptome. Previous studies compared distinct library preparation on whole-cell RNA [48,49] and nuclei [50] using polyA and rRNA depletion-based (Ribo-depletion) strategies. PolyA-based methods were reported to have better read coverage over exonic regions, and higher uniquely mapped reads than ribo-depletion-based techniques [51]. However, it relies mostly on "high"-quality intact RNA, as fragmentation can lead to 3′ coverage bias [52], which is also observed in our study. On the other hand, ribo-depletion based strategies have a higher percentage of mapped reads to intergenic and intronic regions compared to polyA-based strategies; hence, it requires a greater sequencing depth. Additionally, ribo-depletion based methods can be more useful for samples subjected to sequence fragmentation (lower RIN samples) [51]. We emphasize that even though RIN values provide valuable information regarding the RNA fragmentation state and concentration amounts, such values are unreliable considering low-input RNA and, particularly, nuclear RNA [3]. Coupling such low-RIN samples with ribo-depletion RNA-based or total-RNA library preparation strategies offers a suitable combination for nuclear RNA analysis.

To further explore the transcriptional differences between the two techniques, we performed transcriptional comparison for the FANS and INTACT RNA samples. Initial sequencing statistics revealed minor differences between INTACT and FANS. Using PCA clustering analysis, we observed that samples were clustered based on technique, with higher RIN samples leading to better clustering. We did not observe major changes in DEGs between INTACT and FANS when comparing all of the batches together (distinct biological sources). However, when comparing batch-specific DEGs, we identified numerous DEGs between FANS and INTACT, particularly for the batch with the high-RIN values. We reason that as the RIN value increases, the complexity of the RNA population increases leading to an elevated amount of DEGs as observed in our results. These observations agree with previous studies that have reported an association between degraded samples (low RIN) and reduced library complexity [53,54]. Additionally, we observed in our DEGs a large number of small RNA populations, particularly small nucleolar RNAs (snoRNAs). SnoRNAs were reported to be enriched in nuclei compared to the cytoplasm, which might explain the appearance of such RNA populations [55,56]. Further investigations are required to identify the association of such small RNA population with nucRNA-seq.

Additionally, we performed ATAC-seq in order to identify chromatin accessibility changes between the two techniques. Initial sequencing statistics revealed minor differences between INTACT and FANS. We observed reduced read mapping at promoter regions of INTACT samples compared to FANS, despite using the same starting material. This phenomenon was observed repeatedly in replicate ATAC-seq experiments (data not shown). Interestingly, we identified six motifs (NRF, ETS, YY1, SP1, NFY, and GFY-staf) associated with INTACT-reduced accessibility (i.e., FANS-gained) compared to the broad TATA-box motif observed in the INTACT-gained accessibility promoters. These six motifs have been previously labeled as "cardinal cis-regulatory motifs" which frequently co-occur and are suggested to be involved in regulation of chromatin structure by recruitment of secondary co-factors [38]. These results supplement our observations of depleted DEGs and reduced accessibility of GO term enrichment of INTACT compared to FANS that included "transcription, DNA-templated", "RNA splicing", and "mRNA processing". These observations suggest that FANS samples contained an increase of transcriptional regulation associated genes compared to INTACT. We postulate that the physiological changes observed in FANS samples were sufficient to influence or reflect the respective molecular changes observed on transcriptome and chromatin accessibility states of the nuclei. It was

previously reported that several forms of stress on the nuclear membrane, including mechanical force, could lead to chromatin alteration, which ultimately alters transcriptional activity [57–59]. Our results support these remarks, suggesting that nuclei sorting using the two different techniques could lead to different molecular signatures of the same biological materials.

Under our experimental setup, we observed differences between INTACT- and FANS-nuclei both on the physiological and the molecular levels. Both techniques have individual merits and demerits, as summarized in Table 2. We suggest that the choice of either INTACT or FANS for a particular study should be made based on the cell type investigated, starting tissue material, and subsequent molecular analyses. This is inherently supported by the molecular changes observed in our study. We strongly recommend selecting only one method to perform all the subsequent molecular analyses to prevent specific biases and inconsistencies between the different datasets. Overall, in terms of processing speed and costs for multiple samples, INTACT has an advantage over FANS. However, for INTACT protocol to be applied efficiently, the same amounts of starting material must be used. For smaller or higher amounts, the protocol has to be adjusted. Regardless of the starting concentration of nuclei, the FANS protocol need not be changed. In this aspect, FANS is advantageous over INTACT. The presented advantages and disadvantages of the compared techniques can help researchers to select the most suitable methodology for their individual experimental design.

Table 2. Qualitative and quantitative differences between INTACT and FANS.

Parameter Compared	INTACT	FANS
Experimental approach	➢ Affinity purification-based approach of nuclei isolation	➢ Flow cytometry-based approach of nuclei isolation
Processing speed	➢ Relatively high processing speed. ➢ Processing of multiple samples ➢ Reduced experimental waiting time for multiple samples	➢ Relatively low processing speed. ➢ One sample collection at a time ➢ Increased experimental waiting time (if many samples considered)
Quantification accuracy	➢ Decreased accuracy compared to FANS ➢ Quantification based on manual hemocytometer counting	➢ Higher accuracy compared to INTACT
Tissue/cellular amounts requirement	➢ Protocol needs to be modified for different tissue amounts	➢ Protocol remains the same for any type of tissue amount (from low to high)
Effect on nuclear structure	➢ Physiological changes of isolated nuclei undetectable under the experimental setup	➢ Physiological changes detectable under the experimental set-up
Transcriptional alterations	➢ Minor inter-variability between samples ➢ Enriched genes associated with "transport" and "response to ER stress"	➢ Considerable inter-variability between samples ➢ Enriched genes associated with "regulation of transcription and "mRNA processing"
Chromatin accessibility alteration	➢ Accessibility peaks associated with intergenic compared to FANS ➢ Reduced accessibility in promoters of gene associated with "transcription- DNA template", "mRNA-processing" and cellular response to DNA damage stimulus"	➢ Accessibility peaks associated with promoters compared to INTACT ➢ No significant reduced accessibility GO terms compared to INTACT
Cost	➢ Cost-effective	➢ Expensive equipment required

4. Materials and Methods

4.1. Literature Review of INTACT FANS/FACS studies

The literature review was divided into four sections: identification, screening, eligibility, and analysis. Initially, in the identification stage, 335 citations of Mo et al.'s [10] were manually retrieved from the Google Scholar database. Following an initial assortment,

25 publications were removed due to the fact of repetition in the database, duplication in two different journals (peer-reviewed and non-peer-reviewed), or not eligible due to the language of publication (i.e., non-English). In the screening stage, we used an advanced search tool to find articles that included the terms "FANS", "INTACT" or "FACS" on the remaining 310 articles. The articles were then classified further into "relevant" (79) (containing the searched terms) and "non-relevant" articles that consisted of "references" (156) and "reviews papers" (75) (Supplementary Materials Figure S1A). The "relevant" publications used one/both of the techniques investigated, while "references" and "reviews" only cited Mo et al. [10] without using any of the techniques investigated in this study. The 79 "relevant" articles included 40 FACS, 12 FANS, 18 INTACT, and nine both (i.e., INTACT and flow-cytometry methods). We noticed that several studies used the term FACS while describing nuclei sorting. Therefore, we included them in the final summary as FANS (19/40 articles). To obtain a concise comparison of nuclei sorting techniques, we decided to exclude FACS-related articles (21/40 articles) that were sorting cells. Finally, 58 publications were considered for in-depth review and summary (Supplementary Materials Table S1). The data were categorized into a table containing the following information: type of technique used, tissue, cell type, organism, sample size, subsequent analyses, and use of transgenic animals (Supplementary Materials Table S1).

4.2. Animals and Ethics Statement

Thirteen to sixteen week old male and female $Arc^{creERT2(TG/WT)}.R26^{CAG\text{-}Sun1\text{-}sfGFP\text{-}Myc(M/WT\ or\ M/M)}$ were used for this study [10,29]. Habituation in the experimental environment lasted for a week before performing tamoxifen (TAM) injections. All behavioral experiments were performed in accordance with the institutional animal welfare guidelines approved by the ethical committee of the state government of Rhineland-Palatinate, Germany, approved on 2 March 2017 (G-17-1-021)

4.3. Tamoxifen Injection and Behavioral Experiments

Tamoxifen (Sigma–Aldrich, *St. Louis, MI, USA,* T5648-1G) was dissolved in a corn oil:ethanol mixture (9:1) ratio at 42 °C with constant shaking at 500 rpm in light protected Eppendorf tubes (Amber). Animals were injected with tamoxifen at a dosage of 150 mg/kg 5 h before social interaction experiments to activate nuclei sfGFP expression under the control of the Arc promoter. Social interaction (SI) experiments were performed as described in [30]. Test mice were allowed to explore an open field box (40 cm wide × 40 cm depth × 40 cm length) that had an empty cylindrical cage at one side for 150 S in the habituation phase. Then, CD1 mouse was placed in the cylindrical cage and the test mouse was allowed to explore again in the test phase for another 150 S. Mice were sacrificed on the 3rd day following tamoxifen injections and SI to allow for optimal sfGFP expression on the nuclear membrane.

4.4. Nuclei Isolation from Different Brain Regions

Following behavioral experiments, the brain regions—neocortex, pre-frontal cortex, hippocampus, hypothalamus, pituitary, and nucleus accumbens—were dissected according to region specifications in the Allen Brain Atlas for mouse. Nuclei were isolated using the iodixanol-based gradient ultracentrifugation protocol for isolation of micro-dissected brain regions as described in Chongtham et al. [28]. The duration for high-speed ultracentrifugation (7820 rpm) for the neocortex was 12 min, while for the other brain regions, it was kept at 18 min. After the ultracentrifugation process, nuclei were collected from the 30–40% iodixanol layer interface.

4.5. sfGFP Positive Nuclei Separation

4.5.1. INTACT

For sfGFP+ nuclei separation, Dynabeads (Life Technologies, Carlsbad, CA, USA, 10003D) were incubated with anti-GFP antibody (Life Technologies, Carlsbad, CA, USA, G10362) at 4 °C at a ratio of 50:20 (beads: anti-GFP) for downstream molecular biology experiments and at a ratio of 50:10 (beads: anti-GFP) for microscopy in order to decrease the number of beads bound to nuclei. The reduction of beads bound to a nucleus increases the visibility of bead-bound nuclei, which is important for microscopy analyses. The bead-antibody incubation was carried out in a cold room using an end-to-end rotator for 20 min to facilitate bead-antibody interaction in the solution.

In the meantime, wash buffer (0.4% Igepal in homogenization buffer, [28]) was added to the nuclei solution, collected from the 30–40% iodixanol gradient layer (2:1). This was necessary to reduce the solution's viscosity and remove the outer nuclear membrane before affinity purification (as mentioned in [60]) to facilitate anti-GFP binding to sun1sfGFP in the peri-nuclear membrane. The wash buffer-diluted nuclei solution was incubated with anti-GFP bead solution in the ratio of 40:1. Samples were then placed in an end-to end rotator in a cold room for 20 min. After the incubation period, samples were placed on a magnetic rack for 1 min, and the supernatant was removed, retaining the bead-bound sfGFP nuclei clusters. These clusters were washed ones with 500 μL wash buffer and twice with 250 μL wash buffer and subsequently collected in 100 μL wash buffer. For hemocytometer counting, proper dilutions were made so that not more than 200 bead-bound nuclei were present per large square.

Following hemocytometer count, volumes that contained approximately 5000 nuclei for ATAC treatment and 10,000 nuclei for RNA extraction were calculated using a unitary method and collected accordingly.

4.5.2. FANS

For FANS, the nuclei collected from the 30–40% iodixanol layer were diluted with wash buffer in the ratio 2:1 (similar to INTACT), as in Chongtham et al. [28] and Fernandez-Albert et al. [61], to reduce viscosity during sorting. Flow cytometry analysis and FANS were performed using a BD FACSAria III SORP (Becton Dickinson, Franklin Lakes, NJ, USA) equipped with four lasers (405 nm, 488 nm, 561 nm, and 640 nm) and a 70 μm nozzle. GFP expression was detected using the blue laser and a 530/30 BP filter, whereas DAPI was detected using the violet laser and a 450/50 BP filter. Prior sort, 10,000 total events were recorded, and a gating strategy was applied: first, nuclei were gated according to their forward- and side-scatter properties (FSC-A/SSC-A), followed by doublet exclusion using SSC-A and SSC-W. Nuclei were then gated according to their DAPI expression. GFP expression was used as a sorting gate. Sorted nuclei were collected in 1.5 mL Eppendorf tubes, containing the optimal buffers for downstream analyses. The flow cytometry analyses were performed using the BD FACSDiva 8.0.2 Software or FlowJo (v10.6 or higher).

4.5.3. Purity Analysis of INTACT- and FANS-Nuclei

For purity analysis of INTACT-nuclei, the solution was diluted with wash buffer in a ratio of 4:1 before flow cytometry to reduce the density of bead-bound nuclei. For FANS-nuclei, the sorted sfGFP+ nuclei were collected in wash buffer to keep the experimental conditions similar to that of INTACT. The nuclei purity analysis was performed using BD FACS Aria III (Becton Dickinson, Franklin Lakes, NJ, USA). Data were analyzed with FlowJo (v.10.6 or higher, Tree Star, Ashland, OR, USA) from at least 50 single DAPI-positive nuclei.

4.6. Parallel Processing of INTACT- and FANS-Nuclei

For comparing the processing speed, different brain regions (nucleus accumbens, hypothalamus, pituitary, prefrontal cortex, neocortex; see Table 1) with varied combinations of different sfGFP+ percentages sfGFP+ nuclei yield per volume were used. For FANS, duration of sorting to obtain 5k sfGFP+ nuclei were determined for each sample type. INTACT was performed as usual for all sample types. Bead-bound nuclei were then counted using a hemocytometer and the volume that contained 5k bead-bound nuclei was calculated. The duration for sorting 50 k nuclei using both techniques was then calculated using unitary method. For INTACT, the efficiency of sorting (yield) was calculated indirectly by using the percentage of sfGFP+ nuclei that remained in the INTACT supernatant compared to the percentage of sfGFP+ nuclei in the original solution.

4.7. Microscopy

For phase-contrast microscopy, 10 µL of the nuclei:Trypan mixed in a 1:1 ratio was loaded into the hemocytometer. Light intensity was kept the same for all groups. Images were obtained using Leica DM-IL inverted microscope with 40x/0.5, air objective. For fluorescence microscopy, images were obtained using a Leica AF7000 widefield microscope equipped with a Hamamatsu-Flash4-USB3-101292 camera, an LED lamp (Sola Light Engine, SE 5-LCR-VB, Lumencor, Beaverton, OR, USA) and LAS X software (Institute for Molecular Biology, Mainz, Germany). Images were acquired with a HC PL FLUOTAR L 20/0.40 or a 40/1.1 objective lens using the same settings for each image. Images visualizing GFP fluorescence were acquired using an L5 filter (BP 480/40, FT505, BP 527/30), and DAPI was imaged using an A4 filter (BP 360/40, FT400, BP 470/40). Images were analyzed using FIJI (v 1.51 h) as in Chongtham et al. [28]. Manual analysis was performed by drawing an ellipse in the area of the image encompassing the nucleus under observation while automatic analysis was performed using a macroscript [28]. Statistical analyses were performed using Student's unpaired *t*-test (assumption: equal SD between populations) in GraphPad Prism (8.4.2).

4.8. RNA Isolation and nucRNA-Seq Library Preparation

Ten thousand INTACT- or FANS-nuclei were collected in 100 µL of RLT buffer followed by flash freezing. RNA was purified using the RNeasy Micro kit (Qiagen 74004, Hilden, Germany) following the manufacturer's instructions. For the RNA-seq library comparison, we used two different protocols: a ribo-depletion based method, using the Ovation® SoLo RNA-Seq System (NuGEN M01406v2, Redwood City, CA, USA) and a polyA enrichment-based protocol, using SMART-Seq® v4 Ultra® Low Input RNA Kit for Sequencing (Clontech 634894, Mountain View, CA, USA).

NuGEN's Ovation SoLo protocol: NGS library preparation was performed following NuGEN's standard protocol (M01406v2). Libraries were prepared with a starting amount of 1.5 ng and amplified in 14 PCR cycles. *Clontech's SmartSeq protocol*: Clontech's SMART-Seq v4 Ultra Low Input RNA Kit (112219) was used for cDNA generation from 1.5 ng of total RNA, following the manufacturer's recommendations. cDNA was amplified in 11 cycles of LD-PCR. The resulting cDNA were sheared using an S2 focused ultrasonicator (Covaris, Woburn, MA, USA) with the following parameters: 20% duty cycle; 0.5 intensity; 50 cycles/burst; 20 °C; 60 s. The NGS library preparation was performed with 3.16 ng of sheared cDNA with NuGEN's Ovation Ultralow System V2 M01379 v5. Libraries were amplified in 11 PCR cycles.

Both NuGEN and Clontech libraries were profiled in a High Sensitivity DNA Chip on a 2100 Bioanalyzer (Agilent technologies, Santa Clara, CA, USA) and quantified using the Qubit dsDNA HS Assay Kit, in a Qubit 2.0 Fluorometer (Life technologies, Carlsbad, CA, USA). All eight samples (4 NuGEN and 4 Clontech) were pooled together in equimolar ratio and sequenced on 1 NextSeq 500 Midoutput Flowcell, PE for 2 × 72 cycles plus 16 cycles for

the index read and five dark cycles upfront. These dark cycles were included to avoid having unbalanced first bases of Read 1, introduced in the reverse transcription step of the NuGEN's Ovation SoLo protocol. Consequently, there was no need to trim the reads for data analysis. For INTACT and FANS nuclear RNA-seq comparison, libraries were prepared using NuGen Ovation SoLo RNA-Seq System following NuGen's standard protocol. Libraries were prepared with a starting amount of 1.23 ng and amplified in 13 PCR cycles. All samples (INTACT and FANS) were pooled in equimolar ratio and sequenced on 1 NextSeq 500 Highoutput Flowcell, SR for 1 × 70 cycles plus 16 cycles for the index read and five dark cycles upfront. All RNA-seq library preparations and sequencing were performed by the Genomic Core Facility from the Institute of Molecular Biology (IMB, Mainz, Germany).

4.9. RNA-Seq Data Analysis

FANS and INTACT Nugen Ovation RNA Solo library single end sequenced data quality assessment was performed using FASTQC (v. 0.11.8). Read alignment was done using STAR aligner (v2.7.1a) [62] to the *Mus musculus* genome (mm10) UCSC annotations with default parameter. Further, duplicates were removed using UMI (Unique Molecular Identifier) introduced by Nugen Ovation RNA Solo library. Uniquely mapped reads were retained in the output BAM file. Samtools(v1.7) [63] was used to sort and index mapped files. Read count per gene was calculated using HTSeq (v0.11.1) [64]. Normalization and differential expression analysis were conducted using the DESeq [63] Bioconductor package with an FDR rate of 0.05. The DAVID database was used for gene ontology analysis.

4.10. ATAC-Seq Library Preparation

The ATAC-seq was performed in three technical replicates per technique as previously described [37]. Briefly, 50,000 INTACT or FANS nuclei were collected in 50 µL cold lysis buffer (10 mM Tris-HCl, pH 7.4, 10 mM NaCl, 3 mM $MgCl_2$ and 0.1% IGEPAL CA-630) and centrifuged at 750× *g* for 15 min using a cold centrifuge (4 °C). Immediately after centrifugation, the pellet was resuspended in the transposase reaction mix (25 µL 2× TD buffer, 2.5 µL transposase (Illumina FC-121–1030, San Diego, CA, USA) and 22.5 µL nuclease-free water). The transposition reaction was carried out for 30 min at 37 °C. Following transposition, the sample was purified using a Qiagen MinElute kit (Qiagen, 28006, Hilden, Germany) following the manufacturer's instructions. After purification, the library was amplified using 1× NEBnext PCR master mix (NEB M0541, Ipswich, MA, USA) and 1.25 µM of custom Nextera PCR primers 1 and 2 (See [37]). An optimization qPCR quantification was performed as described in Buenrostro et al. [37]. The following PCR conditions were used: 72 °C for 5 min; 98 °C for 30 s; thermocycling at 98 °C for 10 s, 63 °C for 30 s, and 72 °C for 1 min. After 11–12 cycles of PCR amplification, samples were further purified using Qiagen MinElute kit. To remove primer dimers, samples were further purified using AMPure beads XP (Beckman Coulter, Brea, CA, USA) with a ratio of ×0.9 of beads to samples. The purified samples were then analyzed in bioanalyzer (Agilent) and sequenced on NextSeq 500 Highoutput Flowcell (150-cycles PE for 2 × 75bp). Sequencing was performed by the Genomic Core Facility from the Institute of Molecular Biology (IMB, Mainz, Germany).

4.11. ATAC-Seq Data Analysis

The ATAC-seq data quality check was performed using FASTQC (v. 0.11.8). Further, adaptors were removed using Trimmomatic (v0.39) [65]. Paired-end ATAC-seq reads were mapped to *Mus musculus* genome (mm10) UCSC annotations using Bowtie2 (v2.3.5.1) with default parameters. Properly paired end reads with high mapping quality (MAPQ ≥ 10)

were retained in analysis with the help of Samtools (v1.7). Next, using Picard tools MarkDuplicates utility, duplicates were removed. ATAC-seq peaks were called using MACS2 (v2.1.1.20160309) [66] and visualized with UCSC genome browser. Peaks that were reproducible in all samples were considered for differential accessible region analysis. Differential accessible region analysis was performed using DESeq (*p*-value cutoff of 0.05). Further, peaks were annotated using the annotatePeaks.pl utility of HOMER. For motif enrichment analysis findMotifGenome.pl utility (HOMER) was used.

Supplementary Materials: The following are available online at www.mdpi.com/xxx/s1.

Author Contributions: M.C.C. and T.B. planned and performed experiments, analyzed the data, prepared figures, and wrote the manuscript. K.M. analyzed the data, prepared figures, and wrote the manuscript. S.G. and J.W. supervised the project and edited the manuscript. All authors have read and agreed to the published version of the manuscript.

Funding: This work was funded by the Deutsche Forschungsgemeinschaft (grant number CRC1193).

Institutional Review Board Statement: The study was conducted according to the guidelines of the Declaration of Helsinki and approved by the local ethical committee (Landesuntersuchungsamt Rheinland-Pfalz G 17-1-021).

Informed Consent Statement: Not applicable.

Data Availability Statement: The accession numbers reported in this paper are RNA-seq and ATAC-seq (GSE165644). The UCSC browser session link of ATAC data is http://genome.ucsc.edu/s/kanak/INTACTvsFANS_ATACseq. Flow cytometry data were deposited in the FlowRepository (Repository ID: FR-FCM-Z3FX; URL: http://flowrepository.org/id/RvFr7OlCuBDNO3jJvcCSmzBtpm8kB4awZ171aa6EYpEWhRexLS53Huns0tPx3RDR.

Acknowledgments: We would like to thank the Institute of the Molecular Biology (Mainz) and particularly the microscopy, flow cytometry, and genomics core facilities for their assistance and support throughout the study. The use of GCF's NextSeq500 (INST 247/870-1 FUGG) is gratefully acknowledged. We also extend our sincere thanks to the Mouse Behavioral Unit of the Leibniz Institute of Resilience Research. We are grateful to the CRC1193 (DFG) for funding our work.

Conflicts of Interest: The authors declare no conflicts of interest.

References

1. Handley, A.; Schauer, T.; Ladurner, A.G.; Margulies, C.E. Designing Cell-Type-Specific Genome-wide Experiments. *Mol. Cell* **2015**, *58*, 621–631, doi:10.1016/j.molcel.2015.04.024.
2. Stuart, T.; Satija, R. Integrative single-cell analysis. *Nat. Rev. Genet.* **2019**, *20*, 257–272, doi:10.1038/s41576-019-0093-7.
3. Krishnaswami, S.R.; Grindberg, R.V.; Novotny, M.; Venepally, P.; Lacar, B.; Bhutani, K.; Linker, S.B.; Pham, S.; Erwin, J.A.; Miller, J.A.; et al. Using single nuclei for RNA-seq to capture the transcriptome of postmortem neurons. *Nat. Protoc.* **2016**, *11*, 499–524, doi:10.1038/nprot.2016.015.
4. Vembadi, A.; Menachery, A.; Qasaimeh, M.A. Cell Cytometry: Review and Perspective on Biotechnological Advances. *Front Bioeng. Biotechnol.* **2019**, *7*, 147, doi:10.3389/fbioe.2019.00147.
5. Julius, M.H.; Masuda, T.; Herzenberg, L.A. Demonstration that antigen-binding cells are precursors of antibody-producing cells after purification with a fluorescence-activated cell sorter. *Proc. Natl. Acad. Sci. USA* **1972**, *69*, 1934–1938, doi:10.1073/pnas.69.7.1934.
6. Haenni, S.; Ji, Z.; Hoque, M.; Rust, N.; Sharpe, H.; Eberhard, R.; Browne, C.; Hengartner, M.O.; Mellor, J.; Tian, B.; et al. Analysis of C. elegans intestinal gene expression and polyadenylation by fluorescence-activated nuclei sorting and 3′-end-seq. *Nucleic Acids Res.* **2012**, *40*, 6304–6318, doi:10.1093/nar/gks282.
7. Dammer, E.B.; Duong, D.M.; Diner, I.; Gearing, M.; Feng, Y.; Lah, J.J.; Levey, A.I.; Seyfried, N.T. Neuron enriched nuclear proteome isolated from human brain. *J. Proteome Res.* **2013**, *12*, 3193–3206, doi:10.1021/pr400246t.
8. Mo, A.; Mukamel, E.A.; Davis, F.P.; Luo, C.; Henry, G.L.; Picard, S.; Urich, M.A.; Nery, J.R.; Sejnowski, T.J.; Lister, R.; et al. Epigenomic Signatures of Neuronal Diversity in the Mammalian Brain. *Neuron* **2015**, *86*, 1369–1384, doi:10.1016/j.neuron.2015.05.018.

9. Bohlen, C.J.; Bennett, F.C.; Bennett, M.L. Isolation and Culture of Microglia. *Curr. Protoc. Immunol.* **2019**, *125*, e70, doi:10.1002/cpim.70.
10. Box, A.; DeLay, M.; Tighe, S.; Chittur, S.V.; Bergeron, A.; Cochran, M.; Lopez, P.; Meyer, E.M.; Saluk, A.; Thornton, S.; et al. Evaluating the Effects of Cell Sorting on Gene Expression. *J. Biomol. Tech.* **2020**, *31*, 100–111, doi:10.7171/jbt.20-3103-004.
11. Holt, L.M.; Olsen, M.L. Novel Applications of Magnetic Cell Sorting to Analyze Cell-Type Specific Gene and Protein Expression in the Central Nervous System. *PLoS ONE* **2016**, *11*, e0150290, doi:10.1371/journal.pone.0150290.
12. Llufrio, E.M.; Wang, L.; Naser, F.J.; Patti, G.J. Sorting cells alters their redox state and cellular metabolome. *Redox Biol.* **2018**, *16*, 381–387, doi:10.1016/j.redox.2018.03.004.
13. Binek, A.; Rojo, D.; Godzien, J.; Ruperez, F.J.; Nunez, V.; Jorge, I.; Ricote, M.; Vazquez, J.; Barbas, C. Flow Cytometry Has a Significant Impact on the Cellular Metabolome. *J. Proteome Res.* **2019**, *18*, 169–181, doi:10.1021/acs.jproteome.8b00472.
14. Andra, I.; Ulrich, H.; Durr, S.; Soll, D.; Henkel, L.; Angerpointner, C.; Ritter, J.; Przibilla, S.; Stadler, H.; Effenberger, M.; et al. An Evaluation of T-Cell Functionality After Flow Cytometry Sorting Revealed p38 MAPK Activation. *Cytom. A* **2020**, *97*, 171–183, doi:10.1002/cyto.a.23964.
15. Deal, R.B.; Henikoff, S. A simple method for gene expression and chromatin profiling of individual cell types within a tissue. *Dev. Cell* **2010**, *18*, 1030–1040, doi:10.1016/j.devcel.2010.05.013.
16. Henry, G.L.; Davis, F.P.; Picard, S.; Eddy, S.R. Cell type-specific genomics of Drosophila neurons. *Nucleic Acids Res.* **2012**, *40*, 9691–9704, doi:10.1093/nar/gks671.
17. Steiner, F.A.; Talbert, P.B.; Kasinathan, S.; Deal, R.B.; Henikoff, S. Cell-type-specific nuclei purification from whole animals for genome-wide expression and chromatin profiling. *Genome Res.* **2012**, *22*, 766–777, doi:10.1101/gr.131748.111.
18. Stroud, H.; Su, S.C.; Hrvatin, S.; Greben, A.W.; Renthal, W.; Boxer, L.D.; Nagy, M.A.; Hochbaum, D.R.; Kinde, B.; Gabel, H.W.; et al. Early-Life Gene Expression in Neurons Modulates Lasting Epigenetic States. *Cell* **2017**, *171*, 1151–1164 e1116, doi:10.1016/j.cell.2017.09.047.
19. Hrvatin, S.; Tzeng, C.P.; Nagy, M.A.; Stroud, H.; Koutsioumpa, C.; Wilcox, O.F.; Assad, E.G.; Green, J.; Harvey, C.D.; Griffith, E.C.; et al. A scalable platform for the development of cell-type-specific viral drivers. *Elife* **2019**, *8*, doi:10.7554/eLife.48089.
20. Mo, A.; Luo, C.; Davis, F.P.; Mukamel, E.A.; Henry, G.L.; Nery, J.R.; Urich, M.A.; Picard, S.; Lister, R.; Eddy, S.R.; et al. Epigenomic landscapes of retinal rods and cones. *Elife* **2016**, *5*, e11613, doi:10.7554/eLife.11613.
21. Kuboyama, T.; Wahane, S.; Huang, Y.; Zhou, X.; Wong, J.K.; Koemeter-Cox, A.; Martini, M.; Friedel, R.H.; Zou, H. HDAC3 inhibition ameliorates spinal cord injury by immunomodulation. *Sci. Rep.* **2017**, *7*, 8641, doi:10.1038/s41598-017-08535-4.
22. Sharma, N.; Pollina, E.A.; Nagy, M.A.; Yap, E.L.; Di Biase, F.A.; Hrvatin, S.; Hu, L.; Lin, C.; Greenberg, M.E. ARNT2 Tunes Activity-Dependent Gene Expression through NCoR2-Mediated Repression and NPAS4-Mediated Activation. *Neuron* **2019**, *102*, 390–406 e399, doi:10.1016/j.neuron.2019.02.007.
23. Monroe, T.O.; Hill, M.C.; Morikawa, Y.; Leach, J.P.; Heallen, T.; Cao, S.; Krijger, P.H.L.; de Laat, W.; Wehrens, X.H.T.; Rodney, G.G.; et al. YAP Partially Reprograms Chromatin Accessibility to Directly Induce Adult Cardiogenesis In Vivo. *Dev. Cell* **2019**, *48*, 765–779 e767, doi:10.1016/j.devcel.2019.01.017.
24. Zhang, M.; Hill, M.C.; Kadow, Z.A.; Suh, J.H.; Tucker, N.R.; Hall, A.W.; Tran, T.T.; Swinton, P.S.; Leach, J.P.; Margulies, K.B.; et al. Long-range Pitx2c enhancer-promoter interactions prevent predisposition to atrial fibrillation. *Proc. Natl. Acad. Sci. USA* **2019**, *116*, 22692–22698, doi:10.1073/pnas.1907418116.
25. Bhattacharyya, S.; Sathe, A.A.; Bhakta, M.; Xing, C.; Munshi, N.V. PAN-INTACT enables direct isolation of lineage-specific nuclei from fibrous tissues. *PLoS ONE* **2019**, *14*, e0214677, doi:10.1371/journal.pone.0214677.
26. Wang, A.W.; Wang, Y.J.; Zahm, A.M.; Morgan, A.R.; Wangensteen, K.J.; Kaestner, K.H. The Dynamic Chromatin Architecture of the Regenerating Liver. *Cell Mol. Gastroenterol. Hepatol.* **2020**, *9*, 121–143, doi:10.1016/j.jcmgh.2019.09.006.
27. Wang, A.W.; Wangensteen, K.J.; Wang, Y.J.; Zahm, A.M.; Moss, N.G.; Erez, N.; Kaestner, K.H. TRAP-seq identifies cystine/glutamate antiporter as a driver of recovery from liver injury. *J. Clin. Investig.* **2018**, *128*, 2297–2309, doi:10.1172/JCI95120.
28. Chongtham, M.C.; Todorov, H.; Wettschereck, J.E.; Gerber, S.; Winter, J. Isolation of nuclei and downstream processing of cell-type-specific nuclei from micro-dissected mouse brain regions–techniques and caveats. *bioRxiv.* **2020**, doi:10.1101/2020.11.18.374223.
29. Denny, C.A.; Kheirbek, M.A.; Alba, E.L.; Tanaka, K.F.; Brachman, R.A.; Laughman, K.B.; Tomm, N.K.; Turi, G.F.; Losonczy, A.; Hen, R. Hippocampal memory traces are differentially modulated by experience, time, and adult neurogenesis. *Neuron* **2014**, *83*, 189–201, doi:10.1016/j.neuron.2014.05.018.

30. Krishnan, V.; Han, M.H.; Graham, D.L.; Berton, O.; Renthal, W.; Russo, S.J.; Laplant, Q.; Graham, A.; Lutter, M.; Lagace, D.C.; et al. Molecular adaptations underlying susceptibility and resistance to social defeat in brain reward regions. *Cell* **2007**, *131*, 391–404, doi:10.1016/j.cell.2007.09.018.
31. Young, I.T.; Verbeek, P.W.; Mayall, B.H. Characterization of chromatin distribution in cell nuclei. *Cytometry* **1986**, *7*, 467–474, doi:10.1002/cyto.990070513.
32. Dahl, K.N.; Ribeiro, A.J.; Lammerding, J. Nuclear shape, mechanics, and mechanotransduction. *Circ. Res.* **2008**, *102*, 1307–1318, doi:10.1161/CIRCRESAHA.108.173989.
33. Webster, M.; Witkin, K.L.; Cohen-Fix, O. Sizing up the nucleus: Nuclear shape, size and nuclear-envelope assembly. *J. Cell Sci.* **2009**, *122*, 1477–1486, doi:10.1242/jcs.037333.
34. Schreiner, S.M.; Koo, P.K.; Zhao, Y.; Mochrie, S.G.; King, M.C. The tethering of chromatin to the nuclear envelope supports nuclear mechanics. *Nat. Commun.* **2015**, *6*, 7159, doi:10.1038/ncomms8159.
35. Stephens, A.D.; Banigan, E.J.; Adam, S.A.; Goldman, R.D.; Marko, J.F. Chromatin and lamin A determine two different mechanical response regimes of the cell nucleus. *Mol. Biol. Cell* **2017**, *28*, 1984–1996, doi:10.1091/mbc.E16-09-0653.
36. Todorov, H.; Searle-White, E.; Gerber, S. Applying univariate vs. multivariate statistics to investigate therapeutic efficacy in (pre)clinical trials: A Monte Carlo simulation study on the example of a controlled preclinical neurotrauma trial. *PLoS ONE* **2020**, *15*, e0230798, doi:10.1371/journal.pone.0230798.
37. Buenrostro, J.D.; Giresi, P.G.; Zaba, L.C.; Chang, H.Y.; Greenleaf, W.J. Transposition of native chromatin for fast and sensitive epigenomic profiling of open chromatin, DNA-binding proteins and nucleosome position. *Nat. Methods* **2013**, *10*, 1213–1218, doi:10.1038/nmeth.2688.
38. Benner, C.; Konovalov, S.; Mackintosh, C.; Hutt, K.R.; Stunnenberg, R.; Garcia-Bassets, I. Decoding a Signature-Based Model of Transcription Cofactor Recruitment Dictated by Cardinal Cis-Regulatory Elements in Proximal Promoter Regions. *PLoS Genet*. **2013**, *9*, 1003906, doi:10.1371/journal.pgen.1003906.
39. Kozlenkov, A.; Wang, M.; Roussos, P.; Rudchenko, S.; Barbu, M.; Bibikova, M.; Klotzle, B.; Dwork, A.J.; Zhang, B.; Hurd, Y.L.; et al. Substantial DNA methylation differences between two major neuronal subtypes in human brain. *Nucleic Acids Res.* **2016**, *44*, 2593–2612, doi:10.1093/nar/gkv1304.
40. Johnson, B.S.; Zhao, Y.T.; Fasolino, M.; Lamonica, J.M.; Kim, Y.J.; Georgakilas, G.; Wood, K.H.; Bu, D.; Cui, Y.; Goffin, D.; et al. Biotin tagging of MeCP2 in mice reveals contextual insights into the Rett syndrome transcriptome. *Nat. Med.* **2017**, *23*, 1203–1214, doi:10.1038/nm.4406.
41. Xu, X.; Stoyanova, E.I.; Lemiesz, A.E.; Xing, J.; Mash, D.C.; Heintz, N. Species and cell-type properties of classically defined human and rodent neurons and glia. *Elife* **2018**, *7*, doi:10.7554/eLife.37551.
42. Inoue, F.; Eckalbar, W.L.; Wang, Y.; Murphy, K.K.; Matharu, N.; Vaisse, C.; Ahituv, N. Genomic and epigenomic mapping of leptin-responsive neuronal populations involved in body weight regulation. *Nat. Metab.* **2019**, *1*, 475–484, doi:10.1038/s42255-019-0051-x.
43. MacKay, H.; Scott, C.A.; Duryea, J.D.; Baker, M.S.; Laritsky, E.; Elson, A.E.; Garland, T.; Jr Fiorotto, M.L.; Chen, R.; Li, Y.; et al. DNA methylation in AgRP neurons regulates voluntary exercise behavior in mice. *Nat. Commun.* **2019**, *10*, 5364, doi:10.1038/s41467-019-13339-3.
44. Lima, A.F.; May, G.; Diaz-Colunga, J.; Pedreiro, S.; Paiva, A.; Ferreira, L.; Enver, T.; Iborra, F.J.; Pires das Neves, R. Osmotic modulation of chromatin impacts on efficiency and kinetics of cell fate modulation. *Sci. Rep.* **2018**, *8*, 7210, doi:10.1038/s41598-018-25517-2.
45. Strober, W. Trypan blue exclusion test of cell viability. *Curr. Protoc. Immunol.* **1997**, *21*, A-3B, doi:10.1002/0471142735.ima03bs21.
46. Zhu, K.; Didier, A.; Dietrich, R.; Heilkenbrinker, U.; Waltenberger, E.; Jessberger, N.; Martlbauer, E.; Benz, R. Formation of small transmembrane pores: An intermediate stage on the way to Bacillus cereus non-hemolytic enterotoxin (Nhe) full pores in the absence of NheA. *Biochem. Biophys. Res. Commun.* **2016**, *469*, 613–618, doi:10.1016/j.bbrc.2015.11.126.
47. Birch, D.; Christensen, M.V.; Staerk, D.; Franzyk, H.; Nielsen, H.M. Stereochemistry as a determining factor for the effect of a cell-penetrating peptide on cellular viability and epithelial integrity. *Biochem. J.* **2018**, *475*, 1773–1788, doi:10.1042/BCJ20180155.
48. Barthelson, R.A.; Lambert, G.M.; Vanier, C.; Lynch, R.M.; Galbraith, D.W. Comparison of the contributions of the nuclear and cytoplasmic compartments to global gene expression in human cells. *BMC Genom.* **2007**, *8*, 340, doi:10.1186/1471-2164-8-340.
49. Solnestam, B.W.; Stranneheim, H.; Hallman, J.; Kaller, M.; Lundberg, E.; Lundeberg, J.; Akan, P. Comparison of total and cytoplasmic mRNA reveals global regulation by nuclear retention and miRNAs. *BMC Genom.* **2012**, *13*, 574, doi:10.1186/1471-2164-13-574.
50. Price, A.J.; Hwang, T.; Tao, R.; Burke, E.E.; Rajpurohit, A.; Shin, J.H.; Hyde, T.M.; Kleinman, J.E.; Jaffe, A.E.; Weinberger, D.R. Characterizing the nuclear and cytoplasmic transcriptomes in developing and mature human

cortex uncovers new insight into psychiatric disease gene regulation. *Genom. Res.* **2020**, *30*, 1–11, doi:10.1101/gr.250217.119.
51. Cui, P.; Lin, Q.; Ding, F.; Xin, C.; Gong, W.; Zhang, L.; Geng, J.; Zhang, B.; Yu, X.; Yang, J.; et al. A comparison between ribo-minus RNA-sequencing and polyA-selected RNA-sequencing. *Genomics* **2010**, *96*, 259–265, doi:10.1016/j.ygeno.2010.07.010.
52. Ma, F.; Fuqua, B.K.; Hasin, Y.; Yukhtman, C.; Vulpe, C.D.; Lusis, A.J.; Pellegrini, M. A comparison between whole transcript and 3' RNA sequencing methods using Kapa and Lexogen library preparation methods. *BMC Genom.* **2019**, *20*, 9, doi:10.1186/s12864-018-5393-3.
53. Gallego Romero, I.; Pai, A.A.; Tung, J.; Gilad, Y. RNA-seq: Impact of RNA degradation on transcript quantification. *BMC Biol.* **2014**, *12*, 42, doi:10.1186/1741-7007-12-42.
54. Reiman, M.; Laan, M.; Rull, K.; Sober, S. Effects of RNA integrity on transcript quantification by total RNA sequencing of clinically collected human placental samples. *FASEB J.* **2017**, *31*, 3298–3308, doi:10.1096/fj.201601031RR.
55. Mas-Ponte, D.; Carlevaro-Fita, J.; Palumbo, E.; Hermoso Pulido, T.; Guigo, R.; Johnson, R. LncATLAS database for subcellular localization of long noncoding RNAs. *RNA* **2017**, *23*, 1080–1087, doi:10.1261/rna.060814.117.
56. Zaghlool, A.; Niazi, A.; Bjorklund, A.K.; Westholm, J.O.; Ameur, A.; Feuk, L. Characterization of the nuclear and cytosolic transcriptomes in human brain tissue reveals new insights into the subcellular distribution of RNA transcripts. *Sci. Rep.* **2021**, *11*, 4076, doi:10.1038/s41598-021-83541-1.
57. Akhtar, A.; Gasser, S.M. The nuclear envelope and transcriptional control. *Nat Rev. Genet.* **2007**, *8*, 507–517, doi:10.1038/nrg2122.
58. Malhas, A.; Goulbourne, C.; Vaux, D.J. The nucleoplasmic reticulum: Form and function. *Trends Cell Biol.* **2011**, *1*, 362–373, doi:10.1016/j.tcb.2011.03.008.
59. Cho, S.; Irianto, J.; Discher, D.E. Mechanosensing by the nucleus: From pathways to scaling relationships. *J. Cell Biol.* **2017**, *216*, 305–315, doi:10.1083/jcb.201610042.
60. Chitikova, Z.; Steiner, F.A. Cell type-specific epigenome profiling using affinity-purified nuclei. *Genesis* **2016**, *54*, 160–169, doi:10.1002/dvg.22919.
61. Fernandez-Albert, J.; Lipinski, M.; Lopez-Cascales, M.T.; Rowley, M.J.; Martin-Gonzalez, A.M.; Del Blanco, B.; Corces, V.G.; Barco, A. Immediate and deferred epigenomic signatures of in vivo neuronal activation in mouse hippocampus. *Nat. Neurosci.* **2019**, *22*, 1718–1730, doi:10.1038/s41593-019-0476-2.
62. Dobin, A.; Davis, C.A.; Schlesinger, F.; Drenkow, J.; Zaleski, C.; Jha, S.; Batut, P.; Chaisson, M.; Gingeras, T.R. STAR: Ultrafast universal RNA-seq aligner. *Bioinformatics* **2013**, *29*, 15–21, doi:10.1093/bioinformatics/bts635.
63. Li, H.; Handsaker, B.; Wysoker, A.; Fennell, T.; Ruan, J.; Homer, N.; Marth, G.; Abecasis, G.; Durbin, R.; Genome Project Data Processing S. The Sequence Alignment/Map format and SAMtools. *Bioinformatics* **2009**, *25*, 2078–2079, doi:10.1093/bioinformatics/btp352.
64. Anders, S.; Pyl, P.T.; Huber, W. HTSeq--a Python framework to work with high-throughput sequencing data. *Bioinformatics* **2015**, *31*, 166–169, doi:10.1093/bioinformatics/btu638.
65. Bolger, A.M.; Lohse, M.; Usadel, B. Trimmomatic: A flexible trimmer for Illumina sequence data. *Bioinformatics* **2014**, *30*, 2114–2120, doi:10.1093/bioinformatics/btu170.
66. Zhang, Y.; Liu, T.; Meyer, C.A.; Eeckhoute, J.; Johnson, D.S.; Bernstein, B.E.; Nusbaum, C.; Myers, R.M.; Brown, M.; Li, W.; et al. Model-based analysis of ChIP-Seq (MACS). *Genome Biol.* **2008**, *9*, R137, doi:10.1186/gb-2008-9-9-r137.

2.6 Nuclei on the rise: when nuclei-based methods meet next-generation sequencing

Authors: **Tamer Butto**, Jennifer Winter, Beat Lutz and Susanne Gerber

Manuscript in preparation

My contributions to this article are listed in section 4.2 Contributions to individual publications

Nuclei on the rise: when nuclei-based methods meet next-generation sequencing

Tamer Butto [1], Jennifer Winter [1, 2], Beat Lutz [2] and Susanne Gerber [1]

[1] Institute of Human Genetics, University Medical Center of the Johannes Gutenberg University Mainz, Langenbeckstr. 1, 55131 Mainz, Germany
[2] Leibniz Institute of Resilience Research, Wallstr 7, 55122 Mainz, Germany;

Abstract

The upsurge of cell nuclei studies coupled with next-generation sequencing approaches denotes the fast progress in the field of molecular cell biology. Such studies aim at comprehending the molecular (i.e., epigenetic and transcriptomic) states occurring in heterogeneous cell populations by applying various increasingly affordable sequencing approaches. Novel methodologies are being continuously developed to isolate and select nuclei and apply them to cell type-specific studies. However, it is important to recognize potential challenges that can come along in using these techniques. In this perspective article, we outline the emergence of nuclei-based studies, focusing on the methodologies used to obtain specific nuclei populations and the conceivable reasons for their upsurge in recent years. Additionally, we address the intertwining of nuclei-based studies with next-generation sequencing approaches, discussing the advantages and disadvantages of such studies compared to whole cell-based sequencing. We aim at providing a comprehensive overview of nuclei-based studies, pointing out their strengths and weaknesses in order to design and employ improved experimental strategies and to acquire biologically accurate information.

Introduction

The nucleus is the largest organelle in the eukaryotic cell, containing the genetic material (i.e., DNA) of a given organism (Devos et al., 2014). Often, the nucleus contains the instructions to provide the cell with its identity and detailed instruction of its functioning. In terms of its structure, the nucleus has its own double-membrane nuclear envelope (NE), which encapsulates and protects the DNA-histone protein complexes in a highly compacted state as well as the nucleolus (Shah, Wolf and Lammerding 2017; Kemm, Shipony and Greenleaf 2019). Within that state, the chromatin structure is regulated by various chromatin remodeling proteins, structural proteins, and transcription factors, altering the chromatin structure and ultimately determining a given cell's transcriptional profile.

Nuclei-based studies utilize nuclei to identify novel nuclear properties and cell type-specific features combined with supplementary molecular biology techniques. They have come a long way since the initial discovery, exploration, isolation, and use of nuclei in various fields such as genomics and epigenomics. A comprehensive overview of these main trajectories is presented by Pederson (2011), highlighting the significant findings and techniques used to uncover the properties of the nucleus. The key discoveries relevant to the topic of this review are highlighted in Figure 1A. In the last decade, we witnessed an upsurge in nuclei-based studies, particularly combined with high-throughput sequencing. This increase is associated with the growth of next-generation sequencing platforms together with the steady reduction in sequencing cost, which made them both an affordable and valuable research tool (Illumina 2014). On top of that, the introduction of single-cell (and single nucleus) sequencing technologies directed scientists to uncover the unique and heterogeneous molecular properties of a given cell population (Shapiro, Biezuner and Linnarson 2013; Stuart and Satija 2019). The rise of these research fields and technologies, together with the interest in epigenetic studies, led scientists to focus and develop novel tools to isolate cell type-specific populations, focusing mainly on nuclei as tools for molecular investigation. The significant advances in nuclei isolation in addition to nuclei-related sequencing methodologies are highlighted in Figure 1B. One can appreciate the rapid and frequent utilization of nuclei in our current research period marking the shift from the early "discovery era" to the "application era" of nuclei-based research. With such rapid progression, it is essential to highlight the challenges that come along the way. Therefore, in the following overview, we will highlight the main high-throughput sequencing methodologies coupled with nuclei-based investigations, the potential reasons for their upsurge, and upcoming challenges in this fields.

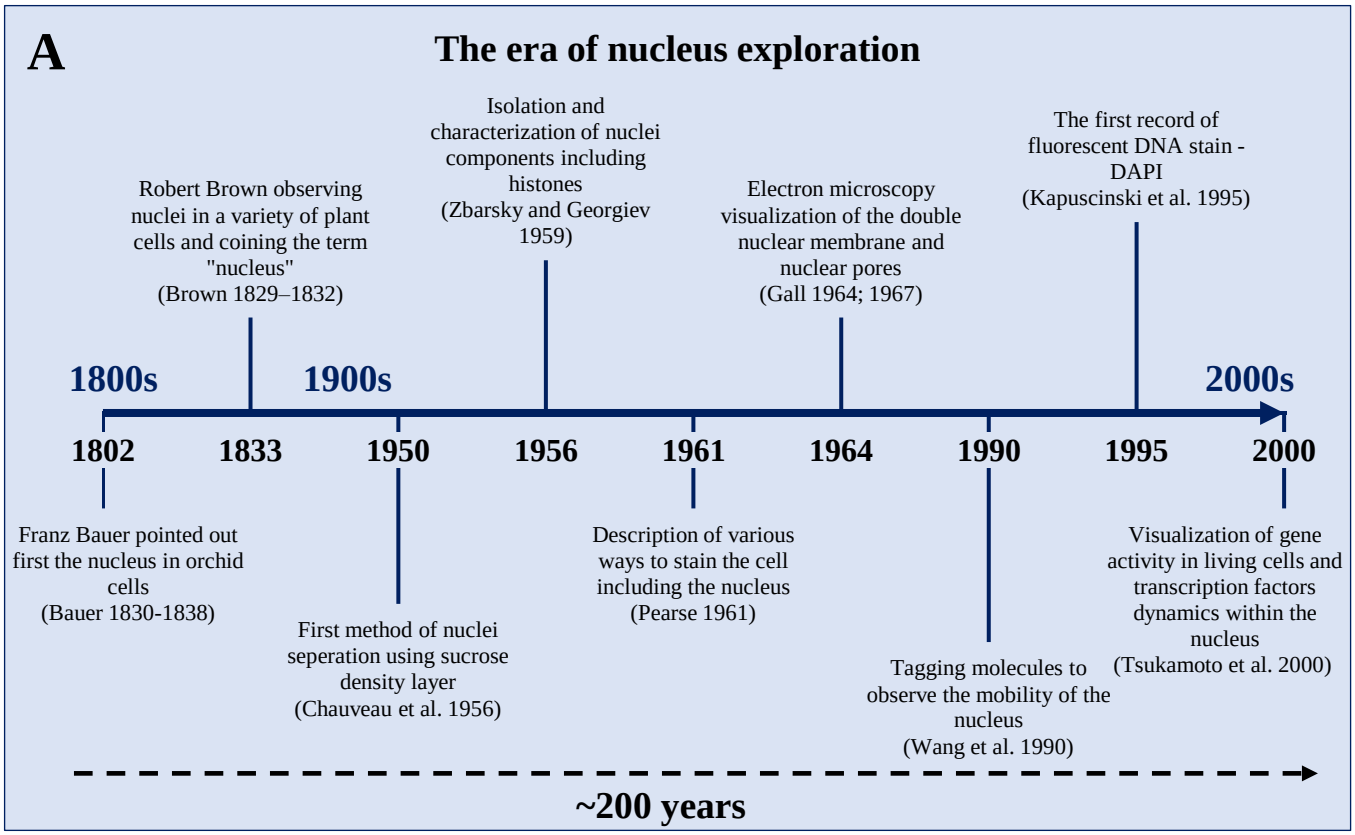
A
The era of nucleus exploration
Robert Brown observing nuclei in a variety of plant cells and coining the term "nucleus" (Brown 1829–1832)
Isolation and characterization of nuclei components including histones (Zbarsky and Georgiev 1959)
Electron microscopy visualization of the double nuclear membrane and nuclear pores (Gall 1964; 1967)
The first record of fluorescent DNA stain - DAPI (Kapuscinski et al. 1995)
1800s
1900s
2000s
1802
1833
1950
1956
1961
1964
1990
1995
2000
Franz Bauer pointed out first the nucleus in orchid cells (Bauer 1830-1838)
First method of nuclei seperation using sucrose density layer (Chauveau et al. 1956)
Description of various ways to stain the cell including the nucleus (Pearse 1961)
Tagging molecules to observe the mobility of the nucleus (Wang et al. 1990)
Visualization of gene activity in living cells and transcription factors dynamics within the nucleus (Tsukamoto et al. 2000)
~200 years

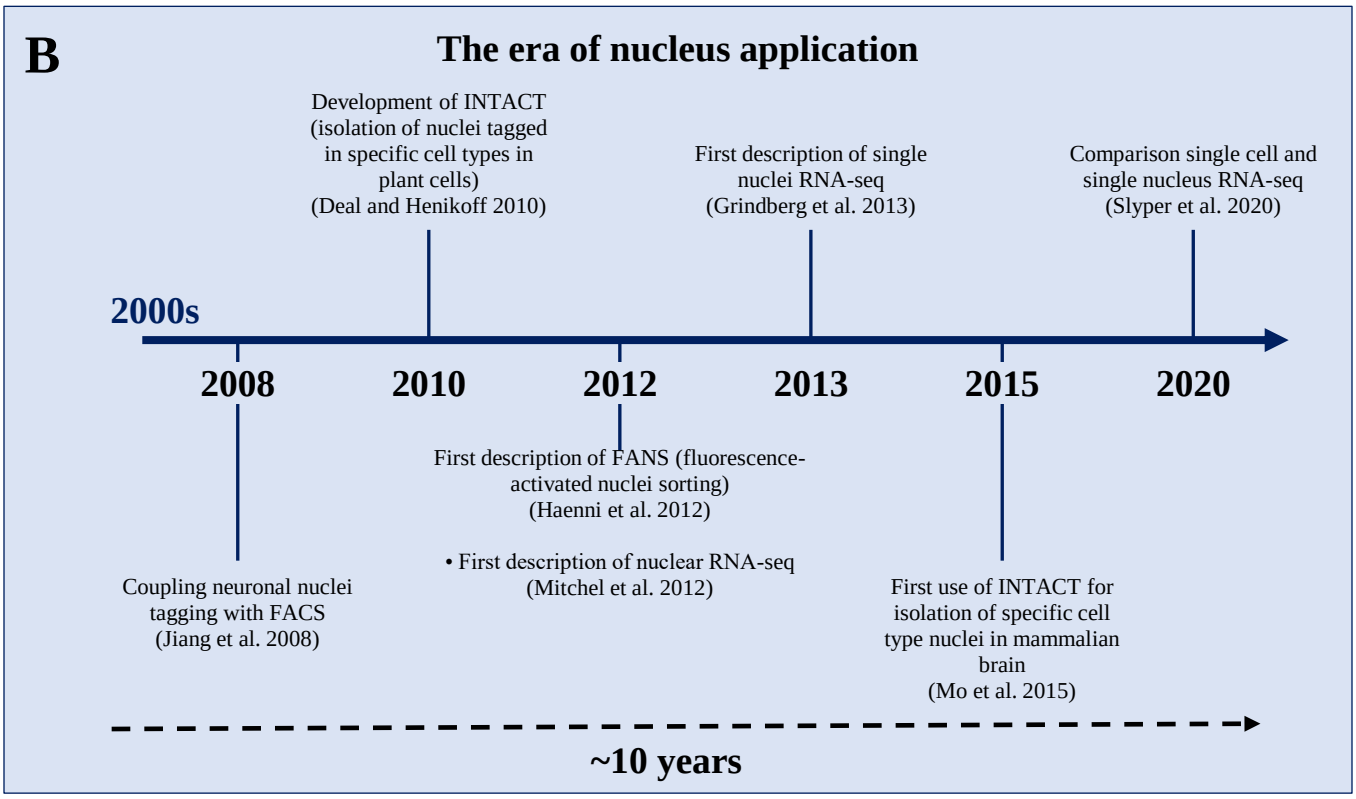
B
The era of nucleus application
Development of INTACT (isolation of nuclei tagged in specific cell types in plant cells) (Deal and Henikoff 2010)
First description of single nuclei RNA-seq (Grindberg et al. 2013)
Comparison single cell and single nucleus RNA-seq (Slyper et al. 2020)
2000s
2008
2010
2012
2013
2015
2020
First description of FANS (fluorescence-activated nuclei sorting) (Haenni et al. 2012)
• First description of nuclear RNA-seq (Mitchel et al. 2012)
Coupling neuronal nuclei tagging with FACS (Jiang et al. 2008)
First use of INTACT for isolation of specific cell type nuclei in mammalian brain (Mo et al. 2015)
~10 years

Figure 1. The trajectory of nuclei-based research, form discovery (A) to the application (B). A. Within the last 200 years, the nucleus was examined in order to identify its distinct properties within a cell. Different methodologies were developed to visualize and isolate the nuclei, uncovering further their role in genome regulation. B. With the increase use of next-generation sequencing approaches, nuclei have been gradually used to uncover the epigenetic and transcriptomic properties of specific cell populations. Novel nuclei isolation methodologies are being applied in combination with next-generation sequencing and increasingly with single-nucleus sequencing approaches.

1. Exploration of cell type-specific populations – focus shifting towards nuclei

Considering the central dogma of molecular biology (DNA to RNA to protein), the nucleus is arguably one of the most critical biological structures in the eukaryotic cell. It contains and regulates two major players, the DNA and RNA (Morange 2009). Transcription is the first step that transforms nucleus-resident information into the first functional product, the RNAs. Regulation of this step requires multi-component mechanisms to ensure proper cellular activity. In the light of complex epigenetic regulation processes, we obtain cell type-specific populations with unique blueprints in the control and expression of specific sets of genes required for each particular cell population. Given that these events occur in the nucleus, it is rational to utilize the nuclei for cell type-specific epigenetic/transcriptomic analyses.

Different methodologies have evolved for the investigation of cell type-specific features. For instance, in 2010, Deal and Henikoff established a method termed "Isolation of Nuclei in Tagged Cell Types" (INTACT). This technique originally consisted of an affinity purification-based method to isolate GFP-tagged nuclei from plant systems (Deal and Henikoff 2010, Deal and Henikoff 2011). While the method was initially used in plant systems, the utilization of INTACT was adapted on other model organisms and gradually shifted towards multiple cell types within the mammalian system, primarily within the mammalian brain (Steiner et al. 2012, Henry et al. 2012, Mo et al. 2015, Mo et al. 2016, Chongtham et al. 2021). Roughly at the same time, the use of flow cytometry-based isolation shifted from sorting whole cells using "Fluorescence-activated cell sorting" (FACS) to specific nuclei populations using "Fluorescence-activated nuclei sorting" (FANS). While isolation of nuclei has been previously reported with the sorting of neurons using the neuronal nuclear marker NeuN (Jiang et al. 2008), it was not until 2012 that the terminology FANS was established (Haenni et al. 2012) and started to be frequently used. Handley and colleagues (2015) provided a detailed review of the methodologies used to isolate particular cell populations following subsequent transcriptomic and epigenomic analyses (Handley et al., 2015). We recently reported a comprehensive comparison between two of the most utilized nuclei isolation techniques, INTACT and FANS (Chongtham et al. 2021). Our report details the observations reported in Handley et al. (2015) and describes the similarities and differences between transcriptomic and epigenetics of nuclei using these two distinct methodologies. The utilization of these techniques often relies on transgenic organisms able to label

selected nuclei populations. For instance, in mammalian systems, the conserved eukaryotic nuclear membrane protein *Sun1* is frequently tagged with GFP, creating a transgene that can be conditionally expressed using Cre recombinase (Mo et al. 2015). Sun1GFP is used to label cell-type specific nuclei that are subsequently isolated and studied using various molecular approaches (Chongtham et al. 2021).

In 2012, for the first time, nuclear RNA-seq (nucRNA-seq) was combined with next-generation sequencing (Mitchell et al. 2012). The authors took the compared the nuclear transcriptome of erythroid cells with RNA polymerase II (RNAPII) occupancy. The authors reported that large unspliced transcripts are detected using nucRNA-seq, henceforth foreseeing some of the challenges, which will be discussed further below. Overall, nuclei-based approaches have moved to an experimental routine, yet so far, with relatively little information about their distinct properties and differences compared to whole-cell studies. In the following, we will address some of the reasons for upsurge of these techniques in the first place.

2. Why have nuclei-based studies increased so much in the past decade?

Since the first description of the nucleus in 1800s, it has become clear that the nucleus, or more specifically, the nuclear content, has a major role in cellular function and regulation. Each cell consists of a "unique nucleus" with seemingly identical DNA sequence, yet with varying transcriptional activities. When such cell populations work in cooperation, by modulating and supplementing each other's function, an entire organism emerges in its entire complexity. The interest in such phenomena led scientists to explore the different attributes of specific cell populations in order to identify their characteristics functions within the organism. Based on the literature, we reason that multiple factors have contributed to the increased use of nuclei in molecular investigations, which will be addressed further in the following sections of the review.

2.1 Availability of next-generation sequencing platforms – particularly transcriptomic and epigenetic approaches

The more frequent utilization of nuclei has come hand-in-hand with the elevated interest and improvement of genomics and epigenetic studies, including various high throughput sequencing platforms (or next-generation sequencing platforms) (Besser et al. 2018). Such technologies have allowed the detection of molecular changes occurring at a genome-wide level, providing both comprehensive databases of specific cell populations as well as loci-specific alterations within a given experimental condition. The curiosity to uncover the internal function and content within the nuclei of unique cellular populations led to the growth of the field of epigenetics and the development of experimental techniques dedicated to uncovering its multifaceted mechanisms. For instance, the three main branches for epigenetic studies include DNA methylation, histone post-translational modification (PTMs), and small RNA regulation (e.g., miRNA) (Chen et al. 2017, Skvortsova, Iovino and Bogdanović 2018). While small RNAs are still transcribed in the

nucleus, their activity also extends to the cytoplasm and, therefore, will be described later in this review. On the contrary, the mechanisms of DNA methylation and histone PTMs, rely on the deposition of chemical modifications on the chromatin or chromatin-associated proteins (histones) located and regulated in the nucleus (Wang, Peterson and Loring 2014). These mechanisms control gene expression, which influences cell function, and ultimately give each cell type its unique epigenetic and transcriptomic blueprint. With the increased interest in epigenetic regulation mechanisms, combined explicitly with high-throughput sequencing, nuclei were found to be sufficient for such applications.

To provide an overview of the different frequently used sequencing methodologies, we conducted a Pubmed database's publication record. Using specific method terminologies (sequencing method labeling), we obtained the number of studies published related to a particular terminology per year. This type of analysis could indicate the dynamic use of a specific method or growth of a particular field investigated. Initially, we collected the most frequently utilized sequencing techniques, including “RNA-seq”, “nucRNA-seq”, “ChIP-seq” and a variety of sequencing methodologies used to investigate DNA methylation, chromatin accessibility, and 3D chromatin conformation (Fig. 2A). The sequencing methodologies for DNA methylation, chromatin accessibility, and chromatin 3D conformation are shown in Figures 2B-D. Overall, we see a dominating use of the term RNA-seq that keeps increasing through time (Fig. 2A). On the other hand, the term nucRNA-seq has not been as frequently used, which might reflect the novelty of nuclear RNA usage for sequencing. Remarkably, the application of chromatin accessibility and 3D conformation methods, particularly ATAC-seq and Hi-C (Fig 2B and 2D), are being increasingly used compared to DNA methylation sequencing techniques, emphasizing the growing interest in chromatin dynamics of specific cell types. For instance, ATAC-seq is a recently popularized technique that utilizes a hypersensitive Tn5 transposase activity to incorporate selected barcodes at chromatin accessible regions. Thereby, ATAC-seq allows detecting genome-wide chromatin accessibility states (Buenrostro 2013, Buerostro et al. 2015). The original protocol utilized cells of which crude nuclei are extracted using cell lysis treatment (Buenrostro et al. 2015). Its relatively short and straightforward protocol made ATAC-seq a rapidly growing technique for identifying chromatin accessibility states, which often indicate chromatin binding, such as transcription factor binding (Li et al. 2019) (Fig 2C). Since its development, different nuclei isolation methods have optimized their protocols, coupling them with ATAC-seq in a variety of organisms and cell-type specific populations (Bhattacharyya et al. 2019). An additional advantage of ATAC-seq is the ability to operate with frozen tissue material (Corces et al. 2017, Milani et al. 2016, Fujiwara et al. 2019) or even cross-linked material for both visualization and detection of chromatin accessible regions (Chen et al. 2016). Another example is the use of Hi-C for the identification of chromatin 3D conformation states and genomic long-distance interaction sites (Lieberman-Aiden et al. 2009). Even though the methodology was developed over a decade ago, the continuous and increased use of Hi-C as the primary chromatin 3D conformation

methodology has been observed particularly in the last few years (Fig. 2D) (Kempfer and Pombo 2019, Oluwardare, Highsmith and Cheng 2019). Surprisingly, even though DNA methylation sequencing techniques has shown a steady usage across the decade and a slight increase in recent years, there is no notable increase in DNA methylation usage as compared to chromatin-associated sequencing methodologies (Fig 2A-D). This could denote a possible reduced interest in the study subject or a need for a simplified and more intuitive method for DNA methylation measurement. Nevertheless, nuclei's isolation is sufficient to obtain the content required for the different epigenetic analyses. The rise of such sequencing platforms is undoubtedly a landmark to molecular genomics and epigenomics, which later has opened the door to the single-cell, and currently also, single nucleus sequencing era.

2.2 Reduction of experimental and biological complexity

Using nuclei instead of whole cells for downstream transcriptomics and epigenetic analyses reduces both experimental and biological complexity. Nuclear isolation procedures were established a half-century ago, providing density gradient platforms that separate the nuclei from the rest of the raptured cell components (Chauveau, Moule and Rouiller 1956, Hadjiolov, Tencheva and Bojadjieva-Mikhailova 1965, Zylber and Penman 1971). In contrary, enzymatic or substance treatments are often required to separate whole cells intro single units (Tomlinson et al. 2013, Almeida, García-Montero and Orfao 2014). Recently, Denisenko and colleagues (2020) has provided a systematic comparison of dissociation protocols using both enzymatic digestions as well as nuclei isolation approaches on adult mice kidney followed by single cell and single nuclei RNA-seq (Denisenko et al. 2020). The enzymatic dissociation protocols including a 37˚C enzyme mix (warm) as well as *B. Licheniformis* protease (cold) tissue dissociations approaches to monitor any transcriptional differences between the methods. Overall, the duration of the warm and cold dissociation protocols was ~50 min and ~40 min, respectively, whereas nuclei isolation protocol was about ~30 min (Denisenko et al. 2020). The authors denote that warm dissociation protocol lead to stress-response transcriptional activation, which was not observed in the cold dissociation protocol.

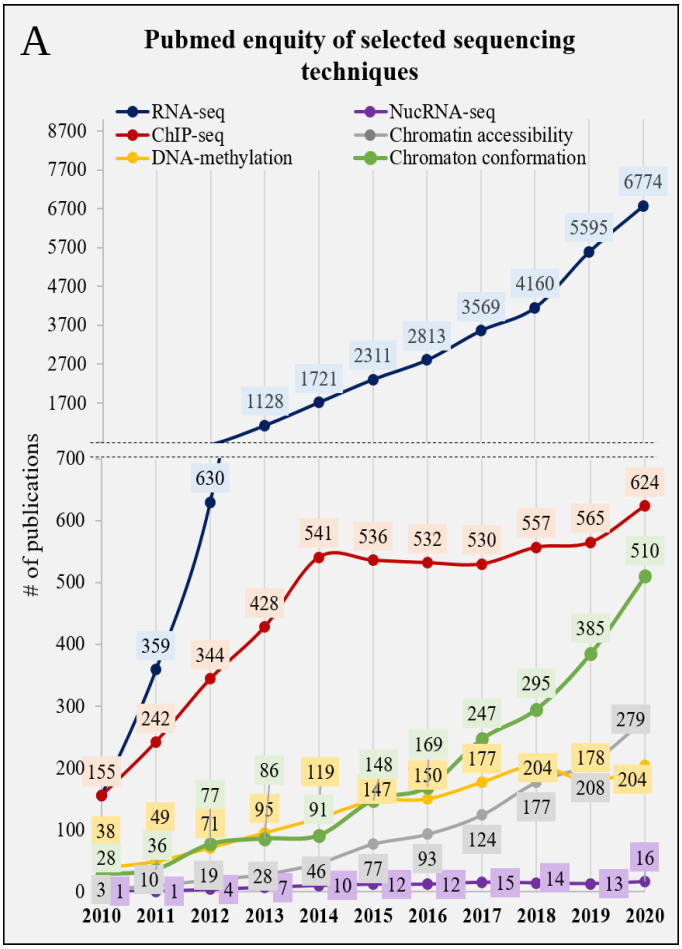
A
Pubmed enquity of selected sequencing techniques
RNA-seq
ChIP-seq
DNA-methylation
NucRNA-seq
Chromatin accessibility
Chromaton conformation
# of publications
2010 2011 2012 2013 2014 2015 2016 2017 2018 2019 2020

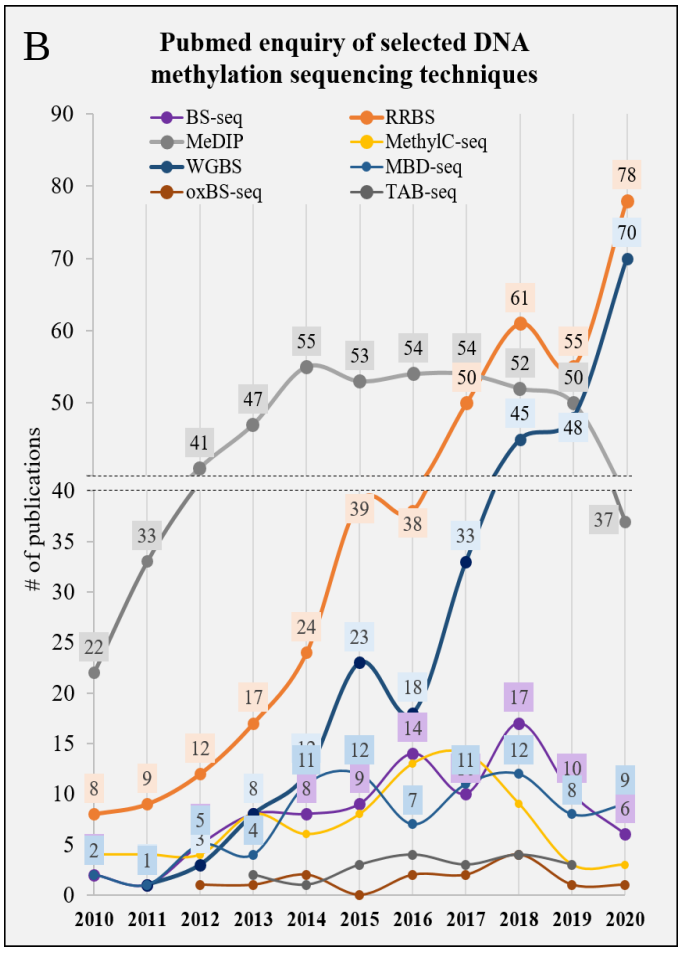
B
Pubmed enquiry of selected DNA methylation sequencing techniques
BS-seq
MeDIP
WGBS
oxBS-seq
RRBS
MethylC-seq
MBD-seq
TAB-seq
# of publications
2010 2011 2012 2013 2014 2015 2016 2017 2018 2019 2020

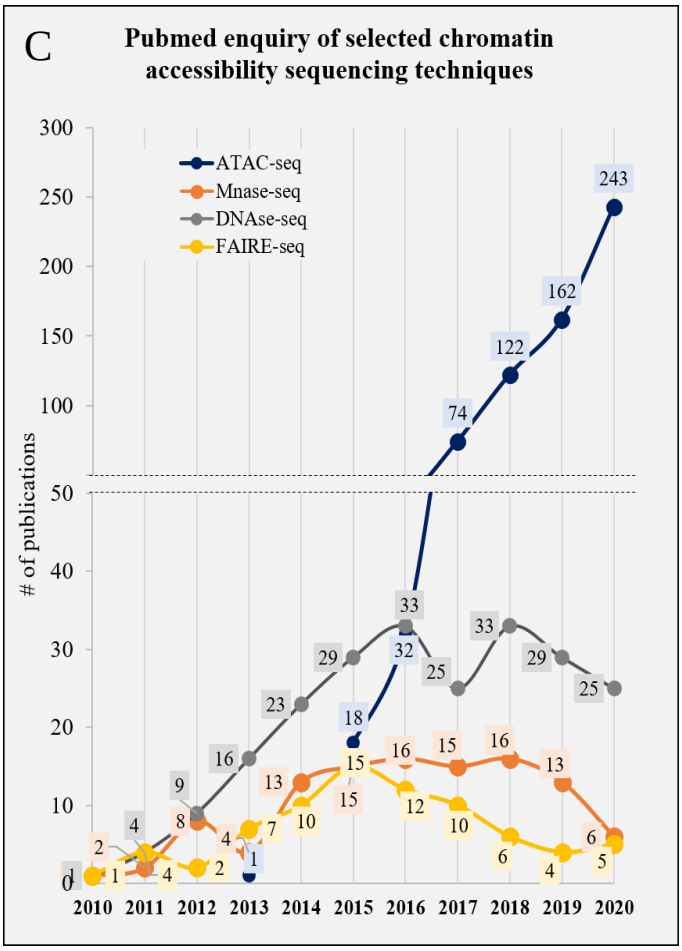
C
Pubmed enquiry of selected chromatin accessibility sequencing techniques
ATAC-seq
Mnase-seq
DNAse-seq
FAIRE-seq
# of publications
2010 2011 2012 2013 2014 2015 2016 2017 2018 2019 2020

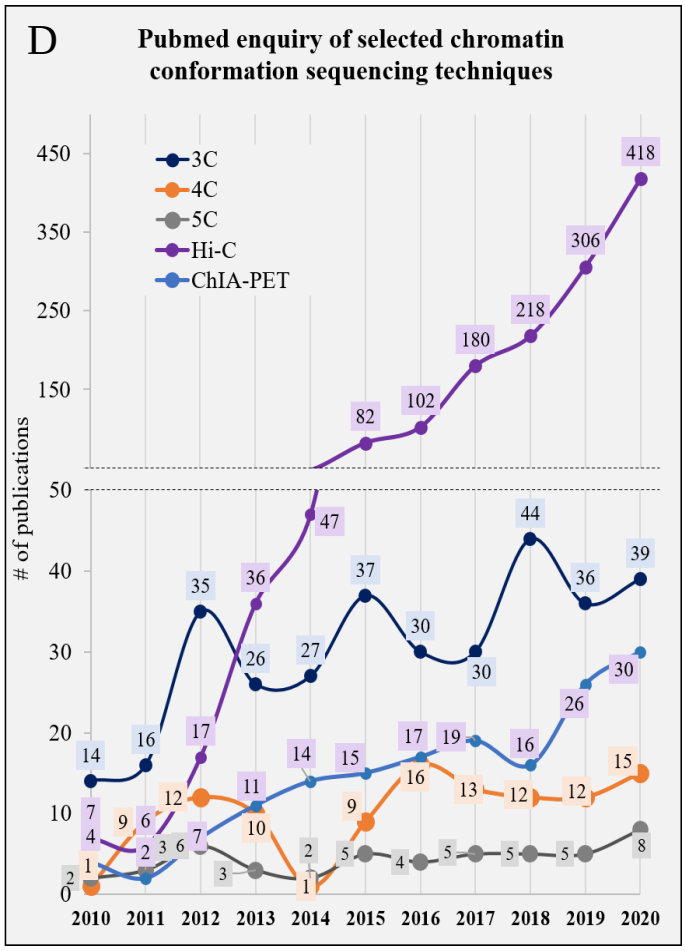
D
Pubmed enquiry of selected chromatin conformation sequencing techniques
3C
4C
5C
Hi-C
ChIA-PET
# of publications
2010 2011 2012 2013 2014 2015 2016 2017 2018 2019 2020

Figure 2*. Pubmed inquiry of selected next-generation sequencing methodologies published in the last century. A. Reported publications of selected sequencing techniques B. Reported publications of DNA methylation sequencing techniques. C. Reported publications of chromatin accessibility sequencing techniques. D. Reported publications of chromatin 3D conformation sequencing techniques. Data were retrieved from the PubMed database using specific, definite terminologies as documented in Supplement data. This type of analysis allows the trends of a particular methodology or field to be represented more robust than merely counting the number of studies using the exact techniques.*

In addition, previous studies reported that enzymatic treatments can lead to major changes affecting different cellular properties such as cell-cycle state, structural alterations, and cellular viability (i.e., apoptosis) (Hwang, Lee and Bang 2018). All these factors contribute to transcriptional changes that could lead to misinterpreted conclusions of the research question investigated (Buettner et al. 2015). Therefore, the process of nuclei isolation provides a slight improvement in speed of isolation in addition to lack of harsh enzymatic treatment procedures. It is important to note nonetheless that nuclei isolation can substantially differ depending on the tissue, isolation method, nuclei storage and suspension time in intermediate buffers (Chongtham et al. 2021). For instance, it has been reported that nuclei isolation is advantageous for tissues difficult to be dissociated, such as bone or adipose (Slyper et al. 2020). This is probably due to the properties of the tissues where enzymatic dissociation would be inefficient compared to the isolation of nuclei, whereby removing the external structural layers of the cell and focuses only on the nuclei. This property relates to the second point to be addressed, the reduction of biological complexity.

The nucleus forms part of a cell, therefore, its separation from the whole cell will reduce the complexity of a cell as a whole. Depending on the application, the nuclei can be sufficient to investigate specific mechanisms such as chromatin structure and DNA methylation states, since the material required is located distinctively in the nucleus. However, in the case of the distinct RNA populations, the content of RNA differs in the nucleus and the cytoplasm (Barthelson et al. 2007, Solnestam et al. 2012, Price et al. 2020). Factors such as transcription rate, splicing rate and transcript export speed could affect the presence of particular RNA population in each compartment. For instance, in the study by Denisenko and colleagues (2020), the authors reported that single nucleus RNA-seq libraries reveled underrepresentation of certain cell types, which was not observed in the single cell RNA-seq (Denisenko et al. 2020). These observations indicate that isolated populations of nuclei and whole cell are not similar in terms of cellular content and therefore also transcriptional states. These points will be elaborated further below (See *Chapter 3* for additional information*).*

2.3 *In-vivo* versus *in-vitro* studies and use of transgenic organisms

Biological research can be divided mainly into two types of studies: *in-vivo* and *in-vitro* studies. The former provides a more realistic system of an organism investigated but a much more complex outlook of a mechanism that is continuously influenced by a broad range of effectors. On the other hand, *in-vitro* studies provide a simple, isolated, relatively homogenous and easy to manipulate component of a biological system (e.g., specific cell type), and to investigates the fundamental role of a component (e.g., gene expression or protein) within the biological system. However, *in-vitro* investigations lack the realistic aspect of complex multi-component systems. Depending on the study and specific cell type investigated, each study can determine sample availability, handling method and input material required for subsequent molecular analyses. Additionally, specific molecular techniques often require defined cell/nuclei numbers for reproducibility purposes and therefore need quantifiable, separated, and homogenized cellular content. The choice between whole cells or nuclei should be planned according to the study requirements and sample availability. Despite the fact that *in-vivo* studies are used both in combination of whole cells or nuclei isolation methodologies, we noticed a prevalent association of nuclei isolation methods with *in-vivo* studies (Chongtham et al. 2021). The rapid and straightforward nuclei isolation approaches, such as density gradient nuclei isolation, are favored for *in-vivo* dissected tissues, in place of enzymatic treatments needed for whole cell isolation, which, as previously noted, can be time-consuming and alter cellular and molecular properties. Additionally, multiple tissue types comprise heterogeneous cell populations that require assortment using for example FACS sorting, of a specific cell population of interest. Depending on the tissue, the sorting of whole cells can be challenging and inefficient due to intermingled cellular population, which makes it hard to asses and sort the required cellular population, even when using transgenic animals (Guez-Barber et al. 2012). On the contrary, sorting of specifically labeled nuclei (e.g., with Sun1GFP) provides a more efficient and rapid way to obtain desired cell populations as the structural properties of the cell are removed.

When considering *in-vitro* systems, the investigated cellular population often consists typically of a specific cell line grown on a dish relatively easy to handle and process to a single-cell suspension. Due to relative ease of handling, *in-vitro* cell lines are directly coupled with a lysis step, molecular processing, and subsequent sequencing techniques without the requirement of nuclei isolation. Even though isolated cells from transgenic animals are also coupled with *in-vitro* handling approaches, they do not require nuclei isolation steps for subsequent molecular analyses. These associations are selected according to the experimental design and rational use of the cellular population investigated.

2.4 Single or combination of "omics" approaches

An additional factor that will determine the use of nuclei over the whole cell is the combination of various sequencing methodologies to investigate a distinct cellular population. An increasing number of studies seek to combine multiple "omics" within a given experimental design to identify specific and shared molecular

properties of a given cellular population (Hasin, Seldin, and Lusis 2017, Pinu et al. 2019). A frequent example of such experiments is the association of RNA-seq in addition to other epigenetic sequencing methodologies such as chromatin accessibility or DNA methylation within a specific experimental scheme. For instance, from our literature review comparing the use of INTACT and FANS techniques, we observed that 60% of the analyzed studies (35/59 studies), combined more than one sequencing technique (Chongtham et al. 2021). This demonstrates the frequent association of various "omics" approaches within the same study, particularly in nuclei-based research. Using these associations, scientists can obtain broader and more comprehensive insights into particular cellular mechanisms *per* given condition. Therefore, sample availability and diversification are crucial aspects of the experimental design of such studies. Depending on the biological question investigated and distinct sample requirements, nuclei are often coupled with additional approaches such as FANS or INTACT to isolate specific populations and diversify their use in various sequencing methodologies.

2.5 The era of single-cell studies – and now also single nuclei

Single-cell studies have also taken an essential role in biological research, gradually rising with time to deepen even further individual cells' characteristics within a given population. One of the most frequently utilized approaches is single-cell RNA-seq (scRNA-seq), which is able to reveal the dynamic transcriptome of individual cells, highlighting the heterogeneity within seemingly identical cell types. However, interestingly enough, the diversification and exploration of a single nucleus, contrary to single cells, had also come into play. In the following, we will use the term "single-cell" to denote the general aspect of single-cell studies unless specified otherwise.

To provide an overview of the association of single nucleus and single cell sequencing technologies, we conducted a similar analysis as in the previous section, using the PubMed database. We utilized the terms "Single Cell/Cells" or "Single Nucleus/Nuclei" in combination with the term "Sequencing" or "RNA-seq" to obtain both wide-range and transcriptome-specific reports for such studies, respectively (Fig 3). The association of "Single Cell/Cells" sequencing methodologies is predominantly applied throughout the last decade, particularly in the previous few years. However, the use of "Single Nucleus/Nuclei" sequencing methodologies is rare compared to "Single Cell/Cells" sequencing yet growing (Fig. 3). Taken together, this search provide further evidence for the increase of nuclear-based studies as well as single cell/nuclei methodologies within the past decade. Similar to the previous sections, we argue that the motivation to use single nuclei for molecular studies are similar to the use of bulk nuclei. Features such as sample availability (Krishnaswami et al. 2016), coupling of multiple "omics" on single cell/nuclei level (Jia et al. 2018, Reyes et al. 2019, Liu et al. 2019), and selection choice between nuclei or cells for molecular analysis (Slyper et al. 2020) are just a few overlapping considerations for the experimental design of single nuclei

methodologies. Since single nucleus RNA-seq (snRNA-seq) is the most frequent methodology among the single nuclei studies used in the field at a single cell level, we will refer mainly to snRNA-seq studies to address specific points.

The first application of snRNA-seq occurred early in this decade, providing the basis for the following snRNA-seq methodologies, which were developed later on (Grindberg et al. 2013). Grindberg and colleagues (2013) applied the first snRNA-seq to uncover the dynamic transcriptome of mouse neuronal progenitor cells (Grindberg et al. 2013). They noted that single nuclei sequencing provides a unique opportunity to explore neuronal transcriptomes since it "*avoids requiring isolation of single-cell suspensions, eliminating potential changes in gene expression due to enzymatic-cell dissociation methods*" (Griberg et al. 2013). In their analysis, they took the opportunity to compare bulk nuclei versus bulk cells as well as single nucleus versus single cell. Their report opened the avenue to the exploration of nuclear transcriptomics on a single-cell level. Since then, the number of studies utilizing snRNA-seq has gradually raised, and with them, the inevitable question: what is the difference between single nuclei and single cell RNA-seq (scRNA-seq)?

Comparing single nucleus and single cell RNA-seq within a single experimental scheme has become more common across studies (Lacar et al. 2016, Bakken et al. 2018, Korrapti et al. 2019, Slyper et al. 2020). We argue that the fundamental differences between nuclei and whole cell are noteworthy, which inevitably led studies to explore and uncover such differences. For instance, Bakken and colleagues (2018) compared scRNA-seq and snRNA-seq from the mouse visual cortex in order to identify the main differences between these two approaches (Bakken et al. 2018). The authors suggest that although the number of transcripts detected from scRNA-seq are higher than snRNA-seq, the latter can be similarly associated with neuronal cell types. Interestingly, the authors highlighted that the incorporation of introns was required for comparable clustering analysis between snRNA-seq and scRNA-seq. They speculated that this is due to the long genes known to be brain-specific which help defining the neuronal population analyzed (Bakken et al. 2018). Additionally, the authors reported that the nuclear fraction of total cellular mRNA varies between 20-50% depending on the cell's size. This suggests that nuclear transcripts could comprise only up to half of the total amount of transcripts, and therefore, could have some implication for nuclear RNA measurements (Bakken et al. 2018).

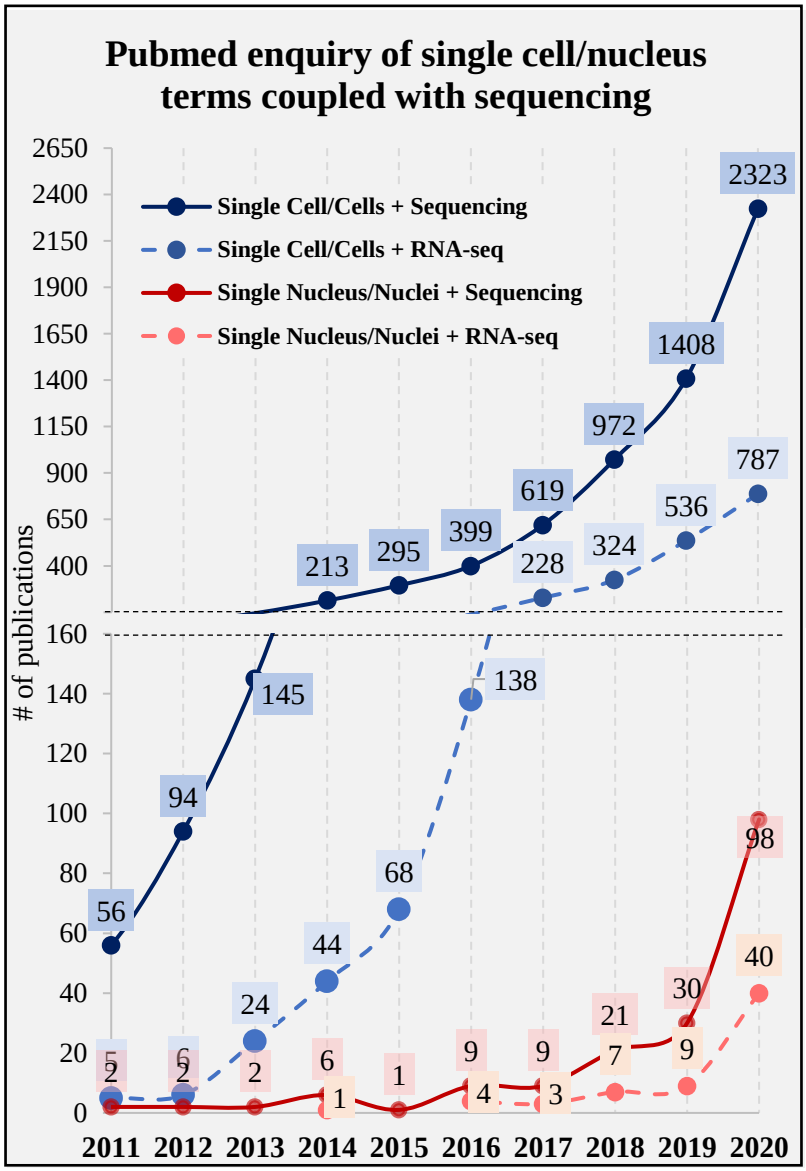

Figure 3. Pubmed inquiry of "Single cell" and "Single nuclei" associated sequencing or RNA-seq published in the last decade.

Another recent study reported a comprehensive database covering various cancer cell types, distinct protocol strategies, tissue acquisition, and sequencing methodologies of scRNA-seq and snRNA-seq data (Slyper et al. 2020). In their study, the authors comment about the choice of using either single cell or nuclei RNA-seq stating, "*The choice between scRNA-Seq and snRNA-Seq is typically driven by sample availability, logistics, and biological question"*. The authors state that the advantages of snRNA-seq include the decoupling of sample acquirement and processing, high recovery from tissues difficult to be dissociated, and sample multiplexing within specific approaches such as Drop-seq (Kang et al. 2018, Stoeckius et al. 2018, Slyper et al. 2020).

All of these considerations stated in the single nucleus/cells section can be applied to bulk analyses as well, especially when considering transcriptome analyses. It is most likely that the combination of the various factors described here leads to the overall selection of nuclei as simple yet effective biological components for the investigation of epigenetic and transcriptomic states within cell type-specific populations. Comparing single nuclei and single cells transcriptomes can provide a great source of information to better understand their transcriptional differences and design more precise transcriptomic analyses. However, at the transcriptomic level, there are some potential challenges that we believe should be addressed.

3. The challenges of nuclei-based studies - Comparison between nuclear and whole cell transcriptomic properties

The field of transcriptomics is a fundamental part of any molecular biological study. Unlike epigenetic studies of DNA methylation or histone PTMs, nuclear transcriptomics faces a more challenging data analysis aspect since nuclear RNA comprises distinct properties compared to total or cytoplasmic RNA. Several studies have compared the differences between nuclear and cytoplasmic RNA fractions (Barthelson et al. 2007, Solnestam et al. 2012, Price et al. 2020). Such differences may be significant depending on the topic of investigation and thus require careful consideration prior to sequencing. Comparing nuclear and cytoplasmic RNA fractions is vital to comprehend, design and utilize better high-throughput sequencing approaches, as each has its advantages and biases, which require reflection.

The following section summarizes the major challenges to be considered when comparing nuclear and whole-cell or cytoplasmic RNA, highlighting each fraction's different properties and their major differences in RNA-seq analysis.

3.1 RNA content - RNA population bias between nuclei and whole cells

Within the eukaryotic cell, transcription is often coupled with RNA post-transcriptional processing steps and transportation to the cytoplasm (Köhler & Hurt 2007). In the specific case of mRNAs, the pre-mRNA splicing machinery is responsible for processing the transcripts, removing the intronic regions, and joining alternative exonic segments by the alternative splicing machinery (Shi 2017). Already at this stage, the composition of the various RNA populations is different between the nuclear and cytoplasmic fractions, since the transcripts contain a different ratio of exonic and intronic sequences. Generally, it was demonstrated that nuclear and cytoplasmic fractions contain overlapping RNA transcripts; however, there are also many transcripts that are unique to a specific fraction. For instance, nuclear mRNA retention could be one form of the mechanism to accumulate specific transcripts in the nucleus as compared to cytoplasm (Bahar Halpern et al. 2015). Nevertheless, protein-coding genes were found to be more equally distributed between these fractions whereas, lncRNAs and snoRNAs were more abundant in the nuclear fractions (Mas-Ponte et al. 2017, Zaghlool et al. 2020). If we consider recent studies that utilized nuclear RNA-seq, we notice that such

RNA populations predominantly re-appear in the transcriptomic analyses (Fernandez-Albert et al. 2019, Chongtham et al. 2021). For instance, Fernandez-Albert and colleagues (2019) reported an elevated induction of snoRNA and miRNA in their nucRNA-seq of neuronal cells (Fernandez-Albert et al. 2019). This suggests that the transcriptional analyses of nuclei could be bias towards these nuclear RNA populations. For this reason, all sequencing approaches that deal solely with nuclear RNA should be critically reflected and analyzed. The study of other RNA populations, such as small RNA, rRNA and RNA modifications, should also be handled with caution when nuclear RNA is analyzed. Future studies should uncover further the properties of nuclear and cytoplasmic (or whole cell) RNA and its different populations and modifications.

3.2 Experimental design of nuclear RNA-seq – Sequencing depth and analysis of exon versus intron reads

If we consider the percentage of intronic and exonic sequences in nuclear RNA, nuclei would contain largely unspliced transcripts (i.e., intron spanning), while the majority of spliced transcripts will be in the cytoplasm. On top of that, introns are known to have long sequences compared to exons, often ranging up to several thousands of base pairs (Wada et al. 2009, Georgomanolis, Sofiadis and Papantonis 2016). Therefore, an important aspect to consider is the sequencing depth and read length, since the distribution of reads can vary depending on the presence or absence of introns. Thus, it is crucial to select a suitable sequencing depth, depending on the biological question investigated. Nuclear RNA-seq will require higher sequencing depth to capture better the diluted exonic fraction compared to conventional RNA-seq. For instance, in the first reported nuclear RNA-seq, the authors analyzed the percentage of intron and exon reads (Mitchell et al. 2012). The authors reported that: "*nucRNA-Seq library showed a strong bias toward intronic reads as introns are generally much larger than exons (36% exonic)*" (Mitchell et al. 2012). In the study by Fernandez-Albert and colleagues (2019), the authors utilized up to 80 million reads for nuclear RNA-seq to obtain sufficient exonic reads for subsequent transcriptional analysis. Nevertheless, 80% of the aligned reads were intronic, revealing the strong bias of nucRNA-seq (Fernandez-Albert et al. 2019). Such differences can be experienced with nuclear RNA-seq, which was not previously considered with conventional RNA-seq (whole cell RNA-seq). Therefore, sequencing depth is an essential factor to consider for efficient interpretation of RNA-seq data (Mortazvi et al. 2008). However, we argue that the nuclear RNA properties are diverse from whole-cell or cytoplasmic RNA, and therefore sequencing properties should be planned accordingly.

3.3 Nuclear RNA quality and library preparation strategies

Two important aspects to consider before sequencing are measuring RNA quality and selecting an appropriate RNA library preparation strategy for sequencing. The investigation of rare cell populations often involves low initial cellular populations, making their subsequent analyses challenging to analyze and

interpret. Krishnaswami and colleagues (2016) provided a detailed protocol for the isolation of single nuclei and subsequent application using snRNA-seq in addition to supplemented bulk nucRNA-seq data. The authors comment on the potential challenges of nuclei transcriptional analyses, especially from neuronal nuclei (Krishnaswami et al. 2016). To detail their arguments, we will divide them into two major potential challenges that may influence nucRNA-seq data: nuclear RNA quality and library preparation.

RNA quality. The RNA integrity number (RIN) has been widely used as RNA quality measurement prior to library preparation and sequencing steps. RIN is measured by analyzing the proportion of 28S:18S rRNA peaks compared to degraded material using bioanalyzer instrument (Schroeder et al. 2006). Commonly, RIN values of >7 are often accepted as high-quality RNA that could be sequenced, whereas values below 7 suggest degraded and therefore lower quality RNA. RIN values can largely vary depending on the handling, storage, and concentrations of RNA material available. As Krishnaswami and colleagues (2016) noted, isolation of total bulk RNA, which is often isolated from high cell numbers, results in higher RIN and hence higher quality RNA. On the contrary, the authors comment that isolation from nuclei can result in varied RIN values (Krishnaswami et al. 2016). We reason that initial nuclei input material will affect the concentrations of the RNA and consequently the RIN values as well. Conceptually, higher concentrations of RNA will result in an increased constant ratio of 28S:18S rRNA peaks, allowing a more accurate estimation of the RIN value. In contrast, low input material will result in lower RNA concentrations that could largely affect the proper detection of 28S:18S rRNA peaks. These changes may be sufficient to result in varied RIN values that ultimately will prevent subsequent sequencing and analysis of such samples. Previous studies demonstrated the effects of RNA degradation and differential RIN values of whole cells on quality of conventional RNA-seq (Gellego Romero et al. 2014, Reiman et al. 2017). Overall, these studies conclude that useful information can be obtained from highly degraded samples (Gallego Romero et al. 2014). However, it is important to be aware of the potential biases that can arise during the experimental handling. It is recommended to minimize intergroup differences, such as in RNA quality (such as RIN values), to obtain comparable data. The emphasis of such studies should be directed towards critical data analysis, with an awareness of the potential effects of RNA quality on data interpretation (Reiman et al. 2017). Krishnaswami and colleagues (2016) go further and suggest that "*if RNA with a RIN score of <7 is all that is available, it should be tested and it may still yield valuable data"*. We agree with such views. However, we argue that further studies should determine the potential reasons for nuclear RNA variations concerning nuclear RNA degradation and its influence on nuclear RNA-seq.

An additional point that we would like to address regarding nuclear RNA quality is the attention of nuclear rRNA (ratio) using the bioanalyzer. We believe that many of the nuclei-based studies initially measure the RIN values as a routine RNA quality measure before library preparation and sequencing. However, due to variable RIN outcomes, which often do not reach the accepted value, such measurements are not always

reported in recent studies. Let's examine the studies that utilized nuclear RNA-seq. We see that several studies explicitly report the RIN values for nuclear RNA (Mo et al. 2015, Krishnaswami et al. 2016, Lacar et al. 2016, Kaul et al. 2020), while many others do not provide such information (Mitchel et al. 2012, Xu and Heller 2018, Lodato et al. 2017, Kenyon et al. 2017, Vilborg et al. 2017, Fernandez-Albert et al. 2019). These inconsistencies might reflect our partial understanding of RIN values together with nuclear RNA as compared to whole cell RNA. Therefore, future studies should evaluate the appropriateness of RIN as a quality indicator for nuclear RNA. As previously noted, all RNA populations' content can vary largely depending on the consideration between nuclear and whole-cell RNA content, including the rRNA fraction. Further investigations should determine if the proportions of rRNA present in the nucleus and whole-cell are comparable. It is possible that nuclear RNA does not reflect a constant ratio of rRNA (depending on transcription speed, transcript processing, or leakage from the nucleus to the cytoplasm), and therefore, nuclear RNA RIN values are not representative of nuclear RNA quality.

RNA library preparation strategies. An additional aspect that should be thoroughly considered is the choice of RNA library preparation strategy for nuclear RNA material. Multiple commercially available RNA library strategies provide different approaches to select specific RNA populations. Stark, Grzelak, and Hadfield (2019) provide an extensive review of the various facets of RNA-seq, including the selection of appropriate RNA library preparation strategies (Stark, Grzelak and Hadfield 2019). For the purposes of this report, we will focus on two main strategies for RNA library preparation: Poly(A) enrichment and rRNA depletion strategies. Poly(A) enrichment strategies are most commonly used for RNA-seq, underlining the selection of poly-adenylated transcripts, such as protein-coding genes (mRNAs) and lncRNA (Hrdlickova, Toloue and Tian 2017). This approach relies on high quality (non-degraded) RNA to select polyadenylated transcripts, since fragmentation or extremely long polyA regions can lead to 3'UTR coverage bias (Ma et al. 2019). Using this strategy, other RNA populations such as miRNAs and enhancer RNAs will not be detected due to the absence of a 3' polyA tail. On the contrary, rRNA depletion strategies rely on the exclusion of rRNA by bead separation or selective degradation (Stark, Grzelak, and Hadfield 2019). Although this approach requires high amounts of total RNA, commercial alternatives are available for low number of input material (Herbert et al. 2018, Haile et al. 2019). The choice between the different RNA library preparation strategies should be suitable for the investigation regardless of any selected type (nuclei or cells) or input amount (high or low) RNA. However, we reason that with the missing evidence regarding nuclear RNA, further investigation should focus on the best potential strategy for nuclear RNA. Nuclear RNA-seq analysis should be used with great caution, especially in combination with concomitant "omics" approaches. Even though multiple studies have compared nuclear and cytoplasmic or total RNA fractions, we displayed in this review many open questions yet to be addressed regarding the properties of nuclear RNA, particularly in association with RNA-seq.

3.4 Nuclear RNA-seq and proper use of novel terminology

Lastly, we would like to comment about the appropriate use of terminology, particularly with the use of nuclear and whole cell/cytoplasmic RNA-seq. We refer to using a specific approach by the defined designation attributed to the particular technique by terminology. Through our previous work and analysis of INTACT and FANS publications, we noticed how the used terminology could be an essential factor for scientific accuracy and interpretation, especially with the development of novel methodologies. For instance, the term FACS has been widely and frequently used to describe the sorting of cells using a flow cytometry approach prior to the report of the first FANS approach (Mitchel et al. 2012). Through the analysis, we found a few studies that even though nuclei were explicitly used in the work, FACS was still described as a technique of cytometry isolation (Krishnaswami et al. 2016, Bakken et al. 2018). Another example of such alteration is the general use of the term RNA-seq contrary to nucRNA-seq (or similarly nuRNA-seq) (Lacar et al. 2016, Krishnaswami et al. 2016, Chamessian et al. 2018). We found a few examples for such misplaced use as well. As we emphasized in this survey, nuclei and whole cells' properties are different at several levels. Therefore, it is crucial to use appropriate terminology to describe specific approaches. It is comprehensible that using a particular term depends on the use frequency and acceptance among the scientific community. However, we underline that appropriate terminology use should be practiced and attained in order to report accurate and reproducible information for future investigations.

Overall, we presented the challenges that nuclei-based studies still face, particularly at the transcriptomic level, summarized in Table 1. Nuclear RNA and total or cytoplasmic RNA are fundamentally different and therefore should be analyzed and interpreted accordingly. Being aware of these challenges can only improve and provide more accurate biological information for various scientific investigations.

Conclusions

The use of nuclei for molecular investigations has become a precedent part of the current scientific practice. We believe that the continuous utilization and application of this particular cellular component is only rational and will rise further, mainly since the multifaceted epigenetic mechanisms are increasingly investigated (Fig 4A). With the development of novel cell type-specific (e.g., INTACT) and epigenetic methodologies (e.g., ATAC-seq), nuclei have become a comfortable biological tool to explore the different properties of cellular specificity, especially in complex *in-vivo* systems. Additionally, due to the simple acquisition, nuclei are gradually incorporated into single cell studies providing an alternative to whole-cell data analyses. However, with the significant advantages that nuclei-based studies offer, it is crucial to identify the future challenges. Here, we presented the potential problems that nuclei-based studies still face, particularly concerning the transcriptomic analyses and data acquisition of nuclear RNA-seq compared to conventional RNA-seq approaches (Table 1, Fig. 4B). We believe that nuclear RNA is still under-studied, as there are many questions about its constitution and comparison to whole-cell RNA, which need to be addressed. As pointed out, future studies should determine the relevance of RIN values on nuclear RNA as well as the most suitable RNA library preparation strategy for nuclear RNA-seq. Understanding these differences between nuclear and whole cell (or cytoplasmic) RNA will be crucial for developing and applying the next phase of nuclei-based studies at bulk and single cell levels. We are confident that with increasing interest and use of nuclei-based studies, these challenges will be addressed, and as a result, the full potential of nuclei-based studies will be unlocked.

Table 1. Considerations for nuclear transcriptomic analyses compared to whole cells

Consideration	Nuclei	Whole cells
Transcripts composition	Mostly full length transcripts (including large introns)	Mixed – spliced and full length transcripts
RNA population bias	Mainly nuclear transcripts including Snors and lncRNA	Mainly protein encoding transcripts
RNA quality (RIN)	Only nuclear rRNA present	Whole cell rRNA present
Library preparation	Depending on investigation and desired RNA population. PolyA enrichment – enrich mainly mRNA populations (require unfragmented RNA) rRNA depletion- enrich general RNA populations excluding rRNA	
	Take in consideration specific cell type transcript's properties in combination with nuclear RNA (e.g. extremely long poly A)	-
Sequencing requirements	Higher sequencing depth due to high intronic mapping bias (depending on purpose)	Classic sequencing depth (depending on purpose)
Terminology	nucRNA-seq or nuRNA-seq	RNA-seq

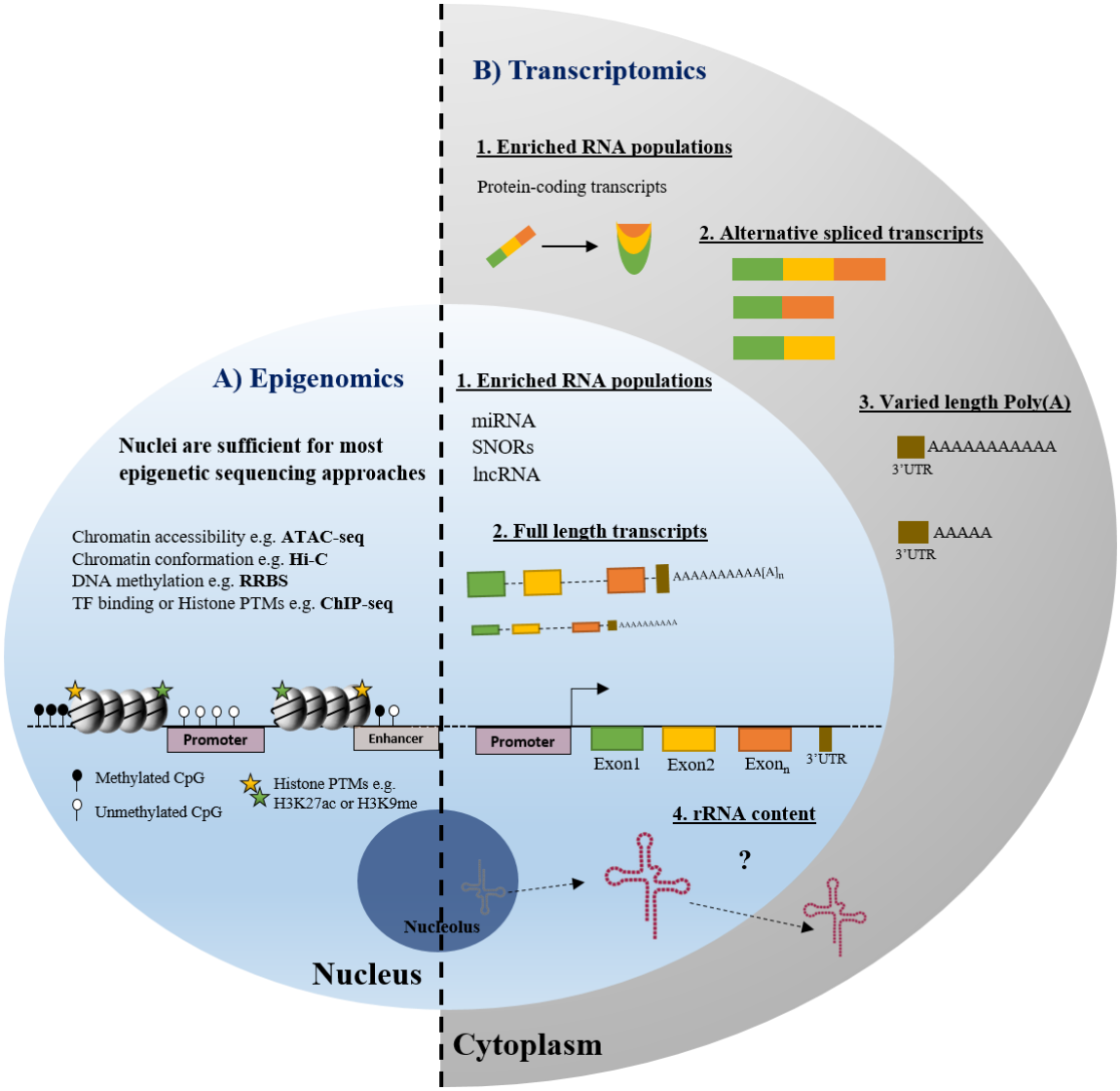

Figure 4. Overview of the application of nuclei-based studies with next-generation sequencing approaches. A. Epigeneomic - The use of nuclei is sufficient for most epigenetic sequencing approaches as the content of interest (e.g. Histones and chromatin-associated modifications) is located within the nucleus. B. Transcriptomics- Differences between nuclear and cytoplasmic transcripts in terms of: 1. Distinct enriched RNA populations, 2. Distinct intronic and exonic transcript ratio, 3. Distinct length of poly-adenylated transcripts, 4. Distinct rRNA content.

Author Contributions

T.B designed and performed the literature study, analyzed the data, and wrote the manuscript. S.G., J.W. and B.L. supervised the project and contributed to writing and editing the manuscript. All authors have read and agreed to the published version of the manuscript.

Funding

The work of T.B. was funded in part by the Resilience, Adaptation, and Longevity (ReALity) initiative of the Johannes Gutenberg University of Mainz and by the DFG through subproject A05 of the Collaborative Research Center (CRC) 1193 (“Neurobiology of Resilience”).

References

1) Devos, D. P., Gräf, R., & Field, M. C. (2014). Evolution of the nucleus. In *Current Opinion in Cell Biology* (Vol. 28, Issue 1, pp. 8–15). Elsevier. https://doi.org/10.1016/j.ceb.2014.01.004

2) Ji, P., Murata-Hori, M., & Lodish, H. F. (2011). Formation of mammalian erythrocytes: Chromatin condensation and enucleation. In *Trends in Cell Biology* (Vol. 21, Issue 7, pp. 409–415). Trends Cell Biol. https://doi.org/10.1016/j.tcb.2011.04.003

3) Garraud, O., & Cognasse, F. (2015). Are platelets cells? And if yes, are they immune cells? In *Frontiers in Immunology* (Vol. 6, Issue FEB, p. 70). Frontiers Media S.A. https://doi.org/10.3389/fimmu.2015.00070

4) Shah, P., Wolf, K., & Lammerding, J. (2017). Bursting the Bubble – Nuclear Envelope Rupture as a Path to Genomic Instability? In *Trends in Cell Biology* (Vol. 27, Issue 8, pp. 546–555). Elsevier Ltd. https://doi.org/10.1016/j.tcb.2017.02.008

5) Klemm, S. L., Shipony, Z., & Greenleaf, W. J. (2019). Chromatin accessibility and the regulatory epigenome. In *Nature Reviews Genetics* (Vol. 20, Issue 4, pp. 207–220). Nature Publishing Group. https://doi.org/10.1038/s41576-018-0089-8

6) Pederson, T. (2011). The nucleus introduced. *Cold Spring Harbor Perspectives in Biology*, *3*(5), 1–16. https://doi.org/10.1101/cshperspect.a000521

7) Illumina. (2014). *An introduction to Next-Generation Sequencing Technology*. Retrieved from www.illumina.com/technology/next-generation-sequencing.html

8) Shapiro, E., Biezuner, T., & Linnarsson, S. (2013). Single-cell sequencing-based technologies will revolutionize whole-organism science. In *Nature Reviews Genetics* (Vol. 14, Issue 9, pp. 618–630). Nat Rev Genet. https://doi.org/10.1038/nrg3542

9) Stuart, T., & Satija, R. (2019). Integrative single-cell analysis. In *Nature Reviews Genetics* (Vol. 20, Issue 5, pp. 257–272). Nature Publishing Group. https://doi.org/10.1038/s41576-019-0093-7

10) Morange, M. (2009). The Central Dogma of molecular biology. *Resonance*, *14*(3), 236–247. https://doi.org/10.1007/s12045-009-0024-6

11) Handley, A., Schauer, T., Ladurner, A. G., & Margulies, C. E. (2015). Designing Cell-Type-Specific Genome-wide Experiments. In *Molecular Cell* (Vol. 58, Issue 4, pp. 621–631). Cell Press. https://doi.org/10.1016/j.molcel.2015.04.024

12) Deal, R. B., & Henikoff, S. (2010). A simple method for gene expression and chromatin profiling of individual cell types within a tissue. *Developmental Cell*, *18*(6), 1030–1040. https://doi.org/10.1016/j.devcel.2010.05.013

13) Deal, R. B., & Henikoff, S. (2011). The INTACT method for cell typeg-specific gene expression and chromatin profiling in Arabidopsis thaliana. *Nature Protocols*, *6*(1), 56–68. https://doi.org/10.1038/nprot.2010.175

14) Steiner, F. A., Talbert, P. B., Kasinathan, S., Deal, R. B., & Henikoff, S. (2012). Cell-type-specific nuclei purification from whole animals for genome-wide expression and chromatin profiling. *Genome Research*, *22*(4), 766–777. https://doi.org/10.1101/gr.131748.111

15) Henry, G. L., Davis, F. P., Picard, S., & Eddy, S. R. (2012). Cell type-specific genomics of Drosophila neurons. *Nucleic Acids Research*, *40*(19), 9691–9704. https://doi.org/10.1093/nar/gks671

16) Mo, A., Mukamel, E. A., Davis, F. P., Luo, C., Henry, G. L., Picard, S., Urich, M. A., Nery, J. R., Sejnowski, T. J., Lister, R., Eddy, S. R., Ecker, J. R., & Nathans, J. (2015). Epigenomic Signatures of

Neuronal Diversity in the Mammalian Brain. *Neuron*, *86*(6), 1369–1384. https://doi.org/10.1016/j.neuron.2015.05.018

17) Mo, A., Luo, C., Davis, F. P., Mukamel, E. A., Henry, G. L., Nery, J. R., Urich, M. A., Picard, S., Lister, R., Eddy, S. R., Beer, M. A., Ecker, J. R., & Nathans, J. (2016). Epigenomic landscapes of retinal rods and cones. *ELife*, *5*(MARCH2016). https://doi.org/10.7554/eLife.11613

18) Chongtham, M.C.; Butto, T.; Mungikar, K.; Gerber, S.; Winter, J. INTACT vs. FANS for Cell-Type-Specific Nuclei Sorting: A Comprehensive Qualitative and Quantitative Comparison. *Int. J. Mol. Sci.* **2021**, *22*, 5335. https://doi.org/10.3390/ijms22105335

19) Jiang, Y., Matevossian, A., Huang, H. S., Straubhaar, J., & Akbarian, S. (2008). Isolation of neuronal chromatin from brain tissue. *BMC Neuroscience*, *9*. https://doi.org/10.1186/1471-2202-9-42

20) Haenni, S., Ji, Z., Hoque, M., Rust, N., Sharpe, H., Eberhard, R., Browne, C., Hengartner, M. O., Mellor, J., Tian, B., & Furger, A. (2012). Analysis of C. elegans intestinal gene expression and polyadenylation by fluorescence-activated nuclei sorting and 3′-end-seq. *Nucleic Acids Research*, *40*(13), 6304–6318. https://doi.org/10.1093/nar/gks282

21) Mitchell, J. A., Clay, I., Umlauf, D., Chen, C. yu, Moir, C. A., Eskiw, C. H., Schoenfelder, S., Chakalova, L., Nagano, T., & Fraser, P. (2012). Nuclear RNA Sequencing of the Mouse Erythroid Cell Transcriptome. *PLoS ONE*, *7*(11). https://doi.org/10.1371/journal.pone.0049274

22) Besser, J., Carleton, H. A., Gerner-Smidt, P., Lindsey, R. L., & Trees, E. (2018). Next-generation sequencing technologies and their application to the study and control of bacterial infections. In *Clinical Microbiology and Infection* (Vol. 24, Issue 4, pp. 335–341). Elsevier B.V. https://doi.org/10.1016/j.cmi.2017.10.013

23) Chen, Z., Li, S., Subramaniam, S., Shyy, J. Y.-J., & Chien, S. (2017). Epigenetic Regulation: A New Frontier for Biomedical Engineers. *Annual Review of Biomedical Engineering*, *19*(1), 195–219. https://doi.org/10.1146/annurev-bioeng-071516-044720

24) Skvortsova, K., Iovino, N., & Bogdanović, O. (2018). Functions and mechanisms of epigenetic inheritance in animals. In *Nature Reviews Molecular Cell Biology* (Vol. 19, Issue 12, pp. 774–790). Nature Publishing Group. https://doi.org/10.1038/s41580-018-0074-2

25) Wang, Y. C., Peterson, S. E., & Loring, J. F. (2014). Protein post-translational modifications and regulation of pluripotency in human stem cells. In *Cell Research* (Vol. 24, Issue 2, pp. 143–160). Cell Res. https://doi.org/10.1038/cr.2013.151

26) Tsompana, M., & Buck, M. J. (2014). Chromatin accessibility: A window into the genome. In *Epigenetics and Chromatin* (Vol. 7, Issue 1, pp. 1–16). BioMed Central Ltd. https://doi.org/10.1186/1756-8935-7-33

27) Kempfer, R., & Pombo, A. (2020). Methods for mapping 3D chromosome architecture. In *Nature Reviews Genetics* (Vol. 21, Issue 4, pp. 207–226). Nature Research. https://doi.org/10.1038/s41576-019-0195-2

28) Barros-Silva, D., Marques, C. J., Henrique, R., & Jerónimo, C. (2018). Profiling DNA methylation based on next-generation sequencing approaches: New insights and clinical applications. In *Genes* (Vol. 9, Issue 9). MDPI AG. https://doi.org/10.3390/genes9090429

29) Buenrostro, J. D., Giresi, P. G., Zaba, L. C., Chang, H. Y., & Greenleaf, W. J. (2013). Transposition of native chromatin for fast and sensitive epigenomic profiling of open chromatin, DNA-binding proteins and nucleosome position. *Nature Methods*, *10*(12), 1213–1218. https://doi.org/10.1038/nmeth.2688

30) Buenrostro, J. D., Wu, B., Chang, H. Y., & Greenleaf, W. J. (2015). ATAC-seq: A method for assaying chromatin accessibility genome-wide. *Current Protocols in Molecular Biology*, *2015*, 21.29.1-21.29.9. https://doi.org/10.1002/0471142727.mb2129s109

31) Li, Z., Schulz, M. H., Look, T., Begemann, M., Zenke, M., & Costa, I. G. (2019). Identification of transcription factor binding sites using ATAC-seq. *Genome Biology*, *20*(1), 45. https://doi.org/10.1186/s13059-019-1642-2

32) Bhattacharyya, S., Sathe, A. A., Bhakta, M., Xing, C., & Munshi, N. V. (2019). PAN-INTACT enables direct isolation of lineage-specific nuclei from fibrous tissues. *PLoS ONE*, *14*(4). https://doi.org/10.1371/journal.pone.0214677

33) Corces, M. R., Trevino, A. E., Hamilton, E. G., Greenside, P. G., Sinnott-Armstrong, N. A., Vesuna, S., Satpathy, A. T., Rubin, A. J., Montine, K. S., Wu, B., Kathiria, A., Cho, S. W., Mumbach, M. R., Carter, A. C., Kasowski, M., Orloff, L. A., Risca, V. I., Kundaje, A., Khavari, P. A., … Chang, H. Y. (2017). An improved ATAC-seq protocol reduces background and enables interrogation of frozen tissues. *Nature Methods*, *14*(10), 959–962. https://doi.org/10.1038/nmeth.4396

34) Milani, P., Escalante-Chong, R., Shelley, B. C., Patel-Murray, N. L., Xin, X., Adam, M., Mandefro, B., Sareen, D., Svendsen, C. N., & Fraenkel, E. (2016). Cell freezing protocol suitable for ATAC-Seq on motor neurons derived from human induced pluripotent stem cells. *Scientific Reports*, *6*(1), 1–10. https://doi.org/10.1038/srep25474

35) Fujiwara, S., Baek, S., Varticovski, L., Kim, S., & Hager, G. L. (2019). High Quality ATAC-Seq Data Recovered from Cryopreserved Breast Cell Lines and Tissue. *Scientific Reports*, *9*(1), 1–11. https://doi.org/10.1038/s41598-018-36927-7

36) Chen, X., Shen, Y., Draper, W., Buenrostro, J. D., Litzenburger, U., Cho, S. W., Satpathy, A. T., Carter, A. C., Ghosh, R. P., East-Seletsky, A., Doudna, J. A., Greenleaf, W. J., Liphardt, J. T., & Chang, H. Y. (2016). ATAC-see reveals the accessible genome by transposase-mediated imaging and sequencing. *Nature Methods*, *13*(12), 1013–1020. https://doi.org/10.1038/nmeth.4031

37) Lieberman-Aiden, E., Van Berkum, N. L., Williams, L., Imakaev, M., Ragoczy, T., Telling, A., Amit, I., Lajoie, B. R., Sabo, P. J., Dorschner, M. O., Sandstrom, R., Bernstein, B., Bender, M. A., Groudine, M., Gnirke, A., Stamatoyannopoulos, J., Mirny, L. A., Lander, E. S., & Dekker, J. (2009). Comprehensive mapping of long-range interactions reveals folding principles of the human genome. *Science*, *326*(5950), 289–293. https://doi.org/10.1126/science.1181369

38) Oluwadare, O., Highsmith, M., & Cheng, J. (2019). An Overview of Methods for Reconstructing 3-D Chromosome and Genome Structures from Hi-C Data. In *Biological Procedures Online* (Vol. 21, Issue 1). BioMed Central Ltd. https://doi.org/10.1186/s12575-019-0094-0

39) Chauveau, J., Moulé, Y., & Rouiller, C. (1956). Isolation of pure and unaltered liver nuclei morphology and biochemical composition. *Experimental Cell Research*, *11*(2), 317–321. https://doi.org/10.1016/0014-4827(56)90107-0

40) Hadjiolov, A. A., Tencheva, Z. S., & Bojadjieva-Mikhailova, A. G. (1965). Isolation and some characteristics of cell nuclei from brain cortex of adult cat. *The Journal of Cell Biology*, *26*(2), 383–393. https://doi.org/10.1083/jcb.26.2.383

41) Zylber, E. A., & Penman, S. (1971). Products of RNA polymerases in HeLa cell nuclei. *Proceedings of the National Academy of Sciences of the United States of America*, *68*(11), 2861–2865. https://doi.org/10.1073/pnas.68.11.2861

42) Slyper, M., Porter, C. B. M., Ashenberg, O., Waldman, J., Drokhlyansky, E., Wakiro, I., Smillie, C., Smith-Rosario, G., Wu, J., Dionne, D., Vigneau, S., Jané-Valbuena, J., Tickle, T. L., Napolitano, S., Su, M. J., Patel, A. G., Karlstrom, A., Gritsch, S., Nomura, M., … Regev, A. (2020). A single-cell and single-nucleus RNA-Seq toolbox for fresh and frozen human tumors. *Nature Medicine*, *26*(5), 792–802. https://doi.org/10.1038/s41591-020-0844-1

43) Tomlinson, M. J., Tomlinson, S., Yang, X. B., & Kirkham, J. (2013). Cell separation: Terminology and practical considerations. In *Journal of Tissue Engineering* (Vol. 4, Issue 1, pp. 1–14). SAGE Publications

Ltd. https://doi.org/10.1177/2041731412472690

44) Almeida, M., Garcia-Montero, A. C., & Orfao, A. (2015). Cell Purification: A New Challenge for Biobanks. *Pathobiology*, *81*(5–6), 261–275. https://doi.org/10.1159/000358306

45) Denisenko E, Guo BB, Jones M, et al. Systematic assessment of tissue dissociation and storage biases in single-cell and single-nucleus RNA-seq workflows. *Genome Biol*. 2020;21(1):130. https://doi.org/10.1186/s13059-020-02048-6

46) Hwang, B., Lee, J. H., & Bang, D. (2018). Single-cell RNA sequencing technologies and bioinformatics pipelines. In *Experimental and Molecular Medicine* (Vol. 50, Issue 8, p. 96). Nature Publishing Group. https://doi.org/10.1038/s12276-018-0071-8

47) Buettner, F., Natarajan, K. N., Casale, F. P., Proserpio, V., Scialdone, A., Theis, F. J., Teichmann, S. A., Marioni, J. C., & Stegle, O. (2015). Computational analysis of cell-to-cell heterogeneity in single-cell RNA-sequencing data reveals hidden subpopulations of cells. *Nature Biotechnology*, *33*(2), 155–160. https://doi.org/10.1038/nbt.3102

48) Barthelson, R. A., Lambert, G. M., Vanier, C., Lynch, R. M., & Galbraith, D. W. (2007). Comparison of the contributions of the nuclear and cytoplasmic compartments to global gene expression in human cells. *BMC Genomics*, *8*(1), 340. https://doi.org/10.1186/1471-2164-8-340

49) Solnestam, B. W., Stranneheim, H., Hällman, J., Käller, M., Lundberg, E., Lundeberg, J., & Akan, P. (2012). Comparison of total and cytoplasmic mRNA reveals global regulation by nuclear retention and miRNAs. *BMC Genomics*, *13*(1), 574. https://doi.org/10.1186/1471-2164-13-574

50) Price, A. J., Hwang, T., Tao, R., Burke, E. E., Rajpurohit, A., Shin, J. H., Hyde, T. M., Kleinman, J. E., Jaffe, A. E., & Weinberger, D. R. (2020). Characterizing the nuclear and cytoplasmic transcriptomes in developing and mature human cortex uncovers new insight into psychiatric disease gene regulation. *Genome Research*, *30*(1), 1–11. https://doi.org/10.1101/gr.250217.119

51) Guez-Barber D, Fanous S, Harvey BK, et al. FACS purification of immunolabeled cell types from adult rat brain. *J Neurosci Methods*. 2012;203(1):10-18. https://doi.org/10.1016/j.jneumeth.2011.08.045

52) Fernandez-Albert, J., Lipinski, M., Lopez-Cascales, M. T., Rowley, M. J., Martin-Gonzalez, A. M., del Blanco, B., Corces, V. G., & Barco, A. (2019). Immediate and deferred epigenomic signatures of in vivo neuronal activation in mouse hippocampus. *Nature Neuroscience*, *22*(10), 1718–1730. https://doi.org/10.1038/s41593-019-0476-2

53) Hasin, Y., Seldin, M., & Lusis, A. (2017). Multi-omics approaches to disease. In *Genome Biology* (Vol. 18, Issue 1, pp. 1–15). BioMed Central Ltd. https://doi.org/10.1186/s13059-017-1215-1

54) Pinu, F. R., Beale, D. J., Paten, A. M., Kouremenos, K., Swarup, S., Schirra, H. J., & Wishart, D. (2019). Systems biology and multi-omics integration: Viewpoints from the metabolomics research community. *Metabolites*, *9*(4). https://doi.org/10.3390/metabo9040076

55) Krishnaswami, S. R., Grindberg, R. V., Novotny, M., Venepally, P., Lacar, B., Bhutani, K., Linker, S. B., Pham, S., Erwin, J. A., Miller, J. A., Hodge, R., McCarthy, J. K., Kelder, M., McCorrison, J., Aevermann, B. D., Fuertes, F. D., Scheuermann, R. H., Lee, J., Lein, E. S., … Lasken, R. S. (2016). Using single nuclei for RNA-seq to capture the transcriptome of postmortem neurons. *Nature Protocols*, *11*(3), 499–524. https://doi.org/10.1038/nprot.2016.015

56) Jia, G., Preussner, J., Chen, X., Guenther, S., Yuan, X., Yekelchyk, M., Kuenne, C., Looso, M., Zhou, Y., Teichmann, S., & Braun, T. (2018). Single cell RNA-seq and ATAC-seq analysis of cardiac progenitor cell transition states and lineage settlement. *Nature Communications*, *9*(1), 1–17. https://doi.org/10.1038/s41467-018-07307-6

57) Reyes, M., Billman, K., Hacohen, N., & Blainey, P. C. (2019). Simultaneous Profiling of Gene Expression and Chromatin Accessibility in Single Cells. *Advanced Biosystems*, *3*(11), 1900065. https://doi.org/10.1002/adbi.201900065

58) Liu, L., Liu, C., Quintero, A., Wu, L., Yuan, Y., Wang, M., Cheng, M., Leng, L., Xu, L., Dong, G., Li, R., Liu, Y., Wei, X., Xu, J., Chen, X., Lu, H., Chen, D., Wang, Q., Zhou, Q., … Xu, X. (2019). Deconvolution of single-cell multi-omics layers reveals regulatory heterogeneity. *Nature Communications*, *10*(1), 1–10. https://doi.org/10.1038/s41467-018-08205-7

59) Grindberg, R. V., Yee-Greenbaum, J. L., McConnell, M. J., Novotny, M., O'Shaughnessy, A. L., Lambert, G. M., Araúzo-Bravo, M. J., Lee, J., Fishman, M., Robbins, G. E., Lin, X., Venepally, P., Badger, J. H., Galbraith, D. W., Gage, F. H., & Lasken, R. S. (2013). RNA-sequencing from single nuclei. *Proceedings of the National Academy of Sciences of the United States of America*, *110*(49), 19802–19807. https://doi.org/10.1073/pnas.1319700110

60) Lacar, B., Linker, S. B., Jaeger, B. N., Krishnaswami, S., Barron, J., Kelder, M., Parylak, S., Paquola, A., Venepally, P., Novotny, M., O'Connor, C., Fitzpatrick, C., Erwin, J., Hsu, J. Y., Husband, D., McConnell, M. J., Lasken, R., & Gage, F. H. (2016). Nuclear RNA-seq of single neurons reveals molecular signatures of activation. *Nature Communications*, *7*(1), 1–13. https://doi.org/10.1038/ncomms11022

61) Bakken, T. E., Hodge, R. D., Miller, J. A., Yao, Z., Nguyen, T. N., Aevermann, B., Barkan, E., Bertagnolli, D., Casper, T., Dee, N., Garren, E., Goldy, J., Graybuck, L. T., Kroll, M., Lasken, R. S., Lathia, K., Parry, S., Rimorin, C., Scheuermann, R. H., … Tasic, B. (2018). Single-nucleus and single-cell transcriptomes compared in matched cortical cell types. *PLOS ONE*, *13*(12), e0209648. https://doi.org/10.1371/journal.pone.0209648

62) Korrapati, S., Taukulis, I., Olszewski, R., Pyle, M., Gu, S., Singh, R., Griffiths, C., Martin, D., Boger, E., Morell, R. J., & Hoa, M. (2019). Single Cell and Single Nucleus RNA-Seq Reveal Cellular Heterogeneity and Homeostatic Regulatory Networks in Adult Mouse Stria Vascularis. *Frontiers in Molecular Neuroscience*, *12*. https://doi.org/10.3389/fnmol.2019.00316

63) Kang, H. M., Subramaniam, M., Targ, S., Nguyen, M., Maliskova, L., McCarthy, E., Wan, E., Wong, S., Byrnes, L., Lanata, C. M., Gate, R. E., Mostafavi, S., Marson, A., Zaitlen, N., Criswell, L. A., & Ye, C. J. (2018). Multiplexed droplet single-cell RNA-sequencing using natural genetic variation. *Nature Biotechnology*, *36*(1), 89–94. https://doi.org/10.1038/nbt.4042

64) Stoeckius, M., Zheng, S., Houck-Loomis, B., Hao, S., Yeung, B. Z., Mauck, W. M., Smibert, P., & Satija, R. (2018). Cell Hashing with barcoded antibodies enables multiplexing and doublet detection for single cell genomics. *Genome Biology*, *19*(1), 224. https://doi.org/10.1186/s13059-018-1603-1

65) Köhler, A., & Hurt, E. (2007). Exporting RNA from the nucleus to the cytoplasm. In *Nature Reviews Molecular Cell Biology* (Vol. 8, Issue 10, pp. 761–773). Nat Rev Mol Cell Biol. https://doi.org/10.1038/nrm2255

66) Shi, Y. (2017). Mechanistic insights into precursor messenger RNA splicing by the spliceosome. In *Nature Reviews Molecular Cell Biology* (Vol. 18, Issue 11, pp. 655–670). Nature Publishing Group. https://doi.org/10.1038/nrm.2017.86

67) Bahar Halpern, K., Caspi, I., Lemze, D., Levy, M., Landen, S., Elinav, E., Ulitsky, I., & Itzkovitz, S. (2015). Nuclear Retention of mRNA in Mammalian Tissues. *Cell Reports*, *13*(12), 2653–2662. https://doi.org/10.1016/j.celrep.2015.11.036

68) Mas-Ponte, D., Carlevaro-Fita, J., Palumbo, E., Pulido, T. H., Guigo, R., & Johnson, R. (2017). LncATLAS database for subcellular localization of long noncoding RNAs. *RNA*, *23*(7), 1080–1087. https://doi.org/10.1261/rna.060814.117

69) Zaghlool, S. B., Kühnel, B., Elhadad, M. A., Kader, S., Halama, A., Thareja, G., Engelke, R., Sarwath, H., Al-Dous, E. K., Mohamoud, Y. A., Meitinger, T., Wilson, R., Strauch, K., Peters, A., Mook-Kanamori, D. O., Graumann, J., Malek, J. A., Gieger, C., Waldenberger, M., & Suhre, K. (2020). Epigenetics meets proteomics in an epigenome-wide association study with circulating blood plasma protein traits. *Nature Communications*, *11*(1), 1–12. https://doi.org/10.1038/s41467-019-13831-w

70) Wada, Y., Ohta, Y., Xu, M., Tsutsumi, S., Minami, T., Inoue, K., Komura, D., Kitakami, J., Oshida, N., Papantonis, A., Izumi, A., Kobayashi, M., Meguro, H., Kanki, Y., Mimura, I., Yamamoto, K., Mataki, C., Hamakubo, T., Shirahige, K., … Ihara, S. (2009). A wave of nascent transcription on activated human genes. *Proceedings of the National Academy of Sciences of the United States of America*, *106*(43), 18357–18361. https://doi.org/10.1073/pnas.0902573106

71) Georgomanolis, T., Sofiadis, K., & Papantonis, A. (2016). Cutting a long intron short: Recursive splicing and its implications. *Frontiers in Physiology*, *7*(NOV). https://doi.org/10.3389/fphys.2016.00598

72) Mortazavi, A., Williams, B. A., McCue, K., Schaeffer, L., & Wold, B. (2008). Mapping and quantifying mammalian transcriptomes by RNA-Seq. *Nature Methods*, *5*(7), 621–628. https://doi.org/10.1038/nmeth.1226

73) Schroeder, A., Mueller, O., Stocker, S., Salowsky, R., Leiber, M., Gassmann, M., Lightfoot, S., Menzel, W., Granzow, M., & Ragg, T. (2006). The RIN: An RNA integrity number for assigning integrity values to RNA measurements. *BMC Molecular Biology*, *7*. https://doi.org/10.1186/1471-2199-7-3

74) Gallego Romero, I., Pai, A. A., Tung, J., & Gilad, Y. (2014). RNA-seq: Impact of RNA degradation on transcript quantification. *BMC Biology*, *12*(1), 42. https://doi.org/10.1186/1741-7007-12-42

75) Reiman, M., Laan, M., Rull, K., & Sõber, S. (2017). Effects of RNA integrity on transcript quantification by total RNA sequencing of clinically collected human placental samples. *The FASEB Journal*, *31*(8), 3298–3308. https://doi.org/10.1096/fj.201601031RR

76) Kaul, T., Morales, M. E., Sartor, A. O., Belancio, V. P., & Deininger, P. (2020). Comparative analysis on the expression of L1 loci using various RNA-Seq preparations. *Mobile DNA*, *11*(1), 2. https://doi.org/10.1186/s13100-019-0194-z

77) Xu, S. J., & Heller, E. A. (2018). Single sample sequencing (S3EQ) of epigenome and transcriptome in nucleus accumbens. *Journal of Neuroscience Methods*, *308*, 62–73. https://doi.org/10.1016/j.jneumeth.2018.07.006

78) Lodato, N. J., Melia, T., Rampersaud, A., & Waxman, D. J. (2017). Sex-Differential Responses of Tumor Promotion-Associated Genes and Dysregulation of Novel Long Noncoding RNAs in Constitutive Androstane Receptor-Activated Mouse Liver. *Toxicological Sciences*, *159*(1), 25–41. https://doi.org/10.1093/toxsci/kfx114

79) Kenyon, A., Gavriouchkina, D., Zorman, J., Napolitani, G., Cerundolo, V., & Sauka-Spengler, T. (2017). Active nuclear transcriptome analysis reveals inflammasome-dependent mechanism for early neutrophil response to Mycobacterium marinum. *Scientific Reports*, *7*(1), 1–14. https://doi.org/10.1038/s41598-017-06099-x

80) Vilborg, A., Sabath, N., Wiesel, Y., Nathans, J., Levy-Adam, F., Yario, T. A., Steitz, J. A., & Shalgi, R. (2017). Comparative analysis reveals genomic features of stress-induced transcriptional readthrough. *Proceedings of the National Academy of Sciences of the United States of America*, *114*(40), E8362–E8371. https://doi.org/10.1073/pnas.1711120114

81) Stark, R., Grzelak, M., & Hadfield, J. (2019). RNA sequencing: the teenage years. In *Nature Reviews Genetics* (Vol. 20, Issue 11, pp. 631–656). Nature Publishing Group. https://doi.org/10.1038/s41576-019-0150-2

82) Hrdlickova, R., Toloue, M., & Tian, B. (2017). RNA-Seq methods for transcriptome analysis. In *Wiley Interdisciplinary Reviews: RNA* (Vol. 8, Issue 1). Blackwell Publishing Ltd. https://doi.org/10.1002/wrna.1364

83) Ma, F., Fuqua, B. K., Hasin, Y., Yukhtman, C., Vulpe, C. D., Lusis, A. J., & Pellegrini, M. (2019). A comparison between whole transcript and 3' RNA sequencing methods using Kapa and Lexogen library preparation methods 06 Biological Sciences 0604 Genetics. *BMC Genomics*, *20*(1), 9. https://doi.org/10.1186/s12864-018-5393-3

84) Herbert, Z. T., Kershner, J. P., Butty, V. L., Thimmapuram, J., Choudhari, S., Alekseyev, Y. O., Fan, J., Podnar, J. W., Wilcox, E., Gipson, J., Gillaspy, A., Jepsen, K., BonDurant, S. S., Morris, K., Berkeley, M., LeClerc, A., Simpson, S. D., Sommerville, G., Grimmett, L., … Levine, S. S. (2018). Cross-site comparison of ribosomal depletion kits for Illumina RNAseq library construction. *BMC Genomics*, *19*(1), 199. https://doi.org/10.1186/s12864-018-4585-1

85) Haile, S., Corbett, R. D., Bilobram, S., Mungall, K., Grande, B. M., Kirk, H., Pandoh, P., MacLeod, T., McDonald, H., Bala, M., Coope, R. J., Moore, R. A., Mungall, A. J., Zhao, Y., Morin, R. D., Jones, S. J., & Marra, M. A. (2019). Evaluation of protocols for rRNA depletion-based RNA sequencing of nanogram inputs of mammalian total RNA. *PLoS ONE*, *14*(10). https://doi.org/10.1371/journal.pone.0224578

86) Chamessian, A., Young, M., Qadri, Y., Berta, T., Ji, R. R., & Van De Ven, T. (2018). Transcriptional Profiling of Somatostatin Interneurons in the Spinal Dorsal Horn. *Scientific Reports*, *8*(1), 6809. https://doi.org/10.1038/s41598-018-25110-7

Chapter 3 – Overall discussion and outlook

3.1 General outlook

As presented in the thesis, epigenetic mechanisms provide a prospect for cellular change and adaptability that could aid in understand specific diseased/healthy phenotypes. The following points summarize the major findings of each study concerning epigenetic role in resilience and adaptability:

Section 1

Case study 1: The HDAC inhibitor (CI-994) is able to partially rescue BBIDS symptoms in the mouse model (*Kcnk9*KO^{mat}). The levels of H3K27ac (as well as H3K4me1) were measured in selected genomic loci (promoter and enhancer) of the hippocampus and locus coeruleus brain regions following CI-994 treatment. CI-994 treatment increased H3K27ac depositions at the tested regulatory regions. Allele-specific ChIP revealed higher H3K27ac deposition at the paternal allele compared to the maternal allele suggesting a targeted mechanism, which is probably influenced by the unique molecular micro-environment present in the *Kcnk9*KO^{mat} mice.

Case study 2: Six fecal miRNA candidates were identified to be differentially expressed following chronic social stress (CSS) exposure. Using a novel alignment strategy (Hewel et al. 2019), we could show that specific miRNAs were strongly related to multiple bacterial genomes. Interestingly, such miRNAs were associated with bacterial GO terms enriched for “Response to stimulus”, “DNA-repair” and “SOS response”, mechanisms known to inflict bacterial phenotypic change. Such a novel outlook could indicate a possible mechanism by which the miRNAs regulates gut microbial gene expression. Based on the study results and available literature, miR200a is an interesting candidate to focus on in future projects.

Case study 3: Transcriptional and chromatin accessibility analyses of activated neuronal populations isolated from chronically defeated mice reveal various gene candidates involved in synaptic regulation and neuronal differentiation. In the PFC, resilient-downregulated targets were enriched for “neurogenesis” and “synaptic signaling” including numerous downregulated synaptotagmins (*Syt*) genes, known to be involved calcium-dependent synaptic vesicle function. Similarly, in the vHIP, resilient-downregulated targets were enriched for “regulation of neuron differentiation” whereas resilient-upwnregulated targets were enriched for “cell-cell adhesion” with various proteocadherins (*Pcdh*) DEGs, known to be involved in regulation cell-cell interaction. Such data offers novel outlook concerning the molecular alterations associated with activated neuronal population of resilient mice to chronic social defeat.

Case study 4: Inhibition of the mTOR pathway (specifically mTORC1) downregulates numerous genes involved in the sterol/cholesterol biosynthesis pathway, both in prenatal and postnatal neurons. Interestingly, the transcription factor binding motifs such as SREBP, SP1 and NF-Y were enriched for the cholesterol gene targets. Despite that the chromatin accessibility states did not significantly change at the promoter of the cholesterol biosynthesis gene targets, ChIP-qPCR of NF-YA revealed increased binding of the transcription factor at these regions, suggesting a potential repressive function of NF-YA. Overall, mTORC1 was identified as an essential transcription regulator in the sterol/cholesterol biosynthesis gene in the developing and developed brain.

Section 2

Case study 5: Quantifiable physiological differences were observed in FANS- isolated nuclei compared to INTACT-nuclei. Transcriptional alterations reveal increased gene targets enriched for "regulation of transcription—DNA templated" and "mRNA processing" in FANS-nuclei compared to INTACT-nuclei. FANS-gained accessibility regions indicate six enriched motifs previously suggested to be involved in regulation of chromatin structure and transcription, suggesting that FANS-nuclei undergo an additional layer of transcriptional alterations compared to INTACT-nuclei. Overall, the choice of either INTACT or FANS for a particular study should be made based on the cell type investigated, starting tissue material, and subsequent molecular analyses. To avoid bias or inconsistencies during the data analysis, it would better to select a single isolation method to perform all the subsequent molecular analyses.

Case study 6: The upsurge in nuclei-based methodologies is associated with the growth of next-generation sequencing platforms, their steady cost reductions, and the increased interest in genome- and epigenome-wide studies. The potential reasons for the increased use of nuclei in molecular biology is attributed to: 1) availability of next-generation sequencing platforms, 2) nuclei as a comfortable biological tool for isolation and use 3) coupling nuclei use with *in-vivo* systems, 4) application of nuclei with "multi-omics" approaches and 5) increased single nucleus sequencing methodologies. Nevertheless, the coupling of nuclei with transcriptomic approaches such as nuclear RNA-seq, still hold a major challenge for nuclei-based studies due to: 1) RNA population bias between nuclei and whole cells, 2) sequencing requirements for suitable coverage of exon versus intron reads, and 3) assessment of nuclear RNA quality and library preparation strategies.

The following section will provide an outlook of the importance of epigenetic mechanisms presented in the thesis, and will review the promising directions for future of the epigenetics field. Finally, the concepts presented are collected to the proposal of basic concepts of epigenetic mechanisms that require further consideration.

3.2 Epigenetics – from the present to the future

3.2.1 Epigenetic modulators as therapeutic agents

An increasing number of studies are exploring epigenetic modulators as therapeutic agents (Morel et al. 2019). Case study 2.1 provides an example of a study investigating the influence of HDAC inhibitor (CI-994) on BBIDS in the mouse model. The epigenetic modulator was shown to influence the histone acetylation deposition (H3K27ac) and thereby activate the expression of the paternal allele which is silenced under normal conditions. Further studies have reported the use of epigenetic modulators to treat additional imprinting disorders such as Prader-Willi syndrome (PWS) (Kim et al 2017) or reveal the genome-wide alterations occurring in distinct cancer cell-lines following treatment (Sanchez et al. 2018, Yousef, El-Fawal and Abdelnaser 2020). Therefore, the power of epigenetic modulators is gradually being uncovered. These insights might provide a tool to alter the epigenetic state (depending on their targeted mechanism of action) that could become routinely utilized for therapeutic purposes.

However, prior to their application as therapeutic agents in humans, it is crucial to investigate further their system-wide and extent of side effects. Tested epigenetic drugs in animals are often administrated intraperitoneally, thereby providing a system-wide effect that could potentially influence other tissue types and cellular populations. Additionally, it would be crucial to understand the full impact of such drugs in the context of the genome within the investigated cell population as their effect could influence the micro-molecular environment. For instance, following CI-994 treatment, not only H3K27ac levels increased within the tested brain regions but also H3K4me1 marks at the *Kcnk9* promoter region. This demonstrates the epigenetic modulators do not only influence specific mechanisms such as histone acetylation levels but, to some extent, also influence the activity of other histone-modifying enzymes. These observations have been documented in additional studies emphasizing the need to comprehend the systematic effect of such drugs on further epigenetic mechanisms and global gene expression states (Sanchez et al. 2018, Huang, Plass and Chen 2011, Calo and Wysocka 2013). It would be essential to monitor the short and long-term effects of such administrations in order to ensure high efficacy and safety of the tested drug.

Nonetheless, novel strategies are being developed to ensure targeted drug delivery, thereby making their administration more efficient and safer by reducing their side effects (Singh et al. 2019). Examples of such targeted drug delivery includes various nanomaterial-based delivery systems that offer precise drug delivery to prevent or treat distinct diseases (Sharma, Crist and Adiseshaiah 2017, Ramaswami, Bayer, Galea 2018, Manzari et al. 2021). These could be combined with epigenetic modulators to precisely deliver the drug,

thereby reducing potential unwanted side effects. Taken altogether, the use of epigenetic modulators shows an exciting and promising avenue for therapeutic usage in the future.

3.2.2 Host-gut microbiota communication

If epigenetic mechanisms provide a "gate" between external environmental stimuli and internal alterations in gene expression, the interaction between the host and gut microbial cellular populations provide an interesting symbiotic relationship that is undoubtedly interconnected (Qin and Wade 2018). More specifically, the dynamic signal interchange between the host and the microbial community has raised several questions regarding the forms of communication between the bacteria and host cells. A rising hypothesis suggests microRNAs can act as both messengers and regulator molecules between the two biological systems (Dong, Tai and Lu 2019, Li, Chen and Wang 2020, Zhao et al. 2021). By their nature, miRNAs are attractive "communication molecules" which can be exchanged easily between the host and gut microbial populations based on their size, relatively unrestricted mobility, and robustness to degradation (Jung et al. 2010). In eukaryotes, apart from regulators of gene expression, it is suggested that miRNAs act as intracellular communicators, affecting neighboring cell gene targets through the exchange of extracellular vesicles (Turchinovich et al. 2013, Bayraktar, Van-Roosbroeck and Calin 2017). However, the extent of such communication between eukaryotic and prokaryotic organisms is poorly understood. Despite the belief that bacteria do not possess miRNA processing machinery, recent evidence demonstrated that these small RNA populations could significantly impact bacterial gene regulation (Liu et al. 2016, Miro-Blanch and Yanes 2019). Additionally, it was revealed that the bacteria often use the host sRNA processing machinery for their own advantage, thereby extending their regulation impact (Weiberg et al. 2015, Hudzik et al. 2020, Kaletsky et al. 2020).

As presented in case study 2.2, multiple fecal miRNAs were associated with specific behavioral conditions (resilient, susceptible and control mice) following chronic social stress (CSS). Interestingly, only six miRNAs were related to multiple bacterial genomes based on sequence alignment and kinetically favorable binding energy (Enright et al. 2003). Bacterial GO term analysis of targeted genes revealed enrichment of mechanisms such as "SOS response" and "response to antibiotic", which are part of the bacterial defense mechanisms, often influenced by the extracellular stimulus. For instance, the SOS response system consists of various factors involved in error-prone DNA repair mechanisms, which induce phenotypic changes and ultimately allow bacteria to survive at the cost of elevated mutagenesis (Baharoglu and Mazel 2014, Maslowska et al. 2019). This observation could elucidate a dynamic network that is constantly influenced by the host cellular activity and potentially mediated by small RNAs such as miRNAs. Additionally, it would be essential to consider the metabolic compounds secreted by the microbial population, which provide a huge potential of influencing

distinct epigenetic mechanisms and thus gene expression (Kho and Lal 2018). Future studies should deepen the relationship between identified miRNAs and gut microbiota to ultimately uncover their role in the host-microbiota communication network and their influence on both systems, host and resident microbial populations.

3.2.3 Prokaryotic epigenetic mechanisms

The majority of epigenetic studies focus on eukaryotic systems as they provide a more practical and direct approach associated with human biology. However, it is important to remark that prokaryotic organisms comprise epigenetic mechanisms as well (Willbanks et al. 2016). Such mechanisms include DNA methylation and regulatory sRNA populations, which are under-investigated and could have massive prospective cellular regulation, both in the bacteria and the host. If we consider discovering the DNA methylation mechanism in the 1950s, it was initially detected in prokaryotes, and a decade later, uncovered in eukaryotes (Morange 2013). DNA methylation in bacteria is believed to recruit specific proteins to the particular bacterial genomic loci and therefore regulate gene expression (Beaulaurier, Schadt and Fang 2019). Similarly, the role of sRNA in prokaryotes is suggested to regulate bacterial gene expression and translation (Watkins and Arya 2019). However, compared to our understanding and documentation of the distinct epigenetic mechanisms in eukaryotes, the epigenetic control mechanisms in prokaryotes are still poorly understood and therefore provides an exciting field to uncover (Casadesús and Low 2006).

3.2.4 Behavioral epigenetics

As the name denotes, behavioral epigenetics aims to investigates the relationship between distinct epigenetic mechanisms and their influence on behavior (Powledge 2011). Nowadays, stress has become a predominant factor associated with various of disorders (Collins et al. 2020). Therefore, it essential to explore the molecular mechanisms underlying the behavioral alterations where epigenetics could be a relevant field to explore. The study of the mammalian brain stands as the central pillar in the field of behavioral epigenetics, connecting the nervous and endocrine systems with the molecular-epigenetic alterations following environmental stimulation. Case study 2.3 focused on the molecular alteration occurring in active neuronal populations using Arc-sun1GFP mice. Studying active neuronal populations could provide a “high resolution” approach to understand how stimulation is processed specifically in a definite set of neurons, which are activated following stimulation (Mo et al. 2015). Recent studies used similar strategies to identify the chromatin structure dynamics underlying neuronal activation during epileptic seizures (Fernandez-Albert 2019) and during engram memory formation (Marco et al. 2020). Studying the individual role of the stimulated neuronal populations is crucial to understand the influence on the overall behavioral phenotypes. An additional example was presented in case study 2.2,

aiming to link the alterations in fecal miRNA in response to stress and their connection with gut microbes. With the increasing investigation of the gut-brain axis, it would be sensible to associate further the gut microbiome and its influence on distinct behavioral phenotypes. As presented, epigenetics can be an appealing mechanism connecting both the host and the gut microbial populations. Therefore, the next phase in the study of behavioral epigenetics would be to combine the various biological systems to identify the "bigger picture", emphasizing the environmental stimuli applied on the biological system, the epigenetic alteration associated with the stimuli, and their overall influence on behavior.

3.2.5 Single-cell sequencing technologies

As noted in case studies 2.5 and 2.6, novel methodologies are continuously developed and applied with the increased interest in epigenetic and "multi-omic" studies. Such methods aim to simplify and explore the distinct cell-type specific populations, uncovering new mechanisms that could assist scientists in understanding the complex cellular system and potentially apply them for therapeutic purposes in humans.

Single-cell (sc) sequencing technologies provide a promising direction in the field of molecular biology, offering a unique opportunity to uncover and deepen further the individual cellular characteristics within different or even seemingly identical cellular populations (Shapiro, Biezuner, and Linnarson 2013, Stuart and Satija 2019). Currently, single-cell RNA-seq (scRNA-seq) is one of the most frequently used single-cell approaches aimed to reveal the dynamic transcriptomes of individual cells (Hwang, Lee and Bang 2018). In addition, most of the epigenomic methodologies mentioned in this thesis, already have a corresponding single-cell resolution counterpart (Kelsey, Stegle, and Reik 2017). Few examples include scATAC-seq (Buenrostro et al. 2015, Cusanovich et al. 2015), scDNA-methylation assays (Smallwood et al. 2014, Farlik et al. 2015), scSmall-RNA-seq (Faridani et al. 2016, Wang et al. 2019), and scChIP-seq (Rotem et al. 2015). However, despite the availability of such techniques, their use is still not as frequent as scRNA-seq or bulk sequencing techniques. This is primarily due to relatively high cost of such approaches as well as the efficacy and analytical issues reported by the scientific community (Kelsey, Stegle, and Reik 2017, Lee, Hyeon, and Hwang 2020). Nevertheless, with gradual improvement and continuous use of single-cell sequencing technologies, such approaches could expand and potentially become a central instrument for molecular investigation in the future.

3.3 Revisiting old concepts with new perspectives

The following chapters will now focus on highlight ideas and personal hypotheses that have emerged in preparing the studies presented above. These reflections, which go beyond the published topics combine the gained knowledge on epigenetics from several subfields, might allow epigenetic mechanisms to be considered from a new perspective and even to re-evaluate some of the basic concepts of epigenetics

3.3.1 "Essential" and "adaptive" epigenetic mechanisms

When examining the presented case studies and the available literature, it became apparent that distinct epigenetic mechanisms could be divided into two groups. The first group comprised mechanisms that acted relatively strictly or fixedly (hard to alter), while the second group included more flexible and dynamic (tend to change) mechanisms. For this reason, this thesis suggests the classification of such mechanisms into "essential" and "adaptive" epigenetic mechanisms. In the following, a potential classification will be introduced using relevant novel terminologies and by providing specific supportive examples. Finally, their importance for our understanding of the general field of epigenetics will be emphasized.

To begin with, the concepts of "essential" and "adaptive" epigenetic mechanisms are analogous to the previously described "constitutive" and "facultative" heterochromatic states (Brown 1966). "Constitutive" heterochromatic states are suggested to be permanently closed, associated with inactive gene activity, and form part of the identity of specific cell types. On the other hand, "facultative" heterochromatic states are suggested to be opportunistic, able to adopt open chromatin confirmations, and thereby are associated with adjustable active transcription (Trojer and Reinberg 2007). However, unlike these definitions that relate exclusively to chromatin conformation states, the proposed "essential" and "adaptive" epigenetic mechanisms relate to all epigenetic states within a cell.

3.3.1.1 "Essential" epigenetic mechanisms

"Essential" epigenetic mechanisms are often associated with tissue-specific cellular populations or particular stages of development where malfunction in these mechanisms or their respective components often result in lethality or disease due to their essential requirement within the system. Case study 2.1 presented the KCNK-imprinting disorder (BBIDS), a heritable, congenital disorder resulting from a mutation in the Kcnk9 maternal allele and therefore is permanent. Hence, the general mechanism of genomic imprinting (and associated regulation of gene expression) can be classified as an "essential" mechanism as allele-specific expression is crucial for certain cell types or stages of development (Weinstein 2001). Additional examples of "essential" mechanisms can include tissue- and cell- specific chromatin accessibility states (Liu et al. 2019, Nott et al.

2019) or developmental-specific miRNA expression (Dexhiemr and Cochella 2020). Their redundancy and broad extent of regulation make their investigation and association with "essential" epigenetic mechanisms challenging for miRNA regulation. Nevertheless, several reports reveal the necessity of such molecules, particularly during specific stages of development (Miska et al. 2007; Park et al. 2012; Chen et al. 2014). The core role of epigenetic mechanisms is to regulate the gene expression of specific genes required for a certain cell population. Therefore, the activity of "essential" epigenetic mechanisms is vital for the regular "maintenance" state and identity of a specific cell population.

3.3.1.2 "Adaptive" epigenetic mechanisms

On the other hand, if we consider "adaptive" epigenetic mechanisms, these are highly dynamic mechanisms more easily influenced by stimulation. "Adaptive" epigenetic mechanisms are probably associated with cell types that are constantly exposed to stimuli and require rapid adaptation. Relevant examples of such biological systems could include the immune system (Zhang and Cao 2019) or the mammalian brain (Houston et al. 2013). In the latter case, the mammalian brain comprises a wide variety of cellular populations, which are constantly influenced by environmental stimuli while maintaining system-wide stability (of the entire organism). Additionally, such "adaptive" epigenetic mechanisms could differ significantly from cell to cell (and eventually from organism to organism) as the activity and adaptability of the biological system rely on environmental stimulation (i.e. experience-specific). The topic of stress exposure is highly associated with "adaptive" epigenetic mechanisms where the stress serves as a perceived stimuli, followed by a cellular/molecular response (e.g. regulation of gene expression) which ultimately leads to adaptability (e.g. resilience or susceptibility). Case studies 2.2 and 2.3 presented such a relationship aiming to identify the molecular alterations in fecal miRNA populations or transcriptional states of active neuronal populations following chronic stress exposure. Additional relevant examples of "adaptive" epigenetic mechanisms include dynamic chromatin structure alterations follow neuronal stimulation (Su et al. 2017, Fernandez-Albert 2019), during engram memory formation (Marco et al. 2020), specific-miRNA association following stress exposure (Leung and Sharp 2010, Allen and Dwivedi 2020) and stress associated long-term alterations in DNA methylation states (Vinkers et al. 2015, Mehta et al. 2020). These are few examples demonstrating the flexibility of "adaptive" epigenetic mechanisms, which alter in response to stimulation and differ through time.

If we go back to the definition of epigenetics, it can be described as the heritable and reversible mechanisms, which ultimately regulate gene expression (Watson 2014). However, in reality, not all epigenetic mechanisms are necessarily heritable nor easily reversible. Thus, the sub classification of such mechanisms to "essential" and "adaptive" epigenetics could assist us to better understand the function and potentially identify the unique

molecular blueprint underlying such mechanisms. Accordingly, “essential” epigenetic mechanisms behave in a classical “genetic” manner, thereby attributing the heritability part to the definition. In contrast, “adaptive” mechanisms highlight the flexible and reversible element of the definition. For these reasons, the notion of epigenetics, particularly associated with “essential” and “adaptive” mechanisms, can both be applied to the previously illustrated concepts of “Nature” and “Nurture”, respectively (Fig 3). It is likely that through evolution, biological systems acquired novel properties, including epigenetic mechanisms, which at some point became “essential” (i.e. required for regular maintenance of a cell). However, the change is raised through the “adaptive” epigenetic mechanisms. Therefore, conceptually, the “adaptive” epigenetic mechanisms can be conceived as the drivers of evolution as they slowly shift the system towards adaptability and possibly altering the “essential” epigenetics mechanisms. Nonetheless, these ideas are merely a hypothesis at this stage and will require further validations to support their legitimacy.

3.3.2 “Stimulation strength” and “epigenetic capacity”

To provide a more detailed description of the concepts of “essential” and “adaptive” epigenetic mechanisms, it is important to define additional key features that could distinguish the two mechanisms. Therefore, the following section will describe the terms “stimulation strength” and “epigenetic capacity”.

3.3.2.1 “Stimulation strength”

It is important to note that practically, all epigenetic mechanisms, including the “essential” ones, are reversible. A great example of such reversibility is the forced reprogramming of induced pluripotent stem cells (iPSCs) using the Yamanaka factors (Liu et al. 2008). The Yamanaka factors consist of 4 components including transcription factors and chromatin remodelers (Oct3/4, Sox2, Klf4, c-Myc), which lead to the global epigenetic reprogramming and induction of the pluripotent cellular state i.e. ability to differentiate to any cell type. This example displays how external factors could alter the cell’s epigenetic state, completely reversing its form and functionality. Therefore, “essential” epigenetic mechanisms are also reversible. However, they require “stronger” induction by external stimuli to alter and inflict change upon the biological system. An additional example is observed in case study 2.1. Treatment with the HDAC inhibitor partially rescues the BBIDS mouse model by increasing the H3K27ac deposition levels at the Kcnk9 promoter region, particularly of the paternal allele. Similarly, this demonstrates that treatment with an epigenetic modulator could have a potent effect to overcome the malfunctioned maternal-allele expression, reduce symptomatic appearance and potentially promote healthier states. Therefore, external chemicals or specific molecules can act as strong inducers for “essential” mechanism reversibility due to their specificity and targeted effect on critical components of the biological system.

On the other hand, “adaptive” epigenetics are influenced by “natural” factors present in the system, which are “less potent” compared to the factors required to inflict change in the “essential” mechanisms. Nonetheless, these influence naturally the gene expression and cellular activity based on the environmental stimuli present (arguably through longer periods of time). Yet, since environmental stimuli influence “adaptive” epigenetic mechanisms, it is tougher to classify the stimulation “strength” as these are often experience-specific or are constantly affected by multiple stimuli at once. Examples of such stimulations can include the gut microbiota. It is estimated that such a population has 150 times more genes than the host (Zhu, Wang and Li 2010). Therefore, it provides a huge repertoire of compounds regulating host cellular activity (Nichols and Davenport 2020). Another example could include stress exposure, where individuals are exposed to countless stressful experiences throughout their lifetime (Yaribeygi et al. 2017); however, it is hard to classify the impact of stressful experiences objectively. An individual might or might not be aware of these stimulations; however, these are perceived, processed and translated to an adaptive response that could benefit (e.g. resilience) or harm (e.g. anxiety-associated disorder) the individual. Nevertheless, studies continuously attempt to classify stressful situations/stimulation based on the symptomatic disorders associated with stressful stimulation. An example of an extremely stressful situation that results in severe physiological disorder is post-traumatic stress disorder (PTSD) (Friedman et al. 2011). These examples demonstrate the need to classify distinct stimulations based on their strength to understand their impact on the biological system, particularly their association with “adaptive” epigenetic mechanisms.

3.3.2.2 “Epigenetic capacity”

The second feature that requires reflection is “epigenetic capacity”, which can be described as the ability of the epigenetic mechanism to change or reverse over time. The following section, gives a highly speculative hypothesis on an integrative understanding of reversibility, speed of change, and transcriptional rate of epigenetic mechanisms to define their individual “epigenetic capacity”.

By their nature, the three branches of epigenetics are relatively different. DNA methylation relies on chemical modification of the DNA molecule, thereby regulating the binding of distinct proteins to the DNA by either preventing or promoting direct binding, or recruiting additional proteins, which regulate such interaction. As previously mentioned (chapter 3.2.3), DNA methylation is also present in prokaryotes. Therefore, it could be presumed that such mechanism is evolutionary ancient. With the emergence of higher eukaryotic organisms, which comprise of larger and more complex genomes, histone post-translational modifications provided an additional layer of regulation aiming to control the dynamic chromatin structure. Such mechanisms can regulate the chromatin accessibility states, allowing or preventing proteins from binding the chromatin and

thereby providing an additional level of regulation over gene expression. On the other hand, miRNA regulation provides an entirely different and perhaps more complicated system, reaching wider extracellular environments and regulating multiple targets at once. It could be argued that miRNA regulation has evolved from the small RNA regulation mechanisms present in prokaryotes. However, there is little evidence to support this hypothesis at this stage (Dutcher and Raghavan 2018). In any case, due to their mechanistic difference, it could be presumed that their "epigenetic capacity" and speed of transcriptional alteration would be distinct in each mechanism.

If we contemplate the mechanism of DNA methylation, it is suggested to be both chemically and genetically stable (Wu and Zhang 2017). Despite its stability, it can be reversed to unmodified states. Processes such as passive dilution of DNA methylation during DNA replications cycles (in cells lacking DNA methylation maintenance machinery) or active demethylation processes using the TET enzymes are commonly studied features of DNA demethylation (Kohli and Zhang 2013). If we consider the "epigenetic capacity" and speed of alteration, rapid DNA methylation, and demethylation activities were previously reported, particularly in specific biological contexts such as early stages of development or specific differentiated cell types (Bhutani, Burns and Blau 2011, Wu and Zhang 2017). However, due to its stability, DNA methylation is often associated with long-term alterations observed in longitudinal studies such as aging (Jiang and Guo 2020, Zhang et al. 2020), cancer (Cheng et al. 2019) or longitudinal consequences of stress (Silberman et al. 2016). Therefore, based on its mechanism, DNA methylation can be perceived mainly as a long-term "essential" epigenetic modification. To provide an analogous simplified illustration, DNA methylation can be paralleled to the "hammer-nail" model where the nail can be introduced and removed; however, its removal requires more effort (Fig. 7B.1)

On the contrary, if we consider the chromatin 3D structure, it is often referred to in the literature as "chromatin plasticity", already hinting at its flexibility and capacity to change (Yadav, Quivy and Almouzni 2018, Fierz and Poirier 2019). Dynamic chromatin accessibility was reported in several studies demonstrating the capacity of the chromatin to change conformation, open and promote transcription and at later time points, close and inhibit transcription (Su et al. 2017, Fernandez-Albert 2019, Marco et al. 2020). One particular study conducted a time-course analysis on neuronal chromatin accessibility states revealing reversible changes 1h, 4h, and 24h following stimulation (Su et al. 2017). The authors comment further: "…*compared to CpG DNA modification, activity-induced chromatin accessibility changes are relatively transient and reversible in neurons in vivo"* (Su et al. 2017). Therefore, the chromatin structure appears to be more easily reversible than DNA methylation mechanisms. The dynamic chromatin can be paralleled to "clay", where it can change

conformation and easily shaped however, like clay, which requires water to bend, the chromatin structure requires specific conditions to achieve this transformation (Fig 7B.2).

Lastly, miRNA regulation could be classified as the mechanism with the highest "epigenetic capacity" due to its redundancy and broad extent of regulation. It is suggested that the number of miRNA genes correlates with the organismal complexity (Berezikov 2011). Additionally, miRNA targets can be easily acquired and lost; thus, suggesting a flexible mechanism that alters according to the complexity and necessity of the biological system. miRNAs were previously described as "fine-tuners", where the expression of miRNAs is required to fine-tune gene expression for a particular cellular population (Michaels et al. 2019). Therefore, miRNA regulation can be paralleled to "radio" aiming to tune-in a specific "expression" quantity required for the cell (Fig. 7B.3).

An interesting aspect of studying a topic like "epigenetic capacity" is the ability of "adaptive" epigenetic mechanisms to alter over time, thereby focusing on fields such as early life experience studies and aging. Early life experiences have a major role in the development of an individual both on the cognitive as well as psychological levels (Fogelman and Canli 2019). Multiple studies revealed that enriched childhood had positive effects on adulthood, resulting in reduced risk to devel op mood-related disorders (Sampedro-Piquero 2017, Ball et al. 2019). On the other hand, further studies report the negative effect of early life stress such as childhood abuse or neglect that could promote the development of psychological and mood-related disorders which can be transformed indirectly into physiological disorders (Albrecht et al. 2017, Vaiserman and Koliada 2017). Therefore, early life experience seems to provide a crucial time window for "adaptive" epigenetic mechanisms to form, operate, and to some extent consolidate, particularly in the brain. As a result of such an adaptability window, early life events could influence and possibly shape the neuronal plasticity capacity of later stages in life, as recent evidence suggests (Kronman et al. 2021). Additionally, it is reported that the regulation and functionality of distinct epigenetic mechanisms decrease with aging (Zhang et al. 2020), suggesting a natural reduction of the "epigenetic capacity" with time. Further studies should aim to perform these longitudinal studies to uncover the dynamic "epigenetic capacity" of the distinct epigenetic mechanism through an individual's life.

Taken together, the ideas presented here provide perspective regarding the classification of the distinct epigenetic mechanisms. One could argue that DNA methylation provides the "basic" regulation required for the regular function of the cells, thus associating more with "essential" epigenetics. On the other hand, chromatin structure regulation, which is more flexible, has evolved to dynamically alter gene expression and therefore could be associated more with the "adaptive" epigenetics. The broad regulation of miRNAs could also be associated with the notion of "adaptive" epigenetics based on their relatively unrestricted nature.

Overall, the hypotheses raised in this thesis, could trigger a re-evaluation of the different branches of epigenetics field and potentially contribute to its progression of the field.

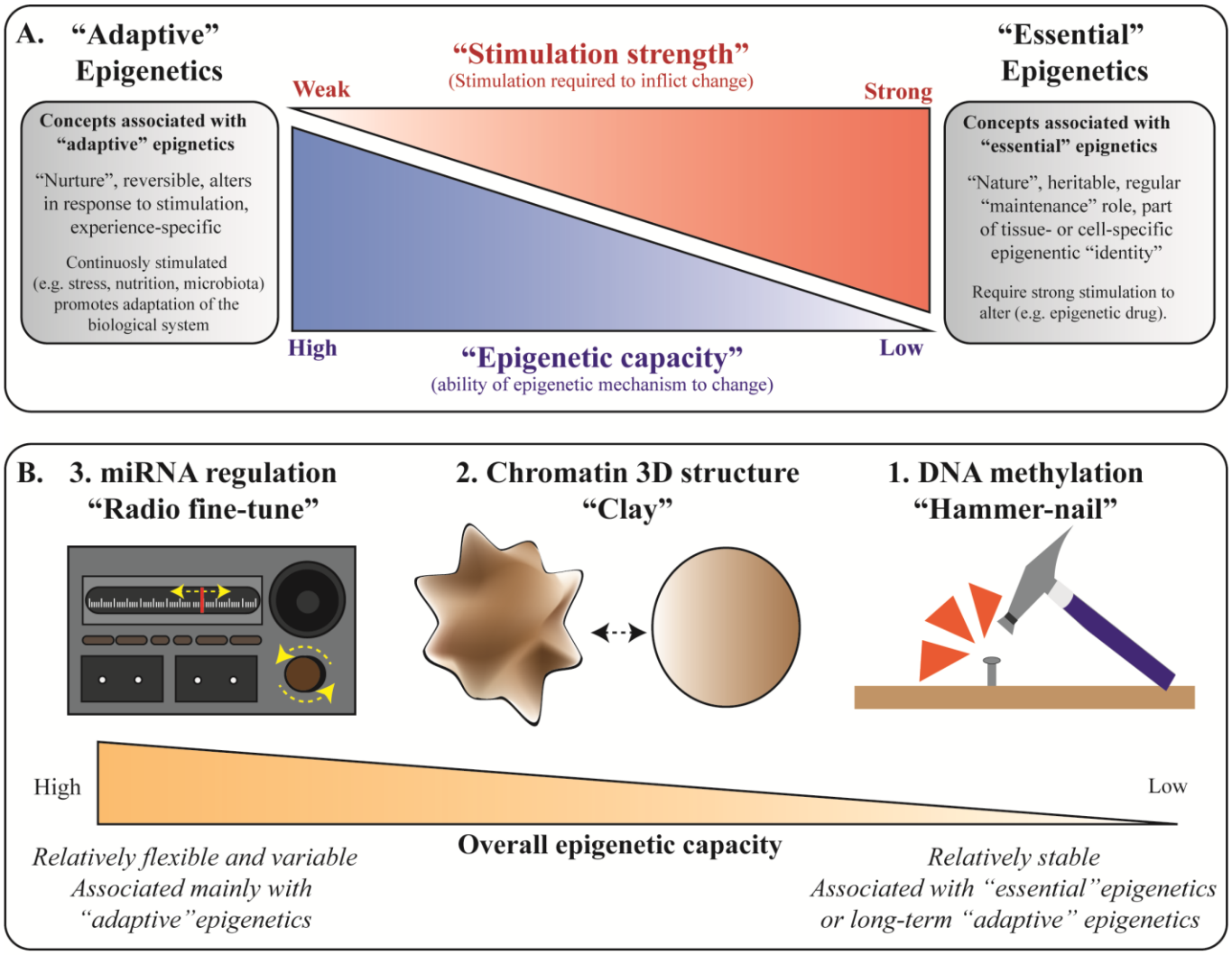

Figure 7. Association of "essential" and "adaptive" epigenetic mechanisms with "stimulation strength" and "epigenetic capacity. A. *Manipulation of "essential" epigenetic mechanisms require a potent stimulation to reprogram the state of the cell since their "epigenetic capacity" is relatively low (hard to alter). On the contrary, "adaptive" mechanisms, which are constantly influenced by environmental stimuli, comprise of a relatively high epigenetic capacity, which allows the biological system to change and adapt.* ***B.*** *Simplified illustrations of the three branches of epigenetics and their proposed associated "epigenetic capacity".* ***1.*** *The "Hammer-nail" model represents DNA methylation where the modification is relatively stable and its removal require extra effort.* ***2.*** *The "Clay" model represents the dynamic chromatin structure, which is constantly influenced and alters its shape in response to environmental stimuli.* ***3.*** *The "Radio fine-tune" represents the influence of the miRNAs by "tuning" and adjusting gene expression.*

Box 1| Proposed terms describing distinct epigenetic mechanisms

"Essential" epigenetics: heritable mechanisms essential for the regular activity of specific cell types, hard to alternate and often act in a classical "genetic" manner.

"Adaptive" epigenetics: Dynamic and reversible mechanisms influenced by environmental stimuli that promote change and adaptation within the biological system.

Stimulation strength: The stimulation required to inflict change (in the epigenetic mechanism) where "essential" mechanisms would require stronger stimulation to change (such as chemicals or direct TF and remodeler molecules) compared to "adaptive" mechanisms.

Epigenetic capacity: the ability of the epigenetic mechanism to change (or reverse) over specific time-periods. The epigenetic capacity of "adaptive" epigenetic mechanism is much higher than "essential" ones.

3.4 Concluding remarks

The field of epigenetics has been previously described as the "Science of change" (Weinhold 2006). The current thesis supports this notion by providing a multi-disciplinary compilation of studies aimed to address the distinct roles of epigenetic mechanisms as a system of change and adaptability and their association with healthy and diseased phenotypes. If we re-assess some of the concepts described in this thesis such as epigenetic alteration, adaptability, allostasis (i.e. stability through change), a repeating pattern can be noticed governed by a system of "stimulation-change-adaptation". However, as proposed, such a system is most likely associated with "adaptive" epigenetic mechanisms, which are more inclined to change following stimulation and less with "essential" epigenetic mechanisms that seem to have a vital cell-specific "maintenance" role. The proposal of concepts presented in this thesis (Fig. 7 Box1) could promote a better understanding of distinct epigenetic mechanisms and direct us towards uncovering their full potential as an evolutionary instrument of change and adaptability.

References

Albrecht, Anne, Iris Müller, Ziv Ardi, Gürsel Çalışkan, David Gruber, Sebastian Ivens, Menahem Segal, Joachim Behr, Uwe Heinemann, Oliver Stork, and Gal Richter-Levin. 2017. "Neurobiological Consequences of Juvenile Stress: A GABAergic Perspective on Risk and Resilience." *Neuroscience and Biobehavioral Reviews* 74(Pt A):21–43.

Allen, Lauren and Yogesh Dwivedi. 2020. "MicroRNA Mediators of Early Life Stress Vulnerability to Depression and Suicidal Behavior." *Molecular Psychiatry* 25(2):308–20.

Anisman, H. and Z. Merali. 1999. "Understanding Stress: Characteristics and Caveats." *Alcohol Research & Health : The Journal of the National Institute on Alcohol Abuse and Alcoholism* 23(4):241–49.

Aramburu, Jose, M. Carmen Ortells, Sonia Tejedor, Maria Buxadé, and Cristina López-Rodríguez. 2014. "Transcriptional Regulation of the Stress Response by MTOR." *Science Signaling* 7(332):re2–re2.

Bae, Sunhee and Bluma J. Lesch. 2020. "H3K4me1 Distribution Predicts Transcription State and Poising at Promoters." *Frontiers in Cell and Developmental Biology* 8.

Baharoglu, Zeynep and Didier Mazel. 2014. "SOS, the Formidable Strategy of Bacteria against Aggressions." *FEMS Microbiology Reviews* 38(6):1126–45.

Ball, Natalie J., Eduardo Mercado, and Itzel Orduña. 2019. "Enriched Environments as a Potential Treatment for Developmental Disorders: A Critical Assessment." *Frontiers in Psychology* 10(MAR):466.

Barel, Ortal, Stavit A. Shalev, Rivka Ofir, Asi Cohen, Joel Zlotogora, Zamir Shorer, Galia Mazor, Gal Finer, Shareef Khateeb, Noam Zilberberg, and Ohad S. Birk. 2008. "Maternally Inherited Birk Barel Mental Retardation Dysmorphism Syndrome Caused by a Mutation in the Genomically Imprinted Potassium Channel KCNK9." *American Journal of Human Genetics* 83(2):193–99.

Barski, Artem, Suresh Cuddapah, Kairong Cui, Tae Young Roh, Dustin E. Schones, Zhibin Wang, Gang Wei, Iouri Chepelev, and Keji Zhao. 2007. "High-Resolution Profiling of Histone Methylations in the Human Genome." *Cell* 129(4):823–37.

Bayraktar, Recep, Katrien Van Roosbroeck, and George A. Calin. 2017. "Cell-to-Cell Communication: MicroRNAs as Hormones." *Molecular Oncology* 11(12):1673–86.

Beaulaurier, John, Eric E. Schadt, and Gang Fang. 2019. "Deciphering Bacterial Epigenomes Using Modern Sequencing Technologies." *Nature Reviews Genetics* 20(3):157–72.

Becker, Justin S., Dario Nicetto, and Kenneth S. Zaret. 2016. "H3K9me3-Dependent Heterochromatin: Barrier to Cell Fate Changes." *Trends in Genetics* 32(1):29–41.

Belkaid, Yasmine and Timothy W. Hand. 2014. "Role of the Microbiota in Immunity and Inflammation." *Cell* 157(1):121–41.

Belmont, John W., Andrew Boudreau, Suzanne M. Leal, Paul Hardenbol, Shiran Pasternak, David A. Wheeler, Thomas D. Willis, Fuli Yu, Huanming Yang, Yang Gao, Haoran Hu, Weitao Hu, Chaohua Li, Wei Lin, Siqi Liu, Hao Pan, Xiaoli Tang, Jian Wang, Wei Wang, Jun Yu, Bo Zhang…Francis S. Collins, Karen Kennedy, Ruth Jamieson, and John Stewart. 2005. "A Haplotype Map of the Human Genome." *Nature* 437(7063):1299–1320.

Ben-Hattar, Jean and Josef Jiricny. 1988. "Methylation of Single CpG Dinucleotides within a Promoter Element of the Herpes Simplex Virus Tk Gene Reduces Its Transcription in Vivo." *Gene* 65(2):219–27.

Benjamin, Don, Marco Colombi, Christoph Moroni, and Michael N. Hall. 2011. "Rapamycin Passes the Torch: A New Generation of MTOR Inhibitors." *Nature Reviews Drug Discovery* 10(11):868–80.

Berezikov E. 2011. "Evolution of MicroRNA Diversity and Regulation in Animals." *Nature Reviews. Genetics* 12(12):846–60.

Bhutani, Nidhi, David M. Burns, and Helen M. Blau. 2011. "DNA Demethylation Dynamics." *Cell* 146(6):866–72.

Borgel, Julie, Sylvain Guibert, Yufeng Li, Hatsune Chiba, Dirk Schübeler, Hiroyuki Sasaki, Thierry Forné, and Michael Weber. 2010. "Targets and Dynamics of Promoter DNA Methylation during Early Mouse Development." *Nature Genetics* 42(12):1093–1100.

Bravo, Javier A., Paul Forsythe, Marianne V. Chew, Emily Escaravage, Hélène M. Savignac, Timothy G. Dinan, John Bienenstock, and John F. Cryan. 2011. "Ingestion of Lactobacillus Strain Regulates Emotional Behavior and Central GABA Receptor Expression in a Mouse via the Vagus Nerve." *Proceedings of the National Academy of Sciences of the United States of America* 108(38):16050–55.

Bridgewater, Laura C., Chenhong Zhang, Yanqiu Wu, Weiwei Hu, Qianpeng Zhang, Jing Wang, Shengtian Li, and Liping Zhao. 2017. "Gender-Based Differences in Host Behavior and Gut Microbiota Composition in Response to High Fat Diet and Stress in a Mouse Model." *Scientific Reports* 7(1):1–12.

Brown, Spencer W. 1966. "Heterochromatin." *Science* 151(3709):417–25.

Buenrostro, Jason D., Paul G. Giresi, Lisa C. Zaba, Howard Y. Chang, and William J. Greenleaf. 2013. "Transposition of Native Chromatin for Fast and Sensitive Epigenomic Profiling of Open Chromatin, DNA-Binding Proteins and Nucleosome Position." *Nature Methods* 10(12):1213–18.

Buenrostro, Jason D., Beijing Wu, Howard Y. Chang, and William J. Greenleaf. 2015. "ATAC-Seq: A Method for Assaying Chromatin Accessibility Genome-Wide." *Current Protocols in Molecular Biology* 2015:21.29.1-21.29.9.

Buenrostro, Jason D., Beijing Wu, Ulrike M. Litzenburger, Dave Ruff, Michael L. Gonzales, Michael P. Snyder, Howard Y. Chang, and William J. Greenleaf. 2015. "Single-Cell Chromatin Accessibility Reveals Principles of Regulatory Variation." *Nature* 523(7561):486–90.

Cadet, Jean Lud. 2016. "Epigenetics of Stress, Addiction, and Resilience: Therapeutic Implications." *Molecular Neurobiology* 53(1):545–60.

Carninci, P., T. Kasukawa, S. Katayama, J. Gough, M. C. Frith, N. Maeda, R. Oyama, T. Ravasi, B. Lenhard, C. Wells, R. Kodzius, K. Shimokawa, V. B. Bajic, S. E. Brenner, S. Batalov, A. R. R. Forrest, M. Zavolan, M. J. Davis, L. G. Wilming, V. Aidinis, J. E. Allen, A. Ambesi-Impiombato, R. Apweiler, R. N. Aturaliya, T. L. Bailey… Suzuki, J. Kawai, and Y. Hayashizaki. 2005. "Molecular Biology: The Transcriptional Landscape of the Mammalian Genome." *Science* 309(5740):1559–63.

Calo E, and Wysocka J. 2013. "Modification of Enhancer Chromatin: What, How, and Why?" *Molecular Cell* 49(5):825–37.

Casadesús, Josep and David Low. 2006. "Epigenetic Gene Regulation in the Bacterial World." *Microbiology and Molecular Biology Reviews* 70(3):830–56.

Chang, Cherng Shyang and Cheng Yuan Kao. 2019. "Current Understanding of the Gut Microbiota Shaping Mechanisms." *Journal of Biomedical Science* 26(1).

Chapman, Nicole M., Hu Zeng, Thanh Long M. Nguyen, Yanyan Wang, Peter Vogel, Yogesh Dhungana, Xiaojing Liu, Geoffrey Neale, Jason W. Locasale, and Hongbo Chi. 2018. "MTOR Coordinates Transcriptional Programs and Mitochondrial Metabolism of Activated Treg Subsets to Protect Tissue Homeostasis." *Nature Communications* 9(1):1–15.

Chen, Ya Wen, Shilin Song, Ruifen Weng, Pushpa Verma, Jan Michael Kugler, Marita Buescher, Sigrid Rouam, and Stephen M. Cohen. 2014. "Systematic Study of Drosophila MicroRNA Functions Using a Collection of Targeted Knockout Mutations." *Developmental Cell* 31(6):784–800.

Cheng, Yuan, Cai He, Manni Wang, Xuelei Ma, Fei Mo, Shengyong Yang, Junhong Han, and Xiawei Wei. 2019. "Targeting Epigenetic Regulators for Cancer Therapy: Mechanisms and Advances in Clinical Trials." *Signal Transduction and Targeted Therapy* 4(1):1–39.

Collins, Nicholas, Natalia Ledo Husby Phillips, Lauren Reich, Katrina Milbocker, and Tania L. Roth. 2020. "Epigenetic Consequences of Adversity and Intervention Throughout the Lifespan: Implications for Public Policy and Healthcare." *Adversity and Resilience Science* 1(3):205–16.

Costa-Mattioli, Mauro and Lisa M. Monteggia. 2013. "MTOR Complexes in Neurodevelopmental and Neuropsychiatric Disorders." *Nature Neuroscience* 16(11):1537–43.

Court, Franck, Cristina Camprubi, Cristina Vicente Garcia, Amy Guillaumet-Adkins, Angela Sparago, Davide Seruggia, Juan Sandoval, Manel Esteller, Alex Martin-Trujillo, Andrea Riccio, Lluis Montoliu, and David Monk. 2014. "The PEG13-DMR and Brain-Specific Enhancers Dictate Imprinted Expression within the 8q24 Intellectual Disability Risk Locus." *Epigenetics and Chromatin* 7(1).

Crews, David, Ross Gillette, Isaac Miller-Crews, Andrea C. Gore, and Michael K. Skinner. 2014. "Nature, Nurture and Epigenetics." *Molecular and Cellular Endocrinology* 398(1–2):42–52.

Creyghton, Menno P., Albert W. Cheng, G. Grant Welstead, Tristan Kooistra, Bryce W. Carey, Eveline J. Steine, Jacob Hanna, Michael A. Lodato, Garrett M. Frampton, Phillip A. Sharp, Laurie A. Boyer, Richard A. Young, and Rudolf Jaenisch. 2010. "Histone H3K27ac Separates Active from Poised Enhancers and Predicts Developmental State." *Proceedings of the National Academy of Sciences of the United States of America* 107(50):21931–36.

Cusanovich, Darren A., Riza Daza, Andrew Adey, Hannah A. Pliner, Lena Christiansen, Kevin L. Gunderson, Frank J. Steemers, Cole Trapnell, and Jay Shendure. 2015. “Multiplex Single-Cell Profiling of Chromatin Accessibility by Combinatorial Cellular Indexing.” *Science* 348(6237):910–14.

De Palma, G., P. Blennerhassett, J. Lu, Y. Deng, A. J. Park, W. Green, E. Denou, M. A. Silva, A. Santacruz, Y. Sanz, M. G. Surette, E. F. Verdu, S. M. Collins, and P. Bercik. 2015. “Microbiota and Host Determinants of Behavioural Phenotype in Maternally Separated Mice.” *Nature Communications* 6(1):1–13.

Dexheimer, Philipp J. and Luisa Cochella. 2020. “MicroRNAs: From Mechanism to Organism.” *Frontiers in Cell and Developmental Biology* 8.

Dimitrova, Emilia, Anne H. Turberfield, and Robert J. Klose. 2015. “Histone Demethylases in Chromatin Biology and Beyond.” *EMBO Reports* 16(12):1620–39.

Dinan, Timothy G. and John F. Cryan. 2017. “Gut Instincts: Microbiota as a Key Regulator of Brain Development, Ageing and Neurodegeneration.” *Journal of Physiology* 595(2):489–503.

Dong, Jiayi, Jesse W. Tai, and Li Fan Lu. 2019. “MiRNA–Microbiota Interaction in Gut Homeostasis and Colorectal Cancer.” *Trends in Cancer* 5(11):666–69.

Duncan, Kenneth W. and John E. Campbell. 2018. “Epigenetic Modulators.” Pp. 227–88 in *Topics in Medicinal Chemistry*. Vol. 28. Springer Verlag.

Dutcher, H. Auguste and Rahul Raghavan. 2018. “Origin, Evolution, and Loss of Bacterial Small RNAs.” Pp. 487–97 in *Regulating with RNA in Bacteria and Archaea*. Vol. 6. American Society of Microbiology.

Düvel, Katrin, Jessica L. Yecies, Suchithra Menon, Pichai Raman, Alex I. Lipovsky, Amanda L. Souza, Ellen Triantafellow, Qicheng Ma, Regina Gorski, Stephen Cleaver, Matthew G. Vander Heiden, Jeffrey P. MacKeigan, Peter M. Finan, Clary B. Clish, Leon O. Murphy, and Brendan D. Manning. 2010. “Activation of a Metabolic Gene Regulatory Network Downstream of MTOR Complex 1.” *Molecular Cell* 39(2):171–83.

Eggermann, Thomas, Guiomar Perez de Nanclares, Eamonn R. Maher, I. Karen Temple, Zeynep Tümer, David Monk, Deborah J. G. Mackay, Karen Grønskov, Andrea Riccio, Agnès Linglart, and Irène Netchine. 2015. “Imprinting Disorders: A Group of Congenital Disorders with Overlapping Patterns of Molecular Changes Affecting Imprinted Loci.” *Clinical Epigenetics* 7(1).

Enright, Anton J., Bino John, Ulrike Gaul, Thomas Tuschl, Chris Sander, and Debora S. Marks. 2003. “MicroRNA Targets in Drosophila.” *Genome Biology* 5(1):1.

Fan, Wenlu, Jing Zheng, Wanzhong Kong, Limei Cui, Maerhaba Aishanjiang, Qiuzi Yi, Min Wang, Xiaohui Cang, Xiaowen Tang, Ye Chen, Jun Qin Mo, Neal Sondheimer, Wanzhong Ge, and Min Xin Guan. 2019. “Contribution of a Mitochondrial Tyrosyl-TRNA Synthetase Mutation to the Phenotypic Expression of the Deafness-Associated TRNASer(UCN) 7511A>G Mutation.” *Journal of Biological Chemistry* 294(50):19292–305.

Fang, Xiaofeng, Gaozhan Zhao, Su Zhang, Yan Li, Qiao Zhao, and Yijun Qi Correspondence. 2019. "Chloroplast-to-Nucleus Signaling Regulates MicroRNA Biogenesis in Arabidopsis." *Developmental Cell* 48:371–82.

Faridani, Omid R., Ilgar Abdullayev, Michael Hagemann-Jensen, John P. Schell, Fredrik Lanner, and Rickard Sandberg. 2016. "Single-Cell Sequencing of the Small-RNA Transcriptome." *Nature Biotechnology* 34(12):1264–66.

Farlik, Matthias, Nathan C. Sheffield, Angelo Nuzzo, Paul Datlinger, Andreas Schönegger, Johanna Klughammer, and Christoph Bock. 2015. "Single-Cell DNA Methylome Sequencing and Bioinformatic Inference of Epigenomic Cell-State Dynamics." *Cell Reports* 10(8):1386–97.

Faye, Charlene, Josephine C. Mcgowan, Christine A. Denny, and Denis J. David. 2018. "Neurobiological Mechanisms of Stress Resilience and Implications for the Aged Population." *Current Neuropharmacology* 16(3):234–70.

Ferguson-Smith, Anne C., Hiroyuki Sasaki, Bruce M. Cattanach, and M. Azim Surani. 1993. "Parental-Origin-Specific Epigenetic Modification of the Mouse H19 Gene." *Nature* 362(6422):751–55.

Fernandez-Albert, Jordi, Michal Lipinski, María T. Lopez-Cascales, M. Jordan Rowley, Ana M. Martin-Gonzalez, Beatriz del Blanco, Victor G. Corces, and Angel Barco. 2019. "Immediate and Deferred Epigenomic Signatures of in Vivo Neuronal Activation in Mouse Hippocampus." *Nature Neuroscience* 22(10):1718–30.

Fierz, Beat and Michael G. Poirier. 2019. "Biophysics of Chromatin Dynamics." *Annual Review of Biophysics* 48:321–45.

Filipowicz, Witold, Suvendra N. Bhattacharyya, and Nahum Sonenberg. 2008. "Mechanisms of Post-Transcriptional Regulation by MicroRNAs: Are the Answers in Sight?" *Nature Reviews Genetics* 9(2):102–14.

Fogelman, Nia and Turhan Canli. 2019. "Early Life Stress, Physiology, and Genetics: A Review." *Frontiers in Psychology* 10(JULY):1668.

Fraga, Mario F., Esteban Ballestar, Maria F. Paz, Santiago Ropero, Fernando Setien, Maria L. Ballestar, Damia Heine-Suñer, Juan C. Cigudosa, Miguel Urioste, Javier Benitez, Manuel Boix-Chornet, Abel Sanchez-Aguilera, Charlotte Ling, Emma Carlsson, Pernille Poulsen, Allan Vaag, Zarko Stephan, Tim D. Spector, Yue Zhong Wu, Christoph Plass, and Manel Esteller. 2005. "Epigenetic Differences Arise during the Lifetime of Monozygotic Twins." *Proceedings of the National Academy of Sciences of the United States of America* 102(30):10604–9.

Franklin, Tamara B., Bechara J. Saab, and Isabelle M. Mansuy. 2012. "Neural Mechanisms of Stress Resilience and Vulnerability." *Neuron* 75(5):747–61.

Friedman, Matthew J., Patricia A. Resick, Richard A. Bryant, James Strain, Mardi Horowitz, and David Spiegel. 2011. "Classification of Trauma and Stressor-Related Disorders in DSM-5." *Depression and Anxiety* 28(9):737–49.

Gallo, Francisco T., Cynthia Katche, Juan F. Morici, Jorge H. Medina, and Noelia V. Weisstaub. 2018. "Immediate Early Genes, Memory and Psychiatric Disorders: Focus on c-Fos, Egr1 and Arc." *Frontiers in Behavioral Neuroscience* 12:79.

Ganesan, A., Paola B. Arimondo, Marianne G. Rots, Carmen Jeronimo, and Mariá Berdasco. 2019. "The Timeline of Epigenetic Drug Discovery: From Reality to Dreams." *Clinical Epigenetics* 11(1):1–17.

Gardiner-Garden, M. and M. Frommer. 1987. "CpG Islands in Vertebrate Genomes." *Journal of Molecular Biology* 196(2):261–82.

Garza-Lombó, Carla and María E. Gonsebatt. 2016. "Mammalian Target of Rapamycin: Its Role in Early Neural Development and in Adult and Aged Brain Function." *Frontiers in Cellular Neuroscience* 10(JUN):157.

Greenberg, Maxim V. C. and Deborah Bourc'his. 2019. "The Diverse Roles of DNA Methylation in Mammalian Development and Disease." *Nature Reviews Molecular Cell Biology* 20(10):590–607.

Heerboth, Sarah, Karolina Lapinska, Nnicole Snyder, Meghan Leary, Sarah Rollinson, and Sibaji Sarkar. 2014. "Use of Epigenetic Drugs in Disease: An Overview." *Genetics and Epigenetics* 1(6):9–19.

Heitman J, Movva NR, and Hall MN. 1991. "Targets for Cell Cycle Arrest by the Immunosuppressant Rapamycin in Yeast." *Science (New York, N.Y.)* 253(5022):905–9.

Hewel, Charlotte, Julia Kaiser, Anna Wierczeiko, Jan Linke, Christoph Reinhardt, Kristina Endres, and Susanne Gerber. 2019. "Common MiRNA Patterns of Alzheimer's Disease and Parkinson's Disease and Their Putative Impact on Commensal Gut Microbiota." *Frontiers in Neuroscience* 13.

Holliday, R. and J. E. Pugh. 1975. "DNA Modification Mechanisms and Gene Activity during Development." *Science* 187(4173):226–32.

Houston, Isaac, Cyril J. Peter, Amanda Mitchell, Juerg Straubhaar, Evgeny Rogaev, and Schahram Akbarian. 2013. "Epigenetics in the Human Brain." *Neuropsychopharmacology* 38(1):183–97.

Huang, Po Hsien, Chun Han Chen, Chih Chien Chou, Aaron M. Sargeant, Samuel K. Kulp, Che Ming Teng, John C. Byrd, and Ching Shih Chen. 2011. "Histone Deacetylase Inhibitors Stimulate Histone H3 Lysine 4 Methylation in Part via Transcriptional Repression of Histone H3 Lysine 4 Demethylases." *Molecular Pharmacology* 79(1):197–206.

Hudzik, Collin, Yingnan Hou, Wenbo Ma, and Michael J. Axtell. 2020. "Exchange of Small Regulatory Rnas between Plants and Their Pests." *Plant Physiology* 182(1):51–62.

Hutvágner, György and Phillip D. Zamore. 2002. "A MicroRNA in a Multiple-Turnover RNAi Enzyme Complex." *Science* 297(5589):2056–60.

Hwang, Byungjin, Ji Hyun Lee, and Duhee Bang. 2018. "Single-Cell RNA Sequencing Technologies and Bioinformatics Pipelines." *Experimental and Molecular Medicine* 50(8):96.

Hyun, Kwangbeom, Jongcheol Jeon, Kihyun Park, and Jaehoon Kim. 2017. "Writing, Erasing and Reading Histone Lysine Methylations." *Experimental and Molecular Medicine* 49(4):324.

Iguchi-Ariga, S. M. and W. Schaffner. 1989. "CpG Methylation of the CAMP-Responsive Enhancer/Promoter Sequence TGACGTCA Abolishes Specific Factor Binding as Well as Transcriptional Activation." *Genes & Development* 3(5):612–19.

Indrieri, Alessia, Sabrina Carrella, Alessia Romano, Alessandra Spaziano, Elena Marrocco, Erika Fernandez-Vizarra, Sara Barbato, Mariateresa Pizzo, Yulia Ezhova, Francesca M. Golia, Ludovica Ciampi, Roberta Tammaro, Jorge Henao-Mejia, Adam Williams, Richard A. Flavell, Elvira De Leonibus, Massimo Zeviani, Enrico M. Surace, Sandro Banfi, and Brunella Franco. 2019. "MiR-181a/b Downregulation Exerts a Protective Action on Mitochondrial Disease Models." *EMBO Molecular Medicine* 11(5).

Jeong, Dae-Eun, Dongyeop Lee, Sun-Young Hwang, Yujin Lee, Jee-Eun Lee, Mihwa Seo, Wooseon Hwang, Keunhee Seo, Ara B. Hwang, Murat Artan, Heehwa G. Son, Jay-Hyun Jo, Haeshim Baek, Young Min Oh, Youngjae Ryu, Hyung-Jun Kim, Chang Man Ha, Joo-Yeon Yoo, and Seung-Jae V Lee. 2017. " Mitochondrial Chaperone HSP -60 Regulates Anti-bacterial Immunity via P38 MAP Kinase Signaling ." *The EMBO Journal* 36(8):1046–65.

Jiang, Haiyin, Zongxin Ling, Yonghua Zhang, Hongjin Mao, Zhanping Ma, Yan Yin, Weihong Wang, Wenxin Tang, Zhonglin Tan, Jianfei Shi, Lanjuan Li, and Bing Ruan. 2015. "Altered Fecal Microbiota Composition in Patients with Major Depressive Disorder." *Brain, Behavior, and Immunity* 48:186–94.

Jiang, Shuang and Yuchen Guo. 2020. "Epigenetic Clock: DNA Methylation in Aging." *Stem Cells International* 2020.

Johnson, David S., Ali Mortazavi, Richard M. Myers, and Barbara Wold. 2007. "Genome-Wide Mapping of in Vivo Protein-DNA Interactions." *Science* 316(5830):1497–1502.

Jung, Monika, Annika Schaefer, Isabel Steiner, Carsten Kempkensteffen, Carsten Stephan, Andreas Erbersdobler, and Klaus Jung. 2010. "Robust MicroRNA Stability in Degraded RNA Preparations from Human Tissue and Cell Samples." *Clinical Chemistry* 56(6):998–1006.

Kaletsky, Rachel, Rebecca S. Moore, Geoffrey D. Vrla, Lance R. Parsons, Zemer Gitai, and Coleen T. Murphy. 2020. "C. Elegans Interprets Bacterial Non-Coding RNAs to Learn Pathogenic Avoidance." *Nature* 586(7829):445–51.

Kalisch, Raffael, Dewleen G. Baker, Ulrike Basten, Marco P. Boks, George A. Bonanno, Eddie Brummelman, Andrea Chmitorz, Guillén Fernàndez, Christian J. Fiebach, Isaac Galatzer-Levy, Elbert Geuze, Sergiu Groppa, Isabella Helmreich, Talma Hendler, Erno J. Hermans, Tanja Jovanovic, Thomas Kubiak, Klaus Lieb, Beat Lutz, Marianne B. Müller…Henrik Walter, Michèle Wessa, Michael Wibral, and Birgit Kleim. 2017. "The Resilience Framework as a Strategy to Combat Stress-Related Disorders." *Nature Human Behaviour* 1(11):784–90.

Karatsoreos, Ilia N. and Bruce S. McEwen. 2011. "Psychobiological Allostasis: Resistance, Resilience and Vulnerability." *Trends in Cognitive Sciences* 15(12):576–84.

Kelly, John R., Paul J. Kennedy, John F. Cryan, Timothy G. Dinan, Gerard Clarke, and Niall P. Hyland. 2015. “Breaking down the Barriers: The Gut Microbiome, Intestinal Permeability and Stress-Related Psychiatric Disorders.” *Frontiers in Cellular Neuroscience* 9(OCT):392.

Kelsey, Gavin, Oliver Stegle, and Wolf Reik. 2017. “Single-Cell Epigenomics: Recording the Past and Predicting the Future.” *Science* 358(6359):69–75.

Kho, Zhi Y. and Sunil K. Lal. 2018. “The Human Gut Microbiome - A Potential Controller of Wellness and Disease.” *Frontiers in Microbiology* 9(AUG).

Kim, Sangdoo, Hyunju Kim, Yeong Shin Yim, Soyoung Ha, Koji Atarashi, Tze Guan Tan, Randy S. Longman, Kenya Honda, Dan R. Littman, Gloria B. Choi, and Jun R. Huh. 2017. “Maternal Gut Bacteria Promote Neurodevelopmental Abnormalities in Mouse Offspring.” *Nature* 549(7673):528–32.

Kim, Yuna, Hyeong Min Lee, Yan Xiong, Noah Sciaky, Samuel W. Hulbert, Xinyu Cao, Jeffrey I. Everitt, Jian Jin, Bryan L. Roth, and Yong Hui Jiang. 2017. “Targeting the Histone Methyltransferase G9a Activates Imprinted Genes and Improves Survival of a Mouse Model of Prader-Willi Syndrome.” *Nature Medicine* 23(2):213–22.

King, Andrew D., Kevin Huang, Liudmilla Rubbi, Shuo Liu, Cun Yu Wang, Yinsheng Wang, Matteo Pellegrini, and Guoping Fan. 2016. “Reversible Regulation of Promoter and Enhancer Histone Landscape by DNA Methylation in Mouse Embryonic Stem Cells.” *Cell Reports* 17(1):289–302.

Kinlein, Scott A. and Ilia N. Karatsoreos. 2020. “The Hypothalamic-Pituitary-Adrenal Axis as a Substrate for Stress Resilience: Interactions with the Circadian Clock.” *Frontiers in Neuroendocrinology* 56.

Kohli, Rahul M. and Yi Zhang. 2013. “TET Enzymes, TDG and the Dynamics of DNA Demethylation.” *Nature* 502(7472):472–79.

Kouzarides, Tony. 2007. “Chromatin Modifications and Their Function.” *Cell* 128(4):693–705.

Kozomara, Ana, Maria Birgaoanu, and Sam Griffiths-Jones. 2019. “MiRBase: From MicroRNA Sequences to Function.” *Nucleic Acids Research* 47(D1):D155–62.

Krishnan, Vaishnav, Ming Hu Han, Danielle L. Graham, Olivier Berton, William Renthal, Scott J. Russo, Quincey LaPlant, Ami Graham, Michael Lutter, Diane C. Lagace, Subroto Ghose, Robin Reister, Paul Tannous, Thomas A. Green, Rachael L. Neve, Sumana Chakravarty, Arvind Kumar, Amelia J. Eisch, David W. Self, Francis S. Lee, Carol A. Tamminga, Donald C. Cooper, Howard K. Gershenfeld, and Eric J. Nestler. 2007. “Molecular Adaptations Underlying Susceptibility and Resistance to Social Defeat in Brain Reward Regions.” *Cell* 131(2):391–404.

Krishnan, Vaishnav and Eric J. Nestler. 2008. “The Molecular Neurobiology of Depression.” *Nature* 455(7215):894–902.

Kronman, Hope, Angélica Torres-Berrío, Simone Sidoli, Orna Issler, Arthur Godino, Aarthi Ramakrishnan, Philipp Mews, Casey K. Lardner, Eric M. Parise, Deena M. Walker, Yentl Y. van der Zee, Caleb J. Browne, Brittany F. Boyce, Rachael Neve, Benjamin A. Garcia, Li Shen, Catherine J. Peña, and Eric J.

Nestler. 2021. “Long-Term Behavioral and Cell-Type-Specific Molecular Effects of Early Life Stress Are Mediated by H3K79me2 Dynamics in Medium Spiny Neurons.” *Nature Neuroscience* 24(5):667–76.

Kunz J, Henriquez R, Schneider U, Deuter-Reinhard M, Movva NR, and Hall MN. 1993. “Target of Rapamycin in Yeast, TOR2, Is an Essential Phosphatidylinositol Kinase Homolog Required for G1 Progression.” *Cell* 73(3):585–96.

Lai, Eric C. 2002. “Micro RNAs Are Complementary to 3' UTR Sequence Motifs That Mediate Negative Post-Transcriptional Regulation.” *Nature Genetics* 30(4):363–64.

Larsen, Frank, Glenn Gundersen, Rodrigo Lopez, and Hans Prydz. 1992. “CpG Islands as Gene Markers in the Human Genome.” *Genomics* 13(4):1095–1107.

Lazar, Veronica, Lia Mara Ditu, Gratiela Gradisteanu Pircalabioru, Irina Gheorghe, Carmen Curutiu, Alina Maria Holban, Ariana Picu, Laura Petcu, and Mariana Carmen Chifiriuc. 2018. “Aspects of Gut Microbiota and Immune System Interactions in Infectious Diseases, Immunopathology, and Cancer.” *Frontiers in Immunology* 9(AUG).

Lee, Hyunmin, Zhaolei Zhang, and Henry M. Krause. 2019. “Long Noncoding RNAs and Repetitive Elements: Junk or Intimate Evolutionary Partners?”

Lee, Jeongwoo, Do Young Hyeon, and Daehee Hwang. 2020. “Single-Cell Multiomics: Technologies and Data Analysis Methods.” *Experimental and Molecular Medicine* 52(9):1428–42.

Lee, Rico S. C., Daniel F. Hermens, Melanie A. Porter, and M. Antoinette Redoblado-Hodge. 2012. “A Meta-Analysis of Cognitive Deficits in First-Episode Major Depressive Disorder.” *Journal of Affective Disorders* 140(2):113–24.

Lee, Rosalind C., Rhonda L. Feinbaum, and Victor Ambros. 1993. “The C. Elegans Heterochronic Gene Lin-4 Encodes Small RNAs with Antisense Complementarity to Lin-14.” *Cell* 75(5):843–54.

Lee, Yoontae, Chiyoung Ahn, Jinju Han, Hyounjeong Choi, Jaekwang Kim, Jeongbin Yim, Junho Lee, Patrick Provost, Olof Rådmark, Sunyoung Kim, and V. Narry Kim. 2003. “The Nuclear RNase III Drosha Initiates MicroRNA Processing.” *Nature* 425(6956):415–19.

Lee, Yoontae, Kipyoung Jeon, Jun Tae Lee, Sunyoung Kim, and V. Narry Kim. 2002. “MicroRNA Maturation: Stepwise Processing and Subcellular Localization.” *EMBO Journal* 21(17):4663–70.

Leung, Anthony K. L. and Phillip A. Sharp. 2010. “MicroRNA Functions in Stress Responses.” *Molecular Cell* 40(2):205–15.

Li, Bing, Michael Carey, and Jerry L. Workman. 2007. “The Role of Chromatin during Transcription.” *Cell* 128(4):707–19.

Li, En, Caroline Beard, and Rudolf Jaenisch. 1993. “Role for DNA Methylation in Genomic Imprinting.” *Nature* 366(6453):362–65.

Li, En and Yi Zhang. 2014. “DNA Methylation in Mammals.” *Cold Spring Harbor Perspectives in Biology* 6(5):a019133.

Li, Meihong, Wei Dong Chen, and Yan Dong Wang. 2020. “The Roles of the Gut Microbiota–MiRNA Interaction in the Host Pathophysiology.” *Molecular Medicine* 26(1):101.

Li, Zhijian, Marcel H. Schulz, Thomas Look, Matthias Begemann, Martin Zenke, and Ivan G. Costa. 2019. “Identification of Transcription Factor Binding Sites Using ATAC-Seq.” *Genome Biology* 20(1):1–21.

Liu, Grace Y. and David M. Sabatini. 2020. “MTOR at the Nexus of Nutrition, Growth, Ageing and Disease.” *Nature Reviews Molecular Cell Biology* 21(4):183–203.

Liu, Longqi, Lizhi Leng, Chuanyu Liu, Changfu Lu, Yue Yuan, Liang Wu, Fei Gong, Shuoping Zhang, Xiaoyu Wei, Mingyue Wang, Lei Zhao, Liang Hu, Jian Wang, Huanming Yang, Shida Zhu, Fang Chen, Guangxiu Lu, Zhouchun Shang, and Ge Lin. 2019. “An Integrated Chromatin Accessibility and Transcriptome Landscape of Human Pre-Implantation Embryos.” *Nature Communications* 10(1):1–11.

Liu, Shirong, Andre Pires Da Cunha, Rafael M. Rezende, Ron Cialic, Zhiyun Wei, Lynn Bry, Laurie E. Comstock, Roopali Gandhi, and Howard L. Weiner. 2016. “The Host Shapes the Gut Microbiota via Fecal MicroRNA.” *Cell Host and Microbe* 19(1):32–43.

Liu, Xiaosong, Jinyan Huang, Taotao Chen, Ying Wang, Shunmei Xin, Jian Li, Gang Pei, and Jiuhong Kang. 2008. “Yamanaka Factors Critically Regulate the Developmental Signaling Network in Mouse Embryonic Stem Cells.” *Cell Research* 18(12):1177–89.

Manzari, Mandana T., Yosi Shamay, Hiroto Kiguchi, Neal Rosen, Maurizio Scaltriti, and Daniel A. Heller. 2021. “Targeted Drug Delivery Strategies for Precision Medicines.” *Nature Reviews Materials* 6(4):351–70.

Marco, Asaf, Hiruy S. Meharena, Vishnu Dileep, Ravikiran M. Raju, Jose Davila-Velderrain, Amy Letao Zhang, Chinnakkaruppan Adaikkan, Jennie Z. Young, Fan Gao, Manolis Kellis, and Li Huei Tsai. 2020. “Mapping the Epigenomic and Transcriptomic Interplay during Memory Formation and Recall in the Hippocampal Engram Ensemble.” *Nature Neuroscience* 23(12):1606–17.

Maslowska, Katarzyna H., Karolina Makiela-Dzbenska, and Iwona J. Fijalkowska. 2019. “The SOS System: A Complex and Tightly Regulated Response to DNA Damage.” *Environmental and Molecular Mutagenesis* 60(4):368–84.

McEwen, Bruce S. 2000. “Allostasis and Allostatic Load: Implications for Neuropsychopharmacology.” *Neuropsychopharmacology* 22(2):108–24.

McEwen, Bruce S. and Ilia N. Karatsoreos. 2015. “Sleep Deprivation and Circadian Disruption: Stress, Allostasis, and Allostatic Load.” *Sleep Medicine Clinics* 10(1):1–10.

Mcewen, Craig A. and Bruce S. Mcewen. 2017. “Social Structure, Adversity, Toxic Stress, and Intergenerational Poverty: An Early Childhood Model.” *Annual Review of Sociology* 43:445–72.

Mehta, Divya, Olivia Miller, Dagmar Bruenig, Georgina David, and Jane Shakespeare-Finch. 2020. "A Systematic Review of DNA Methylation and Gene Expression Studies in Posttraumatic Stress Disorder, Posttraumatic Growth, and Resilience." *Journal of Traumatic Stress* 33(2):171–80.

Michaels, Yale S., Mike B. Barnkob, Hector Barbosa, Toni A. Baeumler, Mary K. Thompson, Violaine Andre, Huw Colin-York, Marco Fritzsche, Uzi Gileadi, Hilary M. Sheppard, David J. H. F. Knapp, Thomas A. Milne, Vincenzo Cerundolo, and Tudor A. Fulga. 2019. "Precise Tuning of Gene Expression Levels in Mammalian Cells." *Nature Communications 2019 10:1* 10(1):1–12.

Mikkelsen, Tarjei S., Manching Ku, David B. Jaffe, Biju Issac, Erez Lieberman, Georgia Giannoukos, Pablo Alvarez, William Brockman, Tae Kyung Kim, Richard P. Koche, William Lee, Eric Mendenhall, Aisling O'Donovan, Aviva Presser, Carsten Russ, Xiaohui Xie, Alexander Meissner, Marius Wernig, Rudolf Jaenisch, Chad Nusbaum, Eric S. Lander, and Bradley E. Bernstein. 2007. "Genome-Wide Maps of Chromatin State in Pluripotent and Lineage-Committed Cells." *Nature* 448(7153):553–60.

Miro-Blanch, Joan and Oscar Yanes. 2019. "Epigenetic Regulation at the Interplay between Gut Microbiota and Host Metabolism." *Frontiers in Genetics* 10(JUL).

Misiak, Błażej, Igor Łoniewski, Wojciech Marlicz, Dorota Frydecka, Agata Szulc, Leszek Rudzki, and Jerzy Samochowiec. 2020. "The HPA Axis Dysregulation in Severe Mental Illness: Can We Shift the Blame to Gut Microbiota?" *Progress in Neuro-Psychopharmacology and Biological Psychiatry* 102.

Miska, Eric A., Ezequiel Alvarez-Saavedra, Allison L. Abbott, Nelson C. Lau, Andrew B. Hellman, Shannon M. McGonagle, David P. Bartel, Victor R. Ambros, and H. Robert Horvitz. 2007. "Most Caenorhabditis Elegans MicroRNAs Are Individually Not Essential for Development or Viability." *PLoS Genetics* 3(12):2395–2403.

Mittal, Rahul, Luca H. Debs, Amit P. Patel, Desiree Nguyen, Kunal Patel, Gregory O'Connor, M'hamed Grati, Jeenu Mittal, Denise Yan, Adrien A. Eshraghi, Sapna K. Deo, Sylvia Daunert, and Xue Zhong Liu. 2017. "Neurotransmitters: The Critical Modulators Regulating Gut–Brain Axis." *Journal of Cellular Physiology* 232(9):2359–72.

Mo, Alisa, Eran A. Mukamel, Fred P. Davis, Chongyuan Luo, Gilbert L. Henry, Serge Picard, Mark A. Urich, Joseph R. Nery, Terrence J. Sejnowski, Ryan Lister, Sean R. Eddy, Joseph R. Ecker, and Jeremy Nathans. 2015. "Epigenomic Signatures of Neuronal Diversity in the Mammalian Brain." *Neuron* 86(6):1369–84.

Mohandas, T., R. S. Sparkes, and L. J. Shapiro. 1981. "Reactivation of an Inactive Human X Chromosome: Evidence for X Inactivation by DNA Methylation." *Science* 211(4480):393–96.

Monk, David, Deborah J. G. Mackay, Thomas Eggermann, Eamonn R. Maher, and Andrea Riccio. 2019. "Genomic Imprinting Disorders: Lessons on How Genome, Epigenome and Environment Interact." *Nature Reviews Genetics* 20(4):235–48.

Morange, Michel. 2009. *Based on the Article Entitled 'Fifty Years of the Central Dogma*. Vol. 33.

Morange, Michel. 2013. "What History Tells Us XXXII. the Long and Tortuous History of Epigenetic Marks." *Journal of Biosciences* 38(3):451–54.

Morel, Daphné, Daniel Jeffery, Sandrine Aspeslagh, Geneviève Almouzni, and Sophie Postel-Vinay. 2020. "Combining Epigenetic Drugs with Other Therapies for Solid Tumours — Past Lessons and Future Promise." *Nature Reviews Clinical Oncology* 17(2):91–107.

Nichols, Robert G. and Emily R. Davenport. 2021. "The Relationship between the Gut Microbiome and Host Gene Expression: A Review." *Human Genetics* 140(5):747–60.

Nightingale, Karl P. 2016. "CHAPTER 1: Epigenetics - What It Is and Why It Matters." Pp. 1–19 in *RSC Drug Discovery Series*. Vols. 2016-January. Royal Society of Chemistry.

Nott, Alexi, Inge R. Holtman, Nicole G. Coufal, Johannes C. M. Schlachetzki, Miao Yu, Rong Hu, Claudia Z. Han, Monique Pena, Jiayang Xiao, Yin Wu, Zahara Keulen, Martina P. Pasillas, Carolyn O'Connor…Fred H. Gage, Bing Ren, and Christopher K. Glass. 2019. "Brain Cell Type–Specific Enhancer–Promoter Interactome Maps and Disease-Risk Association." *Science* 366(6469):1134–39.

Park, Chong Yon, Lukas T. Jeker, Karen Carver-Moore, Alyssia Oh, Huey Jiin Liu, Rachel Cameron, Hunter Richards, Zhongmei Li, David Adler, Yuko Yoshinaga, Maria Martinez, Michael Nefadov, Abul K. Abbas, Art Weiss, Lewis L. Lanier, Pieter J. de Jong, Jeffrey A. Bluestone, Deepak Srivastava, and Michael T. McManus. 2012. "A Resource for the Conditional Ablation of MicroRNAs in the Mouse." *Cell Reports* 1(4):385–91.

Pokholok, Dmitry K., Christopher T. Harbison, Stuart Levine, Megan Cole, Nancy M. Hannett, Ihn Lee Tong, George W. Bell, Kimberly Walker, P. Alex Rolfe, Elizabeth Herbolsheimer, Julia Zeitlinger, Fran Lewitter, David K. Gifford, and Richard A. Young. 2005. "Genome-Wide Map of Nucleosome Acetylation and Methylation in Yeast." *Cell* 122(4):517–27.

Portela, Anna and Manel Esteller. 2010. "Epigenetic Modifications and Human Disease." *Nature Biotechnology* 28(10):1057–68.

Powledge, Tabitha M. 2011. "Behavioral Epigenetics: How Nurture Shapes Nature." *BioScience* 61(8):588–92.

Prachayasittikul, Veda, Philip Prathipati, Reny Pratiwi, Chuleeporn Phanus-Umporn, Ahmad Malik, Nalini Schaduangrat, Kanokwan Seenprachawong, Prapimpun Wongchitrat, Aungkura Supokawej, Virapong Prachayasittikul, Jarl E. S. Wikberg, and Chanin Nantasenamat. 2017. "Exploring the Epigenetic Drug Discovery Landscape."

Purohit, Paresh Kumar and Neeru Saini. 2021. "Mitochondrial MicroRNA (MitomiRs) in Cancer and Complex Mitochondrial Diseases: Current Status and Future Perspectives." *Cellular and Molecular Life Sciences* 78(4):1405–21.

Qin, Yufeng and Paul A. Wade. 2018. "Crosstalk between the Microbiome and Epigenome: Messages from Bugs." *Journal of Biochemistry* 163(2):105–12.

Rada-Iglesias, Alvaro, Ruchi Bajpai, Tomek Swigut, Samantha A. Brugmann, Ryan A. Flynn, and Joanna Wysocka. 2011. "A Unique Chromatin Signature Uncovers Early Developmental Enhancers in Humans." *Nature* 470(7333):279–85.

Ramaswami, Ramya, Ronald Bayer, and Sandro Galea. 2018. “Precision Medicine from a Public Health Perspective.” *Annual Review of Public Health* 39:153–68.

Riggs, A. D. 1975. “X Inactivation, Differentiation, and DNA Methylation.” *Cytogenetic and Genome Research* 14(1):9–25.

Rogers, G. B., D. J. Keating, R. L. Young, M. L. Wong, J. Licinio, and S. Wesselingh. 2016. “From Gut Dysbiosis to Altered Brain Function and Mental Illness: Mechanisms and Pathways.” *Molecular Psychiatry* 21(6):738–48.

Rooks, Michelle G. and Wendy S. Garrett. 2016. “Gut Microbiota, Metabolites and Host Immunity.” *Nature Reviews Immunology* 16(6):341–52.

Rotem, Assaf, Oren Ram, Noam Shoresh, Ralph A. Sperling, Alon Goren, David A. Weitz, and Bradley E. Bernstein. 2015. “Single-Cell ChIP-Seq Reveals Cell Subpopulations Defined by Chromatin State.” *Nature Biotechnology* 33(11):1165–72.

Ruf, Nico, Sylvia Bä;hring, Danuta Galetzka, Galyna Pliushch, Friedrich C. Luft, Peter Nürnberg, Thomas Haaf, Gavin Kelsey, and Ulrich Zechner. 2007. “Sequence-Based Bioinformatic Prediction and QUASEP Identify Genomic Imprinting of the KCNK9 Potassium Channel Gene in Mouse and Human.” *Human Molecular Genetics* 16(21):2591–99.

Ruwe, Hannes and Christian Schmitz-Linneweber. 2012. “Short Non-Coding RNA Fragments Accumulating in Chloroplasts: Footprints of RNA Binding Proteins?” *Nucleic Acids Research* 40(7):3106–16.

Sætrom, Pål, Bret S. E. Heale, Ola Snøve, Lars Aagaard, Jessica Alluin, and John J. Rossi. 2007. “Distance Constraints between MicroRNA Target Sites Dictate Efficacy and Cooperativity.” *Nucleic Acids Research* 35(7):2333–42.

Salleh, Mohd Razali. 2008. “Life Event, Stress and Illness.” *Malaysian Journal of Medical Sciences* 15(4):9–18.

Sampedro-Piquero, P. and A. Begega. 2016. “Environmental Enrichment as a Positive Behavioral Intervention Across the Lifespan.” *Current Neuropharmacology* 15(4):459–70.

Sanchez, Oscar F., Li Lin, Chris J. Bryan, Junkai Xie, and Jennifer L. Freeman. 2019. *Profiling Epigenetic Changes in Human Cell Line Induced by Atrazine Exposure 2 3*.

Schreiber, Katherine H., Sebastian I. Arriola Apelo, Deyang Yu, Jacqueline A. Brinkman, Michael C. Velarde, Faizan A. Syed, Chen Yu Liao, Emma L. Baar, Kathryn A. Carbajal, Dawn S. Sherman, Denise Ortiz, Regina Brunauer, Shany E. Yang, Stelios T. Tzannis, Brian K. Kennedy, and Dudley W. Lamming. 2019. “A Novel Rapamycin Analog Is Highly Selective for MTORC1 in Vivo.” *Nature Communications* 10(1):1–12.

Schreiber, Steven S., Stephen Maren, Georges Tocco, Tracey Jo Shors, and Richard F. Thompson. 1991. “A Negative Correlation between the Induction of Long-Term Potentiation and Activation of Immediate Early Genes.” *Molecular Brain Research* 11(1):89–91.

Senba, Emiko and Takashi Ueyama. 1997. “Stress-Induced Expression of Immediate Early Genes in the Brain and Peripheral Organs of the Rat.” *Neuroscience Research* 29(3):183–207.

Shapiro, Ehud, Tamir Biezuner, and Sten Linnarsson. 2013. “Single-Cell Sequencing-Based Technologies Will Revolutionize Whole-Organism Science.” *Nature Reviews Genetics* 14(9):618–30.

Sharma, Bhawna, Rachael M. Crist, and Pavan P. Adiseshaiah. 2017. “Nanotechnology as a Delivery Tool for Precision Cancer Therapies.” *AAPS Journal* 19(6):1632–42.

Silberman, Dafne M., Gabriela B. Acosta, and María A. Zorrilla Zubilete. 2016. “Long-Term Effects of Early Life Stress Exposure: Role of Epigenetic Mechanisms.” *Pharmacological Research* 109:64–73.

Singh, Akhand Pratap, Arpan Biswas, Aparna Shukla, and Pralay Maiti. 2019. “Targeted Therapy in Chronic Diseases Using Nanomaterial-Based Drug Delivery Vehicles.” *Signal Transduction and Targeted Therapy* 4(1):1–21.

Skvortsova, Ksenia, Nicola Iovino, and Ozren Bogdanović. 2018. “Functions and Mechanisms of Epigenetic Inheritance in Animals.” *Nature Reviews Molecular Cell Biology* 19(12):774–90.

Smallwood, Sébastien A., Heather J. Lee, Christof Angermueller, Felix Krueger, Heba Saadeh, Julian Peat, Simon R. Andrews, Oliver Stegle, Wolf Reik, and Gavin Kelsey. 2014. “Single-Cell Genome-Wide Bisulfite Sequencing for Assessing Epigenetic Heterogeneity.” *Nature Methods* 11(8):817–20.

Stark, Rory, Marta Grzelak, and James Hadfield. 2019. “RNA Sequencing: The Teenage Years.” *Nature Reviews Genetics* 20(11):631–56.

Statello, Luisa, Chun-Jie Guo, Ling-Ling Chen, and Maite Huarte. 2020. “Gene Regulation by Long Non-Coding RNAs and Its Biological Functions.” *Nature Reviews Molecular Cell Biology 2020 22:2* 22(2):96–118.

Sterling, P., & Eyer, J. (1988). Allostasis A New Paradigm to Explain Arousal Pathology. In S. Fisher, & J. Reason (Eds.), Handbook of Life Stress, Cognition and Health (Pp. 629-649). New York John Wiley & Sons. - References - Scientific Research Publishing.”

Stöger, R., P. Kubička, C. G. Liu, T. Kafri, A. Razin, H. Cedar, and D. P. Barlow. 1993. “Maternal-Specific Methylation of the Imprinted Mouse Igf2r Locus Identifies the Expressed Locus as Carrying the Imprinting Signal.” *Cell* 73(1):61–71.

Stuart, Tim and Rahul Satija. 2019. “Integrative Single-Cell Analysis.” *Nature Reviews Genetics* 20(5):257–72.

Su, Yijing, Jaehoon Shin, Chun Zhong, Sabrina Wang, Prith Roychowdhury, Jongseuk Lim, David Kim, Guo Li Ming, and Hongjun Song. 2017. “Neuronal Activity Modifies the Chromatin Accessibility Landscape in the Adult Brain.” *Nature Neuroscience* 20(3):476–83.

Tachibana, Makoto, Kenji Sugimoto, Masami Nozaki, Jun Ueda, Tsutomu Ohta, Misao Ohki, Mikiko Fukuda, Naoki Takeda, Hiroyuki Niida, Hiroyuki Kato, and Yoichi Shinkai. 2002. “G9a Histone

Methyltransferase Plays a Dominant Role in Euchromatic Histone H3 Lysine 9 Methylation and Is Essential for Early Embryogenesis." *Genes and Development* 16(14):1779–91.

Teperino, Raffaele, Kristina Schoonjans, and Johan Auwerx. 2010. "Histone Methyl Transferases and Demethylases; Can They Link Metabolism and Transcription?" *Cell Metabolism* 12(4):321–27.

Tie, Feng, Rakhee Banerjee, Carl A. Stratton, Jayashree Prasad-Sinha, Vincent Stepanik, Andrei Zlobin, Manuel O. Diaz, Peter C. Scacheri, and Peter J. Harte. 2009. "CBP-Mediated Acetylation of Histone H3 Lysine 27 Antagonizes Drosophila Polycomb Silencing." *Development* 136(18):3131–41.

Toth, Miklos. 2021. "Epigenetic Neuropharmacology: Drugs Affecting the Epigenome in the Brain." *Annual Review of Pharmacology and Toxicology* 61:181–201.

Trojer, Patrick and Danny Reinberg. 2007. "Facultative Heterochromatin: Is There a Distinctive Molecular Signature?" *Molecular Cell* 28(1):1–13.

Tronick, Ed and Richard G. Hunter. 2016. "Waddington, Dynamic Systems, and Epigenetics." *Frontiers in Behavioral Neuroscience* 10(JUN).

Turchinovich, A., T. R. Samatov, A. G. Tonevitsky, and B. Burwinkel. 2013. "Circulating MiRNAs: Cell-Cell Communication Function?" *Frontiers in Genetics* 4(JUN):119.

Vaiserman, Alexander M. and Alexander K. Koliada. 2017. "Early-Life Adversity and Long-Term Neurobehavioral Outcomes: Epigenome as a Bridge?" *Human Genomics* 11(1).

Villota-Salazar, Nubia Andrea, Artemio Mendoza-Mendoza, and Juan Manuel González-Prieto. 2016. "Epigenetics: From the Past to the Present." *Frontiers in Life Science* 9(4):347–70.

Vinkers, Christiaan H., Aimilia Lydia Kalafateli, Bart P. Rutten, Martien J. Kas, Zachary Kaminsky, Jonathan D. Turner, and Marco P. Boks. 2015. "Traumatic Stress and Human DNA Methylation: A Critical Review." *Epigenomics* 7(4):593–608.

Vishnoi, Anchal and Sweta Rani. 2017. "MiRNA Biogenesis and Regulation of Diseases: An Overview." Pp. 1–10 in *Methods in Molecular Biology*. Vol. 1509. Humana Press Inc.

Waddington, C. H. 1942. "Canalization of Development and the Inheritance of Acquired Characters." *Nature* 150(3811):563–65.

Walsh, C. P., J. R. Chaillet, and T. H. Bestor. 1998. "Transcription of IAP Endogenous Retroviruses Is Constrained by Cytosine Methylation [4]." *Nature Genetics* 20(2):116–17.

Wang, Nayi, Ji Zheng, Zhuo Chen, Yang Liu, Burak Dura, Minsuk Kwak, Juliana Xavier-Ferrucio, Yi Chien Lu, Miaomiao Zhang, Christine Roden, Jijun Cheng, Diane S. Krause, Ye Ding, Rong Fan, and Jun Lu. 2019. "Single-Cell MicroRNA-MRNA Co-Sequencing Reveals Non-Genetic Heterogeneity and Mechanisms of MicroRNA Regulation." *Nature Communications* 10(1):1–12.

Wang, Yu Chieh, Suzanne E. Peterson, and Jeanne F. Loring. 2014. "Protein Post-Translational Modifications and Regulation of Pluripotency in Human Stem Cells." *Cell Research* 24(2):143–60.

Watkins, Derrick and Dev P. Arya. 2019. “Regulatory Roles of Small RNAs in Prokaryotes: Parallels and Contrast with Eukaryotic MiRNA.” *Non-Coding RNA Investigation* 3:28–28.

Watson, R. E. 2014. “Epigenetics.” Pp. 438–43 in *Encyclopedia of Toxicology: Third Edition*. Elsevier.

Watt, F. and P. L. Molloy. 1988. “Cytosine Methylation Prevents Binding to DNA of a HeLa Cell Transcription Factor Required for Optimal Expression of the Adenovirus Major Late Promoter.” *Genes & Development* 2(9):1136–43.

Weiberg, Arne and Hailing Jin. 2015. “Small RNAs-the Secret Agents in the Plant-Pathogen Interactions.” *Current Opinion in Plant Biology* 26:87–94.

Weiberg, Arne, Ming Wang, Marschal Bellinger, and Hailing Jin. 2014. “Small RNAs: A New Paradigm in Plant-Microbe Interactions.” *Annual Review of Phytopathology* 52:495–516.

Weinhold, Bob. 2006. “Epigenetics: The Science of Change.” *Environmental Health Perspectives* 114(3):A160.

Weinstein, Lee S. 2001. “The Role of Tissue-Specific Imprinting as a Source of Phenotypic Heterogeneity in Human Disease.” *Biological Psychiatry* 50(12):927–31.

Willbanks, Amber, Meghan Leary, Molly Greenshields, Camila Tyminski, Sarah Heerboth, Karolina Lapinska, Kathryn Haskins, and Sibaji Sarkar. 2016. “The Evolution of Epigenetics: From Prokaryotes to Humans and Its Biological Consequences.” *Genetics and Epigenetics* 1(8):25–36.

Wong, Siew Ying, Michelle G. K. Tan, William A. Banks, W. S. Fre. Wong, Peter T. H. Wong, and Mitchell K. P. Lai. 2016. “Andrographolide Attenuates LPS-Stimulated up-Regulation of C-C and C-X-C Motif Chemokines in Rodent Cortex and Primary Astrocytes.” *Journal of Neuroinflammation* 13(1):1–11.

Wu, Xiaoji and Yi Zhang. 2017. “TET-Mediated Active DNA Demethylation: Mechanism, Function and Beyond.” *Nature Reviews Genetics* 18(9):517–34.

Xu, Tian, Dejuan Sun, Yi Chen, and Liang Ouyang. 2020. “Targeting MTOR for Fighting Diseases: A Revisited Review of MTOR Inhibitors.” *European Journal of Medicinal Chemistry* 199.

Yadav, Tejas, Jean Pierre Quivy, and Geneviève Almouzni. 2018. “Chromatin Plasticity: A Versatile Landscape That Underlies Cell Fate and Identity.” *Science* 361(6409):1332–36.

Yan, Chunhong and Douglas D. Boyd. 2006. “Histone H3 Acetylation and H3 K4 Methylation Define Distinct Chromatin Regions Permissive for Transgene Expression.” *Molecular and Cellular Biology* 26(17):6357–71.

Yang, Chun, Yuko Fujita, Qian Ren, Min Ma, Chao Dong, and Kenji Hashimoto. 2017. “Bifidobacterium in the Gut Microbiota Confer Resilience to Chronic Social Defeat Stress in Mice.” *Scientific Reports* 7(1):1–7.

Yang, X. J. and E. Seto. 2007. “HATs and HDACs: From Structure, Function and Regulation to Novel Strategies for Therapy and Prevention.” *Oncogene* 26(37):5310–18.

Yano, Jessica M., Kristie Yu, Gregory P. Donaldson, Gauri G. Shastri, Phoebe Ann, Liang Ma, Cathryn R. Nagler, Rustem F. Ismagilov, Sarkis K. Mazmanian, and Elaine Y. Hsiao. 2015. "Indigenous Bacteria from the Gut Microbiota Regulate Host Serotonin Biosynthesis." *Cell* 161(2):264–76.

Yaribeygi, Habib, Yunes Panahi, Hedayat Sahraei, Thomas P. Johnston, and Amirhossein Sahebkar. 2017. "The Impact of Stress on Body Function: A Review." *EXCLI Journal* 16:1057–72.

Yousef, Mohamed H., Hassan A. N. El-Fawal, and Anwar Abdelnaser. 2020. "Hepigenetics: A Review of Epigenetic Modulators and Potential Therapies in Hepatocellular Carcinoma." *BioMed Research International* 2020.

Zannas, A. S. and A. E. West. 2014. "Epigenetics and the Regulation of Stress Vulnerability and Resilience." *Neuroscience* 264:157–70.

Zhang, Lian, Qianjin Lu, and Christopher Chang. 2020. "Epigenetics in Health and Disease." Pp. 3–55 in *Advances in Experimental Medicine and Biology*. Vol. 1253. Springer.

Zhang, Qian and Xuetao Cao. 2019. "Epigenetic Regulation of the Innate Immune Response to Infection." *Nature Reviews Immunology* 19(7):417–32.

Zhang, Weiqi, Jing Qu, Guang Hui Liu, and Juan Carlos Izpisua Belmonte. 2020. "The Ageing Epigenome and Its Rejuvenation." *Nature Reviews Molecular Cell Biology* 21(3):137–50.

Zhao, Ying, Yan Zeng, Dong Zeng, Hesong Wang, Mengjia Zhou, Ning Sun, Jinge Xin, Abdul Khalique, Danish Sharafat Rajput, Kangcheng Pan, Gang Shu, Bo Jing, and Xueqin Ni. 2021. "Probiotics and MicroRNA: Their Roles in the Host–Microbe Interactions." *Frontiers in Microbiology* 11:3363.

Zheng, P., B. Zeng, C. Zhou, M. Liu, Z. Fang, X. Xu, L. Zeng, J. Chen, S. Fan, X. Du, X. Zhang, D. Yang, Y. Yang, H. Meng, W. Li, N. D. Melgiri, J. Licinio, H. Wei, and P. Xie. 2016. "Gut Microbiome Remodeling Induces Depressive-like Behaviors through a Pathway Mediated by the Host's Metabolism." *Molecular Psychiatry* 21(6):786–96.

Zhou, Xikun, Xuefeng Li, and Min Wu. 2018. "MiRNAs Reshape Immunity and Inflammatory Responses in Bacterial Infection." *Signal Transduction and Targeted Therapy* 3(1).

Zhu, Baoli, Xin Wang, and Lanjuan Li. 2010. "Human Gut Microbiome: The Second Genome of Human Body." *Protein and Cell* 1(8):718–25.